Thiol-Ene "Click"
A Radical Tool for Chemoselective Modification and Labelling of Biomolecules

Mark D. Nolan B.A.

August 2023

Trinity College Dublin

The University of Dublin

Based on research carried out under the supervision of Prof. Eoin Scanlan.

A thesis submitted to the School of Chemistry, Trinity College Dublin, The University of Dublin for the degree of Doctor of Philosophy.

Declaration

I declare that this thesis has not been submitted as an exercise for a degree at this or any other university and it is entirely my own work.

I agree to deposit this thesis in the University's open access institutional repository or allow the Library to do so on my behalf, subject to Irish Copyright Legislation and Trinity College Library conditions of use and acknowledgement.

I consent to the examiner retaining a copy of the thesis beyond the examining period, should they so wish (EU GDPR May 2018).

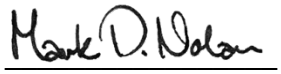

Mark D. Nolan

Abstract

Thiol-Ene Click chemistry represents a venerable reaction in chemical synthesis, allowing the efficient formation of a sulfur-carbon bond from thiol and alkene reaction partners. This reaction has found myriad applications in diverse areas of chemistry, from small-molecule synthesis, to polymer science, and even for modification of large, complex biomolecules. In this work, the development of methodology for modification of peptides and other biomolecules using Thiol-Ene chemistry is explored.

In the first part of this thesis, the use of the UV-initiated Thiol-Ene reaction for the macrocyclisation of peptides to yield disulfide mimetics is investigated. A number of analogues of the neuropeptide hormone oxytocin are obtained in good yields through Thiol-Ene mediated peptide macrocyclisation. This approach is then applied to the synthesis of the therapeutic Carbetocin, with quantitative cyclisation observed. To further expand the scope of this methodology, the cyclisation of small peptide macrocycles is then briefly investigated as this has applications in peptide drug discovery. Further, the use of mild blue LED initiation is developed for cyclisation of these short peptide substrates.

In the third chapter, the use of Thiol-Ene chemistry in Deep Eutectic Solvents for development of a green bioconjugation approach is investigated. Deep Eutectic Solvents represent a newly emerging class of green solvent, with advantageous characteristics such as non-volatility, non-toxicity and recyclability. First, the screening of a range of DESs using a model small-molecule UV-initiated Thiol-Ene reaction reveals successful reaction in a range of solvents, following which a scope focused on biomolecules is established. A subset of the scope examples are then also obtained *via* an oxygen-initiated Thiol-Ene reaction. Following this, the goal of green bioconjugation is investigated. An example peptide based on the minimum binding motif of human angiotensin converting enzyme 2 is synthesised, and Thiol-Ene bioconjugation is achieved to yield lipidated, glycosylated and fluorescent tagged analogues.

The fourth chapter of this work examines the use of the Thiol-Ene reaction in high-throughput for the efficient diversification of peptidic macrocycles to yield high-purity crudes suitable for Direct-to-Biology applications. Initial investigation discussed covers considerations around the compatibility of Thiol-Ene chemistry within the context of high-throughput experimentation. A suitable UV reactor is designed and a small-molecule model Thiol-Ene reaction is studied. With suitable parameters, the application of the conditions to

modification of an alkene-containing peptide macrocycle is then investigated and the reaction conditions optimised. With optimal conditions, a high-throughput approach is envisaged utilising acoustic droplet ejection and automated bulk dispensing. This is then applied to twelve peptide examples and eight thiols for a ninety-six entry scope presented as a heat map.

The fifth chapter covers the development of thiol probes for labelling of alkene groups in a biological context. The synthesis of an alkenyl monosaccharide substrate is first presented. For the thiol probe component, a range of fluorescent probes are synthesised including dansyl, napthyl, fluorescein and aminobenzamide thiols, with only the latter showing successful reaction in UV- or blue LED-initiated Thiol-Ene conditions. To then extend this methodology to fluorophores of use for microscopy, an indirect labelling approach is envisaged. For this purpose, a biotin thiol probe is synthesised which shows successful quantitative consumption of the alkene substrate in UV-initiated conditions. This probe was then applied to labelling of glycans on the cell surface *via* metabolic incorporation of an alkene-containing sugar followed by on-cell TEC.

In the sixth chapter, a brief overall summary of the work discussed in this thesis is given. Experimental details and compound characterisation data are presented in the seventh and final chapter.

Abbreviations

AA	Amino acid
Abz	Aminobenzamide
ACE-2	Angiotensin-Converting Enzyme 2
ADE	Acoustic Droplet Ejection
ADME	Absorption, Distribution, Metabolism and Excretion
AF	AlexaFluor
Agl	Allylglycine
AIBN	2,2'-Azobis(isobutryonitrile)
AIP	Autoinducing Peptide
alloc	*N*-Allyloxycarbonyl
AMP	Antimicrobial Peptide
APCI	Atmospheric Pressure Chemical Ionization
Aq.	Aqueous
Ar	Aromatic
Arg; R	Arginine
Asn; N	Asparagine
Asp; D	Aspartic Acid
ATE	Acyl Thiol-Ene
BDT	1,4-Butanedithiol
Bet	Betaine
BGC	Biosynthetic Gene Cluster
BME	β-mercaptoethanol
Boc	*tert*-butyloxycarbonyl
BOP	Benzotriazol-1-yloxytris(Dimethylamino)Phosphonium Hexafluorophosphate
BPB	Bromophenol Blue
bRo5	Beyond Rule of Five
Br	Broad

BSA	Bovine Serum Albumin
calcd.	Calculated
Cbz	Carboxybenzyl
CDCl3	Chloroform
ChCl	Choline Chloride
CLipPA	Cysteine Lipidation on a Peptide or Amino Acid
COC	Cyclic Olefin Copolymer
COSY	Correlation Spectroscopy
CuAAC	Copper-Catalysed Azide Alkyne Cycloaddition
Cys	Cysteine
d	Doublet
Dansyl	5-(DimethylAmino)Naphthalene-1-Sulfonyl
DAPI	4′,6-Diamidino-2-phenylindole
DCA	Dichloroacetone
DCM	Dichloromethane
dd	Doublet of Doublets
DES	Deep Eutectic Solvent
Dha	Dehydroalanine
DIC	Diisopropylcarbodiimide
DIPEA	Diisopropylethylamine
DMAP	4-(Dimethylamino)pyridine
DMF	Dimethylformamide
DMSO	Dimethylsulfoxide
DNA	Deoxyribonucleic acid
DPAP	2,2-Dimethoxy-2-Phenylacetophenone
DTT	Dithiothreitol
EDC·HCl	1-(3-Dimethylaminopropyl)-3-ethylcarbodiimide Hydrochloride
EDT	Ethanedithiol
EG	Ethylene Glycol

Equiv.	Equivalents
ESI	Electrospray Ionisation
Et	Ethyl
Et_2O	Diethyl Ether
EtOAc	Ethyl Acetate
Fmoc	Fluorenylmethoxycarbonyl
g	Gram
GlucNAc	*N*-Acetyl-D-Glucosamine
Gln	Glutamine
Glu	Glutamic Acid
Gly	Glycine
Glyc	Glycerol
GSH	Glutathione
h	Hour
HAT	Hydrogen Atom Transfer
HBTU	(2-(1H-Benzotriazol-1-yl)-1,1,3,3-Tetramethyluronium Hexafluorophosphate
HCl	Hydrochloric Acid
HF	Hydrofluoric Acid
HGH	Human Growth Hormone
His; H	Histidine
HMBC	Heteronuclear Multiple Bond Correlation
HMPA	Hexamethylphosphoramide
HOBt	Hydroxybenzotriazole
HPLC	High-Performance Liquid Chromatography
HRMS	High Resolution Mass Spectrometry
HSQC	Heteronuclear Single Quantum Coherence
HT	High-Throughput
HTE	High-Throughput Experimentation

Hz	Hertz
IIDQ	2-Isobutoxy-1-Isobutoxycarbonyl-1,2-Dihydroquinoline
Ile; I	Isoleucine
IR	Infrared
J	Coupling Constant
L	Litre
LC	Liquid Chromatography
LC-MS	Liquid Chromatography - Mass Spectrometry
LDV	Low dead volume
LED	Light-Emitting Diode
Leu; L	Leucine
Lev	Levulinic Acid
Lys	Lysine
m	Multiplet
m/z	Mass to Charge Ratio
MAP	4-Methoxyacetophenone
Me	Methyl
Mea	Mercaptoethylamine
MeCN	Acetonitrile
MeOH	Methanol
Met	Methionine
min	Minutes
Mmt	Monomethoxytrityl
M.p.	Melting point
Mpa	3-merceptopropionic acid
mRNA	Messenger ribonucleic acid
MRSA	Methicilin resistant *Staphylococcus aureus*
Mtt	Methyltrityl
NCL	Native chemical ligation

NMM	*N*-methylmorpholine
NMP	*N*-methylpyrolidinone
NMR	Nuclear Magnetic Resonance
PC	Photocatalyst
PCR	Polymerase Chain Reaction
PDA	Photodiode Array
PEG	Polyethylene glycol
PI	Photoinitiator
PPI	Protein-protein interaction
Pro; P	Proline
PTM	Post Translational Modification
PyBOP	benzatriazol-1-yl-oxytripyrrolidinophosphonium hexafluorophosphate
q	Quartet
RA	Rink Amide
RaPID	random nonstandard peptides integrated discovery
R_f	Retention Factor
RiPP	Ribosomally Synthesised and Post-translationally Modified Peptide
Ro5	Rule of five
RP	Reverse Phase
rt	Room Temperature
RVC	Rotary vacuum concentration
s	Singlet
SARS-Cov-2	Severe Acute Respiratory Syndrome Coronavirus 2
Ser; S	Serine
SET	Single Electron Transfer
SPAAC	Strain promoted azide alkyne cycloaddition
SPE	Solid-Phase Extraction
SPPS	Solid phase peptide synthesis
SuFEx	Sulfur(VI) Fluoride Exchange

TBACl	Tetrabutylammonium Chloride
t	Triplet
***t*Bu**	*tert*-butyl
TCEP·HCl	Tris(2-carboxyethyl)phosphine Hydrochloride
TEA	Triethylamine
TEC	Thiol-Ene Click
TEMPO	2,2,6,6-Tetramethylpiperidine 1-oxyl
TES	Triethylsilane
TFA	Trifluoroacetic acid
THF	Tetrahydrofuran
TIPS	Triisopropylsilane
TLC	Thin Layer Chromatography
TOCSY	Total Correlation Spectroscopy
TOF	Time of Flight
Thr; T	Threonine
Trp	Tryptophan
Trityl;Trt	Triphenylmethyl
TYC	Thiol-Yne
Tyr; Y	Tyrosine
Ub	Ubiquitin
UHPLC	Ultra-High Performance Liquid Chromatography
UV	Ultraviolet
UV-vis	Ultraviolet-visible
VAA	Vinylacetic Acid
Val; V	Valine
Vgl	Vinylglycine

Acknowledgements

I would first like to thank Prof. Eoin Scanlan for the guidance and support I received throughout the course of my PhD research. From the pandemic in the first year of my studies, you ensured my work kept moving forward, and trusted in me to pursue my own avenues in the later stages with your expert guidance. Thank you also for supporting me to attend conferences and support my applications which has given me the network and opportunities I have going forward. I could not wish for a more supportive supervisor.

I would also like to thank SSPC, the Science Foundation Ireland Research Centre for Pharmaceuticals for financing this work and for organising the various theme meetings which provided frequent discussion for development of ideas.

I wish to extend my utmost gratitude to Dr. John O'Brien and Dr. Manuel Ruether for their NMR support over the past years. Without a doubt, this work would have been a different undertaking without such brilliant knowledge to lean on. Your skills and enthusiasm kept me going through gigabytes of cyclic peptide NMR data. Additionally, I would like to thank Dr. Gary Hessman for his work on MS analysis, even when I submit countless samples from the HPLC in the desperate search for the product. I would also like to thank Dr. Brendan Twamley for crystallography support and Gavin McManus for microscopy support.

I would like to also thank the collaborators with whom I have worked throughout my PhD studies. I extend my sincere thanks to Prof. Martin Caffrey and his past and present group members, particularly Luke, Kiefer, Samir and Coilín. I would like to thank Prof. Lorenzo Guazzelli and Dr. Andrea Mezzetta for bringing their expertise on green chemistry to our collaborative work. I would also like to thank Prof. Christian Heinis and the whole of the LPPT at EPFL for hosting me on my secondment. In particular, I would like to thank Alex and Mischa who I worked with directly, and Conor. I would also like to thank our collaborator for cell work, Dr. Jerrard Hayes.

I would like to thank the past and present members of Scanlan Lab. Conor and Lucy, I wish you the best of luck with the work I pass on. Le'en, thanks for the meme-ories from first year. Thank you to Conor Webb for the work on the cyclisation project despite the unusual circumstances of the project during the pandemic. I would also like to extend my thanks to the members of the McGouran Lab. Sean, thank you for your work on the protein labelling, and for exploring some of Switzerland with me.

I would like to extend a particular thanks to Dr. Alexander Lund Nielsen. You made me feel extraordinarily welcome at EPFL, whilst also teaching me a great deal about high-throughput chemistry.

To Natalie, thank you for being there for me, for supporting me and for keeping me grounded.

To my family, thank you for your unending support. To all of my grandparents, still with us or not, thank you for always supporting me and nurturing my curiosity. Each of you has played a role in my finding my path and for that I am forever grateful. Mum and Dad, thank you for always supporting me. Sorry I'm not an accountant.

PhD Publications

(1) **Nolan, M.D.**; Scanlan, E.M. Applications of Thiol-Ene Chemistry for Peptide Science. *Front. Chem.* **2020**, *8* (1), 583272. https://doi.org/10.3389/fchem.2020.583272.

(2) McLean, J.T.; Benny, A.; **Nolan, M.D.**; Swinand, G.; Scanlan, E.M. Cysteinyl Radicals in Chemical Synthesis and in Nature. *Chem. Soc. Rev.* **2021**, *50* (1), 10857–10894. https://doi.org/10.1039/d1cs00254f.

(3) **Nolan, M.D.**; Mezzetta, A.; Guazzelli, L.; Scanlan, E.M. Radical-Mediated Thiol-Ene 'Click' Reactions in Deep Eutectic Solvents for Bioconjugation. *Green Chem.* **2022**, *24* (4), 1456–1462. https://doi.org/10.1039/d1gc03714e.

(4) **Nolan, M.D.**; Shine, C.; Scanlan, E.M.; Petracca, R. Thioether Analogues of the Pituitary Neuropeptide Oxytocin via Thiol–Ene Macrocyclisation of Unprotected Peptides. Org. Biomol. Chem. **2022**, *20* (42), 8192–8196. https://doi.org/10.1039/D2OB01688E.

(5) **Nolan, M.D.**; Schüttel, M.; Scanlan, E.M.; Nielsen, A.L. Nanomole-Scale Photochemical Thiol-Ene Chemistry for High-Throughput Late-Stage Diversification of Peptide Macrocycles. *Pept. Sci.* **2023**, e24310. https://doi.org/10.1002/pep2.24310.

(6) Lynch, D.M.;† **Nolan, M.D.**;† Williams, C; Van Dalsen, L.; Calvert, S.H.; Dénès, F.; Trujillo C.; Scanlan E.M. Traceless Thioacid-Mediated Radical Cyclisation of 1,6-Dienes, J. *Org. Chem.* **2023**, *88* (14), 10020-10026. https://doi.org/10.1021/acs.joc.3c00824.

(7) Schüttel, M.; Ji, X.; Assari, M.; **Nolan, M.D.**; Habeshian, S.; Nielsen, A.L.; Zarda, A.S.; Waser, J.; Heinis, C. Reactivity and properties of thiol-thiol peptide cyclization reagents presented as a periodic table, *manuscript submitted*.

(8) Craven, T.W.;† **Nolan, M.D.**;† Bailey, J.;† Olatunji, S.; Bann, S.J.; Bowen, K.; Ostrovitsa, N.; Da Costa, T.M.; Ballantine, R.D.; Weichart, D.; Stewart, L.J.; Bhardwaj, G.; Levine, P.M.; Geoghegan, J.; Cochrane S.A.; Scanlan, E.M.; Caffrey, M.; D. Baker *De novo* design of cyclic peptide inhibitors of a bacterial membrane lipoprotein peptidase, *manuscript submitted*.

†Denotes equal contributions.

Table of Contents

Chapter 1

Introduction

1.1 Peptide Therapeutics

The early 20th century bore witness to the emergence of peptides as therapeutics changing the outlook of many previously life-threatening or fatal ailments. In 1921, Frederick Banting isolated insulin (**1.1**), a 51 amino acid (AA) peptide, and in 1923 insulin became the first commercially available peptide therapeutic.[1] Insulin therapy revolutionised the treatment of diabetes, a previously fatal disease. Since then, research has uncovered peptide-based therapeutics for a range of applications. Examples include Gramicidin S (**1.3**); a topical antibiotic used for treatment of wounds during the second World War, [2,3] and human growth hormone (HGH) (**1.2**); now used to treat Turner syndrome and muscle wasting diseases,[4] but also subject to abuse by athletes for its anabolic effects[5] (**Figure 1.1**).

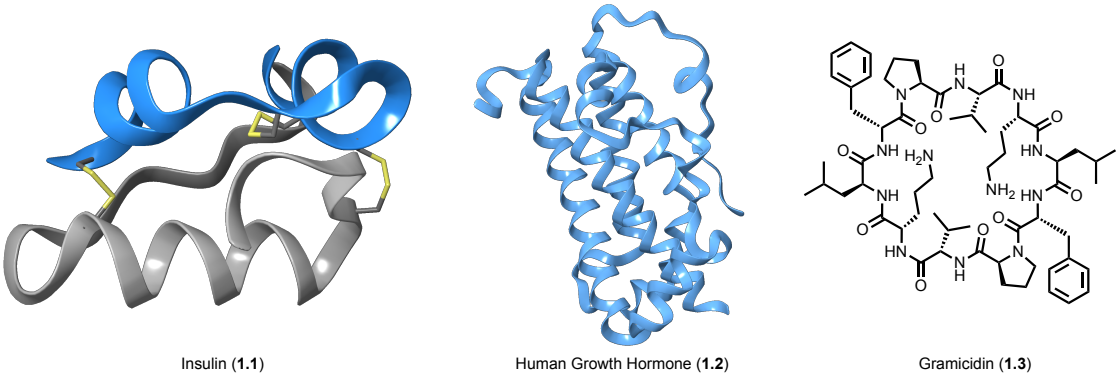

Figure 1.1: Historical examples of therapeutic peptides insulin,[6] HGH[7] and gramicidin.

Given the threat represented by antibiotic resistance, research into peptide antibiotics has become an important theme within peptide science. In particular, peptide natural products have shown significant potential, with multiple types of peptide in either therapeutic use or development. Important examples include the polymyxins including Colistin (**1.4**); a group of cationic cyclic peptides active against Gram-negative bacteria,[8] daptomycin (**1.5**); a cyclic lipopeptide used to treat Gram-positive bacteria including methicillin-resistant *Staphylococcus aureus* (MRSA)[9] and the defensins; a large group of cationic antimicrobial peptides (AMPs) produced by a range of organisms including humans as part of the innate immune system (**Figure 1.2**).[10]

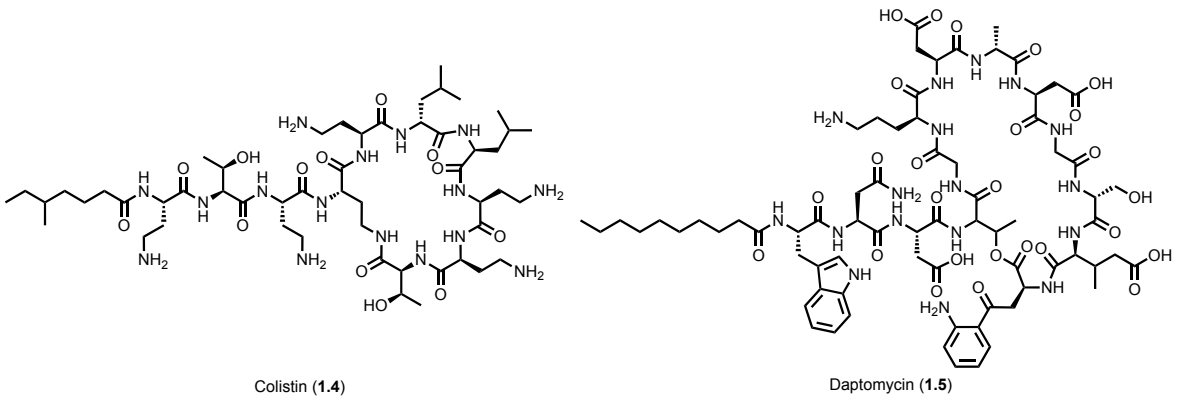

Figure 1.2: Example structures of peptide antibiotics colistin (a polymyxin) and daptomycin.

1.1.2 Therapeutic Properties of Peptides

Peptides have a number of both advantages and disadvantages in their application as therapeutics, though significant research is underway in alleviating disadvantageous properties. From the perspective of adverse effects, peptides are biological molecules found in the human body, and therefore often pose a lower risk of toxicity.[11] Small-molecule binders often require defined binding sites, and thus may only be applied to an estimated 10-15% of the human proteome.[12,13] Peptides however, have shown ability to bind difficult, so-called "undruggable" targets and perturb protein-protein interactions (PPIs) that do not involve a defined binding pocket for targeting with small-molecule inhibitors.[14,15] This has become particularly apparent for cyclic peptides.[16,17] Peptides have come to be appreciated as a privileged class of molecule that occupies an intermediate zone between small-molecule drugs and biologics (**Figure 1.3**). Theoretically, this may facilitate combination of the best characteristics of each class, allowing development of therapeutics that can target a wide range of PPIs whilst also maintaining advantageous drug-like properties.

The disadvantages of peptides as therapeutics are primarily in their bioavailability and a large number of naturally-occurring peptides display poor absorption, distribution, metabolism and excretion (ADME) properties. Such disadvantages are typically observed to be proportional to peptide size. Often, peptides do not conform to the Rule of five (Ro5) and therefore are categorised as 'Beyond rule of five' (bRo5) compounds. Significant hydrogen bonding and polar surface area can hamper membrane permeability and distribution throughout the body. Additionally, some peptides often display low bioavailability. In addition to bRo5 properties, susceptibility to proteases, the body's natural machinery for breaking down naturally-present peptides and proteins, can lead to rapid breakdown of the

therapeutic and removal from the body. A number of approaches have been developed to improve on these properties, including peptide stapling or macrocyclisation and conjugation of functionalities to improve half-life.[18,19] As a result, the therapeutic market for peptides rose to more than $70 billion in 2019.[18] In 2021, 21 of the 200 top selling pharmaceuticals were peptidic compounds, accounting for almost $40 billion in sales despite the COVID pandemic which saw large sales in vaccines and small molecule antivirals.[20]

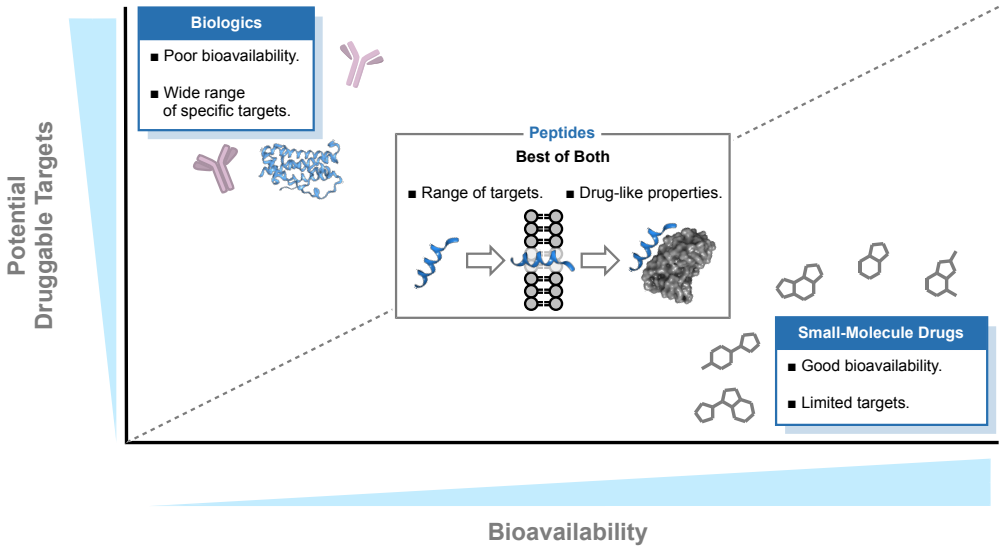

Figure 1.3: Comparison of bioavailability and potential druggable targets for therapeutics of different classes.

Of particular interest and research focus is the use of cyclic peptides, and attempts to develop therapeutic peptides have focused both on development of cyclic analogues of linear peptides and the discovery of therapeutically useful cyclic peptides.[18,21] Cyclic peptides are particularly advantageous for development as drugs for a number of reasons. First, as for linear peptides and proteins, peptide macrocycles possess a large surface area that can provide high affinity, but also high selectivity or specificity. Similarly, they are inherently benign regarding toxicity due to their AA composition.[22] However, cyclic peptides have a number of further advantages over their linear counterparts, arising from their cyclic structure. The conformational restriction provided by cyclisation limits the flexibility of peptide macrocycles, and therefore provides a reduced entropic penalty for binding to the target. This feature can give cyclic peptides enhanced affinities compared to their linear counterparts and is a key principle of peptide stapling. Additionally, peptide cyclisation can afford improved stability to proteases, leading to better half-life.[21] Furthermore, research into cyclic peptides that can passively traverse biological membranes has shown significant

progress.[23] Some such peptides have been shown to be capable of displaying "chameleonic" structures, which switch conformation in a hydrophobic environment to mask polar groups, allowing passive membrane permeability.[24] The cyclosporin natural products display such behaviour,[25] and modern computational methods have even allowed for design of peptides that display such behaviour to embody them with passive membrane permeability.[26]

1.1.3 Peptide Drug Discovery

The goal of discovery of novel peptide-based therapeutics has led to the development of a number of technologies to produce lead compounds for development as pharmaceuticals. Traditionally, peptide leads have often been inspired by natural products or are identified through screening of peptide libraries, while a more modern approach is represented by computational design of peptide binders based on target proteins.

Nature has produced a vast arsenal of peptides for many purposes, from potent toxins to antifreeze peptides to antimicrobials. For this reason, Nature has served as inspiration for a range of peptide-based therapeutics by providing the starting scaffold from which chemists can take inspiration. Natural product or natural-product inspired therapeutics are of vital importance for a range of ailments. Oxytocin, a human cyclic peptide hormone produced in the pituitary gland is important during labour for prevention of excessive bleeding, and has been investigated for treatment of mood disorders.[27] Carbetocin, a synthetic analogue of oxytocin, is used in the clinic to prevent postpartum haemorrhage, particularly following Caesarean section.[28] While this is an example of providing a drug based on a human peptide to fulfil the purpose of that same peptide, natural products from other species have also inspired therapeutic development including as antibiotics and cancer treatments.[29]

Traditional approaches to discovering therapeutically useful natural products have focused on previously isolated compounds or lysates, but has come to be associated with high rediscovery rates of previously identified compounds and compound classes.[30,31] The relatively modern approach of genome mining can identify natural products of interest from organisms that display a favourable relevant characteristic by analysis of the genome. For example, a recent study focused on a *Pseudomonas* strain often found to share a habitat with the amoeba *Dictostelium discoideum*, leading to discovery of a class of antimicrobial nonribosomal lipopeptides therein titled the keanumycins.[32] Genome mining involves identifying or "mining" for biosynthetic gene clusters (BGC) from widely available genetic

data, and then predicting the structures of the secondary metabolites for which they are responsible. This amounts to identifying genes that encode enzymes potentially involved in secondary metabolite biosynthesis, often then comparing them to previously characterised pathways and using this information to predict the product. Often, sequences encoding "reference" enzymes are used to identify homologues. A number of automated genome mining tools exist to comb the available data with more specialised tools available for specific compound types.[33,34] A particular advantage of this approach is the use of an initial *in silico* investigation, thus avoiding library preparation.

Peptide libraries have become an area of wide interest in recent years, and formed part of the Nobel Prize in Chemistry in 2018. Three main methods for peptide library preparation exist; phage display, mRNA display and synthetic libraries. While other library technologies have been developed such as ribosomal or cell-surface display, the field is arguably dominated by the aforementioned methods.[35] The main advantage of phage and mRNA display is the production of huge numbers of peptides for screening. The vast library sizes produced in phage display are often in the region of 10^9 peptides, though up to 10^{12} sequences may be obtained.[36,37] Libraries of 10^9 sequences are most common due to limitation by *in vivo* transformation of *E. Coli*. for propagation. A typical mRNA display library will often contain 10^{12}-10^{14} peptides, mainly depending on the number of positions that are randomised and the number of different monomers included.[38]

In phage display a library of genetic information is inserted into the genomes of bacteriophages for *in vivo* expression. The phage library is exposed to the target so that those encoding a binding sequence can use these to bind. Unbound phages can then be washed away and the target-bound phages recovered. These phage numbers are then amplified by infection of bacterial cells allowing phage reproduction, followed by repeat selection (**Figure 1.4**).[39] Final hit identification is then achieved through sequencing of phages after the desired number of selection rounds.

In mRNA display, a random mRNA library is expressed *in vitro* in the presence of puromycin, which forms a complex in which the mRNA remains bound to the sequence it encodes.[40] This so-called "fusion library" then undergoes selection for the desired property, usually binding affinity, which allows separation of functionally useful sequences. Reverse transcription of these to the complementary DNA, followed by polymerase chain reaction (PCR) amplification then generates more of the functional DNA, which can be expressed as before and then subjected to further rounds of selection (**Figure 1.4**). Final identification of

hits after the desired number of selection rounds can then be performed by DNA sequencing. A key advantage of this method is that it is cell-free and can explore a wide chemical space, including non-natural AAs.

The third library type previously mentioned uses chemical synthesis instead of biological expression to yield peptide libraries, affording both advantages and disadvantages. Production of these libraries are comparatively simple, but often more time consuming and resource-intensive, with each sequence constructed through controlled chemical reactions and in some cases also requiring purification. Advantageously, these libraries can often be obtained in a format such that isolated sequences are used and therefore experimental hit identification negated, i.e. in a "one-well-one-compound" format. However, such libraries are comparatively extremely limited in size, often to the region of 10^5 compounds.[35] This limitation is in part due to differing reactivities of monomers necessitating separate synthesis of sequences instead of pooled combinatorial approaches. However, a significant advantage of this approach is the high degree of control afforded, as well as the ability to incorporate chemistries other than amide bond formation and to use non-natural monomers. Further, combinatorial diversification can incorporate further modifications, greatly enhancing library size and facilitating addition of other binding or otherwise useful moieties.[41] A particularly useful advantage of this approach is the ability to incorporate "anchor" groups with known but weak binding affinity for the target.[42]

Due to the associated advantages and disadvantages of the various peptide discovery approaches, certain methods may be best for specific applications. For example, for a target with no known binder, a large peptide library may be highly useful. On the other hand where a clear environmental constraint exists, genome mining may shed light on useful compounds. Furthermore, where a weak binder is known, smaller targeted synthetic libraries may be useful.

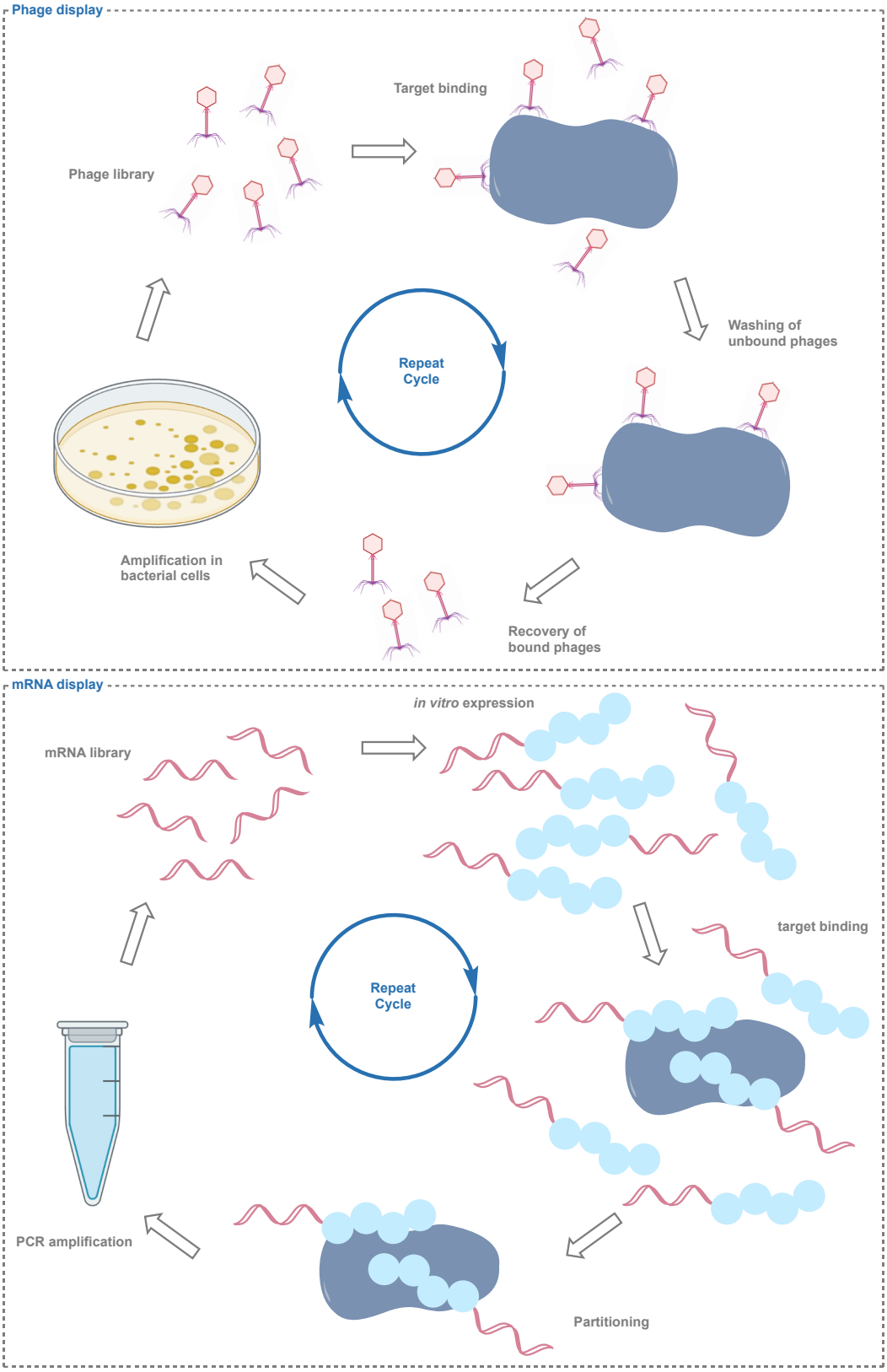

Figure 1.4: Schematics for phage and mRNA display.

1.2 Chemical Peptide and Protein Synthesis

With the advance of peptide and protein therapeutics, methods for their synthesis and modification are of considerable interest. While synthetic methods to access the peptide chain itself are of utmost importance, methodologies for "post-translational" modification of sequences are also vital. Synthetic access to peptides and proteins is achieved through solid phase peptide synthesis (SPPS) and peptide ligation methodologies or combinations thereof. However, each of these have their own limitations. For the modifications of peptides and proteins a large variety of chemistries have been developed to target different amino acids. Of course, a major concern in development of these methodologies is selectivity for the target amino acid as well as tolerance of the range of functional groups found in such biomolecules. To enable efficient access to modified peptides and proteins of interest, a wide variety of chemical methods are required.

1.2.1 Solid Phase Peptide Synthesis

SPPS, reported by Merrifield in 1963, has revolutionised the field of peptide chemistry. Using a functionalised insoluble polymer support, the peptide sequence can be assembled from *C*- to *N*-terminus through successive reactions and filtrations whilst the growing sequence remains bound to the resin. Elongation of the peptide chain is performed by iterative steps of resin-bound amine deprotection and amide bond formation (**Figure 1.5**).

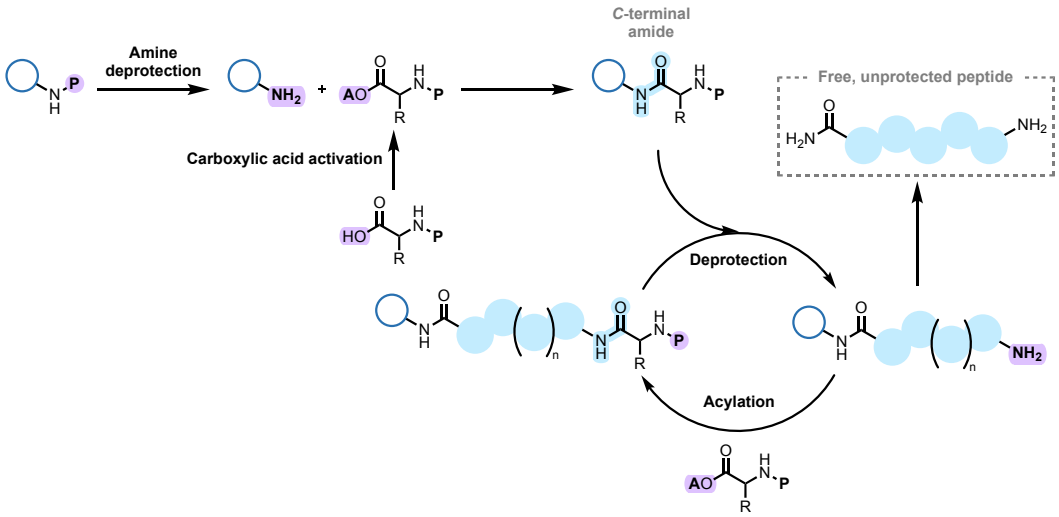

Figure 1.5: Workflow for SPPS. (P = protecting group, A = activating group).

An important advantage of this approach is in allowing facile purification, avoiding tedious recrystallisation or chromatographic purification steps for each intermediate. Instead,

washing and filtration steps remove unbound reactants. A further advantage arising from this facile purification is the ease with which large excesses of reactants can be used, giving complete reactions even for difficult couplings. Large excesses can increase the rate of acylation reactions such that it is common that complete reaction can be achieved in 30 minutes to 1 hour, instead of reaction times of up to 24 hours often applied in solution-phase amide bond formation.[43,44] Additionally, the solid support allows for use of high boiling solvents such as dimethylformamide (DMF) or *N*-methylpyrrolidone (NMP), which circumvents the issue of poor solubility of some sequences or amino acids in more volatile solvents often used in solution-phase chemistry.

The originally reported method utilised the *tert*-butyloxycarbonyl (Boc) amine protecting group, removed by treatment with trifluoroacetic acid (TFA). However, this often necessitates use of dangerous HF to liberate the peptide from the resin at the completion of the synthesis, and cannot be performed in glassware.[45] Introduction of the fluorenylmethoxycarbonyl (Fmoc) protecting group for amine protection allowed use of basic conditions to liberate the amine for successive acylation.[46,47] In turn, peptides are routinely released from acid-labile resins using much more favourable TFA cocktails. For activation of the carboxylic acid a variety of reagents are frequently used, including carbodiimides such as diisopropylcarbodiimide (DIC), hydroxybenzotriazole (HOBt) derivatives such as (2-(1*H*-benzotriazol-1-yl)-1,1,3,3-tetramethyluronium hexafluorophosphate (HBTU) and closely related phosphonium salts such as benzatriazol-1-yl-oxytripyrrolidinophosphonium hexafluorophosphate (PyBOP) which often display improved safety profiles.

1.2.2 Chemical Ligations

A major limitation of SPPS exists in the synthesis of longer sequences, with those above 50 AAs typically giving poor yields or proving inaccessible through such methods. While recent technologies have used an SPPS approach coupled with flow techniques to synthesise large peptides and even proteins, this uses an extreme excess (80-fold equivalents) of reagents and large volumes of solvent and is therefore quite unsustainable for general purposes due to the excessive cost and amount of waste generated.[48] More commonly, ligation approaches are employed in which the *N*- and *C*-termini of two peptide sequences obtained by SPPS or otherwise are chemoselectively reacted to yield the desired peptide or

protein. Native Chemical Ligation (NCL) represents the most important and widely-used technique, reported by Kent and co-workers in 1994.[49] This involves the chemoselective reaction of an *N*-terminal cysteine with a *C*-terminal thioester; first, transthioesterification yields a thioester intermediate, which then undergoes an intramolecular *S*-to-*N* acyl shift to yield the native amide linkage (**Figure 1.6**). While the initial methodology required the presence of a Cys residue in the target peptide or protein, desulfurisation techniques have led to the development of thiol-containing analogues of other naturally occurring amino acids, from which the thiol "scar" can be removed after the ligation step.

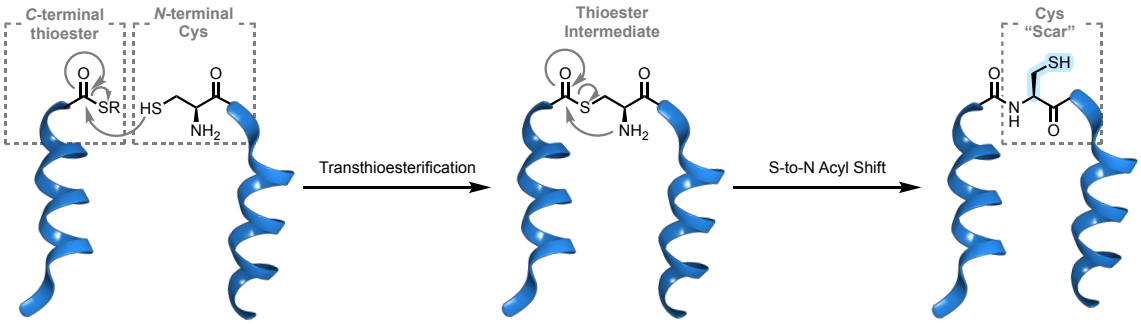

Figure 1.6: Mechanism of Native Chemical Ligation.

While NCL is the most commonly utilised ligation approach, the requirement for the Cys residue and thioester are somewhat limiting. To alleviate the limitation of need for synthetic generation of the thioester component, expressed protein ligation can allow access to recombinantly expressed thioesters. This approach makes use of inteins, self-splicing amino acid sequences that utilise Cys residues to generate the thioester.[50] Through this methodology, synthetic peptides can be ligated onto the *C*-terminal of a recombinant protein. In contrast, ligation of a synthetic peptide onto the *N*-terminal of an expressed protein is more straightforward by recombinant incorporation of the Cys residue. A number of methodologies for generation of the synthetic thioester components through SPPS have been developed.[51]

1.3 Post-Translational Modifications

While only 20 amino acids constitute the diverse range of proteins naturally produced, post-translational modifications (PTMs) vastly increase the diversity of monomers available to the biological machinery of life. These modifications are installed onto an assembled peptide or protein chain, and are not incorporated during main chain biosynthesis. PTMs can have drastic effects on the structure and function of a protein and range from

relatively simple modifications such as methylation of Lys residues, to attachment of whole proteins in ubiquitination. However, despite the seeming simplicity of some PTMs, their installation or removal is a highly important, controlled and regulated process. In biological systems it is not sufficient to simply modify all reactive residues of a certain type, and so specific positions must often be modified by specific enzymes. These PTMs may be either reversible or irreversible,[52] and can occur in various organelles including in the nucleus.[53] Despite the over 400 PTM types known to date, a small subset have attracted the majority of the attention. In fact, phosphorylation, acetylation and ubiquitination comprise more than 90% of the reported PTMs.[54] In order to study the complex phenomena of PTMs, a variety of chemical tools for both selective modification and labelling of PTMs have been developed.[55,56]

In addition to regulating protein function, post-translational processing of smaller peptides can be vital to their function, with many relatively small sequences undergoing significant processing. A particularly prevalent type of PTM often observed for short sequences, particularly those with roles in regulation of biological processes, is peptide cyclisation. In nature, a range of cyclisation types are found, incorporating linkages between side chains, from *N*- to *C*-termini, or between a side chain and one terminus. Cyclic peptides display a number of advantages for achieving their function over their linear counterparts. Firstly, cyclisation of peptide sequences imparts a conformational restriction, therefore reducing the entropic penalty upon binding and improving the affinity for its binding partner, as well as improving selectivity.[21,22] Additionally, cyclisation often leads to improved stability towards proteolysis.[57,58] Recent studies also point towards increased likelihood of passive membrane permeability for cyclic peptides, with some sequences capable of conformational switches depending on the polarity of the environment, allowing them to traverse biological membranes.[26] As a result of the advantages imparted by cyclisation of peptides, sequence macrocyclisation has become an important strategy for improvement of therapeutic characteristics of biologically active peptides. In particular, the advantages of peptide cyclisation have inspired the field of peptide stapling. Through this technique, one starts from a sequence with the desired binding characteristic, often an α-helix. Two residues from the same face of the helix are selected and replaced with residues that can be covalently crosslinked. With careful, often iterative optimisation, the desired conformation can be reinforced.[59]

The group of naturally occurring modified peptides known as ribosomally synthesised and post-translationally modified peptides (RiPPs) comprise a rapidly growing superfamily of natural products observed across the kingdoms of life.[60] These peptides all originate as a gene-encoded precursor, which is read and expressed by the ribosome as a linear chain of AAs. These linear sequences are then modified by a range of enzymes known as RiPP maturation enzymes. The modifications installed on these substrates are seen in great diversity (**Figure 1.7**, compounds **1.6**-**1.8**). While cyclisation is a common modification, the diversity of cyclisation motifs is large, from typical amide backbone cyclisation to thioethers seen in the lanthipeptides, to heterocyclic linkages. These cyclisation modifications can also be highly important for generating complex 3-dimensional peptide folds, such as in lasso peptides or cyclotides, even when the chemical linker itself is relatively simple.[61]

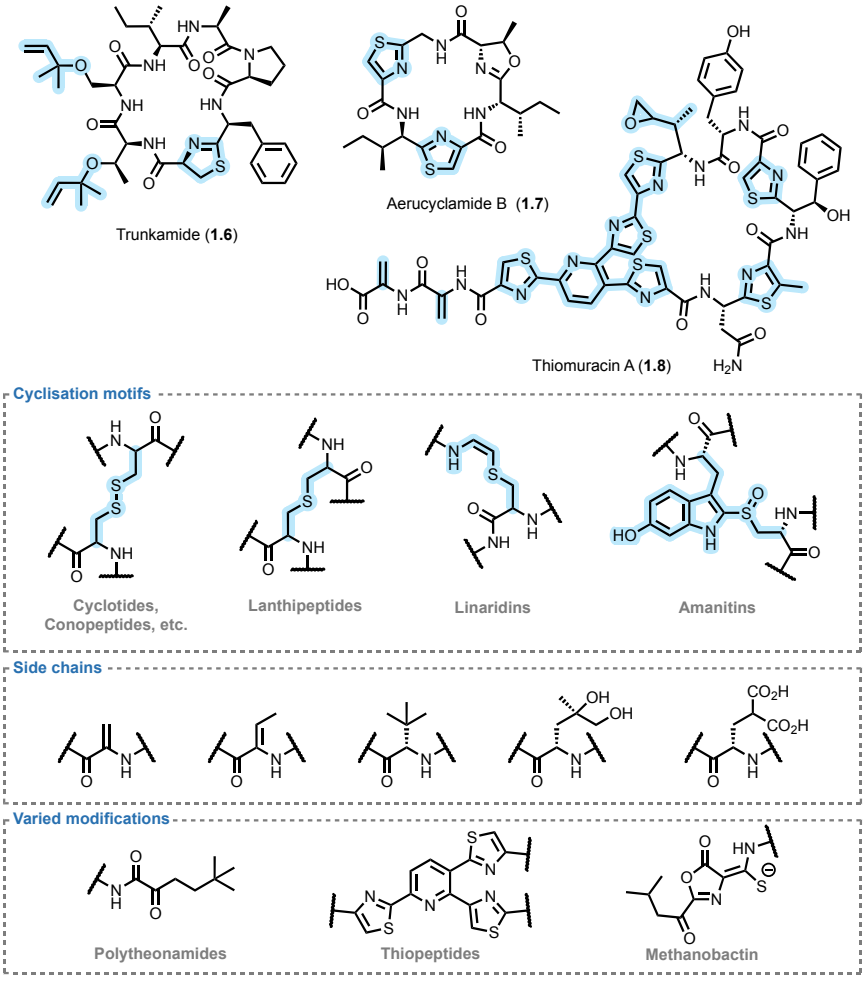

Figure 1.7: Examples of structural diversity observed in RiPPs.[61]

The ability to chemically install PTMs is therefore of high importance for two reasons; to develop diverse, powerful therapeutics, and to understand the function of PTMs in biology. This of course comes with challenges. While nature has made use of complex

enzymes evolved over billions of years, peptide chemists strive to achieve selective modifications through rational design using relatively simple reagents. This has led to the development of residue-specific chemistry, wherein the unique reactivity of a particular AA is harnessed for selective modification. Common targets for such approaches are primarily Cys and Lys, as well as unnatural AAs which may be incorporated in the peptide chain, and current research is constantly expanding methodologies for targeting a range of other AAs.[62]

1.3.1 Cysteine-Selective Chemical Peptide and Protein Modification

Owing in part to the relative low abundance[63] and unique reactivity of the thiol group, Cys is an attractive AA for chemical modification. The ability to selectively react thiols with electrophiles in the presence of other nucleophilic groups such as amines is a result of the lower pKa (approx. 8.2 for Cys compared to 13.0 for the Ser hydroxyl or a pKaH of 10.5 for the Lys amine),[64,65] combined with the "soft" nucleophilic character. This has facilitated the development of Cys-selective electrophiles through careful design and tuning of reactivity (**Figure 1.8**). Additionally, the formation of disulfide bonds is selective for modification of Cys residues,[66] though the disulfide suffers from vulnerability to reductive cleavage. Despite this, disulfide formation has found many applications for Cys modification. A variety of Cys-selective electrophiles have been developed based on alkyl halides, Michael acceptors and even alkynes. More recently developed approaches have used less traditional chemistry, including bromomaleimides,[67] hypervalent iodine reagents,[68–70] and unsaturated phosphonates.[71,72]

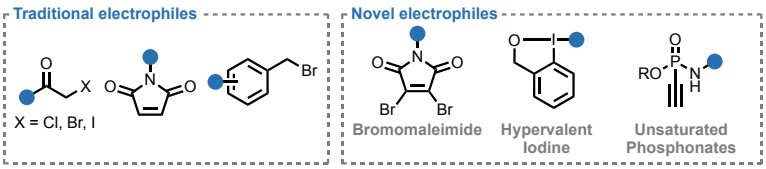

Figure 1.8: Traditional Cys electrophiles and more recently developed functionalities.

A widely applied electrophile group is the haloacetamides or similar compounds containing a halide α to a carbonyl. The addition of thiols to such haloacetamides was originally discovered in the 1930s due to the toxicity of such compounds, which lead to investigation of the reaction of iodo-, bromo- and chloroacetyl reagents with glutathione.[73] One particularly common and important application of such electrophiles is in the cyclisation of peptide libraries through capping of the *N*-terminal with a chloroacetyl group, followed

by intramolecular reaction with a Cys residue. This cyclisation approach is widely applied in the random nonstandard peptides integrated discovery (RaPID) platform for discovery of biologically active peptide macrocycles through mRNA display.[74]

The nucleophilic attack of a thiol at a maleimide, dating back to the 1940s,[75] has since proved particularly useful for modification of proteins such as antibodies. As a result of the success of this reactive handle, variations to facilitate a second thiol addition have also been developed.[67] These incorporate a bromine substituent on the maleimide alkene, which can be lost to regenerate the Michael acceptor system. This can then partake in a second thiol addition. Using these bromomaleimides, up to three groups can be connected; two thiols and one from the nitrogen atom. Furthermore, the linkage can be cleaved by treatment with an excess of external thiol, allowing temporary thiol modification (**Figure 1.9**). Similarly, other Michael acceptors such as vinyl sulfones have been applied for thiol modification.[76]

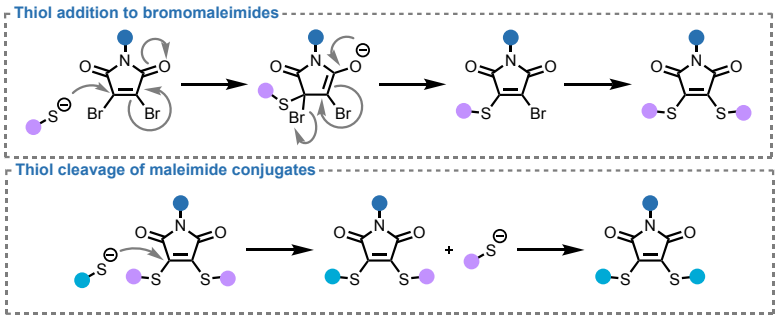

Figure 1.9: Mechanism for reaction of thiols with bromomaleimides showing regeneration of the alkene and thiol-mediated cleavage of linkages formed from bromomaleimides.

Additionally, alkyl halides have been widely applied, in particular for cyclisation of peptide libraries.[77] Aromatic bromomethyl based linkers have shown particular utility in such applications and display highly efficient reaction kinetics and selectivity. However, for most electrophilic modifiers, extended reaction times or excessive electrophilic reagent can lead to modification of other nucleophilic groups, particularly the Lys amines. In fact this amine reactivity itself has also been utilised for peptide cyclisation.[78]

Furthermore, one cannot discuss Cys modifications without also mentioning the use of Cys-reactive warheads in covalent drugs and probes. These predominantly take advantage of the increased nucleophilicity of active-site Cys residues and therefore increased reactivity towards electrophiles such as Michael acceptors or haloacetamides without the need for alkaline conditions. These groups are also synthetically simple to install *via* amide bond formation, also giving a stable linkage. A similar reactive handle less utilised in synthetic

applications for Cys modification are the fumaric acid derivatives often found in covalent inhibitors. A range of other warheads have been developed based on allenamides, propiolonitriles, heteroarenes, terminal alkynes, aromatic substitutions, strain-release reagents, epoxides and more.[79]

The aforementioned approaches to Cys modification share a common theme in targeting nucleophilic residues, and thus often either necessitate alkaline conditions for synthetic applications, or target more nucleophilic active site residues. Recently, however, photochemical methods for modification of peptides or for manipulation of biomolecules *in vivo* have attracted significant attention.

1.3.2 Photochemical Peptide Modification

The ability to use light to drive chemical reactions has opened a new paradigm in organic chemistry, leaving behind the confinements of traditional two-electron nucleophile-electrophile chemistry. Where previously some individual AAs were difficult to target within a sequence using only their capacity to act as nucleophiles, photochemistry unlocks an alternate reactivity with unique reactive intermediates. While many traditional approaches have utilised high energy ultraviolet (UV) light, there is a current shift towards visible light mediated strategies to avoid detrimental side reactions.[80] Additionally, far-red or near-infrared light can allow tissue penetration, while minimising damage to cells.[81]

The use of light to drive chemical reactivity can be achieved by one of two methods; direct excitation of a reactive group or indirect excitation *via* a photoactive additive. Direct excitation is somewhat limited, as the biomolecule itself must be capable of interacting with the light. At the minimum this will require an aromatic or conjugated system, while for lower energy light an extended conjugated system will be required.[80] Indirect formation of reactive intermediates using light can occur *via* one of three methods; hydrogen atom transfer (HAT) in which an initiator radical is formed and abstracts from the substrate to give the reactive intermediate, single electron transfer (SET) from a photocatalyst to a substrate (i.e. photoredox), or sensitisation by energy transfer from a photocatalyst to the substrate. Schematics for these processes are presented in **Figure 1.10**. Unlike the latter methods, use of a radical-generating initiator may not be catalytic as the initiator itself may breakdown to form the radical and is therefore not reobtained at the end of the reaction, though this is not always the case.[82] A particular advantage of these photochemical approaches is that the exact

catalyst or additive structure may be tailored to match the desired substrate in terms of potential for radical abstraction, redox potential or excited-state energy levels. In particular, this can allow targeting of different AA residues or functional groups.

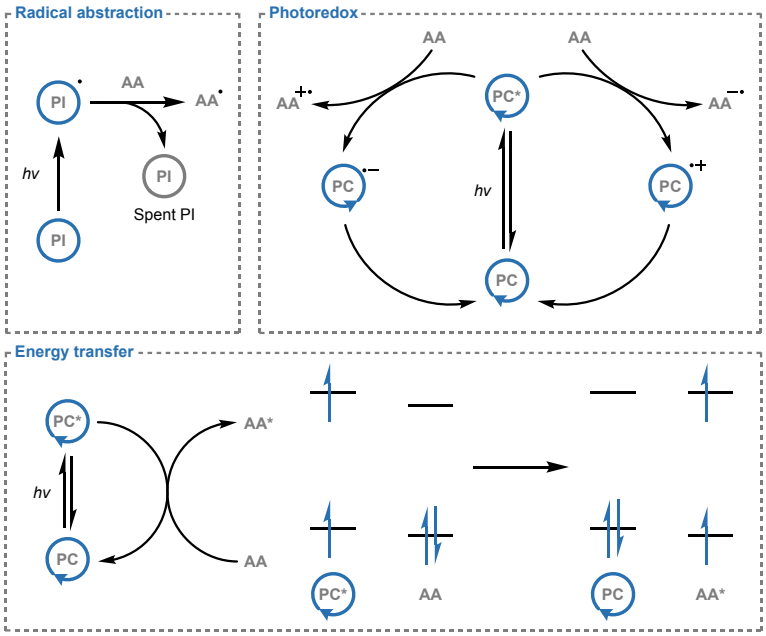

Figure 1.10: Methods for formation of reactive intermediates by photosensitisation. AA = amino acid substrate, PI = photoinitiator, PC = photocatalyst.

In addition to widely targeted Cys residues, photochemical methods have been applied to modification of a range of AAs including Tyr, His, Trp and Met (**Figure 1.11**) using a range of catalysts (**1.9-1.12**). Additionally, modification of *C*-terminal carboxyl groups has also been developed.[80] Visible-light targeting of Tyr residues was developed as early as 1999, with the introduction of Tyr-Tyr photocrosslinking.[83] Since then, tyrosyl radicals have also been applied to Tyr residue modification for conjugation applications.[84] Similarly, His modification has been achieved through SET using thioacetal reaction partners.[85] Trp, the rarest of the 20 naturally-occurring AAs,[86] has also been targeted for photochemical bioconjugation, again using a SET approach.[87] More recently, targeting of Met residues, another low abundance AA, through formation of the α-thio radical *via* HAT has also been developed using an organic flavin-based photocatalyst.[88] Importantly, these methodologies have been able to target less common residues which will be of high utility for generation of homogeneous peptide or protein conjugates.

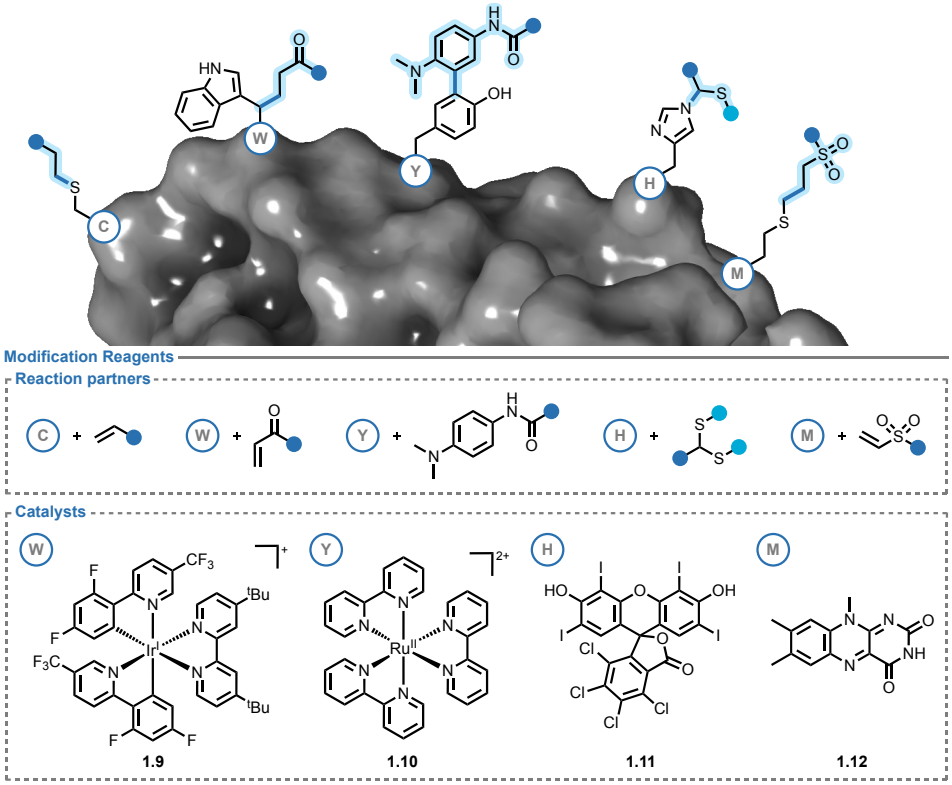

Figure 1.11: Photochemical modifications of naturally-occurring AA residues with the reaction partners and the catalysts for each residue indicated by the single letter code.

1.4 Click Chemistry

Click chemistry was originally conceptualised by Sharpless in referring to "a set of powerful, highly reliable, and selective reactions" that can be used to "click" functionalised building blocks together.[89] This concept has had such a profound impact on scientific research across multiple fields that it earned Sharpless his second Nobel Prize in Chemistry "for the development of click chemistry and biorthogonal chemistry" in 2022, shared with Carolyn Bertozzi and Morten Meldal.[90] Sharpless' 2001 paper identified three click chemistry reaction types (**Figure 1.12**); the nucleophilic opening of "spring loaded" rings such as epoxides and aziridines, cycloadditions such as 1,3-dipolar or hetero-Diels-Alder and so-called "protecting group" reactions such as that of diols with aldehydes or ketones.

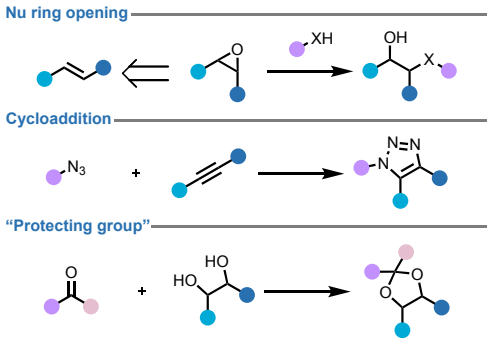

Figure 1.12: The three click chemistry reaction types outlined by Sharpless in 2001.

However, if a single reaction is to be pointed out as synonymous with the concept of click chemistry, it is undoubtedly the 1,3-dipolar cycloaddition of an azide and alkyne, originally referred to as the Huisgen 1,3-dipolar cycloaddition.[91] In 2002, both Sharpless and Meldal independently developed a copper catalysed variation on this venerable reaction, readily affording 1,4-disubstituted triazole conjugates from organic azide and alkyne starting materials.[92,93] This copper-catalysed azide alkyne cycloaddition (CuAAC) has become the reaction of choice for many when the covalent connection of two structural entities is desired without strict linker requirements. This reaction has thus found significant application in organic synthesis, biomolecular ligations, polymer synthesis and even *in vivo* labelling.[94,95]

Carolyn Bertozzi's variation on this reaction in the copper-free strain promoted azide alkyne cycloaddition (SPAAC) is a particularly important development in the field of click chemistry, and has somewhat come to define the concept of biorthogonal chemistry.[96] While CuAAC had previously been used *in vivo*, the toxicity of the catalyst precludes its application where cell viability is of importance. The use of strained alkynes contained within a ring structure provides an alternative means of activation in place of a Cu catalyst, and this system allowed for chemical modification in living cells without observed toxicity. Through metabolic incorporation of synthetically prepared azide-containing carbohydrate monomers in place of the native carbohydrates, treatment of cells or even whole organisms with a probe bearing a strained alkyne allowed labelling of functionalised cells (**Figure 1.13**).[97] This biorthogonal SPAAC approach has since been applied to study of a myriad of systems.

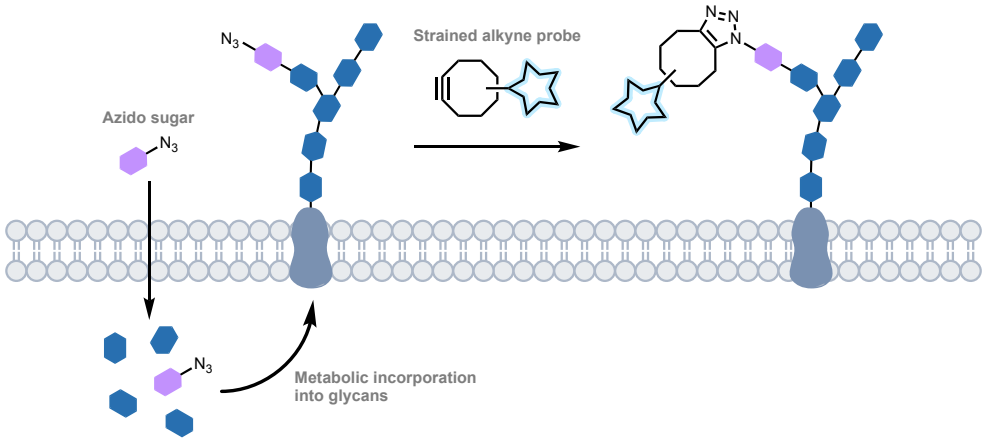

Figure 1.13: Cell-surface glycan labelling using SPAAC.

Despite the many applications thus far, further developments in click chemistry for *in vivo* applications are still sought after, with key problems including intracellular delivery, retention of biological function upon modification of native structures, and utilisation of conditional activation conditions.[98] However, click chemistry has been highly instrumental in improving the accessibility of powerful synthesis, providing tools for many scientists.

1.5 Thiol-Ene Click

The Thiol-Ene Click (TEC) reaction was first reported by Posner in 1905[99] and has since become a highly useful component of the synthetic chemist's toolbox. The TEC reaction amounts to the anti-Markovnikov hydrothiolation of an alkene to give a thioether product. Often, this may be considered in two forms; the addition of a thiyl radical or a thiolate. TEC possesses characteristics of a "Click" reaction, as idealised by Sharpless[89] in his Nobel Prize winning work. The reaction is highly efficient, simply executed and often yields no side products. TEC has brought click chemistry to a wide range of fields beyond the original visions of click chemistry according to Sharpless.[98]

While radical TEC can be initiated through thermal or photoinitiation, the latter is the most common approach.[100] Through utilisation of a variety of photosensitisers or initiators, a range of wavelengths from UV to red irradiation[101] and even ambient light[102] have been utilised for initiation of the TEC reaction. Most of these initiation mechanisms rely on the generation of a radical through homolytic fragmentation of the photoinitiator, which can then abstract a proton (i.e. HAT) from the thiol to generate the thiyl radical. Arguably the most common initiators for organic synthesis are 2,2'-azobis(isobutryonitrile) (AIBN) (**1.13**) and 2,2-dimethoxy-2-phenylacetophenone (DPAP) (**1.15**) (**Figure 1.14**).

AIBN (**1.13**) can be initiated thermally to give **1.14**, often requiring high temperatures (up to 90 ºC)[103] which may preclude some applications. DPAP (**1.15**) on the other hand, is initiated using UV light which causes fragmentation to produce carbon-centred radicals **1.16** and **1.17**. This radical species readily abstracts a proton from a thiol to give the thiyl radical. Recently, the Scanlan lab has also demonstrated initiation of TEC using atmospheric oxygen.[104,105] Throughout this thesis the work will focus on radical TEC, and thus TEC is intended to refer to the radical reaction. TEC has been applied extensively in carbohydrate,[106] polymer,[107] surface[100] and peptide and protein chemistry.[108–110] The exquisite selectivity afforded through the use of thiyl radicals lends useful orthogonality to other two-electron reactive groups such as hydroxyls or amines often found in biomolecules such as carbohydrates and proteins.

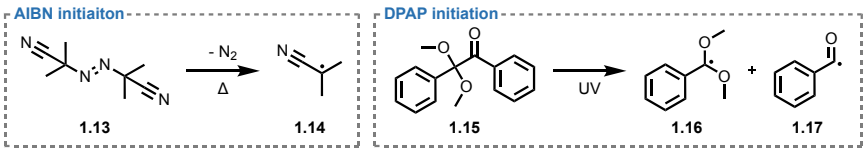

Figure 1.14: Initiation reactions for AIBN and DPAP.

The mechanism of this reaction first involves the formation of the reactive thiyl radical through homolytic cleavage of the S-H bond. This reactive intermediate then attacks the alkene (or alkyne) reactive partner, forming a carbon-centred radical intermediate. Importantly, this step is reversible, and in some systems fragmentation to the thiyl radical and alkene can be observed. This is primarily dictated by carbon-centred radical stability, where highly unstable species may fragment rapidly. Otherwise, the carbon-centred radical can abstract a proton from another thiol, forming the thioether product whilst also generating a new reactive thiyl radical and hence propagating the reaction (**Figure 1.15**). For this reason TEC may be described as a radical chain process.

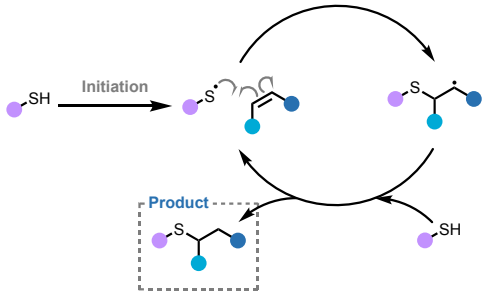

Figure 1.15: Mechanism of radical TEC.

The rate-limiting step for this reaction depends on both the alkene and thiol reaction components. While previously it has been thought that the overall rate was determined by

the alkene structure,[110,111] more recent studies have shown that the thiol is also important as it dictates the rate of propagation, which will vary with thiol reactivity, electrophilicity and radical stability.[112] The key steps for rate determination are the attack of the thiyl radical and the propagation of the reaction *via* thiol proton abstraction by the carbon-centred radical. Where radical attack is significantly slower than propagation, the concentration of alkene is the determining factor. This will occur where the alkene component is less reactive, and is primarily dependent on the alkene electron density and the stability of the carbon-centred radical intermediate.[113] Conversely, when the propagation is limiting, the thiol becomes the rate-limiting reactant. This can occur for thiols with lower propensity to form thiyl radicals.

1.5.1 Acyl-Thiol-Ene and Thiol-Yne

While the previously discussed reaction between a thiol and alkene is arguably the most common and foundational form of TEC, two analogous reactions exist. The acyl-thiol-ene (ATE) reaction refers to the reaction of a thioacid with an alkene partner, while the thiol-yne (TYC) reaction refers to the reaction of a thiol with an alkyne partner (**Figure 1.16**). The combination of both in the acyl-thiol-yne reaction has also been reported.[114]

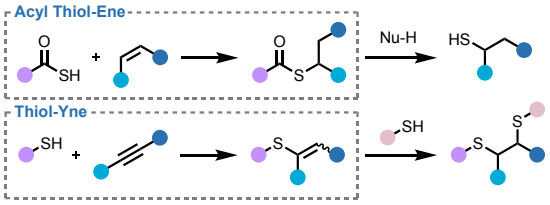

Figure 1.16: Products of ATE and TYC and their utility.

The ATE reaction relies on the generation of a thioacid component, carboxylic acid analogues with greater acidity and nucleophilicity.[115] Similar to thiols, abstraction of the H atom produces a sulfur-centred radical capable of addition to an alkene. The product of this reaction is the thioester, itself a useful synthon. Additionally, thiols may be accessed through ATE followed by thioester hydrolysis in good yields.[116] The thioacid reactants however are highly prone to hydrolysis to the corresponding carboxylic acids, and as a result often must be prepared directly for use from precursors. An example of such a precursor is the trityl thioester, which may be converted to the corresponding thioacid by treatment with TFA in the presence of a cation scavenger.

On the other hand, the TYC reaction generates an unsaturated thioether from a thiol and alkyne. These unsaturated conjugates can then be further functionalised through the

alkene handle, including by a subsequent TEC reaction. In fact, it is often difficult to terminate the reaction after the initial TYC reaction and prevent the TEC addition. Importantly, the *Z*/*E* selectivity of TYC varies, though some examples show favouring of the *Z* isomer.[117,118]

1.6 Thiol-Ene Click in Peptide Chemistry

TEC has found significant application towards modification of peptides and proteins, owing in part to its potential for modifying native Cys residues. The major applications of TEC for such systems may be grouped into peptide stapling, glycosylation or lipidation as well as a number of miscellaneous applications.[108,109] The potential of Cys for formation of thiyl radicals has also been used in development of peptide-based catalysts for synthetic applications.[119–121] In these applications, three UV initiators are prominent; DPAP, VA-044 and irgacure. While VA-044 and irgacure have the added advantage of water solubility, DPAP is the most common initiator used and can be solubilised with small amounts of organic co-solvent.

1.6.1 Peptide Macrocyclisation and Stapling

The stapling of peptide sequences using TEC has incorporated both one-component and two-component approaches, and has additionally been extended to TYC. Interestingly, in these applications a stoichiometric or near stoichiometric amount of initiator is often used, which is not the case in many intermolecular applications. Both solution-phase and solid supported methodologies have been reported. While the solid support approach provides a *pseudo* dilution effect, on-resin cyclisation often gives reduced yields. This is possibly a result of the hampered radical propagation, as the radical species cannot freely diffuse through solution. Notably, these systems do not all require stoichiometric initiator,[122,123] which implies that radical propagation can still occur for resin-bound peptides.

Single-component methodologies refer to those in which the alkene and thiol reactive partners are on the same molecule, and so the overall modification is an intramolecular reaction, though propagation still requires an intermolecular process (**Figure 1.17**). This requires the strategic installation of an alkene moiety within the peptide sequence. Partially due to the previous success in the use of ring-closing metathesis for peptide stapling,[124] a variety of alkene-containing amino acids are commercially available. Additionally,

modification of the Lys side chain amine has been utilised, either *via* use of alloc-protected Lys or a norbonene functionalised Lys.[125] Stapling at simple, otherwise unfunctionalized alkene AA residues has utilised carbon chains of four to six atoms in length bearing a terminal alkene.[126] Hoppmann *et al*. have also established the incorporation of photoswitchable azobenzene AAs with a terminal alkene that are suitable reactive partners for TEC peptide stapling.[122,127] Notably, these aromatic alkenes were found to lead to formation of the sulfoxide linkage, unlike that reported for other approaches. This oxidation is attributed to the proximal aromatic system facilitating a light-induced reaction of the thioether linkage. Both on-resin and solution-phase stapling approaches have been investigated, and neither approach has proved superior. For example, Aimetti *et al.* focused on resin-bound peptides for ease of purification,[125] while Levalley *et al.* reported low yields for solid-supported reactions and focused on solution phase peptide stapling.[128] These one-component stapling applications achieved through TEC have led to a number of staple structures, from simple alkenes to photoswitchable linkers. Further, Levalley *et al*. have reported the cyclisation of azide-containing peptides, which were then functionalised by azide-alkyne cycloaddition.[128] Importantly, this demonstrates highly useful orthogonality of the TEC and CuAAC reactions.

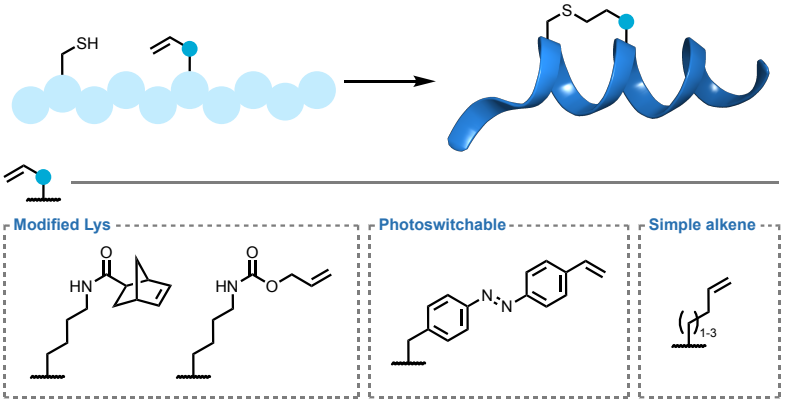

Figure 1.17: One-component peptide stapling *via* TEC.

Two-component methodologies rely on a peptide and an external modifier, resulting in a two-step cyclisation. First, the intermolecular TEC reaction introduces the external staple, which will then react with the second stapling residue in an intramolecular TEC step. An advantage of this approach is that it can be achieved using only native residues *via* stapling of Cys residues using a variety of dienes (**Figure 1.18**). The first report of such a stapling approach was from Wang and Chou, who investigated a range of diene staples including simple aliphatic dienes (**1.18**), PEG derivative **1.19**, and aromatic-containing alkenes (**1.20**-**1.22**).[129] In this study, a TEC stapled peptide was also compared to an example

obtained *via* ring-closing metathesis, showing comparable helicity. Interestingly, while the thiyl radical-initiated 5-*exo*-trig cyclisation of 1,6-dienes to form 5-membered rings is known,[130] such products are not observed. This is possibly due to the second proximal thiol providing a more favourable reaction pathway, further strengthened by the precyclic native peptide conformation which possesses a degree of helicity already. This stapling approach was then extended to aqueous conditions through use of diallylurea staples (**1.23**) and the water soluble initiator VA-044. The same study also extended the methodology to stapling *via* TYC, as well as a tandem TYC-TEC approach.[131] The staples used have also been extended to divinyl diesters **1.24-1.26**, again with good helical properties.[132]

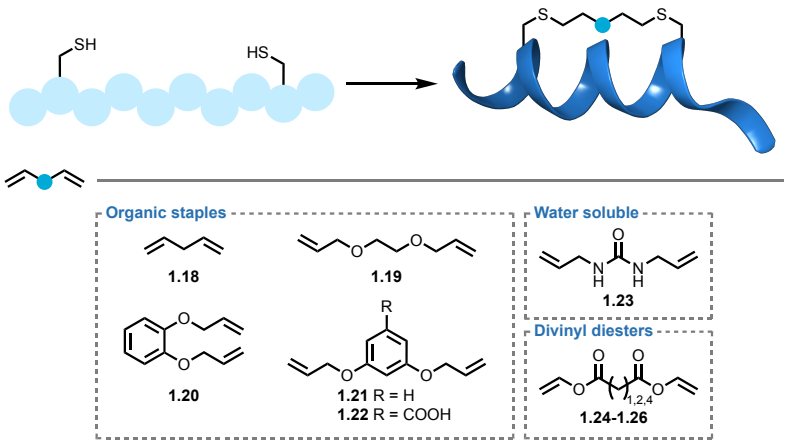

Figure 1.18: Two-component peptide stapling *via* TEC.

However, despite extensive study of peptide stapling using TEC and TYC, application of this chemistry to access peptide macrocycles is poorly developed. These reported methodologies have instead focused on the stabilisation of already helical structures. With the potential of TEC having been established, future development of such TEC macrocyclisation methods to access potential therapeutic leads is of importance.

1.6.2 Glycosylation and Lipidation

It has been estimated that more than 50% of all human proteins are glycosylated,[133] and glycosylation is the most abundant PTM observed on secreted and extracellular membrane associated proteins.[134] *In vivo* protein glycosylation results in a large degree of heterogeneity, whereas chemical methods allow access to homogeneous conjugates. TEC has been applied to synthesis of glycosylated AA monomers for use in SPPS, as well as modification of peptides or proteins in a more "post-translational" approach. TEC chemistry has also been applied to synthesis of thiosugar monomers.[106,135] Approaches towards the

synthesis of peptide or protein glycoconjugates using TEC have used either alkene or thiol containing peptides or proteins with their respective carbohydrate partner.

Initial work in this area by Dondoni *et al.* applied TEC to the synthesis of Fmoc-Cys conjugates through reaction with sugars functionalised with an alkene-containing chain at the anomeric position (**1.27**). This was then extended to glycosylation of glutathione and then a model nonapeptide. Finally, the methodology was applied to modification of native bovine serum albumin (BSA).[136] A "tag-modify" approach to glycosylation of BSA has also been developed by the Davis group, in which homoallylglycine was incorporated in the expressed protein, providing the alkene functionality. This was then reacted with glycosyl thiols (**1.28**) in mild, aqueous conditions using VA-044 initiator. The methodology was then extended to three further model protein systems. Model peptides contained up to 180 alkene residues, all of which were successfully modified (**Figure 1.19**).[137] Use of tandem TYC-TEC has also been used for double glycosylation of alkyne-tagged peptides.[138] Since these reports, TEC has been applied to modification of NCL products,[139] and synthesis of glycoprotein vaccines[140] and heteroglycoclusters.[141] This approach has also been extended to large polysaccharides.[142,143] The prevalence of examples of the use of TEC for glycoconjugate synthesis demonstrates its utility. Notably, this approach can furnish constructs with large numbers of glycosylation sites, single sites, or on the reverse can modify polysaccharides with peptides.

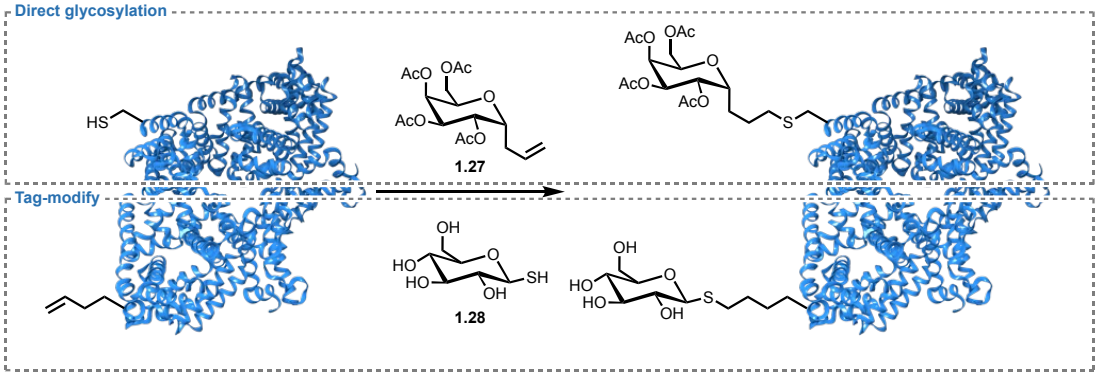

Figure 1.19: TEC-mediated glycosylation of BSA.[144]

As with glycosylation, recombinant approaches to lipidation can lead to significant heterogeneity, and therefore synthetic approaches towards peptide and protein lipidation are of high utility. Lipidation of peptides has been shown to positively impact stability, bioavailability and membrane permeability.[145–147] Further, use of naturally occurring lipopeptides as therapeutics has shown promise for combating microbial infections.[148,149] As

was seen for glycosylation, TEC has been used both to synthesise modified AAs for SPPS as well as for modification of peptide sequences.

While previous methods for the synthesis of alkylated Cys monomers relied on basic conditions and produced low yields, Triola *et al.* demonstrated the high yielding synthesis of lipo-AAs for use in SPPS by TEC reaction of Cys derivatives with lipid alkenes.[103] This lowers the degree of racemisation of the α position compared to previous approaches. However, the most prominent demonstration of peptide lipidation is in the Cysteine Lipidation on a Peptide or Amino Acid (CLipPA) approach developed by the Brimble group. First reported in 2013, this approach uses vinyl esters bearing lipid chains to modify Cys residues.[150] The methodology has since been extensively optimised,[151] and applied to cyclic peptides obtained *via* NCL[152] as well as analogues of antimicrobial peptides.[153,154]

1.6.3 Further Applications

The TEC reaction has been applied to other areas in peptide chemistry, demonstrating its wide utility. Applications from synthesis to probe development have made use of the selective nature of this reaction, with particular focus on biological studies.

The use of TEC for synthesis of either modified AAs or peptide sequences for biological study has garnered significant attention (**Figure 1.20**). Due to the click nature of this reaction, incorporation of a range of functionalities is readily achieved to furnish a range of analogues from a single substrate. TEC was demonstrated as a useful approach to access modified AA monomers by Karmann and Kazmaier. This study focused on the modification of Boc-protected allylglycine (Boc-Agl) to synthesise amino acids with a variety of side chains, from simple aliphatic chains to diamino diacids. Additionally, the approach was extended to short peptides containing an allylglycine (Agl) residue.[155] In a similar vein, the modification of glutathione (GSH) (**1.29**) with a range of alkenes has also been investigated for application in the study of the bacterial GSH-binding protein Kef. While the objective of this study was to build a fluorescent-tagged glutathione analogue, a range of alkenes were investigated, primarily more simple aliphatic or aromatic compounds. Notably, styrene derivatives afforded lower yields, while pinene derivatives **1.30** and **1.31** gave very poor yields. This is hypothesised to be due to either poor propagation by the relatively stable carbon-centred radical intermediates or rearrangement or fragmentation reactions of radical intermediates. A further interesting observation from this study was the necessity for

incorporation of TCEP·HCl to prevent disulfide formation for some more challenging substrates, while significant desulfurisation was not observed.[156] While previous studies have used TEC for synthesis of unnatural AAs either as monomers or within chains, Petracca *et al.* have reported the ATE reaction of dehydroalanine (Dha) with thioacids, yielding Cys thioester derivatives. Further, treatment with base can facilitate the *S*-to-*N* shift of the acyl group for *N*-terminal Dha, furnishing *N*-terminally modified peptides. While this study focused primarily on the nucleophilic thiol-Michael addition, it was also shown that the thioester could be formed using radical conditions.[157] A recent example improving the Green properties of the TEC approach to peptide modification lead to the development of water-soluble blue LED photosensitiser **1.32**, termed Q_{PEG}. The sensitiser itself could be attached to the Cys peptide substrate *via* TEC through incorporation of an alkene group (**1.33**), or it could be used to modify the peptide with a range of biologically relevant alkenes including biotin, azides, drugs and carbohydrates.[82]

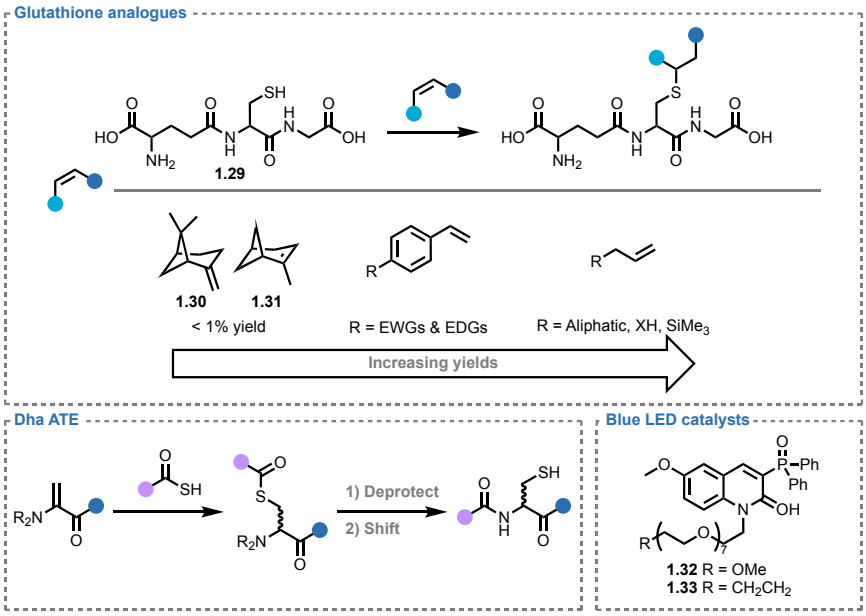

Figure 1.20: Synthetic applications of TEC to access modified peptides and AAs.

TEC has been applied to the study of native PTMs through generation of thioether analogues of the native species. The attachment of a uridine diphosphate modification to peptide chains using TEC has been demonstrated using an alkene-containing uridine diphosphate analogue (**1.34**) for reaction at Cys residues. These conjugates showed inhibition of human β-*N*-acetylglucosamine transferase as was the aim of the study. Further conjugation of uridine diphosphate peptides with cell penetrating peptides yielded cell-penetrant inhibitors.[158] The TEC reaction of Cys-containing peptides with *N*-vinylacetamine **1.35** to

yield analogues of acetylated Lys residues has been applied to study of site-specific protein acetylation (**Figure 1.21**). The modification of ubiquitin and histone proteins was also demonstrated, and biological studies showed the *N*-acetylthialysine residues to be suitable mimetics of native acetylated Lys residues.[159] Access to larger conjugates *via* TEC has also been shown in the synthesis of branched ubiquitin dimers. Incorporation of Cys residues in a ubiquitin monomer as well as terminal modification of the reactant partner with allylamine followed by TEC coupling afforded a homothialysine isopeptide bond linker between monomers. Hydrolytic cleavage of the products using isopeptidases showed comparable activity to native substrates. Similarly, deubiquitinase activity towards trimers produced by this approach showed comparable results to the native constructs.[160]

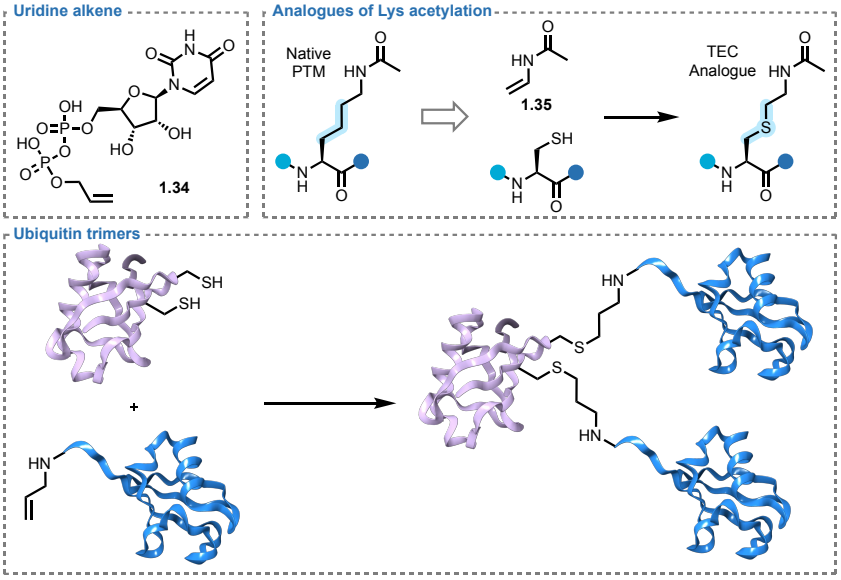

Figure 1.21: Applications of TEC for generation of analogues of native PTMs.[161]

The TEC reaction has also found utility in probe development, both directly and as a capping agent. To study protein phosphorylation, Garber and Carlson aimed to use a thiophosphate analogue which, once incorporated on a protein, could be reacted with suitable electrophile probes. However, these probes would also be reactive towards Cys residues. To prevent these reactions, the authors first capped Cys residues using TEC, in which conditions the incorporated thiophosphates are not reactive. This then allowed selective labelling of the desired PTM (**Figure 1.22**).[162] The TEC reaction has also been applied to development of activity based probes to target deubiquitinase enzymes. Alkene-containing probes were incubated with the corresponding enzymes containing an active site Cys residue. Upon irradiation, covalent labelling could be achieved. Notably, and likely due to close proximity of reactive groups, a short irradiation time of only 1 minute was required.[163] The authors have

since improved on this approach to use eosin Y as the catalyst, allowing covalent labelling using ambient light instead of the previous UV initiation.[102]

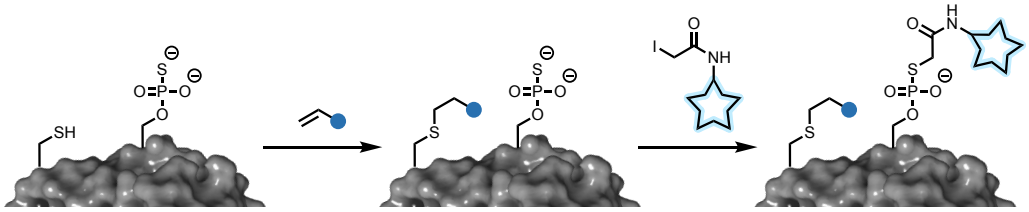

Figure 1.22: Cys capping using TEC to allow study of protein phosphorylation.

1.7 Work Outlined in this Thesis

As discussed in this chapter, TEC has shown significant potential for use in chemoselective modification of complex substrates, including for application to biomolecular systems. However, there are a number of areas which could be developed further through application of TEC where it has not previously been studied.

In **Chapter 2**, the use of TEC for synthesis of a disulfide mimetic of the macrocyclic neuropeptide hormone oxytocin through formation of short side chain linkages is discussed. First, synthesis of the linear alkene-containing precursors is detailed, followed by investigation and optimisation of the cyclisation reaction conditions. In the optimised reaction, analogues with different alkene placement and stereochemistry are investigated. Additionally, this cyclisation methodology is applied to the rapid and efficient synthesis of the clinically approved drug Carbetocin, allowing a protecting-group free cyclisation approach and thus reducing the number of required synthetic steps. The use of this cyclisation approach for smaller macrocycles is then briefly discussed, and the methodology extended to initiation using blue LEDs for such substrates.

Chapter 3 discusses the development of a green bioconjugation platform through the use of TEC chemistry in Deep Eutectic Solvents (DESs), an emerging class of green solvent. Initially, a range of DESs are screened for compatibility with the TEC reaction using a small molecule model reaction. With success in all DESs, the substrate scope for UV-initiated TEC is investigated, incorporating a range of biologically relevant and synthetically useful alkenes and thiols. Additionally, the use of oxygen mediated initiation is investigated and a subset of the original scope reacted using these conditions. Further green chemistry considerations including reaction scale-up and the potential for the presence of peroxides in the reaction

mixture are then discussed. Finally, peptide bioconjugation is investigated. An analogue of the minimal binding motif of human angiotensin-converting enzyme 2 (ACE-2) for the SARS-CoV-2 spike protein containing a Cys residue is synthesised and, through UV-initiated TEC in a water/DES mixture, examples of conjugation with a lipid, carbohydrate and fluorophore are achieved.

In **Chapter 4**, the development of a high-throughput platform for diversification of alkene-containing peptide macrocycles for direct-to-biology applications is discussed. Initially, development of a suitable reactor and investigation into the compatibility of TEC with high-throughput conditions is investigated leading to successful performance in a small molecule model reaction. Next, synthesis of two model peptides is achieved through use of recently developed disulfide-tethered resins, yielding a disulfide and dithioether macrocycle. Test reactions on these substrates revealed a good reaction profile for the dithioether substrate and so the reaction was further optimised and investigated using this material. With optimised conditions in hand, further scope peptides were synthesised. An unexpected oxidation of aromatic thioethers was observed during the reaction, which was prevented through further optimisation to exclude atmospheric air from the reaction and lower the reaction time. A workflow for high-throughput automation of the reaction was then developed and applied to a scope incorporating 12 peptides and 8 thiols for a 96-entry scope presented as a heatmap. Crude reaction mixtures were of high purity, averaging 95% desired product purity, with a large number of the mixtures exhibiting a single peak by LC-MS analysis.

Chapter 5 details progress towards TEC mediated labelling of alkenes metabolically incorporated into glycans on the cell surface, further investigating the potential for use of TEC as a biorthogonal reaction. First, synthesis of a suitable GlucNAc analogue is achieved for metabolic incorporation. Then, the development of a thiol fluorophore with suitable reactivity in TEC conditions is investigated. A range of fluorescent cores are investigated including dansyl, napthalimide and BODIPY groups, showing surprising lack of reactivity. As a result, investigation into a "disulfide-ene" approach and into distancing of fluorescent and thiol groups was conducted with no successful TEC reaction being achieved. Then, simplification of the fluorescent group was performed through synthesis of an aminobenzamide thiol. This compound displayed both fluorescence and successful alkene hydrothiolation of both a model alkene and the GlucNAc alkene synthesised in *in vitro* experiments. However, the excitation wavelength of 320 nm precludes its application for

microscopy. Nevertheless, successful TEC was demonstrated using a fluorescent thiol, and further applied to fluorescent labelling of a modified BSA. Following this, a fluorescein-based thiol more suited to microscopy applications was also synthesised, but again showed no TEC reactivity. Finally, an indirect labelling approach was envisaged, for which a biotin thiol was synthesised which demonstrated excellent reactivity *in vitro*. This probe was applied to an indirect fluorescent labelling of a metabolically incorporated alkene-containing carbohydrate by treating labelled cells with a streptavidin-AF647 conjugate.

Chapter 6 presents a brief final summary of the work discussed in this thesis. And **Chapter 7** contains experimental details and characterisation data for the compounds synthesised over the course of this work.

Chapter 2

Thiol-Ene Mediated Peptide Macrocyclisation

"Radicals don't care about your two-electron problems"
- Prof. Phil Baran on selectivity of radical reactions.

2.1 Introduction

Peptide macrocyclisation is a common approach towards improvement of the therapeutic properties of peptides. As detailed in **Chapter 1**, cyclisation of peptide sequences often results in improved stability and higher binding affinity. Disulfide bonds are found in many naturally-occurring peptides of therapeutic relevance, from larger peptides such as insulin which contains three disulfide linkages, to smaller examples such as oxytocin incorporating a single disulfide. However, disulfide bonds possess inherent instability to reducing conditions, wherein the dithiol is obtained. This makes disulfide-containing peptides poorly suited to therapeutic development. Recently, the replacement of disulfide bonds with suitable mimetics has become a common approach to improving stability of peptides for therapeutic applications.[164]

Oxytocin (**2.1**), a neuropeptide hormone produced in the hypothalamus, has clinical application in inducing labour and treating postpartum bleeding and has also been linked to social behaviour, anxiety and depression.[165] Oxytocin (**2.1**) has a historic place in the development of peptide chemistry, as the first polypeptide hormone to be sequenced[166] and synthesised,[167,168] earning Vincent du Vigneaud the Nobel Prize in Chemistry in 1955.[169] Its structure consists of 9 residues, with cysteines at position one and six linked *via* a disulfide bond. Therefore, oxytocin presents an interesting scaffold for investigation of peptide macrocyclisation for synthesis of disulfide mimetics.

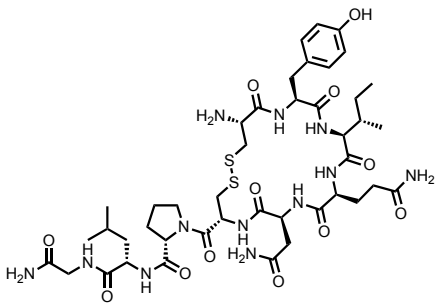

Figure 2.1: Structure of Oxytocin.

Recently, in the context of peptide drug discovery towards novel therapeutics or drug leads, smaller peptides have garnered considerable interest.[22] Such compounds display improved Ro5 properties, of course possessing lower molecular weight, but also fewer hydrogen bond donors and acceptors, and having lower flexibility. However, such peptides can be more challenging to cyclise, possessing ring sizes that are too small to show *pseudo*-intermolecular characteristics in their kinetics, but are too large to readily organise into

conformations that favour cyclisation through proximity of reactive groups. Novel methods for cyclisation of such sequences are of course required to access to diverse compounds for therapeutic discovery.

2.2 Aims

The primary aim of this project was to develop methodology for synthesis of disulfide mimetics using thiol-ene chemistry. The robust thioether linkage afforded through this reaction provides an ideal scaffold for cyclic peptides possessing improved stability compared to disulfide macrocycles, whilst resulting in a minimal structural perturbation.

A second aim of this work was to develop conditions for TEC cyclisation of small peptide chains, particularly using mild blue LED irradiation. This will provide a platform for synthesis of small peptide macrocycles with therapeutic potential.

2.3 Results & Discussion

2.3.1 Synthesis of Linear Peptide Precursors

For our initial investigations we focused on the use of Agl as the alkene-containing residue, as Fmoc-protected Agl is commercially available and is suited to use in standard SPPS conditions. The selected model peptide Oxytocin (**2.1**) contains a disulfide between the Cys residues in the first and sixth positions, and theoretically either residue could be exchanged for the alkene-containing reactive partner to give two analogues. As the model peptide contains a *C*-terminal amide, the sequence was synthesised on Rink Amide (RA) (aminomethyl)polystyrene resin to give the desired amide upon cleavage by treatment with a TFA cocktail. Additionally, this resin was selected due to the mid-level loading of approx. 0.7 mmol/g being suited to the desired scale.

Manual synthesis of the peptide sequences (**Figure 2.2**) was performed by standard Fmoc SPPS, with Fmoc deprotection achieved upon treatment of the resin with 20% (v/v) piperidine in DMF twice, each for ten minutes. Acylation of the deprotected peptide amine was achieved through use of PyBOP coupling agent with *N*-methyl morpholine base. PyBOP (**2.2a**) allows the *in situ* generation of the HOBt anion (**2.2b**), avoiding direct handling of explosive HOBt. Furthermore, PyBOP avoids the formation of the carcinogenic hexamethylphosphoramide (HMPA, **2.2c**, R = Me) side product associated with

benzotriazol-1-yloxytris(dimethylamino)phosphonium hexafluorophosphate (BOP) coupling. Formation of the activated ester of the *N*-protected amino acid in solution can then take place, followed by acylation upon attack by the peptide free amine. Each acylation reaction was qualitatively monitored by bromophenol blue test, wherein a small sample of beads were treated with a solution of bromophenol blue in DCM. Fmoc-protected amino acids were coupled sequentially in nine rounds of coupling and deprotection using a mixture of Fmoc-AA (4 equiv.), PyBOP (4 equiv.) and *N*-methylmorpholine (NMM) (8 equiv.) for the first coupling, so as to ensure efficient and complete coupling to the resin, and Fmoc-AA (3 equiv.), PyBOP (3 equiv.) and NMM (6 equiv.) for all subsequent couplings. For the Asn, Gln and Cys residues, trityl (Trt) side chain protection was utilised, allowing for removal during TFA-mediated cleavage from the solid support. Similarly, protection of the tyrosine (Tyr) hydroxyl group as a *tert*-butyl (tBu) ester allowed deprotection during resin cleavage. In the case of the Cys Trt protection, on-resin removal can also be achieved by treatment with 5% TFA solution. In these syntheses it was assumed that the first coupling to the resin was quantitative and all equivalents were calculated based on resin loading. However, should it be desired, quantification of resin loading may be achieved through deprotection of the Fmoc of the coupled AA, followed by determination of the concentration of cleaved Fmoc.[170]

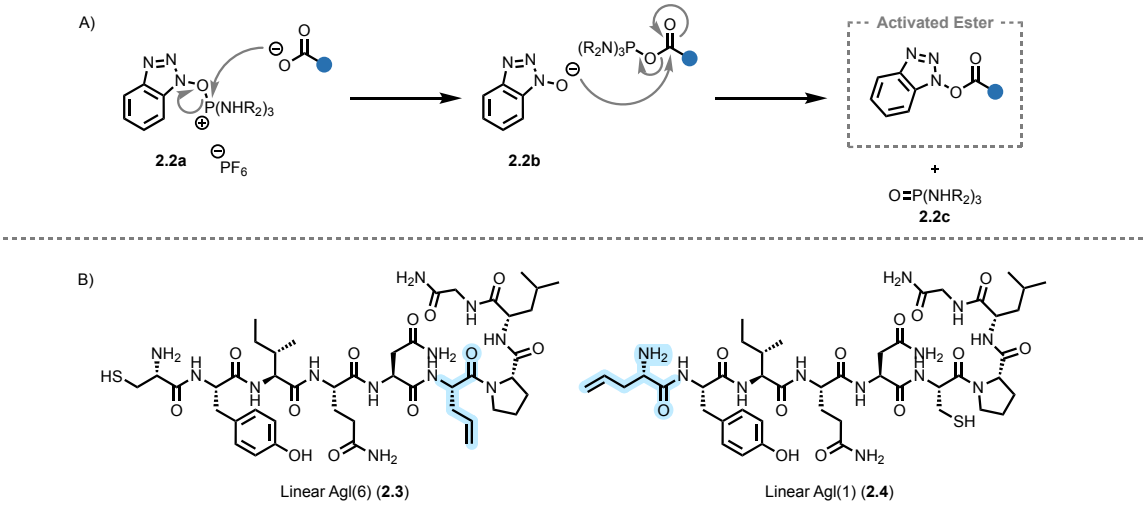

Figure 2.2: A) Mechanism of amide formation using benzotriazole phosphonium coupling reagents. B) Structures of linear peptides prepared for initial investigation.

For characterisation of linear precursors, peptides were universally deprotected and cleaved from the resins upon treatment with TFA cleavage cocktail. Due to the presence of the Cys residue, it was necessary to incorporate an additional scavenger in the deprotection cocktail. The free thiol of a deprotected Cys is known to scavenge carbocations, as are

generated during TFA removal of Boc, tBu and Trt protecting groups. While scavenging of Trt cations would still allow production of the thiol following a second deprotection, the tBu cation is not as easily removed and leads to *S*-alkylated by-products. Incorporation of ethanedithiol (EDT) in the cleavage cocktail provides a thiol-based scavenger, suppressing side-reactions at Cys. Additionally, EDT can help to maintain the thiols in their reduced sulfhydryl state, preventing formation of disulfide dimers. Thus, a cleavage cocktail consisting of TFA, triethylsilane (TES), H_2O and EDT in a 94:1:2.5:2.5 ratio was used for release of the peptide from the resin along with removal of side chain protecting groups.

SPPS furnished the linear peptides **2.3** and **2.4** in good purity, allowing purification through reverse-phase flash chromatography. Peptides were purified on C_{18} stationary phase using a gradient of 0-100% acetonitrile (MeCN) in H_2O and lyophilised to a white powder.

2.3.2 Initial Investigation of the Macrocyclisation Reaction[a]

Initially, we investigated the on-resin cyclisation of the peptides prepared. Selective removal of the Cys Trt group was achieved by treatment with 5% TFA in DCM and confirmed qualitatively using the Ellmann test. The resin was then suspended in DMF with catalytic DPAP and MAP, and irradiated at 365 nm for 1 hour. Following this, peptides were cleaved from the resin for analysis, exclusively revealing the acyclic product. Further attempts using larger equivalents of initiator and sensitiser as well as longer reaction times gave no improvement. It is likely that the lack of reaction was due to poor propagation of the reaction as the thiol is resin-bound and cannot freely diffuse through solution. Since TEC is a radical chain reaction, this drastically inhibits or prevents the reaction. Additionally, the presence of neighbouring protecting groups may cause steric hindrance or effect organisation of the peptide into a conformation suitable for cyclisation.

Following from these results, alkene-containing peptides were cleaved from the resin. Peptides were dissolved in deuterated ammonium acetate buffer for ease of reaction monitoring by ^{1}H NMR spectroscopy. DPAP (1 equiv.) and MAP (1 equiv.) were added and the mixture was irradiated for 1 hour at 365 nm. In these conditions, partial conversion (c. 50%) of the Agl(6) analogue (**2.2**) and no conversion of the Agl(1) analogue (**2.3**) to the macrocyclic product (**2.5** or **2.6** respectively) was observed.

[a]Initial investigation of reaction solvent was performed by Dr. Rita Petracca.

Table 2.1: Solvent systems investigated for peptide macrocyclisation.

Solvent System	Initiator	Solubility
D_2O/NH_4OCOCH_3	-	Suspension
D_2O/NH_4OCOCH_3	DPAP + MAP	Suspension
THF	-	Suspension
MeOH	DPAP + MAP	Solution after sonication
MeCN/H_2O (2:1) + 0.1% TFA	**DPAP + MAP**	**Solution**

Given that some conversion of the Agl(6) analogue had been achieved, optimisation of the solvent system used for this substrate was undertaken. Use of tetrahydrofuran (THF) and methanol gave similar results. In these cases, incomplete solvation of the peptide and/or additives was observed. It was hypothesised that this was what led to poor conversion. Fortunately, upon switching to a H_2O/MeCN solvent system with 0.1% TFA, the cyclic analogue of the Agl(6) peptide (**2.5**) was obtained in high conversion of 91% (**Figure 2.3**). The solvent systems used are summarised in **Table 2.1**.

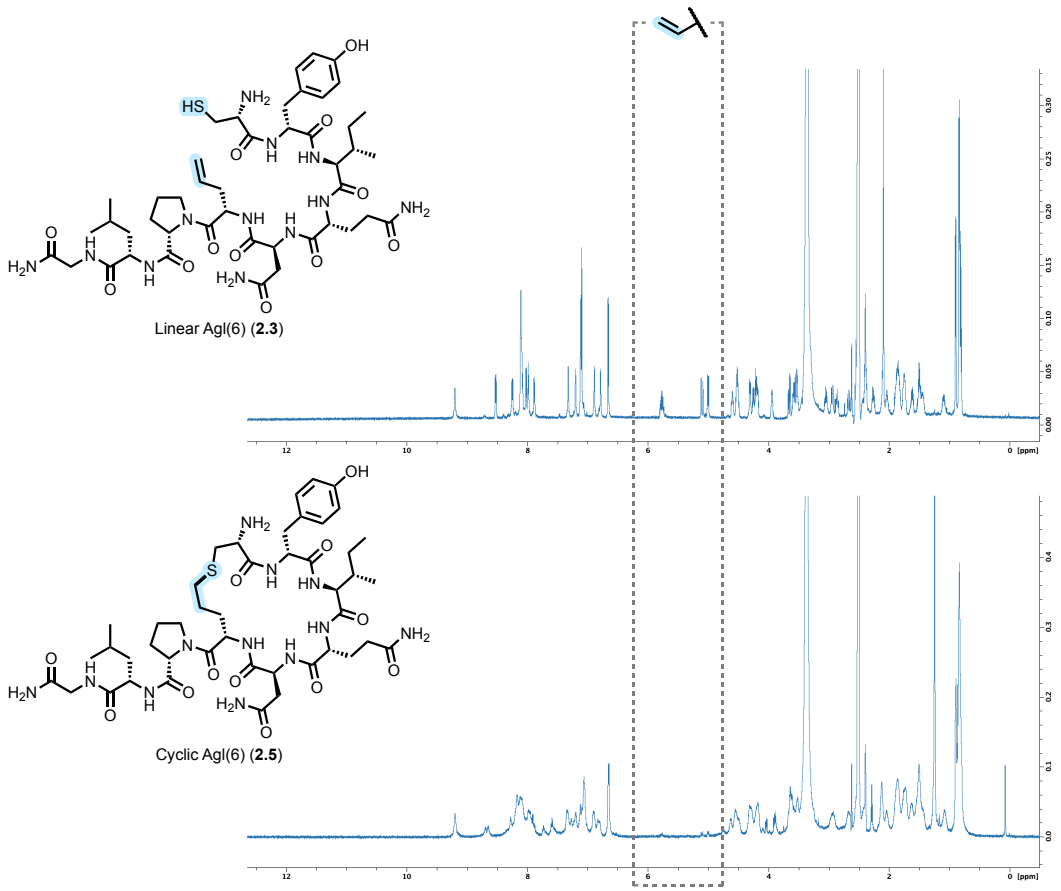

Figure 2.3: ^{1}H NMR spectra for the linear Agl(6) alkene-containing peptide and the corresponding cyclic product in DMSO-d_6.

Additionally, in this reaction dilute conditions of 7 mM (~20 mg in 3.0 mL) were used to minimise formation of intermolecular products. However, unlike typical cyclisation methodologies that rely on a nucleophilic attack type reaction, propagation of the thiol-ene chain reaction requires interaction of the *C*-centred radical intermediate with another thiol. Therefore, excessively dilute conditions could hamper the progression of this process. It is in part for this reason that a full molar equivalent of DPAP was used, as this would make reaction completion less reliant on efficient propagation of the radical chain process.

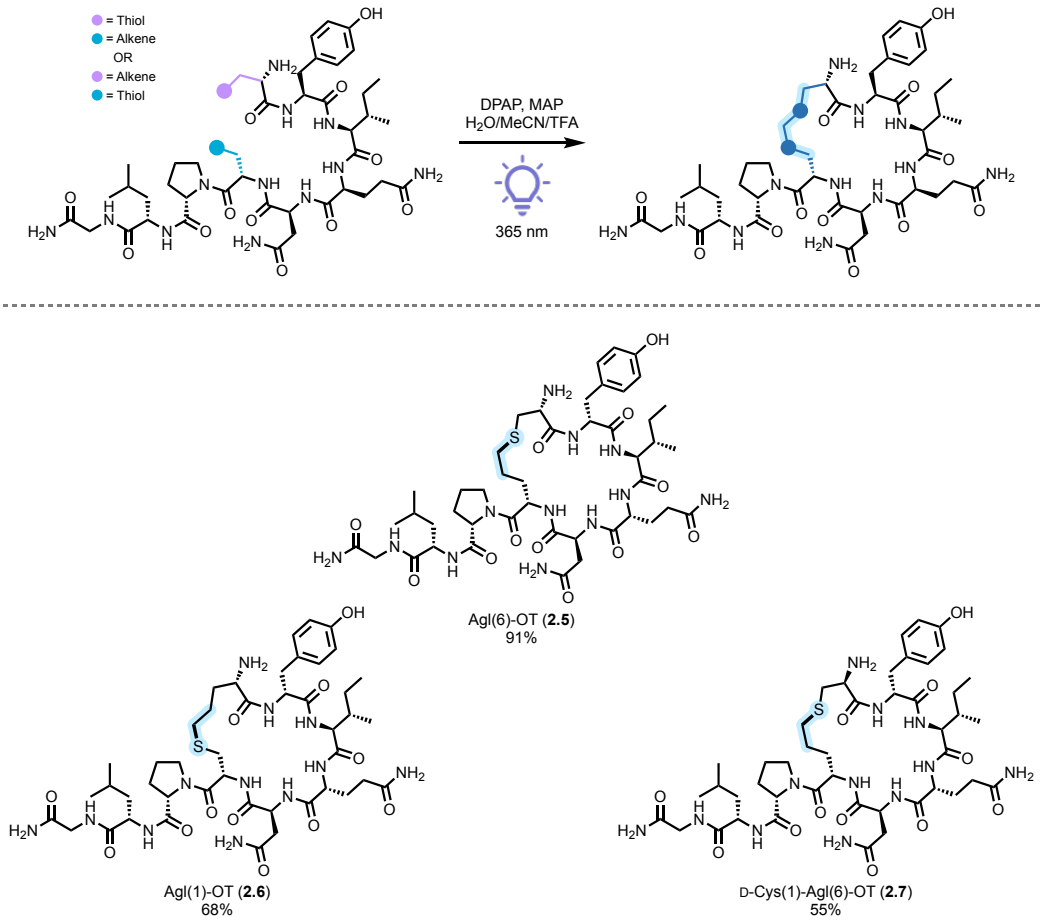

Figure 2.4: Structures of analogues examined in the cyclisation methodology.

Application of these conditions to Agl(1) analogue **2.4** also furnished the cyclic product **2.6**, albeit at lower conversion of 68% (**Figure 2.4**). Previously, it has been suggested that use of internal Cys residues in TEC gave lower yields, however, these reports involved intermolecular reactions. This result indicates that the accessibility of the thiol is of key importance, although it is also possible that the peptide conformation plays a key role. To investigate the latter aspect, an additional linear Agl(6) analogue bearing a D-Cys residue in the first position was synthesised and subjected to the cyclisation conditions. The use of a residue with D stereochemistry may allow the peptide to better fold back on itself into a

precyclic conformation instead of adopting the largely linear conformation. However, to our surprise, use of D-Cys in the peptide chain gave a lower yield of **2.7** at 55%, lower than either the Agl(6) or Agl(1) substrates **2.3** or **2.4**. This suggests that preorganisation of the peptide chain may be of greater importance or influence on the reaction outcome.

2.3.3 Native Ring Size Analogues

With conditions conducive to TEC macrocyclisation in hand, we turned attention to the synthesis of analogues of the same macrocycle size as the native disulfide, which have a 4 atom backbone-backbone linker compared to the 5 atom linker generated in the analogues synthesised (**Figure 2.4**). While longer connections have previously been shown to serve as suitable disulfide mimetics, it is desirable to investigate the shorter connection. However, this is not a trivial step due to the requirement for the shorter dehydro-AA vinylglycine (Vgl). Vgl is not widely commercially available (> €500/g for the HCl salt **2.11**) and is sensitive to basic conditions such as in Fmoc deprotection or standard SPPS coupling conditions. In the Scanlan lab, Vgl was observed to undergo racemisation and isomerisation to the internal alkene in basic conditions, and thus could not be incorporated by standard conditions and must use different *N*-protection. Due to these limitations, it is most convenient to install the Vgl residue on the *N*-terminal position, avoiding further on-resin manipulation. Boc-protection of the amine allows for deprotection to occur during TFA mediated cleavage from the resin and thus avoids basic conditions.

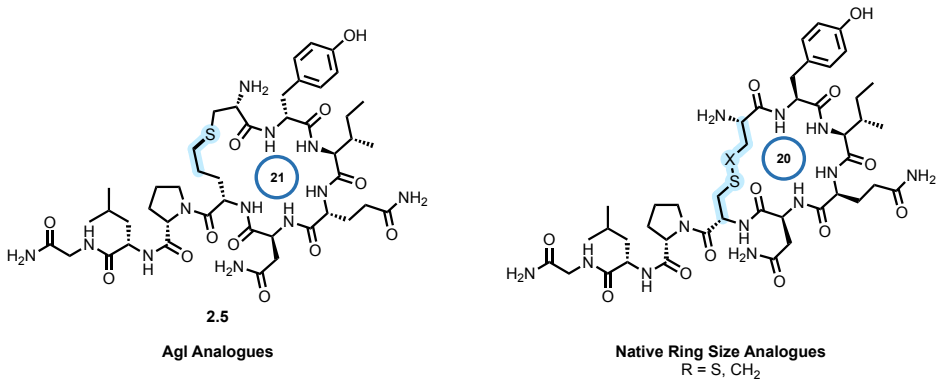

Figure 2.5: Comparison of ring size of allylglycine analogues and analogues with the native ring size.

Synthesis of Boc-Vgl-OH (**2.12**) was achieved from the widely available Cbz-Met-OMe **2.7** (< €5/g) starting material (**Scheme 2.1**). This synthesis is based on the original reported by Rapoport and co-workers in 1980[171] and has been previously optimised within

the Scanlan group.[172] In the first step, the thioether of the Cbz-Met-OMe (**2.7**) starting material is oxidised to the sulfoxide (**2.9**) using sodium periodate. The reaction proceeds in near quantitative yield and with good purity, not requiring chromatographic purification. The elimination reaction to yield the alkene (**2.10a**) is then effected *via* heating to reflux in xylene for 72 h. This step also yields internal *Z* and *E* alkene side products (**2.10b**) which are responsible for the low yield. The desired terminal alkene represents the kinetic Hofmann product, where the internal alkene is the thermodynamic Zaitsev product. In the high temperatures and long reaction times required for the reaction, significant formation of the thermodynamic product occurs. Use of flow chemistry approaches to avoid formation of such thermodynamic products has been reported, but necessitates specialised equipment. Use of Kugelrohr apparatus may also help to reduce the extent of formation of the Zaitsev product. However, sufficient material to proceed was obtained. As such, removal of the Cbz and methyl ester protections could be achieved through heating to reflux in 6 M HCl for 1.5 h to give the Vgl HCl salt **2.11**. It was then necessary to install an amine protecting group that could be removed without base, and thus Boc anhydride was used to give the final Boc-Vgl product **2.12** in overall 10% yield.

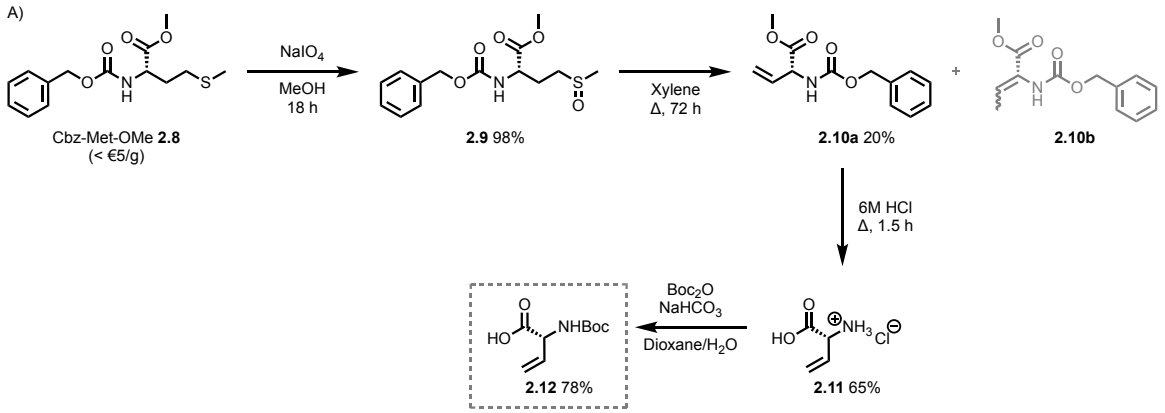

Scheme 2.1: A) Synthesis of *N*-Boc-L-Vinylglycine.

With the desired alkene-containing AA in hand, synthesis of the corresponding linear peptide macrocyclisation substrate was undertaken. As described previously, the first eight AAs were coupled using PyBOP and NMM. A base-free coupling strategy was then undertaken for acylation using the Vgl derivative prepared. 2-Isobutoxy-1-isobutoxycarbonyl-1,2-dihydroquinoline (IIDQ) was employed as the coupling reagent with no base additive.[173] Following deprotection of the Tyr amine, the resin was dried and re-swelled in THF, followed by acylation of the amine *via* treatment with a solution of Boc-Vgl (**2.10**) and IIDQ (**2.11**) in THF for 120 h, after which the coupling was qualitatively checked

using the bromophenol test. Following successful coupling, the resin was again washed and dried. TFA mediated cleavage and deprotection as before then afforded the crude linear peptide **2.13**, which was purified by reverse-phase flash chromatography as for the previous analogues.

Upon subjecting linear Vgl(1) precursor **2.14** to the optimised cyclisation conditions, no cyclisation to **2.16** was observed (**Figure 2.5**). Efforts to force the reaction using longer reaction time or higher equivalents of DPAP and MAP proved ineffective. To investigate the cause of this lack of reactivity, the experiments were performed using external thiol coupling partners, which could be used in larger excess. First, the Vgl(1) peptide **2.14** was irradiated in the presence of five equivalents of benzyl mercaptan with DPAP and MAP, and again no consumption of the alkene was observed. Following from this result, the reaction with thioacetic acid was investigated due to the increased reactivity of thioacids towards alkenes in the acyl ATE reaction, but again no conversion to the desired thioester was observed.

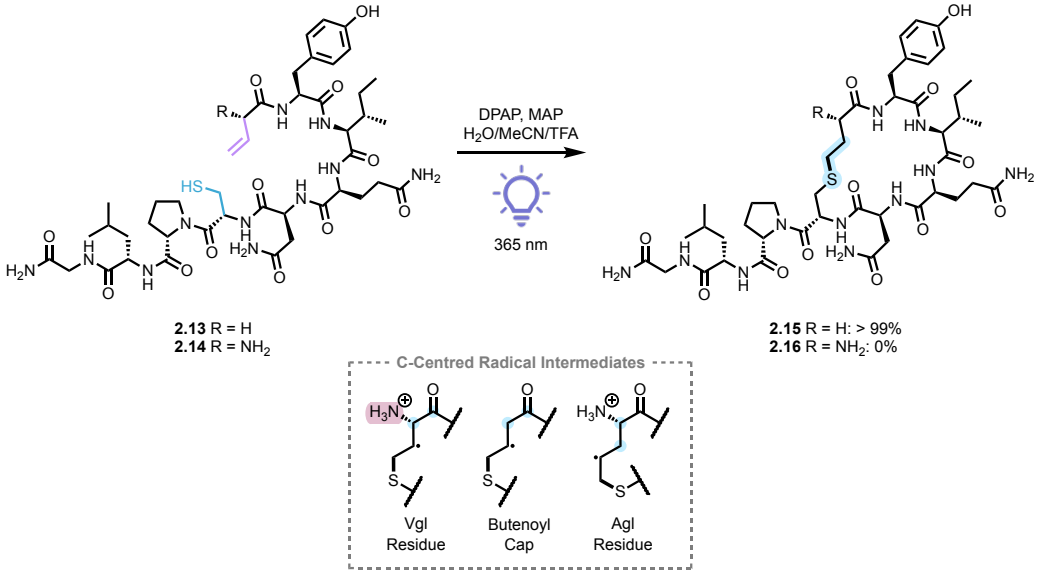

Figure 2.5: Cyclisation to yield analogues of native ring size.

We next turned our attention to the alkene component of the reaction. Previously, the distance between the alkene and *N*-terminal amine had been greater and gave successful reaction and so it was hypothesised that the lack of reactivity was due to the proximal amine. Amine inhibition of TEC has been previously reported.[174] As such, the deamino analogue **2.13** of this Vgl peptide was synthesised following procedures used for the Agl analogues, with butenoic acid (vinylacetic acid, VAA) coupled in place of the Vgl residue (**Figure 2.5**). Interestingly, this substrate **2.13** gave quantitative conversion to **2.15** in the previously used conditions, indicating that the amine was indeed the factor preventing reaction. Previous

studies have shown that in systems such as the *C*-centred radical intermediate generated in TEC, orbitals located up to two atoms away will contribute to the stability of the radical.[175] In both the deamino and Agl peptide substrates, this involves contribution from orbitals centred on a neutral C atom. However, for the Vgl substrate **2.14**, this intermediate will have a contribution from the basic amine, which is likely protonated in the reaction conditions. This reduces the stability of the radical and increases the likelihood of fragmentation of this radical intermediate to give the thiyl radical and alkene. Combined with the dilute conditions for macrocyclisation which slow overall kinetics, this causes the fragmentation to become the dominant pathway, and thus the starting material is regenerated.

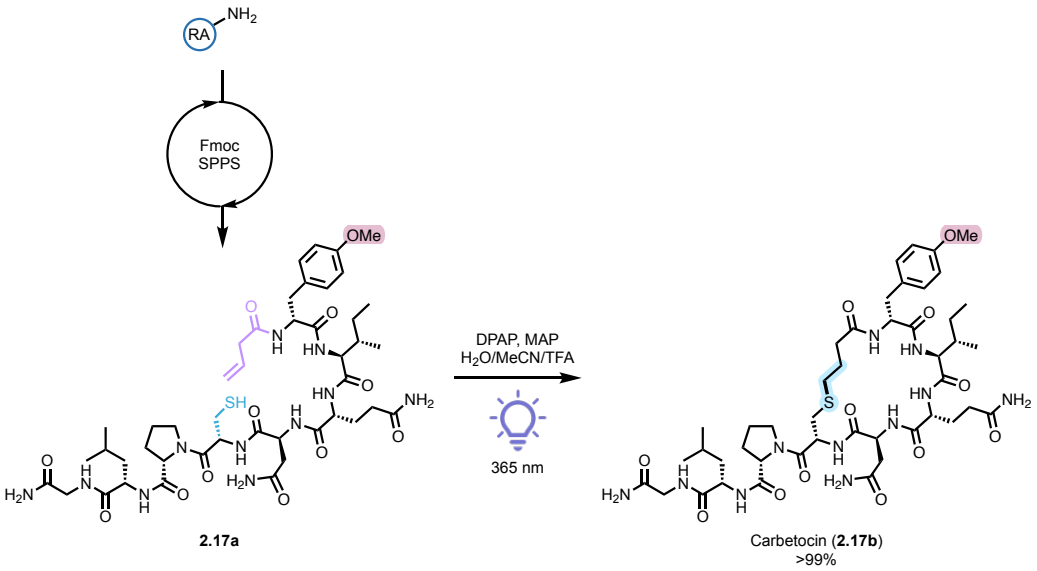

Scheme 2.2: Synthesis of Carbetocin *via* TEC mediated cyclisation of the unprotected peptide precursor.

However, this investigation inspired us to investigate our methodology for application in the synthesis of the clinically-approved therapeutic Carbetocin (**2.17b**) (**Scheme 2.2**), which is used in clinic to treat postpartum bleeding, particularly following Caesarean section. This drug is an Oxytocin analogue, in which the *N*-terminal amine has been removed and the disulfide replaced with a thioether, as well as the Tyr hydroxyl replaced with a methoxy group. Approaches to synthesis of this drug that rely on amide couplings necessitate orthogonal protections and multiple deprotection steps, one of which is selective for the desired reacting groups. We envisioned a more efficient synthesis whereby the unprotected peptide could be cyclised *via* TEC with Cys and an *N*-terminal butenoyl cap. As such, the requisite linear peptide **2.17a** was synthesised on resin as previously described and cleaved, yielding the linear peptide **2.16** in sufficient purity for cyclisation without

chromatographic purification. Cyclisation of this precursor under optimised conditions then gave quantitative formation of **2.17**. This approach provides a highly efficient synthetic route, necessitating only linear synthesis and a single solution-phase step. This is in contrast to aforementioned approaches requiring additional protecting group manipulation.

2.3.4 Attempts Towards On-Resin Macrocyclisation

To further develop applications of this methodology, adaptation for on-resin macrocyclisation is desirable, facilitating simple purification as well as potentially allowing further chain elongation subsequent to cyclisation. In particular, this would be advantageous for Vgl-containing peptides for which the base-sensitivity of Vgl limits its use except for as the *N*-terminal residue due to extensive coupling times. Use of *N*-protected Vgl residues may allow masking of the amine and therefore facilitate successful macrocyclisation, followed by deprotection and then further manipulation either on-resin or in solution. Therefore, on-resin macrocyclisation would allow this methodology to be extended to a larger range of disulfide analogues.

For on-resin macrocyclisation, it is necessary to selectively deprotect the Cys sulfhydryl group without cleavage of the peptide. An additional concern in the case of further chain extension would be deprotection of other nucleophilic side chains which may be protected using Trt groups. The selective deprotection of Cys(Trt) on resin has previously been reported using 3% TFA solutions in DCM along with a cation scavenger. However, the analogous monomethoxytrityl (Mmt) group allows for deprotection in 1% TFA, thus minimising the loss of other Trt protecting groups. This is a result of the ability of the Mmt group to better stabilise the cationic intermediate (**2.18a** vs. **2.18b**) through the oxygen lone pair (**Scheme 2.3**) before quenching to form a neutral species (**2.18c**, **d**). For this reason, synthesis of the resin-bound peptide was undertaken to incorporate Fmoc-Cys(Mmt)-OH.

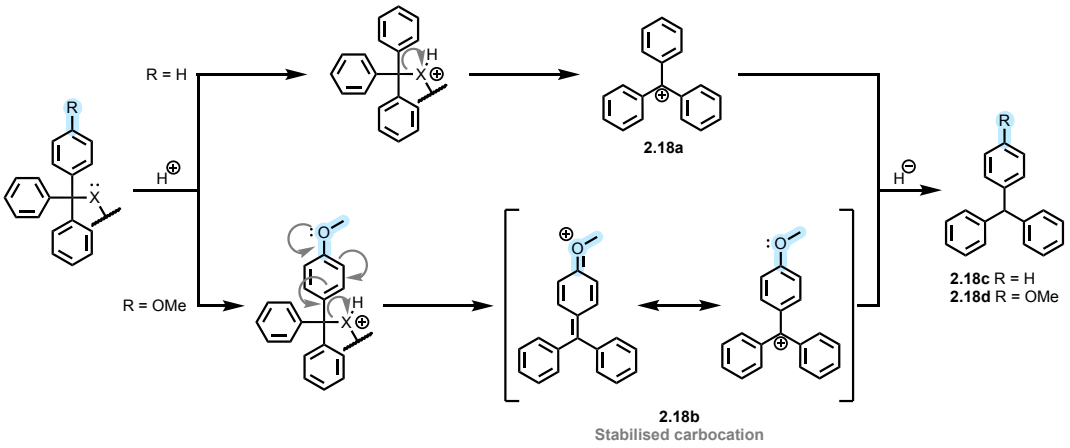

Scheme 2.3: Mechanism for deprotection of Trt and Mmt groups highlighting stability of *C*-centred carbocation intermediates. H^+ denotes use of an acid, while H^- denotes a radical quenching species such as a triorganosilane.

As with previous analogues, the peptide was prepared on resin using standard Fmoc-SPPS with PyBop and NMM coupling mixtures and the Mmt-protected Cys derivative installed in the *N*-terminal position. A sample of the resin was then exposed to a mixture of DCM/EDT/TFA (94:5:1). The resin was subjected to six rounds of 10 minute deprotections, and the solution after each deprotection was examined for UV activity resulting from the cleaved Mmt group. In the first three deprotection cycles a yellow colour characteristic of Trt deprotection was observed, while subsequent mixtures remained colourless. All six solutions were UV-active, possibly due to very small amounts of either Mmt or Trt deprotection occurring. Evaporation of the solvent revealed the majority of the cleaved material in the third mixture. The resin was then subjected to an Ellmann test in which a strong yellow colour was observed, indicating the presence of a free thiol.

The resin was then transferred to a glass flask, rather than the polypropylene SPPS vessel which is not fully UV-permeable or stable to prolonged intense UV irradiation. As a result of the peptide being resin-bound, the use of DMF was convenient, ensuring efficient solvation of the peptide chain and small molecule additives DPAP and MAP. Additional equivalents of both DPAP and MAP were incorporated in the reaction mixture due to the inability of the thiol to freely diffuse through the solution. Further additions of DPAP were performed every ten minutes over the hour-long irradiation. Following the irradiation, the resin was washed thoroughly and the peptide was then cleaved from the resin as the linear peptides were previously. The crude peptide was then subjected to NMR spectroscopic analysis to examine reaction progress, unfortunately revealing no reaction had occurred.

Given the use of an excess of initiator, it is unlikely that the limiting factor is insufficient formation of thiyl radicals. However, chain propagation is required to prevent fragmentation of the *C*-centred radical intermediate which may impact the reaction outcome. Further, it is possible that either of the reactive groups is not accessible for reaction when resin bound. Despite this, previous reports have suggested that on-resin TEC cyclisation is possible (See **Chapter 1**),[108] and research into on-resin TEC is ongoing in the Scanlan lab.

2.3.5 Short-Chain Substrates For Smaller Macrocycles

Having successfully cyclised the 9-mer model peptide oxytocin in solution under UV irradiation, extension of the approach to include smaller peptide macrocycles and also shift towards milder and greener blue LED initiation was investigated. Smaller peptide macrocycles may possess better qualities as lead compounds for pharmaceutical development, as they of course have smaller mass and less hydrogen bond donors and acceptors, but also often display better structural rigidity. This combination of features makes them ideal drug candidates due to their potential for bioavailability and potency.

To investigate the cyclisation of shorter sequences, a simple and flexible 4-mer (**2.19**, **Scheme 2.4**) was synthesised composed of Ser-Gly-Gly-Cys, and *N*-terminally capped with an acrylate group. The Gly residues were incorporated to afford high flexibility, allowing investigation of the potential for cyclisation, while the Ser residue was included to provide a degree of polarity to the substrate. Synthesis of the linear precursors was performed as previously for oxytocin analogues, using Rink amide resin and PyBop/NMM coupling conditions. The acrylate cap was then incorporated similarly, using acrylic acid with PyBop and NMM for activation. The peptides were obtained as a single peak by analytical HPLC following cleavage from the resin under standard conditions previously utilised for oxytocin analogues.

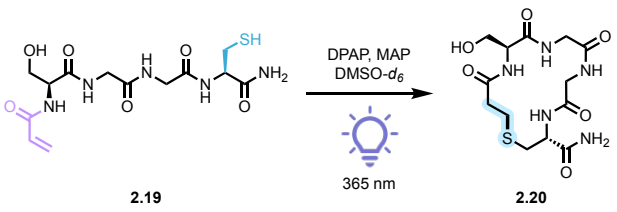

2.19 **2.20**

Scheme 2.4: Test cyclisation of a short tetrameric peptide.

To test the cyclisation of this substrate type, the peptide was dissolved in DMSO-d_6, along with 0.2 equiv. DPAP and MAP, and irradiated for 2 hours. Gratifyingly, this afforded quantitative cyclisation to **2.20** as measured by ^{1}H NMR spectroscopic analysis.

2.3.6 Optimisation of Blue-LED Initiation

While UV initiated conditions had given good results, the use of milder conditions may allow for use of TEC cyclisation in the presence of UV-sensitive groups. Additionally, blue LEDs offer a safer irradiation option. Prolonged exposure to powerful UV irradiation can also lead to side reactions such as dimerisation of Tyr residues, and thus blue LED initiation may facilitate longer irradiation times for reactant combinations with slower kinetics without such side-product formation.

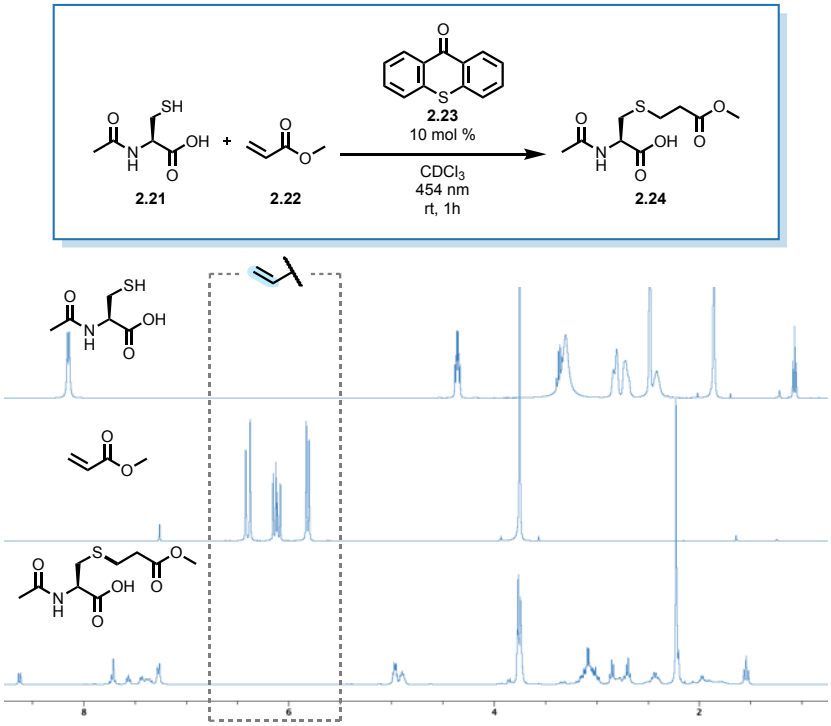

Figure 2.6: Intermolecular test reaction of Ac-Cys-OH (**2.21**) and methyl acrylate (**2.22**) under blue LED conditions.

Prior to investigation of the reaction in an intramolecular context, the simplified model reaction between *N*-acetyl-cysteine (**2.21**) and methyl acrylate (**2.22**) to give **2.24** was investigated (**Figure 2.6**). Alongside blue-LED conditions, the atmospheric oxygen-initiated reaction was also tested for this model reaction. Previously, the Scanlan group has reported an additive-free thiol-ene reaction, in which TEC can be performed by leaving the reaction

vessel open to air and providing heating.[104] However, for the model reaction chosen, no conversion was achieved using these conditions. Application of blue LED initiation to the model reaction, however, showed significant promise. An initial test reaction in $CDCl_3$ with 0.1 equiv. thioxanthene-9-one (**2.23**) as initiator and 1 hour reaction time gave quantitative conversion.

It was then sought to investigate different catalysts for cyclisation of **2.19** to give **2.20**, with the aim to decrease the catalyst loading required for quantitative conversion, likely leading to more facile purification (**Table 2.2**). The initial test in UV conditions was promising, giving quantitative conversion (**entry 1**). Utilising blue LED photocatalyst **2.23** at various concentrations (**entries 2-5**) also gave promising results, though high loading was required for quantitative conversion (**entry 5**). Use of 50 mol% acridine orange (**2.25**) afforded lower conversion of 64% (**entry 6**), compared to 90% achieved for the same loading with **2.23**. Eosin Y (**2.26**), however, when used at 50 mol%, gave 93% conversion (**entry 7**). Changing of the solvent to aqueous phosphate buffer (pH 7) with 10% DMF facilitated quantitative conversion with only 20 mol% Eosin Y (**entry 8**).

Table 2.2: Optimisation of blue LED initiated peptide TEC cyclisation.

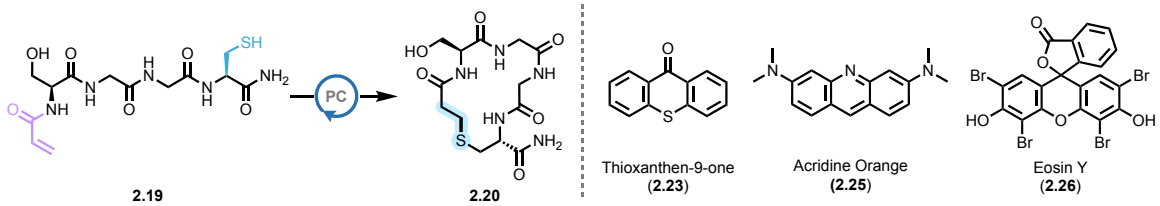

Entry	Initiator	λ (nm)	Loading (mol%)	Solvent	Time (h)	Conversion (^{1}H NMR)
1	DPAP/MAP	365	20	DMSO	2	> 99%
2	**2.23**	454	10	DMSO	1	64%
3	**2.23**	454	20	DMSO	2	72%
4	**2.23**	454	50	DMSO	2	90%
5	**2.23**	454	100	DMSO	2	> 99%
6	**2.25**	454	50	DMSO	2	64%
7	**2.26**	454	50	DMSO	2	93%
8	**2.26**	**454**	**20**	**Aq. buffer/DMF (9:1)**	**2**	**> 99%**

2.4 Conclusions & Future Work

Herein, macrocyclisation methodology for efficient synthesis of disulfide peptide mimetics *via* the photochemical thiol-ene reaction was developed. Linear analogues of the model peptide oxytocin were synthesised, replacing one of the cysteine residues with an allylglycine residue to provide the alkene reaction component. Initial investigations into on-resin cyclisation were unsuccessful, however, solution-phase cyclisation showed potential. Investigation of reaction solvent lead to identification of an acidified H_2O/MeCN mixture as the ideal reaction medium. Using stoichiometric DPAP and MAP as the photoinitiator/photosensitiser pair, UV irradiation lead to good conversions to the desired products.

Attempts towards cyclisation of Vgl-containing linear oxytocin analogues, which would yield products of the native ring size were unfortunately not successful. The incorporation of Vgl on the *N*-terminal leads to the formation of an unstable *C*-centred radical intermediate, for which fragmentation is predominant over abstraction of a proton to quench the radical. Incorporation of Vgl within the peptide chain was not investigated due to the synthetic challenges associated with such a base-sensitive residue. Future work towards cyclisation at Vgl residues should investigate use of protected or otherwise acylated (i.e. non-terminal) residues. This may improve the stability of the *C*-centred radical intermediate and thus allow the reaction to proceed. Use of Boc-SPPS may allow incorporation of Vgl at a non-terminal position, however, the use of hazardous HF would be required. Alternatively, different peptide targets may be amenable to *N*-terminal acetylation which may facilitate the reaction.

Application of the developed methodology to the synthesis of the highly important therapeutic Carbetocin facilitated a highly efficient synthesis of the target cyclic peptide. SPPS was followed by thiol-ene macrocyclisation, which gave quantitative conversion to the desired product. Importantly, this approach limits the requirements for protecting group manipulation in the macrocyclisation step, thereby improving overall atom economy and synthetic efficiency.

Following development of the solution phase macrocyclisation approach, on-resin cyclisation was revisited. The use of Mmt-protected Cys allowed for facile on-resin thiol deprotection, as observed by Ellmann test. Disappointingly, cyclisation was not observed despite use of additional DPAP/MAP or supplementation of the reaction mixture with

additional DPAP/MAP aliquots. A number of factors may be responsible for the lack of reactivity, likely poor accessibility of reactive groups and lack of thiol diffusion through solution leading to poor radical propagation.

The cyclisation of smaller peptides was also investigated to allow cyclisation of these often challenging substrates. Due to improved Ro5 properties owing to smaller size, fewer amide bonds and better rigidity, small cyclic peptides offer attractive scaffolds for drug development. A 5-mer model peptide was synthesised and successfully cyclised using DPAP/MAP and UV irradiation.

Following successful results using UV irradiation, the use of milder initiation conditions was investigated. Initial intermolecular experiments using oxygen-initiation conditions did not provide conversion. However, a quantitative reaction was observed using blue LED initiation. Application of identical conditions to the 5-mer model peptide previously used gave good conversion, and optimisation of the reaction solvent and photocatalyst lead to conditions for quantitative cyclisation using eosin Y in aqueous conditions.

Future work inspired by these results will investigate cyclisation of peptides using the analogous thiol-yne and acyl-thiol-ene reactions. The use of thiol-yne chemistry for cyclisation will furnish macrocycles displaying an alkene, suitable for a second hydrothiolation *via* TEC. This may be used in a one-pot cyclisation-conjugation approach, with potential for synthesis of compound libraries. For this purpose, the cyclisation of short peptides is also of particular importance for improved pharmacological properties. Alternatively, the alkene handle may be exploited for investigation of biological properties of the cyclic peptide, for modification of biomolecules or covalent inhibition of active site Cys residues. Meanwhile, the acyl-thiol-ene reaction will provide a novel route to cyclic thiodepsipeptides. These are an important group of peptide natural products with potential applications as antimicrobials.[176,177] Further, cyclisation *via* acyl-thiol-ene, followed by pH-mediated acyl transfer will allow access to other linkages otherwise reliant on protecting group chemistry for formation.

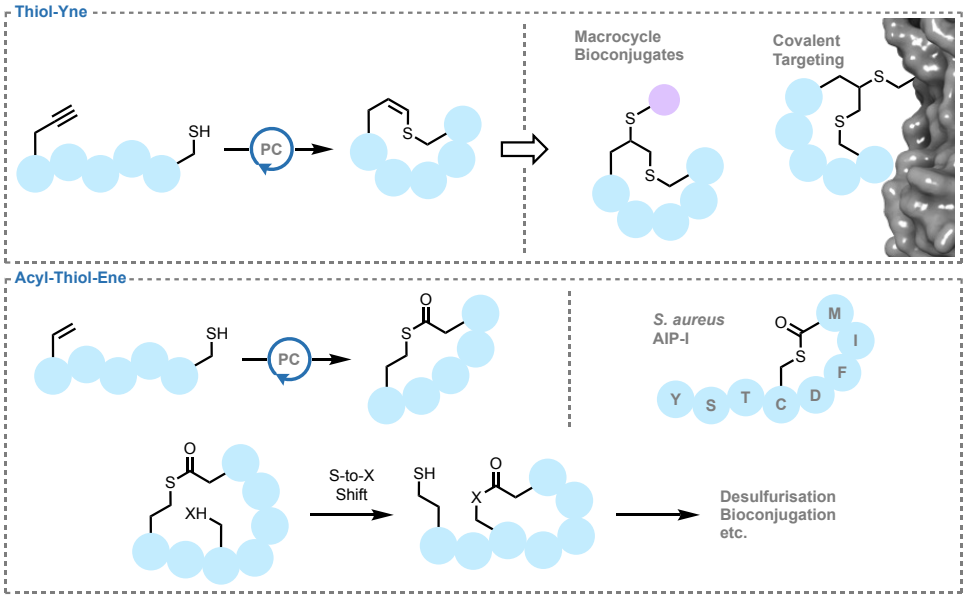

Figure 2.7: Future work on peptide cyclisation using the thiol-yne and acyl-thiol-ene reactions.

Chapter 3

Green Bioconjugation *via* Thiol-Ene Click

"The status quo is somewhere between absurdity or obscenity"
- Prof. Paul Anastas on current practises in chemistry.

3.1 Introduction

The United Nations Sustainable Development Goal 12, responsible consumption and production, aims to improve on existing patterns that contribute to climate change, biodiversity loss and pollution. A primary theme of this particular goal is set around chemicals and waste. As well as the more well-known aim of reducing waste, the management of toxic chemicals was identified as another important aim.[178]

Previously, studies on greening peptide synthesis have focused on chain assembly, whereas side-chain modifications have attracted less attention.[179] In regards to Green Chemistry, traditional bioconjugations fall short in two particular areas; use of harmful solvents such as DMF, and use of large excesses of reactants (>10-fold). In particular, the most critical aspect of a chemical process to consider in regards to waste is the solvent. In the pharmaceutical manufacturing industry, solvents employed amount to 80-90% of the chemicals employed, and it is estimated that < 50% of solvent is reused.[180,181]

In recent years, the use of DESs has attracted significant interest as alternatives to volatile organic solvents for a myriad of applications from biomass treatment[182,183] to natural product extractions[184,185] and have shown utility in areas from electrochemistry[186,187] to biotechnology.[188] DESs have also become an active area of study for application as solvents or catalysts in organic reactions, with examples including cross-coupling reactions,[189] amide bond formation,[190] and organometallic chemistry[191] among others.[192] DESs usually consist of two parts; a hydrogen bond acceptor, usually a quaternary ammonium salt, and a hydrogen bond donor. When both components are present in nature, the mixture may be referred to as a Natural DES. These individual components can form strong interactions which cause an overall decrease in the melting point compared to an ideal mixture.

However, despite the clear potential of this solvent class, use of the TEC reaction in DESs had not been previously explored. As a robust method for thioether formation, and requiring only catalytic additives, TEC represents a strong candidate for improvement of Green characteristics of organic processes, including bioconjugation. Furthermore, TEC often does not require a large excess of reactants to achieve completion, in part due to its nature as a radical chain reaction.

3.2 Aims

The primary aim of this project was to develop a thiol-ene bioconjugation platform with improved Green Chemistry characteristics by replacing harmful solvents such as DMF with a more sustainable alternative. For this purpose, DESs present an appropriate choice, however the thiol-ene reaction has not been previously investigated in this reaction medium.

First, it was necessary to investigate the compatibility of the thiol-ene reaction with this newly-emerging solvent class. In this vein, two initiation methods were investigated; UV and atmospheric oxygen. A range of DESs were studied as well as a diverse range of substrates. In particular, biologically relevant compounds such as AAs, carbohydrates and lipids were to be of particular focus for scope investigations. Other important considerations of relevance to application of this methodology in a pharmaceutical setting, namely scale-up, solvent recycling, and potential formation of peroxides in the reaction mixture were also investigated. Finally, application of the methodology to a model peptide containing a Cys residue for demonstration of green bioconjugation *via* TEC was undertaken.

3.3 Results & Discussion

3.3.1 Initial Solvent Screening[b]

To begin our investigation into the compatibility of the thiol-ene chemistry with DESs, a range of common DESs were prepared[193–196] and screened. We sought to demonstrate compatibility of the reaction with a diverse range of DESs to allow for wider applicability of the reaction. The DESs included in the initial investigation were composed of combinations of the quaternary ammonium salts; choline chloride (ChCl, **3.1a**), betaine (Bet, **3.1b**), and tetrabutylammonium chloride (TBACl, **3.1c**) and H-bond donors; urea (**3.2a**), ethylene glycol (EG, **3.2b**), glycerol (Glyc, **3.2c**) and levulinic acid (Lev, **3.2d**) (**Table 3.1**).

This selection of DESs includes those with a variation in properties. The properties of primary interest for application of these solvents in synthetic chemistry are the melting temperature (T_m) and viscosity (η), although for some applications the degradation temperature (T_{deg}) may be of relevance. An important consideration for the ChCl:Urea DES

[b]Solvent selection, synthesis and measurement of properties was performed by Dr. Andrea Mezzetta and Dr. Lorenzo Guazzelli at the University of Pisa.

is the high T_m value, which can lead to solidification of samples if stored only slightly below room temperature. Additionally, this DES shows high viscosity in comparison to other DESs studied, with only Bet:Glyc showing a higher h value. For other solvents with lower T_m values, often well below 0 ºC, this factor is not often of significant concern unless the reaction requires significant temperature control, for example, addition of reactants at -78 ºC. Notably, this factor would restrict solvent choice to only ChCl:Glyc, although this is not of relevance for TEC. The viscosity of the solvent represents an important consideration for efficient stirring, and all solvents could be stirred sufficiently for synthetic reaction. Where lower h is required, addition of a small amount of water gives a less viscous mixture. Of course, for isolation of the DES after use, it is important that T_{deg} is higher than the boiling point of any additives to be removed *in vacuo*.

Table 3.1 Structures and select properties of DESs used in this study.

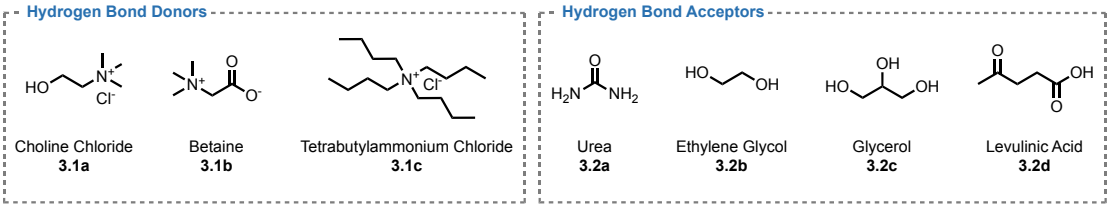

DES	Ratio	T_m (°C)	T_c (°C)	T_{deg} (°C)	h @25°C (cP)	r @25°C (Kg/m^3)
ChCl:Urea	1:2	12[197]	--	211[198]	1398[199]	1197[199]
ChCl:EG	1:2	-25.8	0.0	199[200]	46	1116
ChCl:LevA	1:2	[a]-76.1	--	180[200]	256	1138
ChCl:Glyc	1:2	<-90	--	202[200]	375	1191
Bet:EG	1:2	-17.9 59.6	-11.9	183	-	-
Bet:Glyc	1:2	[a]-74.1	--	176	2102	1216
TBACl:EG	1:2	[a]-60.8 -30.1[201]	-	154[202]	[b]127[201]	1020[203]
TBACl:LevA	1:2	[a]-57.5	-	238	258	1019

Initially, we sought to apply this reaction directly to peptide or AA examples, and thus Cys and reduced GSH were chosen as the thiol component. These would serve as initial model substrates for individual AA functionalisation and also for modification of a Cys residue within a peptide sequence. These thiol components proved fully soluble in the range of DESs tested. Test reactions with allyl acetate were conducted *via* irradiation at 365 nm for 1 hour in the presence of DPAP and MAP. However, due to the non-volatile nature of the DESs, it was necessary to extract the product from the reaction mixture instead of using

vacuum concentration. The DES was minimally diluted with water to give a viscosity suitable for traditional workup. However, extraction with a range of aqueous immiscible solvents failed to extract the product, instead only giving the organic breakdown products of the initiator and photosensitiser. Extraction using solid phase extraction (SPE) cartridges was then attempted but also failed to separate the product for either the reaction with Cys or GSH. It was then decided that initial investigation should be conducted with organic soluble small molecules, which should be readily extracted from the aqueous DES after reaction completion.

The reaction between thioacetic acid (**3.3**) and allyl acetate (**3.4**) to give **3.5**, mediated by UV irradiation in the presence of DPAP and MAP was then chosen as a model reaction. Reaction mixtures were irradiated at 365 nm for 1 hour, after which time they were minimally diluted to reduce viscosity and then extracted with the biodegradable solvent ethyl acetate (EtOAc). This extraction facilitated separation of the organic components of the mixture; namely the product, DPAP breakdown products (benzaldehyde and benzaldehyde dimethyl acetal) and MAP from the DES solvent which was recovered by concentration of the aqueous layer *in vacuo*. This allows for traditional analysis of the crude reaction mixture by ^{1}H NMR spectroscopic analysis and thin layer chromatography (TLC) following concentration of the organics *in vacuo*. Additionally, the DESs could be studied by ^{1}H NMR spectroscopic analysis in D_2O to ensure no breakdown or reaction of individual components.

The organics underwent ^{1}H NMR spectroscopic analysis (**Figure 3.1**), showing successful formation of the product in all DES systems examined. In all examples except for those based on Bet, quantitative consumption of the alkene was observed, with no observable side products. The DESs consisting of ChCl and either Glyc or EG gave the cleanest organic extracts, with none of the DES component being extracted. While the extracts from the reaction run in the ChCl:Urea DES appeared to be of comparable purity by ^{1}H NMR spectroscopic analysis, small amounts of solid impurity were observed that was not soluble in the $CDCl_3$ NMR solvent used, likely the urea component. The ChCl:LevA reaction extract gave a significant impurity, which accounted for the bulk of the crude mass. For both TBACl based DESs examined, minor impurities were again observed due to presence of small amounts of DES components. While the Bet based DESs showed good extract purity, a colour change and precipitate was noticed in the DES, indicating poor potential for recyclability, in addition to the reaction not reaching completion in these examples. From these results, it was clear that ChCl:Glyc or ChCl:EG were the optimum DESs for further

investigation. It may also be noted that EG possesses a degree of oral toxicity,[204] making Glyc more favourable for maintenance of the principles of "Green" chemistry. For this reason, ChCl:Glyc was selected for use in further investigation of these systems for "Green" bioconjugation. A key point from these results is, however, that the reaction proceeded to very high conversion in all DESs examined, allowing for potential tailoring of the DES to individual reaction components. Tailoring of the DES used to the reaction being performed is a particular advantage of DESs, allowing for solvation of different reactants or even use of the DES as a catalyst in the reaction. As a comparison, the reaction was also attempted in neat Glyc, but upon extraction a large amount of the Glyc solvent was obtained in the organics. It was therefore concluded that the DES system is necessary for ease of recyclability and product isolation.

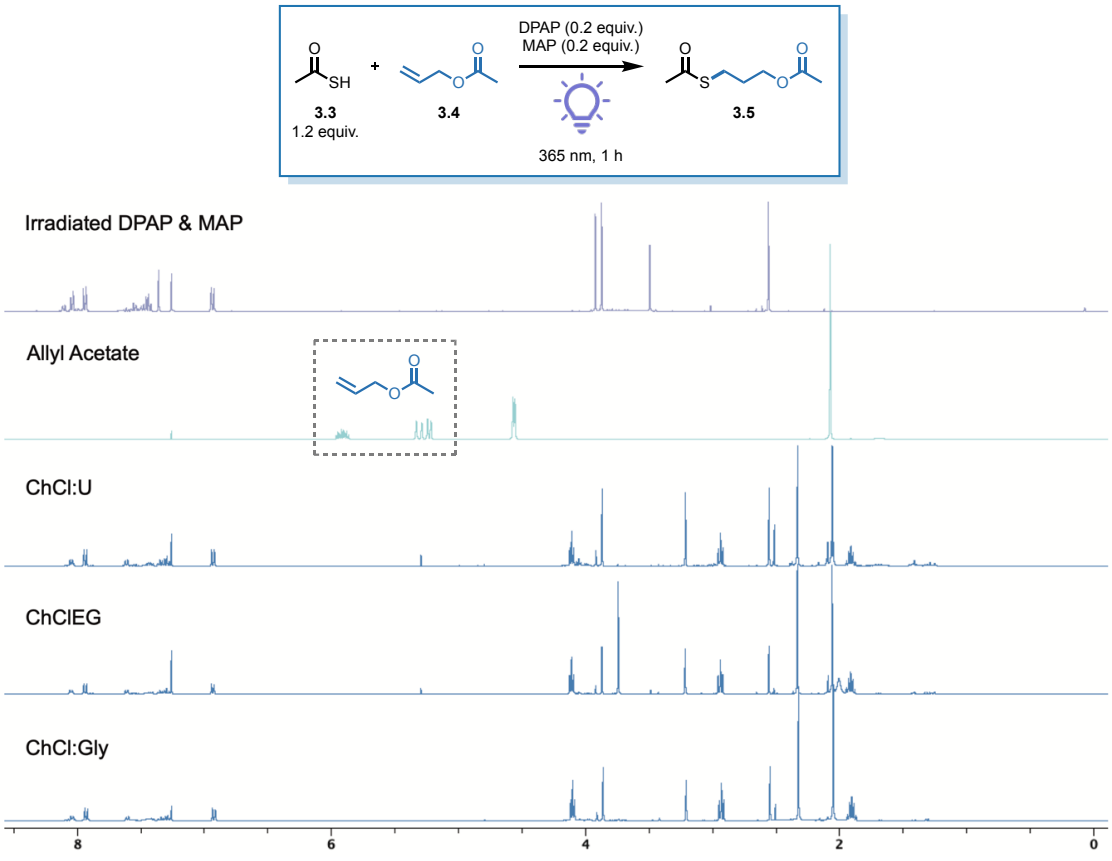

Figure 3.1: ^{1}H NMR spectroscopic analysis of crude reaction mixtures for the TEC reaction of thioacetic acid and allyl acetate in selected DES solvents show good profile with no DES components present or remaining alkene. Consumption of the alkene is observed through disappearance of the peaks between 5 and 6 ppm.

3.3.2 Substrate Scope for TEC in DESs

Initially, the modification of GSH in the DES system was investigated. GSH was soluble in DES/H_2O mixtures, along with the required DPAP/MAP additives. Therefore, a test reaction of GSH with allyl alcohol was attempted. After irradiation of GSH, DPAP/MAP and allyl alcohol in a H_2O/ChCl:EG (1:2) mixture, isolation of the product from the non-volatile DES was attempted. Attempts towards precipitation were entirely unsuccessful, as was use of solid phase extraction cartridges. As a result, the investigation of more simple reactants that could be extracted using organic solvents was undertaken.

The scope of this reaction was then investigated (**Figure 3.2**), incorporating biological examples with the aim of building towards the goal of bioconjugation within these systems. Initially, a number of relatively simple thiol and alkene combinations (**3.6a-b**) were investigated, showing promising yields of up to 91%. Following this, the reaction was applied to the synthesis of modified AAs through reaction of Boc-Cys-OMe with a range of alkenes. First a simple alkene, cyclohexene was utilised, giving thioether **3.6c** in a 67% yield. The reaction conditions were subsequently applied to synthesis of lipo-AA **3.6e**, protected diol-containing AA **3.6f**, and steroid-conjugated AA **3.6g**. Notably, the yield of **3.6g** is low due to poorer solubility of the hydrophobic estrone moiety in the polar DES solvent. The reaction with cyclohexene was also investigated for Boc-Cys-OH, showing compatibility with the free carboxylic acid, and producing a modified AA **3.6d** that could be directly used in SPPS without further protecting group manipulation. Additionally, thioglucose, example **3.6j**, underwent successful carbohydrate ligation. The reaction conditions were subsequently applied to the Acyl Thiol-Ene reaction to furnish thioester products. Use of thioacetic acid **3.3** as the thiol source furnished thioester products (**3.7a-c**) with yields of up to 91%. The synthesis of *S*-acetylated homocysteine **3.7d** was also performed through this methodology with a modest yield. Furthermore, the conditions were applied to a radical cascade cyclisation of diethyl 2,2-diallylmalonate to furnish diastereomeric cyclopentane product **3.7e**. Notably these produced lower yields, possibly due to lower alkene reactivity. Thus, the scope of this reaction was shown to incorporate a range of biologically important functionalities and molecules, as well as useful intermediates for synthesis of larger bioconjugates. This, importantly, shows good potential for attainment of the goal of "Green" bioconjugation of biomolecules in these DES systems via Thiol-Ene chemistry.

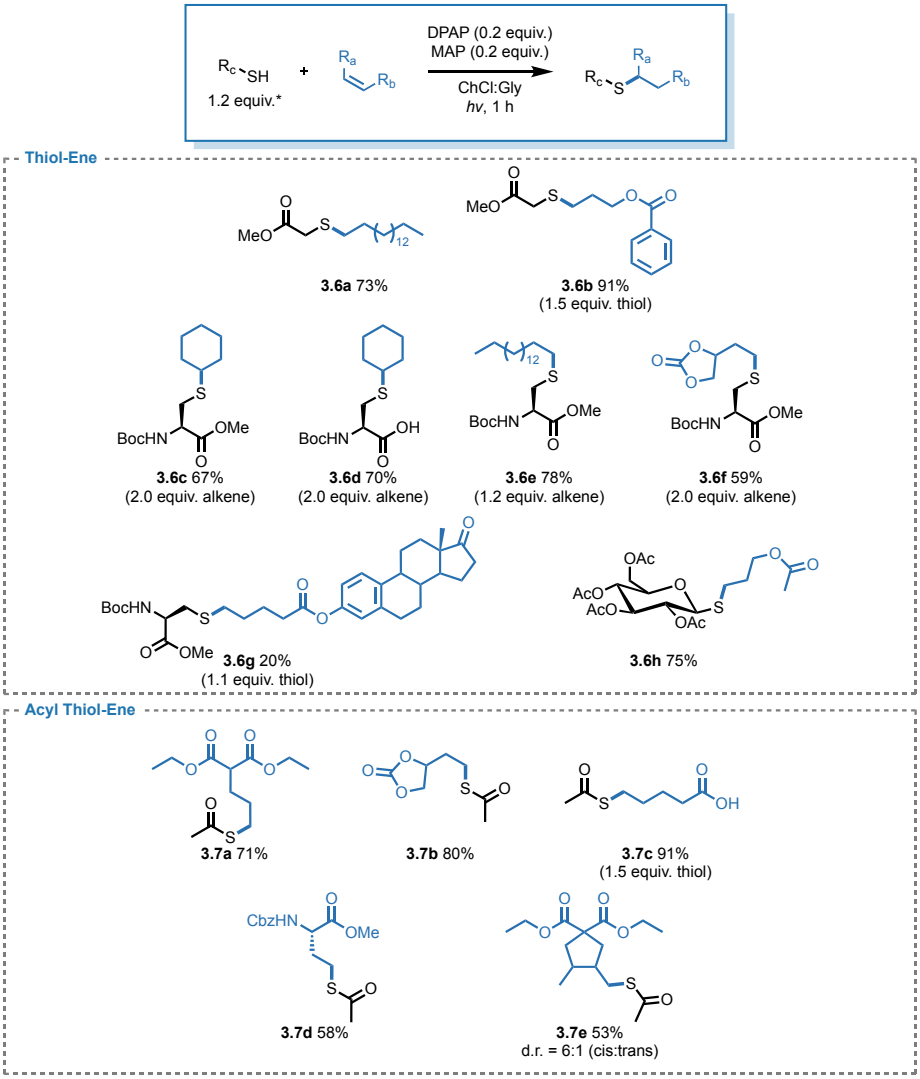

Figure 3.2: Scope of UV-initiated TEC and ATE in DESs. *Thiol equivalents and concentrations were tailored to examples as detailed in section 7.3.1.

Next, we sought to further improve the "Green" potential of Thiol-Ene chemistry in DESs through investigation of the O_2-initiated reaction. This will allow the reaction to be performed without any additives for initiation, instead using only atmospheric O_2, offering improved atom economy. The conditions applied in this reaction may also facilitate benchtop chemistry, though it is important to consider the toxicity of individual reactants, along with the often-acrid nature of small molecule thiols. However, the limitation of this initiation protocol is in the extended reaction times required for full conversion. In the Scanlan group's previous studies, reporting the atmospheric O_2-initiated Thiol-Ene reaction, heating of the reaction mixture to reflux encouraged efficient gas dissolution.[104] However, this is not possible for the non-volatile DESs. A recent study from Zhang *et al*. investigated the O_2 transfer rate, and included investigation into potential methods for tailoring reaction

conditions, favouring O_2 incorporation.[205] This study suggests that viscosity is of particular influence on gaseous incorporation, with reduced viscosity increasing dissolution. Conveniently, this factor can be influenced through heating or incorporation of water into the reaction mix. Additionally, enhanced stirring speeds have been shown to improve yields in O_2-dependant reactions in DESs.[206] Use of rapid stirring and gentle heating was therefore employed in our investigations into the O_2-initiated TEC reaction in DESs.

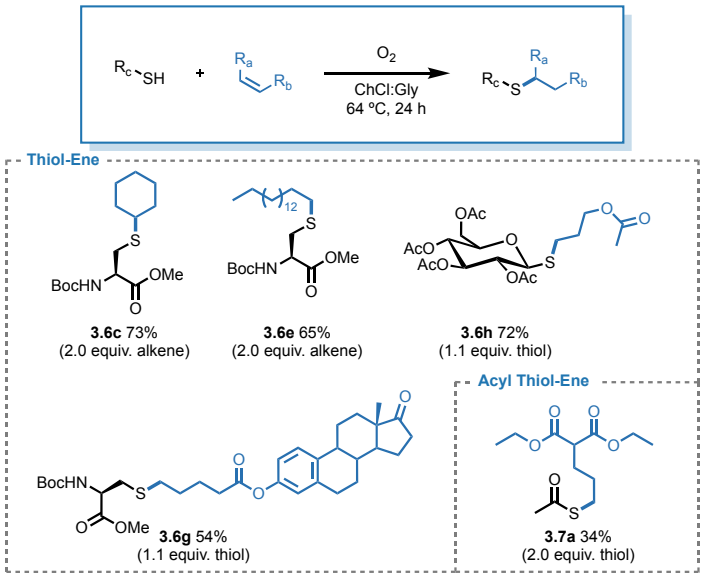

Figure 3.3: Scope of O_2-initiated TEC and ATE in DESs. Thiol equivalents and concentrations were tailored to examples as detailed in section 7.3.2.

Fortunately, our initial attempt into applying these conditions was successful, showing that the DES was capable of sufficient O_2 incorporation for thiyl radical formation. Additionally, the addition of a small amount of water as co-solvent for select examples further reduced viscosity to improve the O_2 transfer rate. To explore the scope of these conditions (**Figure 3.3**), thiol (**3.6c, 3.6e, 3.6g, 3.6h**) and thioacid (**3.7a**) examples were investigated. As for the UV-initiated conditions, cysteinyl radicals were investigated for synthesis of biologically relevant AA monomers. For the cyclohexene and hexadecene examples **3.6c** and **3.6e**, reduced yield was observed in these conditions when compared to the UV-initiated conditions. However, for steroid AA example **3.6g**, these conditions offered an improved yield. It is likely that this is due to improved solubility due to the higher temperature, while it may also be influenced by the longer reaction time. This, importantly, demonstrates further potential for tailoring of the reaction conditions to individual substrates that may exhibit difficult solubilities.

3.3.3 Recycling, Scale-Up and Investigation of Reaction Peroxide Content

A key advantage often noted for DES systems is the potential for reuse of the solvent in successive iterations of the reaction. For this reason, recycling of the reaction medium in TEC was investigated. The reaction between diethyl 2-allylmalonate and thioacetic acid was selected, initiated by UV irradiation in the presence of DPAP/MAP. In fresh DES solvent, this reaction was previously found to give a yield of 71%. The DES solvent was reisolated following the reaction by concentration of the aqueous layer *in vacuo* following reaction workup. Following addition of the alkene, thioacid and DPAP/MAP to the DES, the mix was irradiated, the isolation repeated and after each reaction the DES was examined by ^{1}H NMR spectroscopic analysis. A total of 5 repeats (6 reactions) were performed in the same solvent sample, with the 5th and final repeat showing undiminished yield. Additionally, no change in the solvent structure was observed by ^{1}H NMR spectroscopic analysis. This is an important consideration for the green characteristics of this methodology. In addition to the DES, only small amounts of H_2O and biodegradable EtOAc were used as solvents, and only 0.2 equiv. of the photoinitiator/photosensitiser DPAP/MAP combination were required for the UV-initiated conditions. In the oxygen-initiated conditions, the additives can also be excluded.

An important aspect of this methodology that is directly related to its potential impact in pharmaceutical manufacture is in scale-up of the reaction. To investigate the potential for scale-up, a multi-gram scale synthesis of **3.6e** was performed using O_2-initiated conditions for favoured "Green" characteristics. As may be expected in scale-up, a reduced yield of 47% (compared to 65% at approx. 200 mg scale) was achieved. Another consideration that is important in scale-up of this particular reaction is the potential presence of peroxides. Proposed mechanisms for generation of thiyl radicals *via* atmospheric O_2 suggest that an intermediate hydroperoxyl radical may be formed.[104,207] Although only a small amount will be required for initiation of the radical chain process in the TEC reaction, at large scale this may become significant. For this reason, throughout the course of the reaction the peroxide concentration was monitored using MerkQuant peroxide test strips. The peroxide concentration was quantified at t = 0, 0.5, 1, 1.5, 2, 3, 5, 24, 30, 48, 54 and 72 hours. In all cases, the peroxides concentration remained below the detectable limit of 0.5 mg/L after the 15 seconds required for quantitative results and remained negative at the three minute limit for a positive result. While this shows that no significant quantities of peroxides are produced, it does not completely disprove the presence of any peroxide species and their involvement in the reaction mechanism. Since the TEC reaction is a radical chain process, very low

concentrations of oxygen-centred radical species are required for initiation and the by-products of these may not be detectable at small scale. A putative mechanism for the oxygen mediated reaction is presented in **Figure 3.4**.[104]

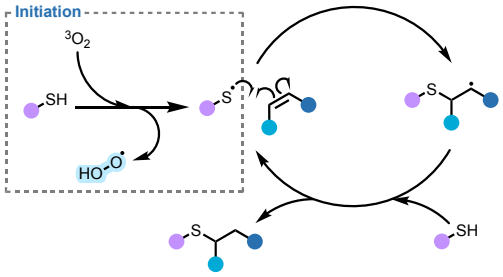

Figure 3.4: Mechanism for oxygen-initiated TEC.

3.3.4 Peptide Bioconjugation *via* TEC in DESs

With the successful application of this methodology to individual AA monomers having been achieved, it was then sought to apply the methodology to a peptide example. Recently, the minimal sequence required for binding of the SARS-CoV-2 spike protein to human angiotensin-converting enzyme 2 (ACE-2), the *C*-terminal EDLFYQ portion, was identified (**Figure 3.5**).[208] This interaction serves as an essential entry route for entry of SARS-CoV-2 into cells.[209] An analogue of this sequence, bearing a Cys residue on the *N*-terminal (CEDLFYQ, **3.9**) for modification was therefore chosen for investigation bioconjugation *via* TEC in DESs, in which the Cys replaces an Ala residue in human ACE-2. The desired sequence was prepared by Fmoc-SPPS, to afford the peptide in sufficient purity such that further purification was not required.

With this peptide in hand, the UV-initiated conditions were applied to reaction of the peptide with cyclohexene, as this alkene is commercially available and previously resulted in good isolated yields under both UV- and O_2-initiated conditions. For more efficient solvation of the peptide, as well as reduced viscosity, a DES-water mixture was utilised. Hammond *et al*. have shown that the DES nanostructure of a range of ChCl-based DESs is maintained up to 42 wt % H_2O, while above 51 wt % the structure is disrupted.[210] With this in mind, a DES/H_2O (3:2) mix was used for the reaction. Additionally, this serves as further demonstration of the potential for tailoring of DES systems as designer solvents, through manipulation of the hydrophobic or hydrophilic character of the reaction mix.

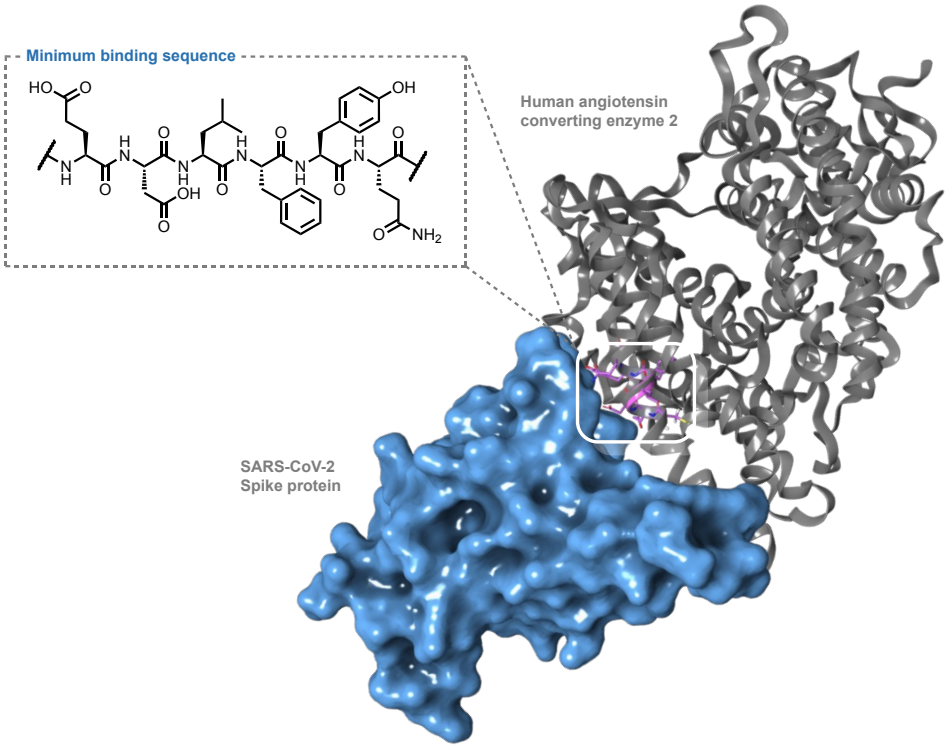

Figure 3.5: Minimum binding sequence for the SARS-CoV-2 spike protein to human angiotensin converting enzyme 2.

Disappointingly, in these conditions only trace product was observed by HPLC and MS analysis, and significant disulfide formation could be observed. To overcome the formation of this side-product, the use of the reducing agent TES was investigated, along with degassing of the reaction mix. The peptide was dissolved in degassed DES/H_2O (3:2) mix, along with DPAP (1 equiv.), MAP (1 equiv.), TES (1 equiv.) and cyclohexene (5 equiv.), and stirred under UV irradiation for 3 hours (**Figure 3.6**). An aliquot of the reaction mix was then taken and analysed by RP-HPLC, showing 86% conversion to the desired product **3.8a** and clean reaction profile. A new peak with increased retention time of 16.93 min and the desired mass was identified as the product. Semi-preparative RP-HPLC of the reaction mix afforded **3.8a** in 56% isolated yield. It is likely that this isolated yield is reduced when compared to the measured conversion is as a consequence of the necessity to isolate the product from the DES, as the large injection volume necessary causes some product to be carried through the column as the injection peak.

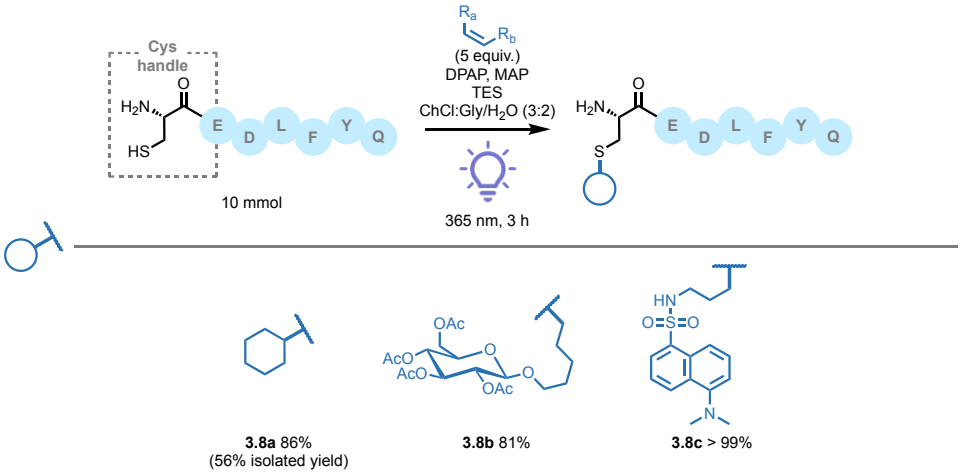

Figure 3.6: Scope for peptide bioconjugation by TEC in DESs.

To further demonstrate this methodology for peptide conjugation, the reaction conditions were applied to functionalisation with a carbohydrate (**3.8b**) and dansyl fluorophore (**3.8c**), affording 81% and quantitative conversions respectively. Importantly, this demonstrates the use of this methodology for "post-translational" glycosylation of a fully deprotected sequence, as well as the modification of a biologically relevant sequence for potential application in study of SARS-CoV-2.

The application of the O_2-initiated conditions to peptide functionalisation were then applied to the functionalisation of the CEDLFYQ sequence with a cyclohexyl moiety. Again, one equivalent of TES was incorporated in the reaction mix due to the high likelihood of disulfide formation in the presence of atmospheric O_2. After 24 h, HPLC analysis of the reaction mixture showed no conversion of the starting material. The mixture was again analysed at 48 h, with still no formation of the desired product. Despite the presence of TES, small amounts of the disulfide were observed. It is possible that the incorporation of atmospheric oxygen in the DES/water mixture used leads to rapid disulfide formation, thereby preventing formation of the desired product.

3.4 Conclusions & Future Work

A range of DESs with varied properties were screened for compatibility with the TEC reaction. All solvents tested were compatible with the reaction, however the degree of success of product isolation and potential for recycling gave three optimal DES mixtures, all of which were based on the ChCl hydrogen bond acceptor. The urea, EG and Glyc hydrogen bond donors in combination with ChCl gave clean organic extracts after the reaction, with

no observed effect on the DES itself. The remaining ChCl and TBACl DESs gave good reaction profile, but with DES components in the organic extract. However, it is likely that chromatographic purification would readily facilitate separation of products and extracted DES components. For the Bet examples, significant degradation of the DES during the reaction was observed.

Investigation of the substrate scope for this methodology covered a range of thiol and alkene substrates including AAs, carbohydrates, lipids, and steroids as well as more simple small molecule examples. Generally, moderate to good yields were observed for the UV-initiated conditions. To further the Green characteristics of this methodology, the initiation of the TEC reaction using atmospheric oxygen was also investigated. Again, generally moderate to good yields were obtained. Notably, a general trend of higher yields for either initiation method was not observed, suggesting that the optimal method depends on the combination of thiol and alkene.

The important aspects of solvent recycling, scale-up and peroxide content was then investigated, as these are important considerations for use of this methodology in a pharmaceutical manufacturing setting. The solvent was successfully recycled five times, with no effect on reaction outcome or DES. A multi-gram scale oxygen-initiated modification of Cys *via* TEC reaction was therefore performed. Additionally, during the course of this reaction the mixture was monitored for presence of peroxides and was found to be below the detectable limit throughout the reaction time.

Finally, the goal of bioconjugation of a peptide example was undertaken. The 6-mer minimal binding sequence of human ACE-2 for the SARS-CoV-2 spike protein was synthesised with an additional *N*-terminal Cys residue to serve as a conjugation handle. Using the UV initiated conditions, lipid, carbohydrate, and fluorophore tagged peptide conjugates were synthesised in high to quantitative yields. Notably, this required the addition of TES as a reductant to prevent disulfide formation. Unfortunately, application of the oxygen-initiated conditions gave no desired product. It is possible that this lack of reactivity results from competition between formation of the thiyl radical by triplet oxygen and reaction with TES, thus preventing reaction initiation. However, exclusion of TES from the reaction mixture gives only disulfide formation.

Future work towards improving the Green properties of this bioconjugation approach will combine the use of DESs with the added benefits of flow chemistry. An important

consideration in flow applications is solvent viscosity, and for this reason the varied DES compatibility is highly advantageous. The continued improvement of Green characteristics of synthetic methodologies for the pharmaceutical industry is of great importance for ensuring a sustainable future.

Chapter 4

High-Throughput Thiol-Ene Click for Direct-to-Biology Applications

"More peptides, more problems."
- Prof. Stephen Kent on peptide chemistry.

4.1 Introduction

High throughput chemistry is an area of particular recent interest for discovery of lead compounds towards biological targets. These methods often rely on highly efficient reactions for combinatorial syntheses of libraries of compounds. Often, in preparation of synthetic libraries, the most resource-intensive step is the purification of large numbers of compounds. A recent trend in the area of high-throughput experimentation (HTE), therefore, is the so-called "direct-to-biology" approach, in which crude reaction mixtures are used directly in initial assays.[211] This approach relies on the use of highly efficient reactions that yield the desired product in quantitative yields and good purity. Examples of reactions that have been employed in such approaches to date include amide bond formation,[42,212,213] CuAAC[214] and Sulfur(VI) Fluoride Exchange (SuFEx) chemistry.[215,216]

Recently, the Heinis lab has developed a highly efficient methodology for synthesis of macrocyclic peptide libraries using disulfide resins which facilitate on-resin deprotection, followed by peptide release in a separate step (as detailed in **section 4.3.2**). Release can be either cyclative to yield disulfide macrocycles[217] or reductive to yield linear dithiol peptides.[218] Dithiol peptide products can then be cyclised in solution using *bis*-electrophilic reagents, allowing further diversification of the library, or themselves oxidised to disulfide macrocycles. Disulfide peptide libraries have been combined with solution-phase amide bond formation on amine-containing side chains with carboxylic acid libraries. The synthesis of macrocycle libraries through such approaches has led to discovery of biologically active inhibitors against protein targets.[42,78,219]

However, the current available approaches each have limitations, for example amide bond formation and SuFEx chemistry is not tolerant of other amines which may be important groups for binding. While CuAAC provides exquisite selectivity, the presence of a copper catalyst can limit the compatible biological applications, while the triazole linkage may impact binding properties.

4.2 Aims

The primary aim of this project was to develop a novel method for high-throughput compound diversification suitable for direct screening without chromatographic purification through utilising the click characteristics of the TEC reaction. This will facilitate the rapid production of targeted chemical libraries toward desirable drug targets.

Initially, it was necessary to design a reactor suitable for UV irradiation of microwell plates, and for this purpose an in-house built LED array was to be employed to provide uniform irradiation across the base of the plate. Additionally, TEC had not been previously reported in a high-throughput context in microwell plates. In such approaches a number of restrictions become relevant when compared to traditional larger scale batch chemistry. Of primary concern in this context is the lack of stirring or agitation for this diffusion-limited TEC reaction. Thus, the compatibility of TEC with both the custom reactor and the limitations of high-throughput setups was to be investigated.

At this stage the modification of varied peptides could be investigated. A variety of peptide macrocycles were to be included, along with a range of thiols and the reaction conditions thoroughly optimised to afford high purity crude products. Following this, a high-throughput workflow was to be devised, incorporating a high degree of automation amenable to the preparation of large libraries without a significant drain on resources. This overall approach was then to be applied to a scope library to investigate and demonstrate the utility of this technology.

4.3 Results & Discussion

4.3.1 Reactor and Reaction Compatibility[c]

Prior to application of the methodology to complex substrates in peptidic macrocycles, it was necessary to a) obtain a suitable reactor for irradiation in microtiter plates and b) ensure that the TEC reaction is compatible with a number of considerations related to HTE. For the design of a suitable reactor, a 7 W 96 UV LED array was constructed in dimensions appropriate for microtiter plates (**Figure 4.1**). 96 LEDs are arranged on an electrical circuit to align with the wells of a standard microtitre plate. The LED driver provides power control, in combination with a dimmer to allow varying degrees of irradiation. Further components include earthing and a mains power supply.

Of course this is well-suited to irradiation of samples in 96 well-plates, but also to 384 and 1,536 well-plates which share similar dimensions and well layout. Furthermore, it was necessary to obtain a housing for the reactor which would protect the user from significant exposure to UV light. For this purpose, a commercially available nail curing lamp

[c]Reactor development was performed by Dr. Mischa Schüttel.

was obtained. This particular choice had the added advantage of providing further irradiation by means of 4 x 9 W UV bulbs, and additional reflective interior coating, allowing efficient radiation of the entire plate. Additionally, this setup is highly cost-efficient with a cost of less than €80 for the array and less than €100 in total.

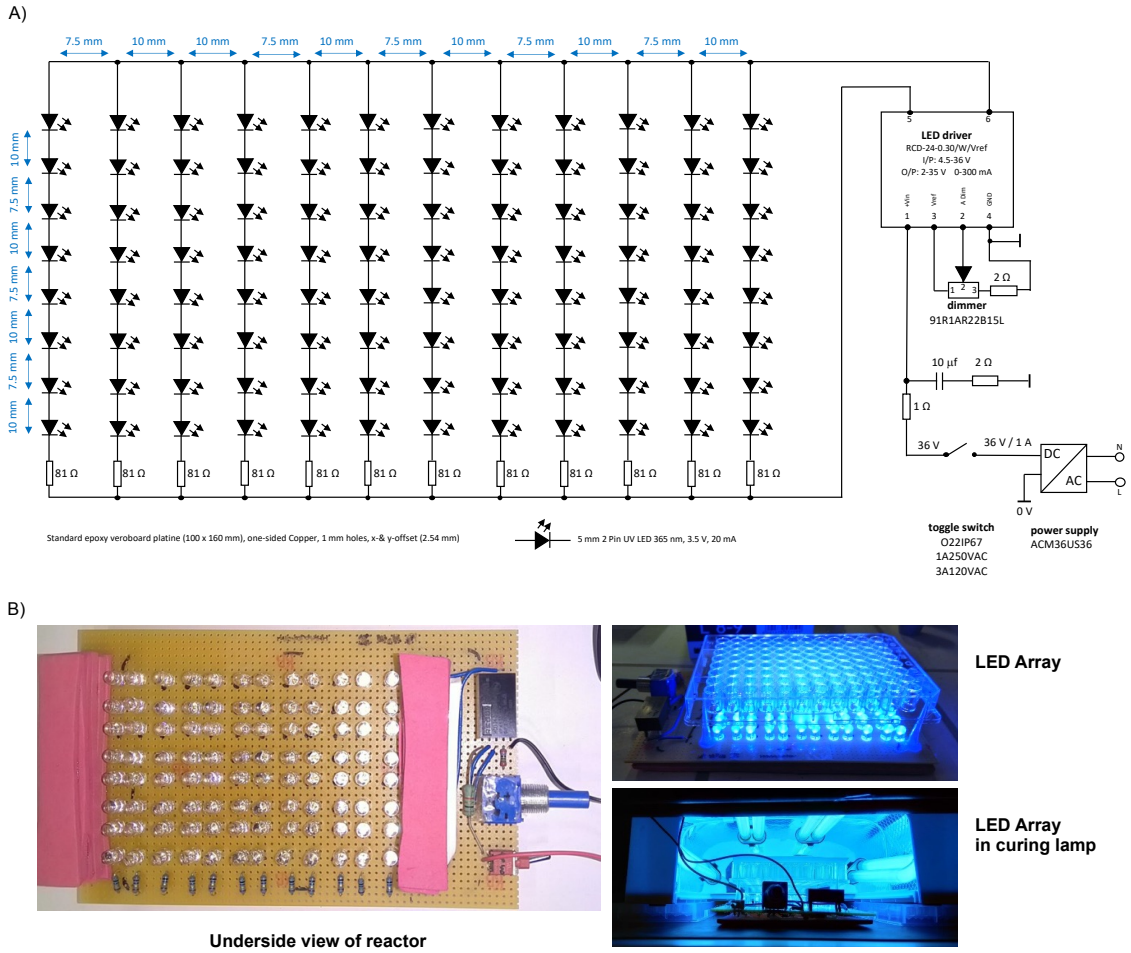

Figure 4.1: HT UV photoreactor. A) Schematic drawing of the array. B) Images of the reactor.

In relation to the elements of HTE that must be considered, the primary condition is the limited ability to agitate solutions to ensure sufficient mixing or diffusion of reactants. This is of particular relevance for a reaction such as TEC as it is a diffusion limited radical chain reaction. Insufficient mixing may result in premature quenching of radical species and thus insufficient propagation of the chain reaction. While at volumes in the range of 100 µL an agitation of the well plate may provide mixing, in single digit µL volumes the surface tension reduces such agitation significantly. Additionally, it was necessary to ensure that the reaction is compatible with typical HTE solvents, for example, DMSO. Use of small reaction volumes in HTE limits the applicability of volatile solvents, including MeCN. Thus, a solvent

that is sufficiently non-volatile but can also dissolve the necessary components and facilitate the reaction is required.

Initially, to examine the potential for initiation using the designed apparatus, the breakdown of DPAP (**4.4**) into benzaldehyde (**4.6**) was to be used as a test reaction (**Figure 4.2**). In this case, a characteristic aldehyde peak would be observed in the ^{1}H NMR spectrum of the reaction at approx. 10 ppm upon breakdown of **4.4**. The reaction was investigated at concentrations of 2 or 10 mM **4.4**, with either equimolar or no MAP sensitiser added and 1 hour of irradiation time. The reactions were conducted in 6 x 100 µL aliquots in a UV-transparent glass 96 well-plate and in DMSO-d_6 to facilitate direct ^{1}H NMR spectroscopic analysis by combination of aliquots. However, the results of this experiment were not clear, with inconsistent formation of the expected aldehyde.

It was then decided that a different compatibility experiment should be conducted, utilising a model TEC reaction of allyl acetate **4.1** and mercaptopropionic acid **4.2** to give **4.3** (**Figure 4.2**). This reaction was similarly performed with concentrations of 2 or 10 mM DPAP in 6 x 100 µL aliquots in a UV-transparent glass 96 well-plate and in DMSO-d_6, but with 3 h irradiation time. The concentration of alkene **4.1** was 10 mM, and 3 equivalents of thiol **4.2** were used for a 30 mM concentration. This experiment was expected to reveal the same aldehyde peak as for the previous experiment, but also to allow monitoring of the alkene consumption. Thus, this would verify both sufficient initiation *via* the DPAP/MAP initiator/sensitiser system and a successful TEC reaction. Gratifyingly, ^{1}H NMR spectroscopic analysis revealed complete consumption of the alkene along with formation of the characteristic aldehyde peak in all cases, indicating a complete reaction was indeed achieved even in the absence of MAP and with as little as 20 mol% DPAP (**Figure 4.2**, 2nd and 4th spectra from bottom).

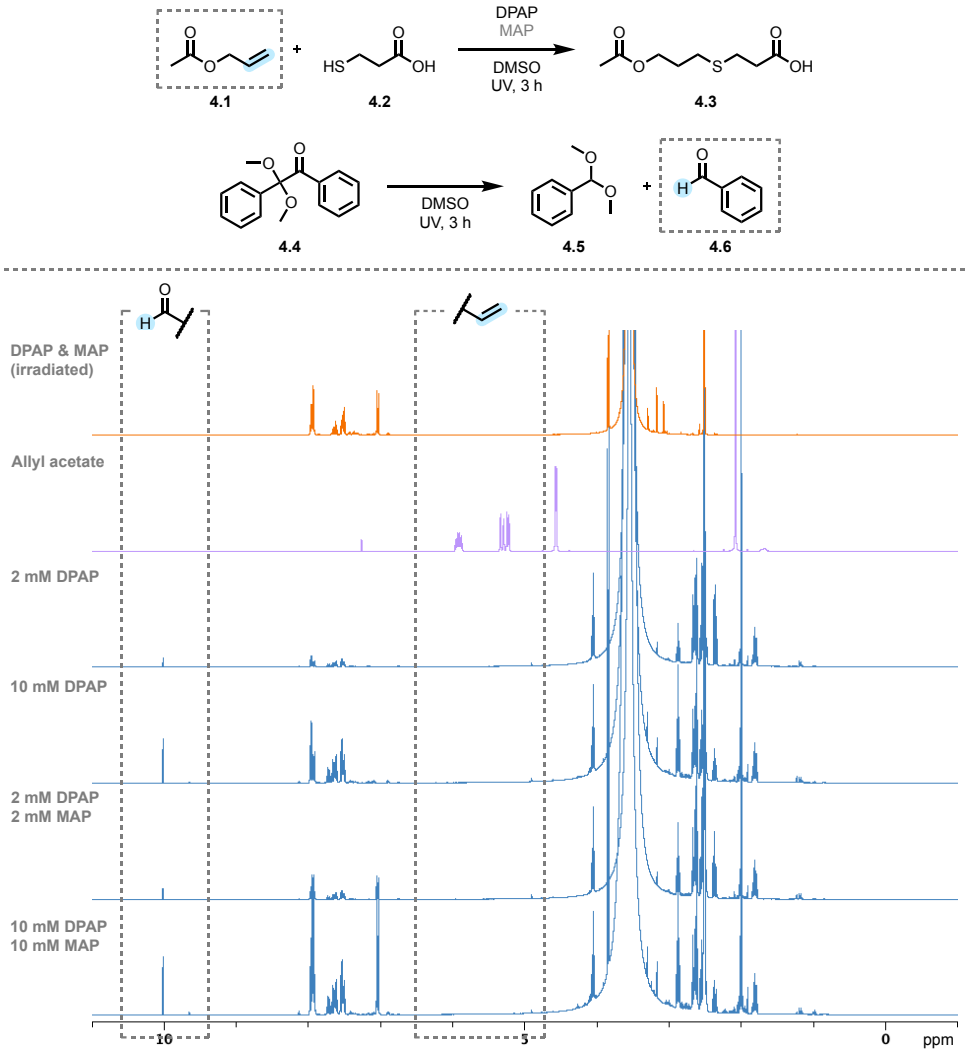

Figure 4.2: Initial TEC compatibility test through a model reaction. ^{1}H NMR spectroscopic analysis shows quantitative consumption of the alkene, along with appearance of the characteristic aldehyde peak due to UV-initiated DPAP breakdown.

4.3.2 Synthesis of Model Peptides

With these promising results in hand, we sought to apply the reaction to modification of alkene-containing cyclic peptides. Recently, the Heinis lab have developed highly efficient methodologies for synthesis of dithioether and disulfide macrocycles, utilising a disulfide linked resin (**Figure 4.3**). This disulfide linkage is stable to standard Fmoc-SPPS conditions, as well as acid-mediated side-chain deprotection conditions. This allows for on-resin universal deprotection of side-chains, followed by washing steps to remove side-products. The peptide can then be released from the resin by either a reductive[218] or cyclative[217] release in high purity.

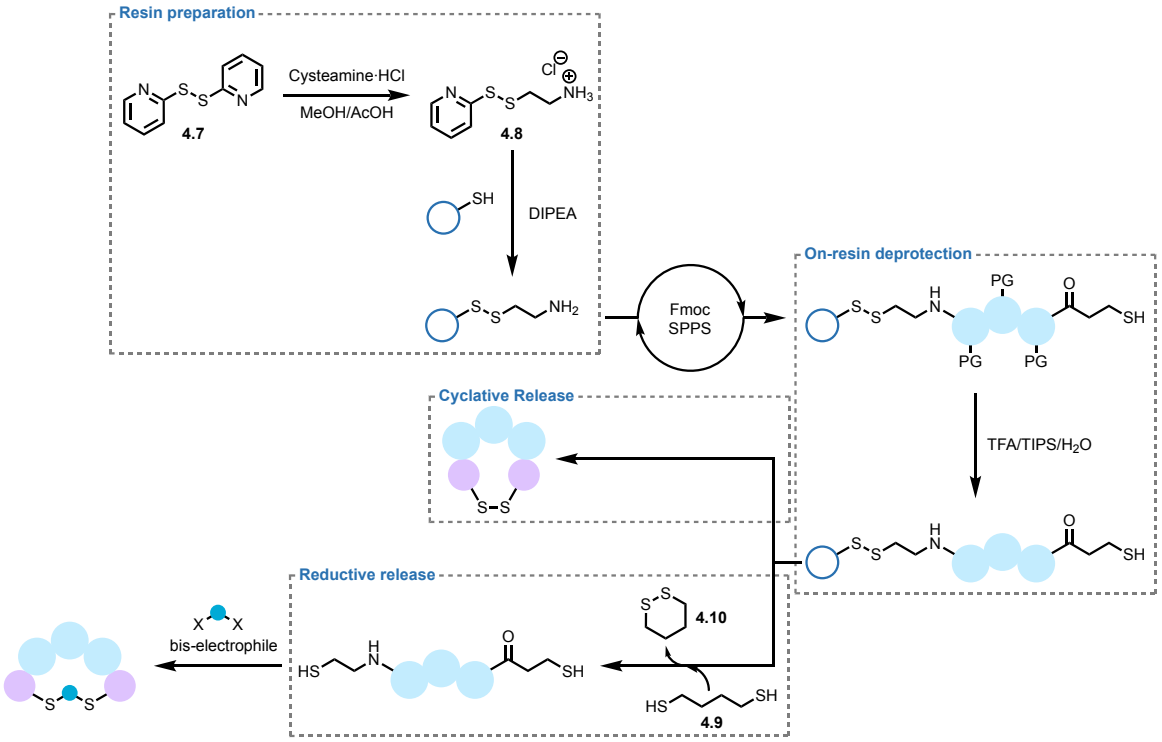

Figure 4.3: Synthesis of cyclic peptides on disulfide-linked resin allows for on-resin removal of protecting groups, followed by either cyclative or reductive release to yield peptides in high crude purity.

Synthesis of the disulfide-linked resin was achieved as reported by Bognar *et al.* to yield a cysteamine-functionalised resin.[218] Firstly, 2-(2-pyridyldithio)ethylamine) hydrochloride **4.8** was prepared from dipyridyl disulfide **4.7** to function as a disulfide exchange reagent, from which the cysteamine moiety is readily transferred to another thiol. Treatment of thiol-functionalised polystyrene resin with this exchange reagent in the presence of base then resulted in disulfide exchange to furnish the resin with disulfide-linked mercaptoethylamine (Mea) bearing a free amine on which the peptide chain can be constructed. Chain extension was performed using standard Fmoc-SPPS coupling conditions with HBTU as a coupling reagent, as HBTU had been previously utilised as a suitable coupling agent for this SPPS approach.[218] To minimise loss of material by premature release from the resin due to base sensitivity, Fmoc deprotections in 20% piperidine in DMF were limited to 2 x 3 minute treatments. Following chain elongation, side chain protecting groups were cleaved using a mixture of TFA/TIPS/H_2O (95:2.5:2.5), leaving the unprotected peptide still resin bound. The resin was then split into two portions for both cyclative and reductive release of the peptide from the resin. The first portion was treated with 150 mM triethylamine (TEA) in DMF, leading to deprotonation of the *N*-terminal thiol which undergoes disulfide

exchange at the *C*-terminal to release the peptide as a disulfide macrocycle. The second portion was treated with 100 mM 1,4-butanedithiol (BDT, **4.9**) and TEA in DMF. This releases the peptide by reduction of the resin disulfide tether. Use of BDT over the similar but more common reducing agent dithiothreitol (DTT) gives the volatile side product **4.10** which may be removed *in vacuo*, affording high purity crude peptides. Importantly, for linear dithiol products, acidification of the cleaved mixture prior to rotary vacuum concentration (RVC) is necessary to avoid oxidation.

This methodology was applied to the synthesis of a short model peptide bearing a Gly, Agl and Tyr residue, capped with 3-mercaptopropionic acid (Mpa). The linear peptide afforded by the reductive release was cyclised using the dichloroacetone linker reported by the Dawson group to yield the dithioether model peptide **2.11a**.[220] From released material, a 50% yield from SPPS was assumed and dissolved to 1 mM in 1:1 freshly prepared degassed NH_4HCO_3 buffer (60 mM, pH 8.0) and MeCN, to which dichloroacetone was added. Once the reaction was observed to be complete by LC-MS, β-mercaptoethanol (BME) was added to quench excess electrophile. This cyclisation approach for dithiol peptides has previously been demonstrated as a highly efficient process yielding few side products.[218] However, use of large excess of electrophilic reagent or extended reaction times can result in alkylation of other nucleophilic groups such as amines.[219] Additionally, an additional sample of linear peptide was similarly treated with DMSO in place of the *bis*-electrophile to yield disulfide macrocycle **2.11b**.

4.3.3 Initial Test Reactions

With model dithioether and disulfide cyclic peptides in hand, we turned to investigation of their functionalisation *via* TEC chemistry (**Figure 4.4**). In addition, further downscale of the reaction to the nanomole scale was investigated. For reactions in single-digit microlitre volumes, 1,536-well low dead volume (LDV) plates provide an attractive reaction vessel, allowing performance of a large number of reactions in volumes of approximately 2-8 µL. At a 10 mM concentration, 40 nmol of peptide precursor can therefore be functionalised in a 4 µL reaction. This is particularly advantageous for precious substrates, as peptides often are. From a relatively small amount of material, a large number of analogues could be produced. For example, 1 mg of peptide with a molecular weight of 500 g/mol would be sufficient for 50 reactions at this scale, allowing for investigation of a large variety

of different modifications of the original sequence. Additionally, at this scale and for high throughput application, automated dispensing of both reagents and substrates is desirable. Therefore, 1,536-well LDV cyclic olefin copolymer (COC) plates with organic solvent and acoustic droplet ejection (ADE) technology[221–223] compatibility were selected. To ensure completion of reaction, stoichiometric DPAP was used, particularly considering the poor potential for agitation of such small reaction volumes due to surface tension.

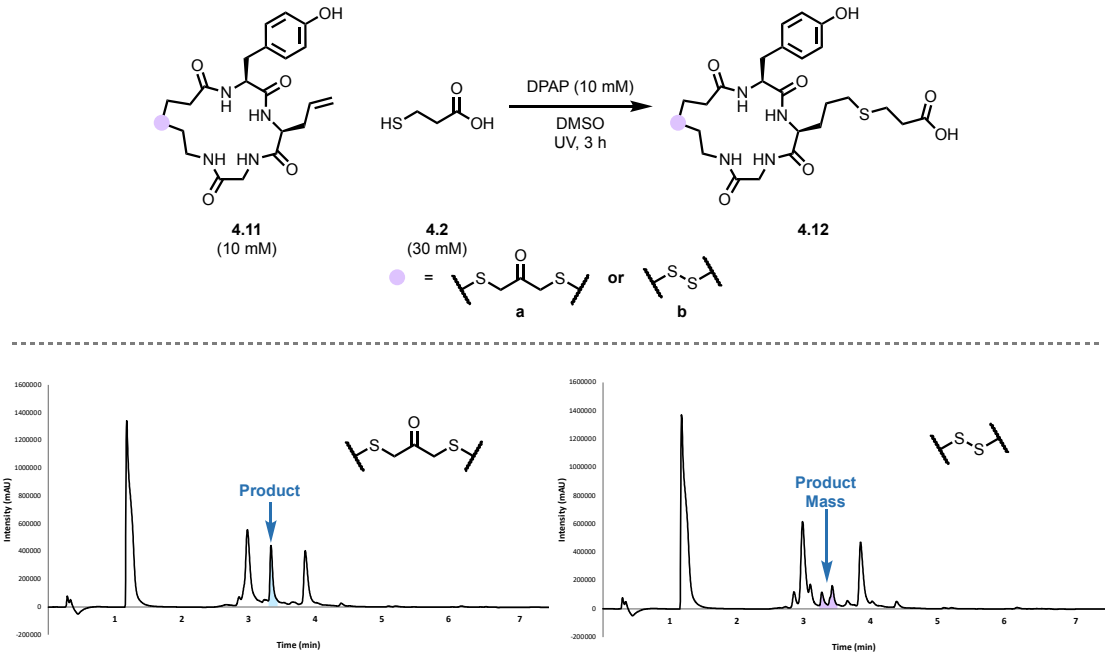

Figure 4.4: LC-MS traces for reaction mixtures for initial test reactions of dithioether (left) and disulfide (right) substrates.

Peptides were dispensed *via* pipette from 40 mM stock solutions in DMSO, followed by addition of reactants, also *via* pipette from DMSO stocks, for final concentrations of 10 mM peptide, 3 mM thiol and 10 mM DPAP. After dispensing of substrates and reagents, the plates were sealed with a transparent seal, centrifuged to ensure combination of individual droplets, and irradiated for 3 hours. In the case of the dithioether macrocycle, quantitative conversion to the desired product **4.12a** was observed by LC-MS. However, LC-MS analysis of the reaction mixture for the disulfide substrate revealed two peaks with mass corresponding to the target product **4.12b**, possibly due to disulfide exchange with the thiol reaction component. Additionally, a peak with mass corresponding to reduced disulfide was observed.

To attempt to curb side reactions for disulfide substrate **4.11b**, use of 0.1% TFA in DMSO was utilised as reaction solvent, preventing thiolate formation which could result in

disulfide exchange. Unfortunately, this only gave a slight change in intensities of the peaks corresponding to the product mass. Use of three equivalents of TFA gave no further improvement. As the dithioether macrocycles possess greater potential both in this methodology and for structural diversity in macrocycle libraries, it was decided to focus on dithiol peptides cyclised *via* reaction with *bis*-electrophiles. However, this methodology should also be more generally applicable to linear peptides or head-to-tail cyclised peptides, and may also be compatible with other non-redox-active or more stable cyclative linkages.

4.3.4 Investigation of Experimental Considerations

To improve the potential for application to production of high-purity crude mixtures for direct screening applications, two key factors were also investigated; substrate concentration and removal of DPAP breakdown by-products. In production of libraries, it may be desirable to work at different concentrations to reduce the need for solvent removal and dissolution steps. While TEC is frequently applied at concentrations up to 0.1 M, lower substrate concentrations have not been thoroughly investigated, and particularly not at μL volumes. The previous reaction conditions were again applied at 2.5 mM, 5 mM and 10 mM alkene concentrations (maintaining previous reactant equivalents), giving conversions of 46, 81 and > 99% respectively (**Figure 4.5**). This shows that alkene concentration is of high importance, likely for propagation of the radical chain mechanism. However, it is possible that further large excesses of thiol may allow functionalisation at low concentrations. Nevertheless, further investigations were conducted at a 10 mM macrocycle concentration.

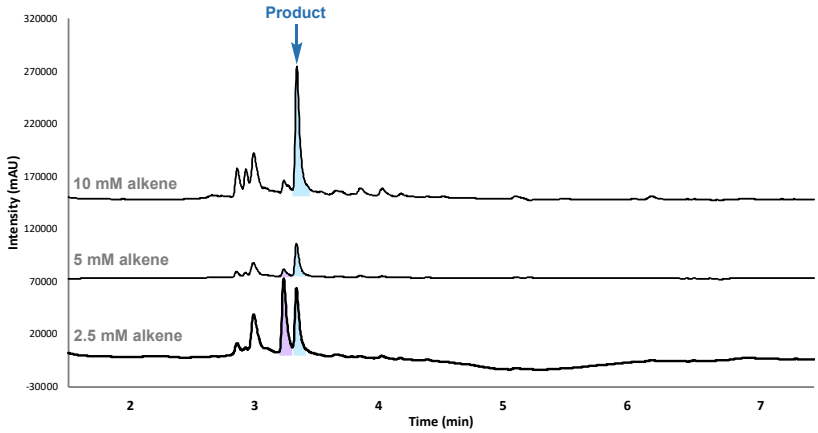

Figure 4.5: LC-MS traces for reactions at different alkene substrate concentration.

Secondly, it was of particular interest to investigate the removal of DPAP breakdown products *in vacuo*. UV irradiation of DPAP produces benzaldehyde (**4.6**) and benzaldehyde

dimethyl acetal (**4.5**), with boiling points of 178 and 196 ºC respectively,[224] and so the quantities present may be at least drastically lowered during RVC. Indeed, RVC for as little as 2 h removed the majority of the material, as seen *via* LC-MS analysis. If desired, the reaction mixtures could be resuspended in DMSO and subjected to RVC overnight to almost completely remove these breakdown products (**Figure 4.6**). For a number of thiols, removal of excess reagent may also be achieved through RVC, making this a highly useful approach to improvement of the reaction purity profile without the need for chromatographic approaches.

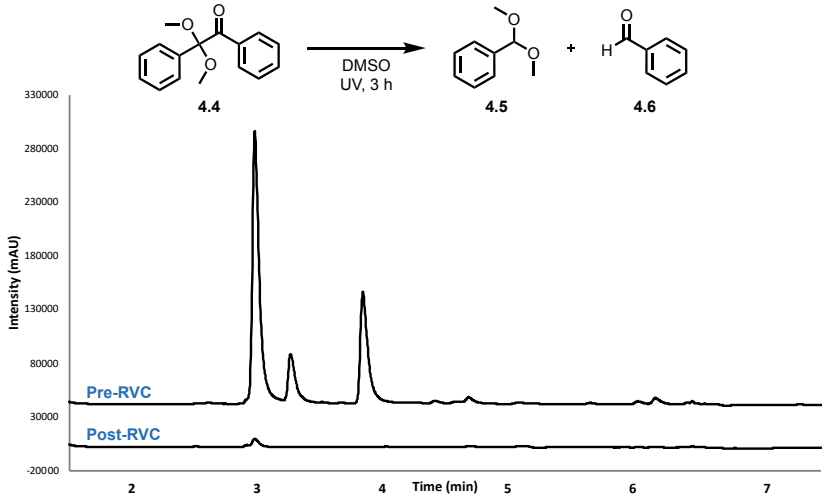

Figure 4.6: LC-MS traces for samples of irradiated DPAP before RVC and after 2h of RVC. Compound **4.5** can be seen at 3 min and compound **4.6** at 3.9 min/

4.3.5 Oxidation at Aromatic Thioethers

From the original investigation, extension of the methodology to macrocycles bearing different functionalities in their side chains, as well as different linkers was desired. In the course of these investigations a model peptide sequence was synthesised and cyclised using 1,5-dibromomethylpyridine to yield macrocycle **4.13b** (see section 4.3.8). However, subjecting this precursor to the previously optimised reaction conditions gave only 54% desired product. LC-MS analysis showed, in addition to the product peak, the formation of two +16 peaks and a single +32 peak, along with quantitative hydrothiolation of the alkene (**Figure 4.7**).

While a myriad of uses of TEC for peptide and protein substrates have been reported, oxidation of thioethers is rarely observed.[108] In cyclisation of peptides through TEC reaction

of photoactive azobenzene alkene AAs with Cys residues, Hoppmann *et al.* observed oxidation of the thioether moiety and hypothesised that this was due to the proximal aromatic group.[122,127] Recent studies have also shown oxidation of thioethers in proximity to aromatic groups in thiyl radical reactions.[225] The observation of two +16 peaks implies the oxidation of two thioethers, which could occur at those in the macrocycle substrate backbone, or singly at the backbone or at the side chain after hydrothiolation. However, no triply oxidised +48 adduct was observed. This combination of experimental evidence and literature precedent lead to the conclusion that the oxidation of the backbone thioethers was responsible for formation of these side products. To further strengthen this conclusion, cyclisation with non-aromatic linkers such as in the original model peptide did not yield oxidation side products.

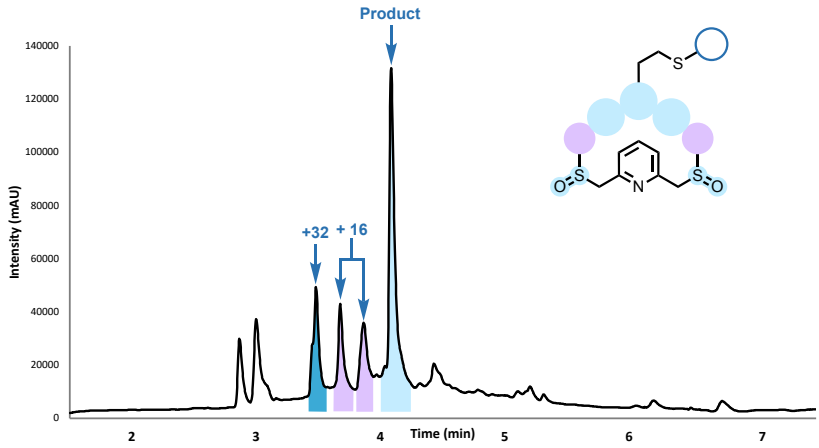

Figure 4.7: LC-MS analysis of crude reaction mixture for substrate containing pyridyl linker showing oxidation products.

To improve the reaction profile to yield only one major product, prevention of the oxidation was investigated. First, inclusion of one equivalent of the reducing agent TES was investigated, giving slight improvement with a product/+16/+32 ratio of 7:2:1. Use of DMF as the solvent for addition of thiol and initiator surprisingly gave a greater extent of oxidation, at 55%. Due to the oxidation occurring at the thioether groups not partaking in the TEC reaction, it was hypothesised that changing of factors that would improve TEC kinetics and allow for shorter reaction time may allow avoidance of thioether oxidation. Higher thiol equivalents can give faster reaction kinetics for the TEC reaction, while the oxidation kinetics remain unchanged and slower. Thus, shorter reaction time may be utilised to avoid oxidation. The use of 1 hour reaction time with 3, 5 and 10 equivalents of thiol was investigated. In each case, the oxidation products were reduced to a total of only 9% (~3% each). For the reaction with 10 equivalents of thiol, quantitative reaction was achieved. Use of 5 equivalents

of thiol gave high but incomplete conversion of 69%, whilst only 3 equivalents gave poorer conversion of 52%. Importantly, despite the extent of conversion, the amount of oxidised product was constant for each reaction. This implies a slower oxidation reaction occurring on the hydrothiolated product. Use of degassed reaction solvent was investigated, further lowering the extent of oxidation to 4%. Again, degassed DMF gave poorer results even than DMSO without degassing, at 11% oxidation. Finally, sealing the plate in an inert argon atmosphere using a simple plastic Aldrich® AtmosBag after distribution of reactants gave >99% desired product (**Figure 4.8**).

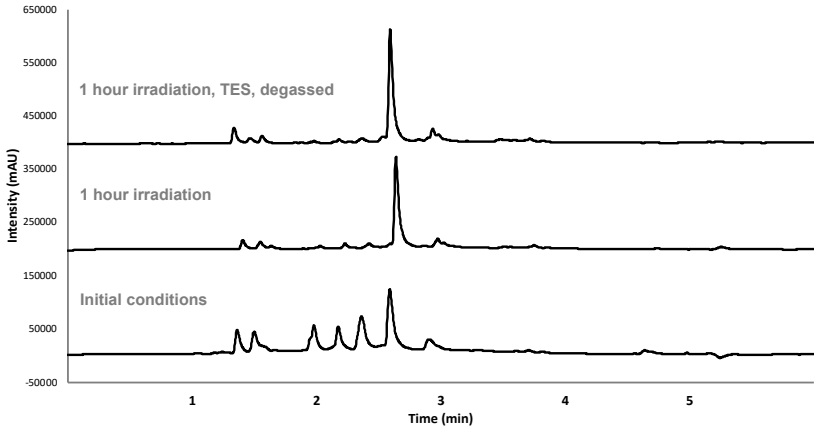

Figure 4.8: LC-MS analysis of crude reaction mixtures with varying measures to prevent oxidation.

Of course, it is still possible to apply this methodology to substrates that are not sensitive to oxidation without the need for extensive oxygen expulsion measures and with milder conditions using longer reaction times. Alternatively, if small amounts of oxidation are tolerated, varying measures may be used or excluded.

4.3.6 Thiol Scope

With suitable conditions in hand for different peptide substrates, it was necessary to investigate the thiol scope compatible with the methodology. Initial tests using the simple aliphatic thiol Mpa were successful, but use of aromatic thiols was not trivial, in part due to their potential for oxidation as was seen for aromatic thioether linkers. Initially, the use of thiophenol (**4.14h**) and benzyl thiol (**4.14d**) in the reaction gave little to no conversion. It was therefore hypothesised that this was due to their increased propensity to form disulfide dimers (**4.15d** and **4.15h**) in comparison to aliphatic thiols. Due to the significantly higher

concentration of the thiols in the reaction mixture in comparison to the peptide precursor, this may become the dominant pathway for consumption of the thiol component.

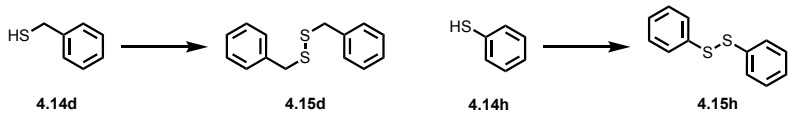

Scheme 4.1: Formation of disulfides for aromatic thiols.

To avoid this dimerization side reaction, the inclusion of the volatile reducing agent TES in the reaction mixture was investigated. Whilst Tris(2-carboxyethyl)phosphine (TCEP) is often the reducing agent of choice for disulfide cleavage, TCEP has been shown to desulfurise thiol groups, forming a reactive primary *C*-centred radical.[226,227] This is likely to lead to a mixture of products, including hydrothiolated and hydroalkylated substrate, but also unconsumed starting material. The presence of multiple peptide products would hamper applications of the crude reaction mixtures. Additionally, TCEP is non-volatile and therefore, unlike TES, would not be removed during RVC.

Inclusion of TES in the mixture gave full conversion of the substrate in the case of the benzylic thiol, with no difference observed whether 5 or 10 equivalents of TES were used. Unfortunately, the thiophenol example gave no conversion to the desired product. Reactions using 4-methoxythiophenol or 4-hydroxythiophenol were also unsuccessful.

4.3.7 High-Throughput Considerations

ADE has previously been applied both to automate and miniaturise reactions for optimisation investigations[228] and in library applications. ADE provides a highly useful approach in avoiding tedious, inefficient and error-prone manual pipetting steps.[42,229–231] To apply this TEC functionalisation approach in HT, inclusion of such automated dispensing technology was also desirable (**Figure 4.9**). Peptide substrates in DMSO stock solutions were distributed into 1,536 well-plates compatible with acoustic dispensing by ADE using a Labcyte Echo 650 acoustic liquid handler. ADE allows automated dispensing of 2.5-5000 nL volumes, which are often either difficult or not possible by other means such as pipette transfer. Stock solutions to be dispensed are placed in a compatible source plate used by the instrument. The user then determines the destination plate layout in terms of selecting source wells and transfer volumes for each destination well. The instrument then uses acoustic waves to transfer exact volumes from the source plate to the inverted destination plate.

Further, the transfer is contactless, so no tips or tubing that may lead to waste or require cleaning are used. A significant advantage of this approach is the very low dead volume, often in the µL range, which applies to the source plate. This makes the approach particularly useful for dispensing valuable stocks.

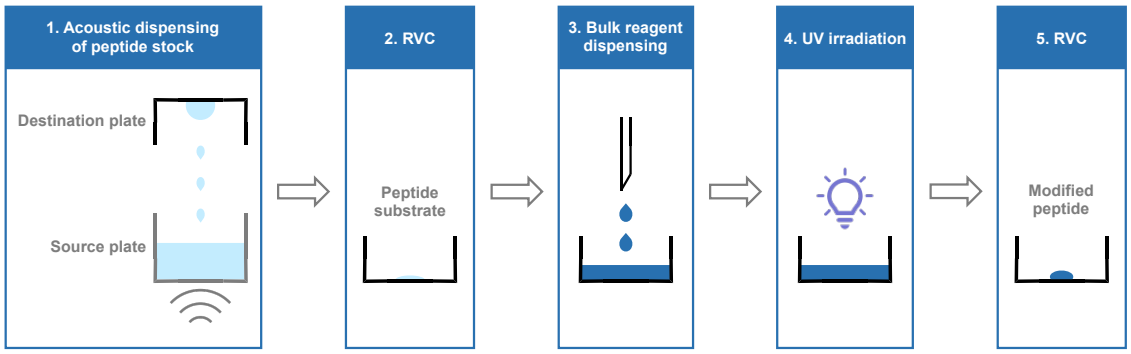

Figure 4.9: Schematic for ADE and HT-TEC workflow.

Following dispensing of substrate stocks, removal of the stock solution solvent was achieved by RVC, followed by dispensing of thiol, DPAP and TES in degassed DMSO using a Certus FLEX automated bulk dispenser. Use of bulk dispensing allows a significant reduction in repetitive pipetting steps and greatly speeds up the process. For example, 500 nL can be dispensed into 1,536 wells in as little as 39 seconds.[232] Stock solutions of reagents are dispensed accurately through microvalves using controlled air pressure typically in volumes of 10 nL to 5 µL. This process is highly efficient for dispensing of bulk solutions to multiple wells. However, unlike ADE, this approach to bulk dispensing has considerable dead volume both in the tubing and syringes or bottles used to hold stock solutions. Often, dead volume can be in the mL range, making this method unsuitable for valuable peptide stocks. For dispensing of commercial reactants such as in this case however, this bulk dispensing method provides a highly convenient and rapid method.

4.3.8 High-Throughput Scope Evaluation

Having developed the methodology thus far on single examples, the application of this approach in a HTE scope evaluation was undertaken. For this purpose, 12 peptide substrates divided into three groups were prepared using an identical synthetic approach as described for the initial model peptides (**Figure 4.10**). Peptides **4.13a-d** were included to allow investigation of varying functionality observed in canonical AAs. Following coupling of a Tyr and Agl residue to the Mea disulfide resin previously used, either Lys (**4.13a**), Val

(**4.13b**), Trp (**4.13c**) or Asp (**4.13d**) were coupled, followed by deprotection and cleavage as before. Lys was included to examine compatibility with basic residues and amines, as amines have previously been shown to slow the rate of TEC.[174] Val shows compatibility with alkyl groups for which hydrogen abstraction would form a relatively stable tertiary radical. Trp was included as its side chain indole possesses sp^2 character and therefore may allow generation of side products due to thiyl radical attack. Asp shows compatibility with negatively charged functional groups such as the carboxylic acids found in peptides and proteins. Peptides **4.13e-f** were synthesised using the same sequence, with the previously varied AA replaced by a Gly residue. In turn, four different *bis*-electrophilic linkers were used to cyclise the linear dithiol peptide obtained. This included 2,6-*bis*(bromomethyl)pyridine (**4.13e**), 2,6-*bis*(bromomethyl)benzene (**4.13f**), dichloroacetone (**4.13g**) and divinylsulfone (**4.13h**). These peptides were used as crudes from the cyclisation mixture to examine the potential for application in diversification of crude libraries. Finally, peptides **4.13i-l** incorporated different alkene structures in a backbone containing a Trp and Ala residue. Agl (**4.13i**) was incorporated as the standard alkene previously used. An alloc amine protecting group (**4.13j**) was also included as this allows ready access to varied alkene AAs. β-allylglycine (**4.13k**) was included to allow access to a greater variety of peptide backbones. *N*-allylglycine (**4.13l**) was included to investigate the compatibility of allyl amine type substrates.

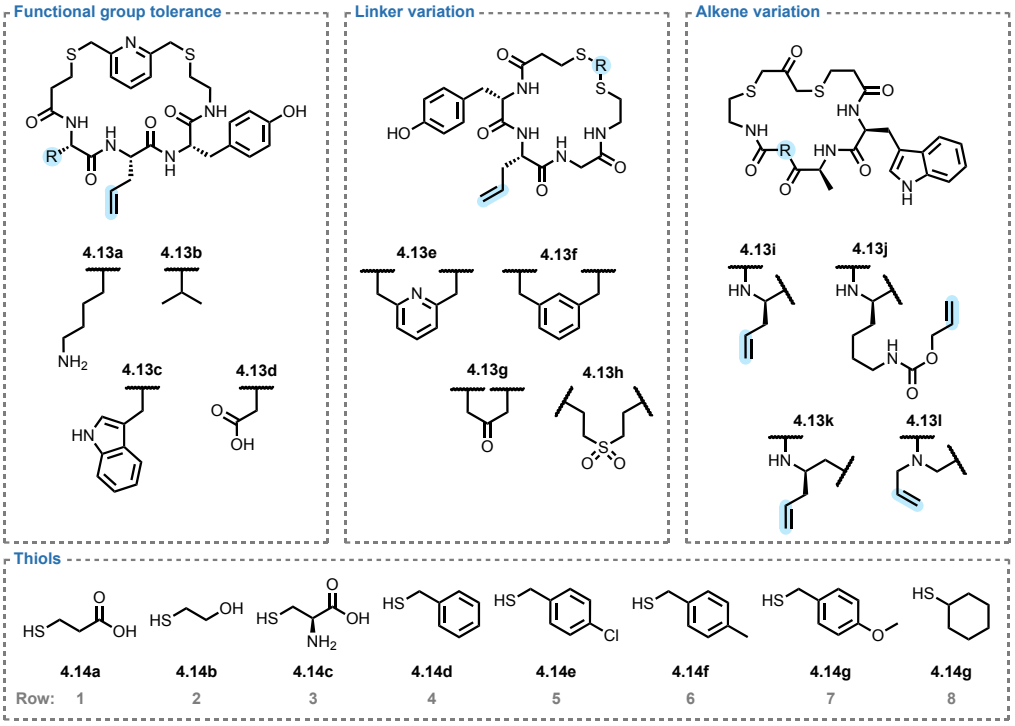

Figure 4.10: Structures of scope peptide substrates **4.13a-l** and thiols **4.14a-g** distributed in rows 1-8.

In addition to varied alkene macrocycle substrates, a variety of thiols were included, both aliphatic (**4.14a-c**, **g**) and aromatic (**4.14d-g**). Notably, dissolution of cysteine (thiol 3) in DMSO to the desired 100 mM concentration could not be achieved, and inclusion of up to 20% water did not provide significant improvement.

For dispensing of peptide stocks, ADE was utilised. 40 mM stock solutions were transferred into 384-well source plates by pipette and from this, an Echo 650 acoustic liquid handler was used to transfer 1 μL peptide stock into each destination reaction well by ADE. The solvent was then removed by RVC to leave the peptide substrate pellet. Reactant solutions of 100 mM thiol, 50 mM TES and 10 mM DPAP in degassed DMSO were prepared and distributed by bulk dispensing using a Certus FLEX and the plate was centrifuged to ensure combination and mixing of droplets. The plate was then sealed in Ar atmosphere using an Aldrich® AtmosBag. The plate was next irradiated for 1 h followed by removal of volatiles by RVC. Each peptide was individually reacted with each thiol, for a total of 96 entries. Each entry was analysed by LC-MS and the relative amounts of peptidic materials used to evaluate the reactions. The results are therefore expressed as the percentage conversion to the desired product as a heatmap in **Figure 4.11**. Over all of the reactions, the peptide species observed were the desired product, starting material, oxidised product and dithiolated peptide.

As expected, peptide **a** gave the lowest average desired product across the range of thiols at 89%, likely due to the amine moiety in combination with the oxidisable linker. Peptides **b**-**d** all gave slightly above 95% conversion to the desired product on average, implying that the amine is at least partly responsible for the poorer performance. Of the substrates containing varying linker structures, the sulfone substrate **h** showed the best results, averaging more than 99% desired product. Not surprisingly, the pyridyl linker substrate **e** was the worst performing at 93% desired product, as this linker combines basicity that can hamper TEC with oxidation sensitivity. Of the varied alkene substrates, little difference was observed for peptides **i**-**k**, each averaging around 95% desired product, showing potential for wide alkene compatibility. For peptide **l**, an average of 92% desired product was observed. This result is likely a result of the less stable *C*-centred radical intermediate formed during TEC for allyl amine substrates. The lower stability increases the

rate of the fragmentation that amounts to reversal of the initial thiyl radical attack on the alkene.

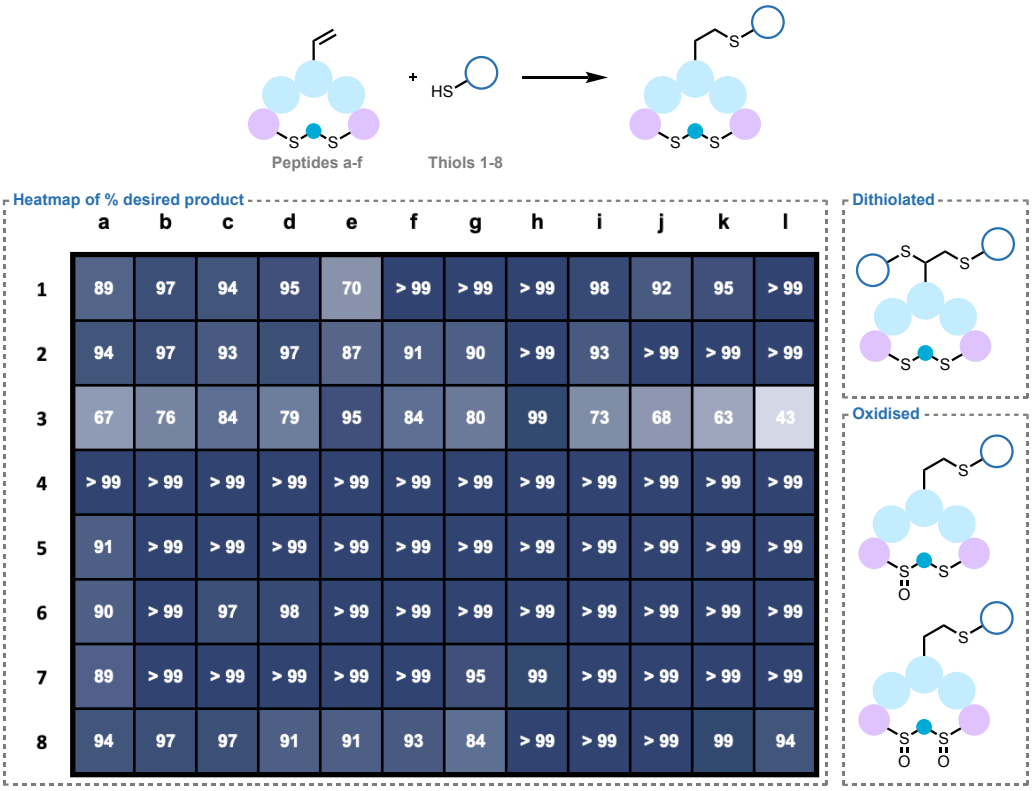

Figure 4.11: Heatmap for HT-TEC peptide modification and structures of observed peptide components of reaction mixtures. Peptides **4.11a-l** are distributed down the columns a-l while thiols **4.12a-g** are distributed across the rows 1-8. The % conversion to the desired product is calculated by identification and integration of all peaks observed in the LC-MS trace for each well.

For the thiols used, Mpa and BME gave good conversions, averaging 94 and 95% of the desired product respectively. Cys represents by far the worst performing thiol, though this is due to the lower solubility of the thiol reaction component, and gives an average of 76% desired product. The benzylic thiols performed exceptionally well in this methodology. Benzyl thiol gave quantitative conversion to the desired product in all cases, while (4-chlorophenyl)methanethiol gave greater than 99% desired product on average, with only one example not showing a quantitative result. The remaining *p*-tolylmethanethiol and (4-methoxyphenyl)methanethiol both averaged 99% desired product. The bulkier aliphatic cyclohexanethiol gave slightly lower conversion to the desired product, often with some staring material remaining, but still gave an average result of 95%. The results obtained for

the range of thiols show excellent tolerance for a range of structures, with the limiting factor being thiol solubility.

Overall, of 96 examples, 81 (85%) gave > 90% conversion to the desired product, with an average of almost 95% conversion to the desired product for the whole set. The range of both peptide substrates and thiol modifiers was well tolerated. In particular, the benzylic thiols 4-7 gave particularly clean results with an average of over 99% conversion to the desired product.

4.4 Conclusions & Future Work

A suitable reactor for UV irradiation of samples in a microwell plate was successfully constructed and tested. This reactor was subsequently used to investigate the compatibility of TEC with the particular limitations imposed in high-throughput chemistry, principally the lack of potential for stirring or agitation. The TEC reaction showed good compatibility, with suitable initiation of DPAP observed *via* the formation of benzaldehyde, and quantitative consumption of an alkene substrate even in mild conditions and without a photosensitiser additive.

To test this approach for diversification of peptide macrocycles to yield high purity crudes for direct screening, two types of macrocycle substrates were synthesised. Furthermore, the reaction was downscaled to 4 µL volumes, using only 40 nmol of substrate. The macrocycle containing a disulfide bond showed multiple products in the reaction mixture and therefore was not investigated further. However, the dithioether cyclised substrate showed excellent reaction profile. Investigation of substrate concentration effects showed that a relatively low concentration of 10 mM is compatible with the approach, while good conversion can still be obtained as low as 5 mM. Additionally, RVC of the crude reaction mixture can remove the DPAP photoinitiator additive. Upon extension of the peptide macrocycle scope to those incorporating aromatic linkers, oxidation of the thioethers contained within the macrocycle was observed. Further optimisation of the reaction conditions facilitated avoidance of such oxidation through use of TES additive and inert atmosphere.

A high-throughput approach was then devised, allowing automated handling of macrocycle substrates and additives through use of an Echo system for peptide stock dispensing and a Certus Flex bulk dispensing system. For a small scope library

demonstration, 12 peptide substrates were synthesised, incorporating different AAs, linkers and alkene structures. These were combined with 8 thiols, both aromatic and aliphatic, in a 96-entry substrate scope. LC-MS analysis of each entry in the scope revealed an average of 95% desired product, with excellent reaction profiles. Aromatic thiols demonstrated the best profile, with many affording almost pure desired product.

Future work will apply this technology to the optimisation of therapeutic peptide sequences (**Figure 4.11**). In particular, lipopeptides often pose challenges for both synthesis and purification. In contrast, synthesis of an alkene tagged peptide lacking the lipid chain will not pose the same solubility challenges. A variety of lipid chains can then be readily installed *via* high-throughput TEC and directly screened to rapidly optimise lipid structure, following which individual hits may be individually scaled up and synthesised. Similarly, individual residues of other biologically active peptides may be optimised through this approach. Additionally, it is important to emphasise that this technology is not limited to peptide substrates, and small molecule therapeutics may also be optimised or combined through this approach, providing a new reaction for combinatorial syntheses. Additionally, further work will investigate the use of thiol-reactive resins that could be used to scavenge non-volatile thiols, thus facilitating formation of higher molecular weight dimers and use of thiols that may themselves possess significant bioactivity.

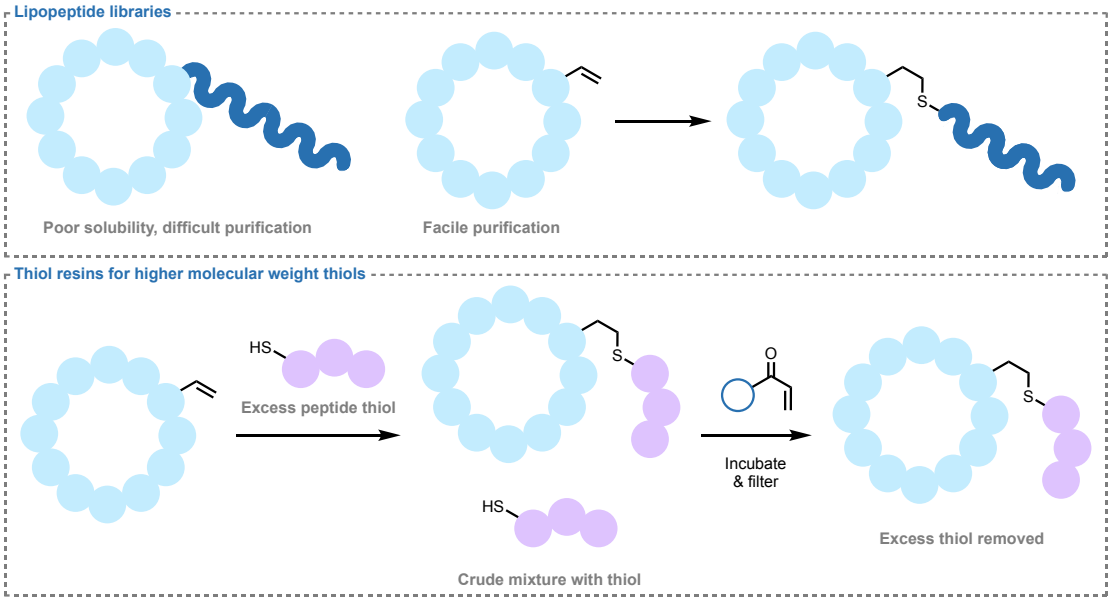

Figure 4.11: Future work on optimisation of lipopeptide structure and incorporation of non-volatile thiols that can be removed using a thiol-reactive resin.

Chapter 5

Thiol-Ene Mediated Labelling of Alkenes on the Cell Surface

"If you learned something from it, it's not a failure."
- Prof. Carolyn Bertozzi on scientific research.

5.1 Introduction

Glycosylation is a key PTM effecting protein function and localisation, and cell surface glycans play vital roles in cell adhesion, signalling and interaction. Furthermore, glycosylation also varies depending on a cell's physiological state. Variations are observed depending on the developmental state of a cell as well as in disease.[233,234] As a result, cell surface glycans can provide useful information in the study of many important biological processes.[97] For such studies chemical tools are often needed. One highly prominent approach is that discussed in **Chapter 1** (section 1.4), in which click reactive analogues of native sugars can be incorporated into glycans by engineering of the cells own metabolism, and then labelled with fluorophores for microscopy, or with other probes. While SPAAC has become prominent in this application, use of only one click reaction only allows study of one monomer type per cell sample. The introduction of new biorthogonal chemistries,[235] however, allows labelling of different monomer analogues bearing different reactive groups with orthogonal reporter molecules, allowing direct comparative observation of different sugars on the same cells.[236]

To date, the TEC reaction has yet to be fully investigated in the context of biorthogonality for applications such as cell surface glycan labelling. Application of alkene hydrothiolation in a cellular system has not yet been reported. Recent advances[102] and the work included in this thesis have developed on methods for initiation of TEC without the need for high energy UV light, improving on the biocompatibility of the reaction. While the presence of cellular thiols is a concern still to be overcome for intracellular applications, the labelling of cell surface structures on the extracellular side in cell culture presents a more controlled environment for investigation of the bioorthogonal potential of this reaction.

5.2 Aims

The overall aim of this project was to apply TEC to covalent labelling of alkenes in a cellular context. For this demonstration, incorporation of an alkene-containing sugar monomer into cell-surface glycans by metabolic engineering was to be used. This allows the study of glycan synthesis and protein PTMs, and while other chemistries have been used for such a purpose, an additional orthogonal approach in use of TEC chemistry will provide a useful tool.

First, it was necessary to synthesise a suitable alkene-containing sugar. For this purpose an *N*-acyl glucosamine analogue was selected, allowing attachment of the alkene to the acyl group. The synthesis of this target molecule was therefore undertaken. The second component necessary for investigation of cell surface glycan labelling is a suitably reactive thiol fluorophore. To date, reports of such compounds are limited and show poor or inconsistent results or require complicated and well-controlled reaction mixtures. To identify a suitably reactive thiol fluorophore, a range of fluorescent cores were to be investigated and their thiol derivatives synthesised. The reactivity of such compounds was then to be investigated in an easily quantifiable manner in *in vitro* experiments to confirm their efficiency prior to application to cell glycan labelling.

Finally, the modified sugar was to be fed to cells, allowing incorporation onto cell surface glycans. The designed fluorescent thiol was then to be applied to covalent labelling of the modified sugar within the glycans, allowing visualisation of their expression. Further experiments may then apply orthogonal SPAAC labelling of an azide analogue of another sugar monomer of interest, allowing comparative or dual investigation of monomers in the same cell sample.

5.3 Results & Discussion

5.3.1 Synthesis of Alkene-Containing GlucNAc Analogue

It was first necessary to synthesise the alkene-modified GlucNAc analogue, which would be metabolically incorporated for labelling. This would consist of an acetyl protected glucosamine ring, with a pentenoic chain installed at the amine.

Starting from glucosamine hydrochloride (**5.**1, Scheme **5.1**), the amine is protected using anisaldehyde **5.2** in 1.0 M NaOH to give the imine-protected sugar **5.3** in reasonable yield of 62%, with purification achieved through washings to remove both unreacted sugar and anisaldehyde. Following this, acetylation of the hydroxyl groups using conditions previously utilised within the Scanlan lab afforded fully protected sugar **5.4** in rather poor yield of 15%. Increasing the reaction time to 18 h and adding catalytic DMAP however, gave 68% yield of the desired product at multigram scale without need for chromatographic purification. The imine was then readily deprotected in 5.0 M HCl to give the amine salt **5.5** in high yield of 88%. Finally, reaction of the free amine with pentenoyl chloride yielded the target compound **5.6** in a good yield of 80%.

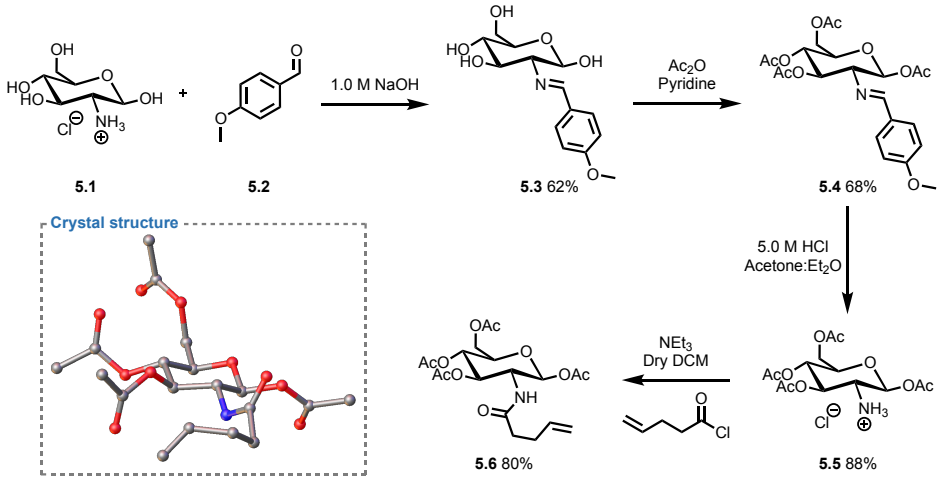

Scheme 5.1: Synthesis of alkene-modified GlucNAc analogue.

Additionally, following purification of the target by flash chromatography, it was observed that the product formed crystalline needles when the solvent was allowed to slowly evaporate. A small sample of the compound was taken and dissolved in DCM and placed in a sample vial in an ether chamber to crystallise by Et_2O diffusion. By this process, as the Et_2O antisolvent evaporates and condenses into the DCM, formation of product crystals is slowly induced, allowing formation of larger and higher quality crystals. After 3 days, the formation of large crystals was observed. A single crystal specimen was examined by X-ray diffraction to determine the molecular structure.

5.3.2 Dansyl Thiol Fluorophores

Initially, a simple dansyl fluorophore was selected for investigation, in part due to the ready availability of dansyl chloride, facilitating ready modification to install a thiol group (**Scheme 5.2**). The reaction of dansyl chloride **5.7** with cystamine dihydrochloride in aqueous alkaline conditions yielded bi-dansyl cysteamine **5.8**, in which the thiols are protected as a disulfide. This disulfide is readily cleaved using reducing conditions, for which a myriad of approaches are possible. In this case the reduction of this disulfide using zinc dust in the presence of acid then furnished the free thiol **5.9**, while the zinc dust was easily removed *via* filtration.[237] This synthetic approach yielded the target compound in an efficient manner requiring no chromatographic purification.

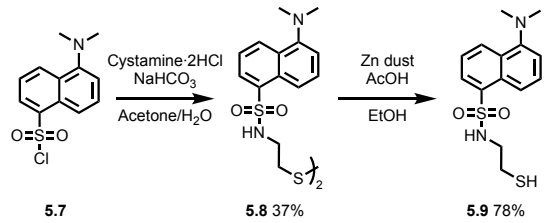

Scheme 5.2: Synthesis of a simple dansyl thiol.

With the dansyl thiol in hand, a test reaction was undertaken with the previously synthesised GlucNAc alkene reaction partner **5.6** (**Figure 5.1**). Initially, the reaction was tested with no photoinitiator or photosensitiser additives to examine if they would be necessary. Use of DMSO-d_6 as the reaction solvent allowed for direct determination of reaction progress *via* monitoring of the alkene peaks in the ^{1}H NMR spectrum. Unfortunately, no consumption of the alkene to give **5.10** was observed. As a result, the reaction was repeated using DPAP photosensitiser, but again no consumption was observed. Finally, the reaction was repeated in EtOAc and using both DPAP and MAP. Previous optimisation studies for TEC applications with small molecules have often shown EtOAc to be the most favourable solvent, and so it was investigated to examine if the DMSO had been the cause of the lack of reaction. However, still no alkene consumption was observed. Additionally, the peak corresponding to the thiol proton in the ^{1}H NMR spectrum was no longer visible, whilst the remaining peaks for the starting material did not show significant change. It is therefore possible that disulfide formation was occurring during the reaction. HRMS analysis showed no presence of desulfurised products.

To examine which reaction component was the cause for the lack of reaction, each was individually reacted with a different reaction partner for which TEC had previously been performed. The GlucNAc analogue **5.6** was reacted with thioacetic acid (**5.12**) in EtOAc in the presence of DPAP and MAP, giving quantitative alkene consumption to form **5.14** and showing that the alkene component was indeed reactive. On the other hand, the dansyl thiol **5.9** was reacted with allyl acetate (**5.11**) in EtOAc in the presence of DPAP and MAP to form **5.13**, but gave no alkene consumption. Thus, it was concluded that the thiol component was responsible for the lack of successful reaction.

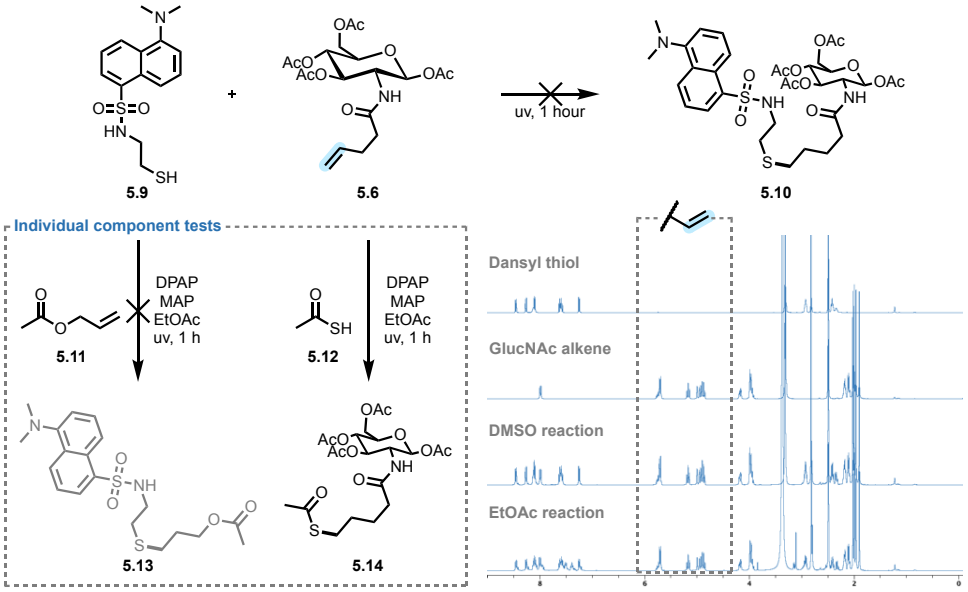

Figure 5.1: Unsuccessful reaction of dansyl thiol with GlucNAc alkene and reactions of individual components.

It was therefore hypothesised that the proximal NH of the sulfonamide group was responsible for the lack of reactivity, as it may allow abstraction of the proton to quench the thiyl radical. For this reason, the synthesis of an *N*-methylated dansyl thiol was undertaken. Additionally, the chosen synthetic route would incorporate a TEC reaction with a dansyl alkene rather than the thiol, which would verify the compatibility of the fluorophore core with the reaction. First, dansyl chloride (**5.7**) was reacted with *N*-allylmethylamine (**5.15**) to afford the methylsulfonamide containing dansyl alkene **5.16** in a quantitative yield. This was then reacted with thioacetic acid using DPAP and MAP photoinitiator and photosensitiser, successfully yielding the desired acetyl thioester product **5.17**. Notably, this also shows compatibility of an alkene fluorophore with TEC. The thioester is then readily cleaved in basic conditions to yield the target thiol **5.18**, with an overall 33% yield for the three-step synthesis (**Scheme 5.3**). This dansyl thiol was then subjected to the same reaction conditions as previously with allyl acetate in EtOAc in the presence of DPAP and MAP, and again no alkene consumption was observed.

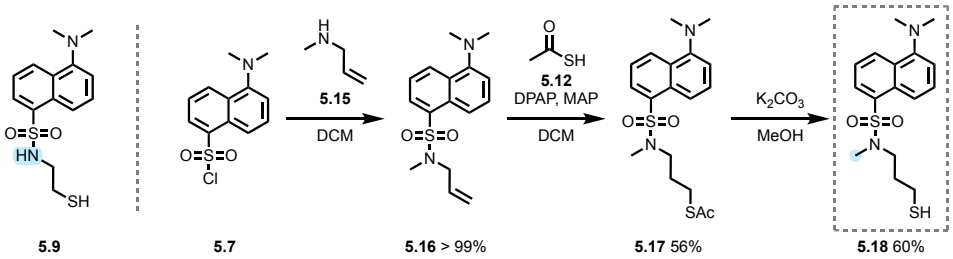

Scheme 5.3: Synthesis of *N*-methylated dansyl thiol.

Meanwhile, investigation into the use of BODIPY thiols for TEC was under investigation in the Scanlan lab, and was meeting similar challenges. It was therefore concluded that alternative fluorophores should be investigated, with the aim to develop a TEC compatible thiol fluorophore.

5.3.3 Napthalimide Thiol Fluorophores

Next, the napthalimide core was chosen for investigation. The use of napthalic anhydride derivatives to synthesise a range of napthalimides provides a convenient route towards synthesis of a napthalimide thiol. Initially, the reaction of cysteamine dihydrochloride with 4-nitro napthalic anhydride **5.19a** was performed (**Scheme 5.4**). As in the synthesis of the initial dansyl thiol, the thiol is conveniently protected as a disulfide. The nitro group then provides a convenient functional handle for further modification to improve fluorescent properties, likely through reduction to the amine, which may then be further modified if desired. The coupling of the cysteamine to the napthalic core yielded a brown solid. However, the poor solubility of this compound limited its manipulability for both characterisation and further synthetic manipulation. Nevertheless, ^{1}H NMR spectroscopic analysis showed promise and so the material was telescoped directly for reduction of disulfide **5.19b** using DTT. Attempts to work up the reaction led to formation of precipitate, as well as partial dissolution in both aqueous and organic layers. The reaction was repeated and the napthalimide components precipitated using ice-cold H_2O and isolated by filtration, however it is important to note that this will also include any unreacted starting material. ^{1}H NMR spectroscopic analysis of the crude showed little conversion to the desired thiol **5.19c**, with no visible thiol peak or change in splitting of the CH_2 α to the thiol compared to the disulfide as would be expected. Attempts towards more forcing conditions including higher DTT equivalents, additional DIPEA as a base additive or extended reaction times with heat proved fruitless in formation of the desired product.

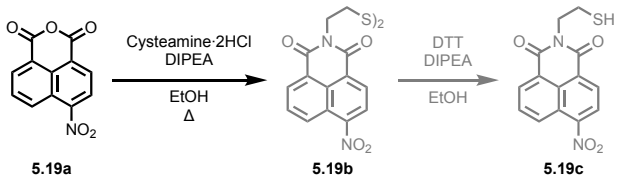

Scheme 5.4: Attempted route for synthesis of a napthalimide thiol.

It was then decided to modify the target to remove the nitro group, with the aim of improving solubility and therefore the ease of handling and purification. Additionally, a modified synthesis to use cystamine was envisaged. For this reaction, nucleophilic attack by the thiol was not of concern, as the thioester product formed is quite labile. Indeed, a product corresponding to napthalimide formation was obtained, however no thiol peak was observed in the ^{1}H NMR spectrum. Acidification of the mixture did not result in observation of a thiol peak. However, an Ellman test was positive for the presence of a thiolate. At this point, due to the poor solubility of napthalimide derivatives and the difficulty of forming a thiol, it was decided to pursue an alternative approach.

5.3.4 Peptide-Inspired Fluorophores

As TEC using peptide thiols has previously been extensively developed both in this thesis and elsewhere, the synthesis of a fluorescent peptide thiol was undertaken. The design for such a target would incorporate three elements; a reactive thiol, a fluorescent group, and a diamine linker (**Figure 5.2**). The simplest design envisaged would compose of a Cys-Lys dipeptide, in which the Lys sidechain is functionalised with a fluorophore (**5.20a**). In this case, the dansyl fluorophore was again included, as it could provide a direct comparison to the simple dansyl thiol previously obtained. However in this case, the thiol is at a much more distant position with 9 atoms between the fluorophore and sulfur atom. Modifications to the design included use of an amide *C*-terminus to avoid acidic quenching of the dansyl group, removal of the unnecessary Cys amine group (**5.20b**), as well as swapping the positions of the thiol and fluorophore component to provide a highly flexible thiol (**5.21**). Additionally, the Lys *C*-terminus could provide a modification point for installation of useful functionalities for solubility or other tags in later generations.

An added advantage of such a peptidic thiol is that is amenable to SPPS, allowing rapid synthesis of the desired product with minimal purification steps. First, a sidechain methyltrityl (Mtt) lysine derivative was coupled to Rink amide resin. As for the Mmt group

discussed in **Chapter 2**, this protecting group can be selectively removed on resin, and was done so using a DCM/TFA/TES (90:5:5) cocktail, with 5 x 1 minute treatments of the resin. Successful deprotection can then be verified using the bromophenol blue test. Then, *S*-trityl protected mercaptopropionic acid was coupled to the Lys sidechain using traditional SPPS amide bond formation. Following this, the Lys *N*-terminal amine Fmoc group was removed using 20% piperidine in DMF. Installation of the dansyl group was then achieved through treatment of the resin with dansyl chloride in DMF for 2 h, with capping of the amine again verified by the bromophenol blue test. Removal from the resin and trityl deprotection was then achieved by standard resin cleavage conditions using a TFA/EDT/H_2O/TES (94:2.5:2.5:1) cocktail for 90 min to yield the target compound **5.21**. NMR spectroscopic and HRMS analysis showed that the desired product **5.21** was successfully obtained.

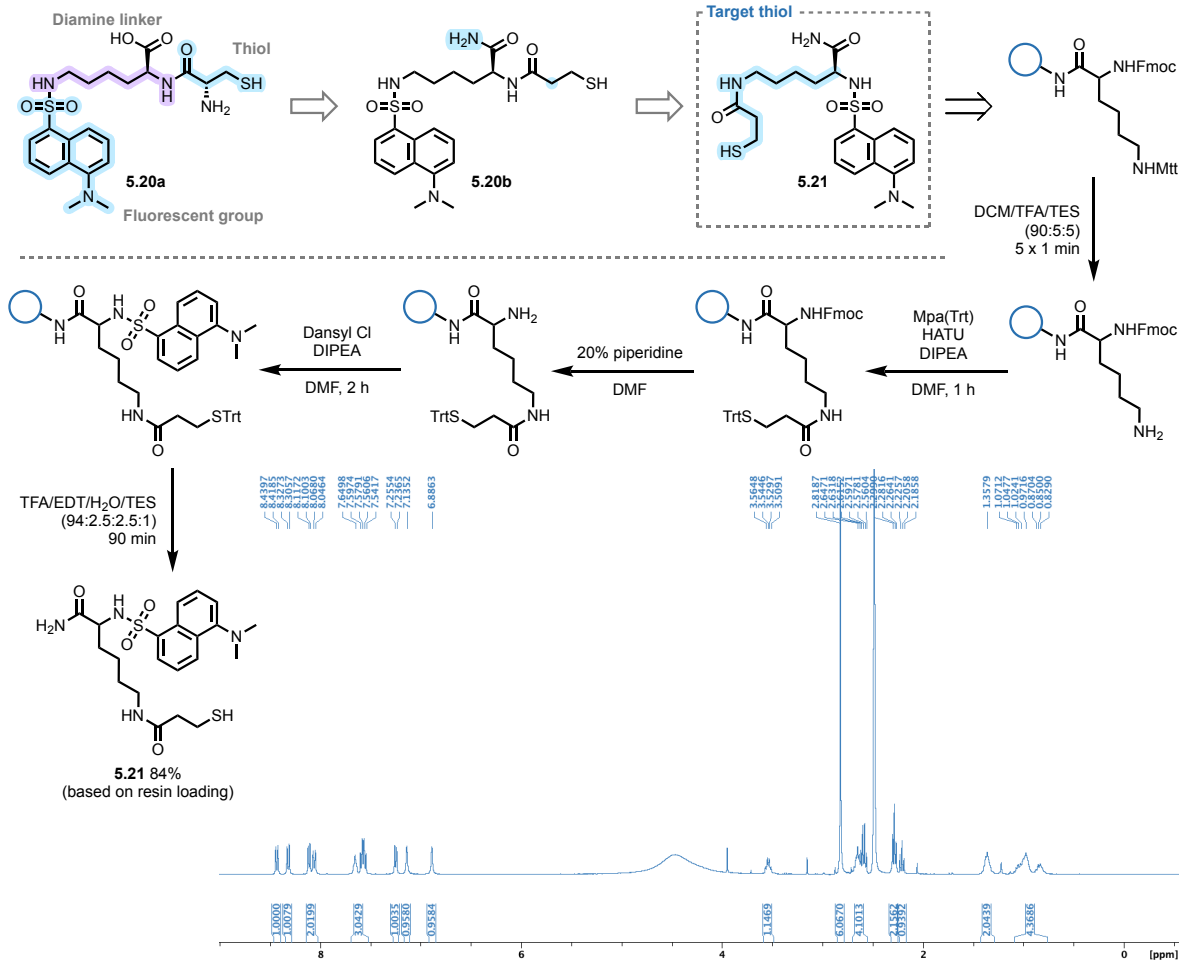

Figure 5.2: Design of the synthesised peptide thiol, synthesis by SPPS and ^{1}H NMR spectrum of the product obtained.

With the fluorescent dipeptide thiol in hand, investigation of its compatibility with TEC was undertaken. Due to the lack of solubility of the thiol compound in EtOAc, the

reaction was investigated in DMSO-d_6, again allowing direct determination of alkene consumption by ^{1}H NMR spectroscopic analysis. The reaction was again performed with both DPAP and MAP, however again no alkene consumption was observed.

It was then hypothesised that, for the case of the dansyl fluorophore, absorption of the 365 nm light used to initiate TEC was hindering reaction progress. Therefore, it was decided to investigate the use of blue LED initiation. For this purpose, an alternative initiator was required. Previous work in the lab had investigated the use of thioxanthene-9-one as a blue LED TEC photoinitiator with success and therefore this was chosen. Unfortunately, use of catalytic photoinitiator did not result in any alkene consumption, nor did an excess of photoinitiator.

5.3.5 The "Disulfide-Ene" Approach

Recently, an analogous reaction to TEC was reported by the Glorius group in which thiyl radicals were produced from a small range of disulfides, and reacted with alkenes.[238] It is reported that the formation of the thiyl radical takes place *via* an energy transfer activation, rather than the more traditional fragmentation of an initiator leading to proton abstraction from the thiol. Additionally, Li *et al.* reported the use of dansyl disulfide **5.8** in a radical mediated alkene hydrothiolation.[239] It was therefore reasoned that attempting to react a disulfide fluorophore with an alkene may provide insight into the issues experienced previously.

The Glorius group reported the use of a range of photocatalysts, among them benzophenone was included and was on hand. The reaction was therefore performed using harsh conditions in attempt to force conversion. Two equivalents of dansyl disulfide **5.8** (4 equivalents of reactive thiol) and equimolar benzophenone were irradiated at 365 nm in the presence of allyl acetate. However, disappointingly no alkene conversion was achieved. This experiment implies that the mode of activation is not the factor limiting the reactions under investigation, and so it was decided to continue with traditional TEC chemistry.

5.3.6 Aminobenzamide Thiol Fluorophores

With still no successful fluorophore having been obtained, the use of the simple aminobenzamide (Abz) fluorophore was investigated. These derivatives of anthranilic acid possess a very simple core, without an extended aromatic or largely unsaturated system. The most simple Abz thiol designed consists of anthranilic acid coupled to cysteamine. To access this compound, three possible routes were envisaged incorporating different protecting group approaches (**Scheme 5.5**); (1) completely unprotected reactants, (2) Boc-protected anthranilic acid and disulfide protected thiol and (3) Boc-protected anthranilic acid and Trt-protected thiol.

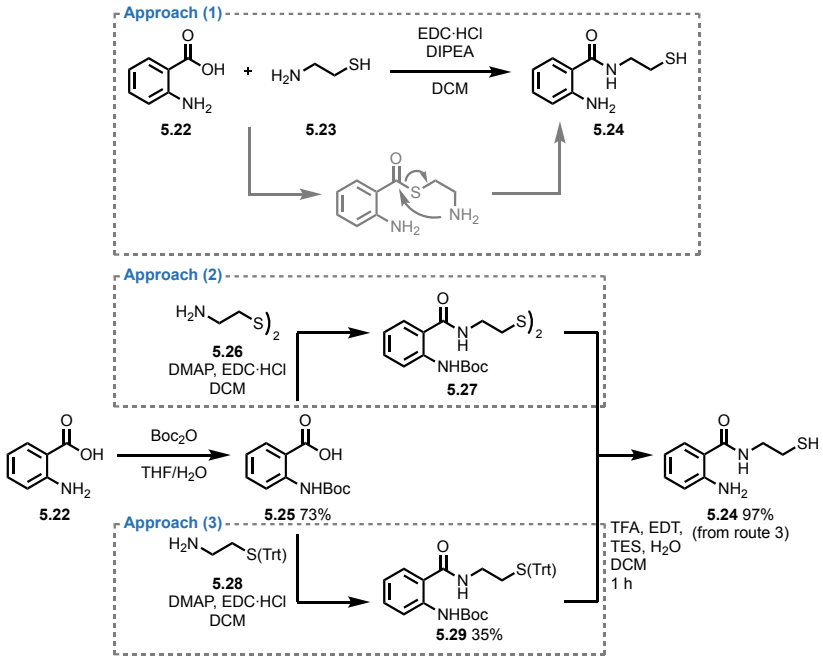

Scheme 5.5: Different synthetic approaches to the AbzSH target.

For approach (1), the use of unprotected anthranilic acid (**5.22**) and cysteamine **5.23** was investigated. The lower nucleophilicity of the aromatic amine should prevent significant formation of the acylated anthranilic acid derivative. Additionally, and as mentioned previously, the thioester formed by attack of the thiol as the nucleophile should be labile and readily acylate the amine of cysteamine to give the desired product. However, attempts towards coupling of these two components using EDC·HCl gave no desired product.

Approach (2) utilises cheap cystamine dihydrochloride (**5.26**) starting material and therefore was investigated next. Additionally, it was decided to protect the amine of the anthranilic acid coupling partner. This is readily achieved using Boc_2O, with any unreacted amine starting material readily removed by washing of the organics with acid. The amide

bond formation was then attempted again using EDC·HCl. After stirring overnight, significant precipitate was observed in the reaction mixture, with no product observed by TLC. Addition of DMF with the aim to dissolve precipitated components gave no significant improvement.

Finally, approach (3) was attempted, in which the individual components are protected using the acid-labile Boc and trityl protecting groups which may be simultaneously removed. In this case, the coupling of Trt-cysteamine (**5.28**) with Boc-anthranilic acid (**5.25**) was successful, albeit in moderate yield. With the doubly protected Abz thiol **5.29** in hand, deprotection was achieved using TFA in DCM to yield the desired Abz thiol (AbzSH, **5.24**) target.

The TEC reaction of this simple AbzSH fluorophore was then investigated (**Figure 5.3**). An initial small scale test reaction with allyl acetate **5.11** and DPAP in DMSO-d_6 was first attempted, and graciously gave quantitative alkene consumption. The reaction of this thiol with the GlucNAc alkene analogue **5.6** to give **5.30** was then attempted on a larger scale in EtOAc. However, after irradiation for 90 minutes, a significant colour change to an orange solution with orange precipitate was observed, and no alkene consumption was achieved. Due to this result, it was decided to investigate the reaction further at a small scale with direct NMR spectroscopic analysis. The reaction between AbzSH **5.24** and the GlucNAc analogue **5.6** was performed in both DMSO and EtOAc. As for the large scale reaction, the small scale EtOAc reaction gave an orange colour and precipitate, and no alkene consumption was observed. However, the same reaction performed in DMSO-d_6 gave quantitative alkene consumption. Examination of the reaction mixture by TLC, NMR spectroscopy and HRMS confirmed the formation of the desired product with excellent profile for the reaction performed in DMSO.

Following from this promising result, the reaction was performed in a 1:1 mixture of DMSO and H_2O, again giving quantitative formation of the desired product. Further, a 1:1 mixture of DMF and H_2O gave the same result. It was therefore clear that the EtOAc has an inhibitory effect on the reaction, possibly due to poorer solubilisation of the radical. However, for applications to cell labelling, aqueous solvent mixtures with DMSO for solubilisation of components are most desirable and therefore this system should be appropriate.

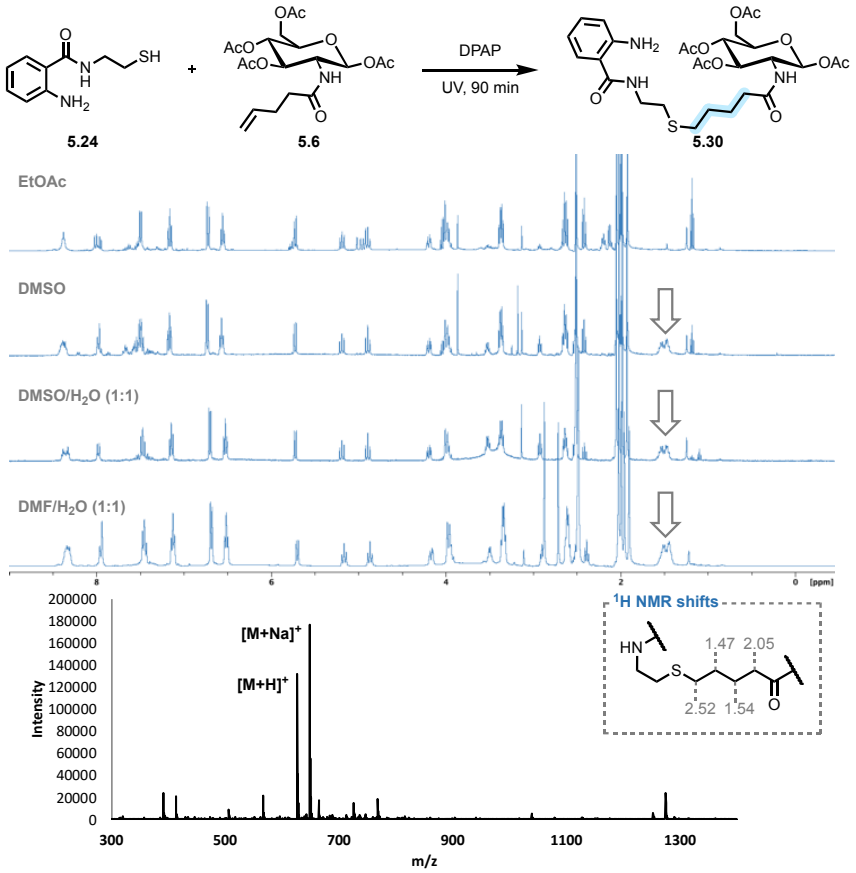

Figure 5.3: Analyses of reaction mixtures showing quantitative consumption of the alkene with clear formation of new peaks at ~ 1.5 ppm corresponding to the two CH_2s formed in the desired product. HRMS of the crude shows product mass.

However, the use of the Abz fluorescent group is not suitable for cell fluorescence labelling experiments for microscopy due to the low excitation wavelength of the Abz core at 320 nm which is not compatible with most microscopes. As a result, it was necessary to further investigate alternative fluorophore cores, with the knowledge in hand that a reactive thiol fluorophore can be designed. Importantly, the successful reaction of this thiol fluorophore with an alkene under UV initiation demonstrates that it is possible to perform a TEC reaction with a thiol fluorophore.

Nevertheless, AbzSH probe **5.24** may be useful for labelling of alkenes where the application is not limited to microscopy. For example, fluorescence of the Abz core may be quenched by a proximal nitrotyrosine moiety through a FRET process, making this pair highly useful for assay development.[240] Thus, this probe may be applied to such an assay in which alkene incorporation may be quantitatively measured *via* FRET quenching.

Additionally, the fluorescence resulting from this fluorescent group may be observed and/or quantified using gel imaging instrumentation.

A brief investigation into the utility of AbzSH **5.24** in labelling alkenes in a model system was then conducted.[d] To serve as a substrate, a modified BSA was prepared. This was achieved through synthesis of alkenyl NHS ester **5.31**, with which BSA was incubated for 5 h at pH 10 to acylate exposed Lys residues and provide the alkene handle. This material was then treated with a TEC cocktail consisting of AbzSH **5.24**, DPAP, and MAP in varying concentrations, and irradiated with UV light for 5 min. At 2.25 mM probe **5.24,** 0.7 mM DPAP and 4.9 mM MAP, clear fluorescent labelling of the BSA material was observed.

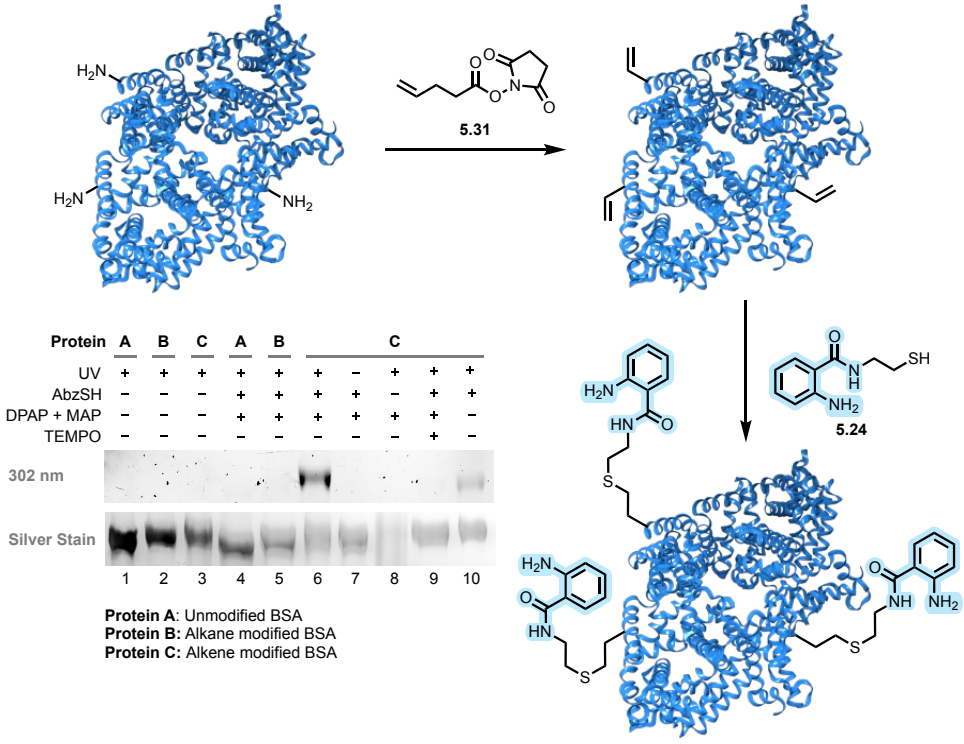

Figure 5.4: Fluorescent labelling of alkene-modified BSA[144] using the AbzSH probe.

A follow-up experiment incorporating a range of controls was then conducted (**Figure 5.4**). In this experiment, final concentrations for labelling of alkene-tagged BSA were 2.25 mM AbzSH probe, 0.7 mM DPAP and 4.5 mM MAP in 5% DMSO, irradiated under UV light for 5 min. Lanes 1-3 show two control proteins (unmodified or alkane modified) and the alkene-modified BSA without any additives but exposed to the same workflow. In lanes 4 and 5, the controls have been exposed to the labelling conditions, but show no labelling. This demonstrates that labelling does not occur as a result of either

[d]Protein labelling work was performed by Sean McKenna.

nonspecific binding with BSA or by hydrophobic interactions with the aliphatic Lys modifications installed. Lane 6 shows clear labelling of the modified BSA with AbzSH fluorescent probe **5.24**. Lack of irradiation shows no labelling, as seen in lane 7, implying that the TEC reaction is indeed the mechanism through which BSA is labelled. Of course, exclusion of the probe produced no labelling (lane 8). However, the silver stain reveals clear breakdown of the protein in this sample. This is likely due to reaction of the protein with the carbon-centred radicals produced through breakdown of DPAP. Interestingly, similar degradation is not observed in samples where the thiol is present, indicating that the thiol may intercept these radicals and prevent protein damage. In lane 9, the prevention of labelling by the radical scavenger TEMPO is observed, again indicating that the radical TEC reaction is the mechanism by which labelling is achieved. Finally, it was also possible to achieve labelling without the use of DPAP and MAP in lane 10, demonstrating successful labelling of alkenes using a single-component probe cocktail.

5.3.7 Fluorescein Thiol Fluorophores

Having successfully developed a reactive thiol fluorophore using the Abz core, it was necessary to focus on a fluorophore type suitable for microscopy. The fluorescein core forms a structural basis to which a number of other fluorophores are related, including the common Alexa Fluor variants. As a result, it is an attractive choice as a starting point for development of novel fluorophores. However, synthetic manipulation of fluorescein is somewhat limited due to its poor solubility, often meaning reactions must be performed in high-boiling DMF. For other non-synthetic applications, solubilisation can often be achieved in alkaline aqueous solution or with addition of DMSO.

Initially, a multi-step synthesis was envisaged (**Figure 5.5**), in which coupling of propargyl amine **5.33** with fluorescein-5(6)-carboxylic acid **5.32** would yield a fluorescein alkyne **5.34**. This would then be coupled with a synthetically prepared thiol azide through CuAAC to give **5.35**. To prevent poisoning of the copper catalyst, it is also necessary to protect the thiol moiety. However, the amide bond formation proved problematic in yielding a mixture of products. These three compounds were inseparable by column chromatography and likely consisted of both 5- and 6- substituted isomers which are desired, as well as product **5.37** resulting from ring opening of the lactone in the fluorescein core (**5.36**) and coupling to the resultant acid.

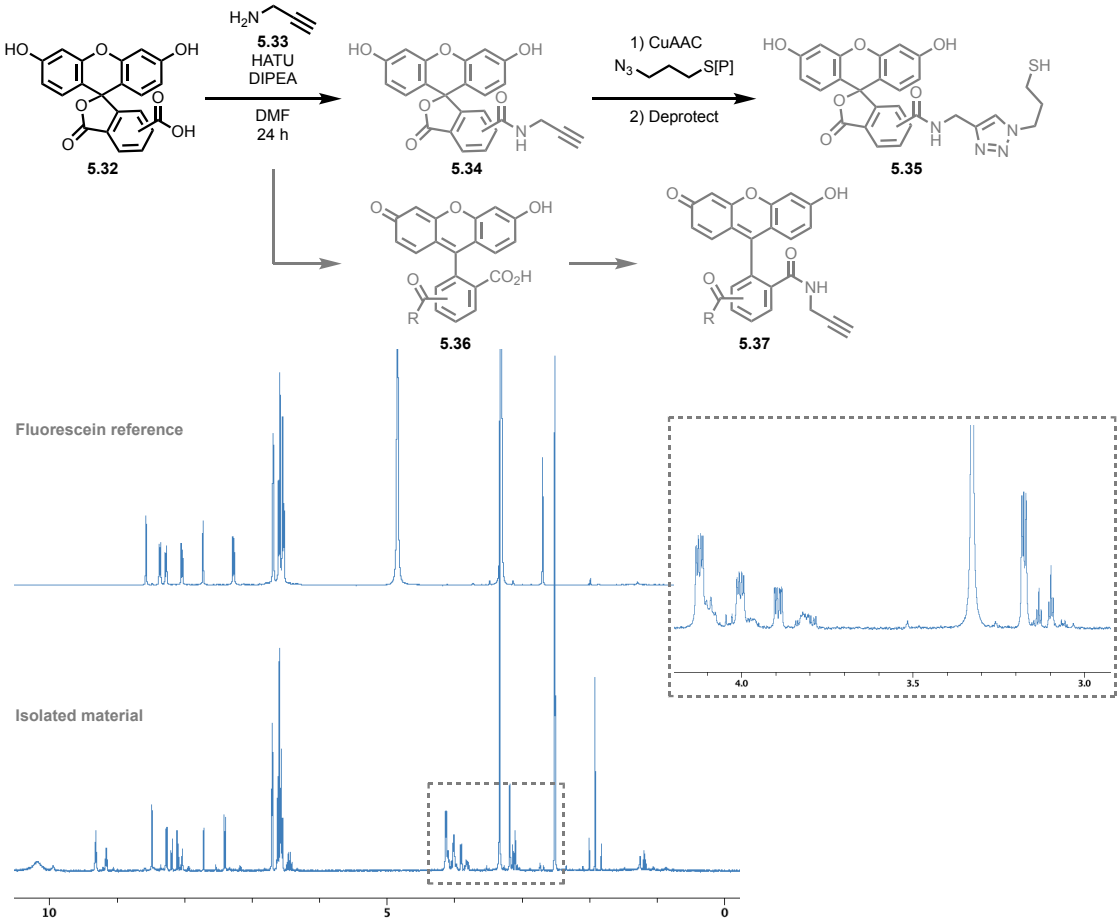

Figure 5.5: Initial synthetic plan and ^{1}H NMR spectroscopic analysis of mixture isolated from propargyl amine coupling, showing incorporation of multiple propargyl amine moieties.

As a result of this unsuccessful result, it was decided to attempt coupling of a thiol or thiol precursor to a preactivated fluorescein derivative, fluorescein isothiocyanate **5.38** (**Figure 5.6**). This can be readily reacted with an amine to yield the corresponding thiourea without the need for activating agents. The target compound **5.41** has previously been investigated by the Dondoni and Davis groups for use in TEC to modify biomolecules[241] and so was chosen for investigation. To install the thiol, fluorescein isothiocyanate was reacted with cysteamine (**5.39**) in the presence of DIPEA in DMSO overnight. The product was then precipitated out by diluting with ice-cold water followed by acidification using TFA, and then collected *via* centrifugation. NMR spectroscopic analysis showed successful thiourea formation, however no thiol was observed. It was therefore hypothesised that the thiol had been oxidised to the disulfide to give **5.40**, and so the product was dissolved in DMF and treated with TCEP·HCl for 3 h, following which it was again precipitated with cold water

and isolated by centrifugation. Usually, the presence of a thiol can be confirmed by an Ellmann test, producing a yellow coloured solution in the presence of a thiol. However, the strong red to yellow coloured solution of the product precluded this test. However, NMR spectroscopic analysis of this reduced material showed presence of the thiol peak and formation of the desired product **5.41**, which was obtained in an 83% yield.

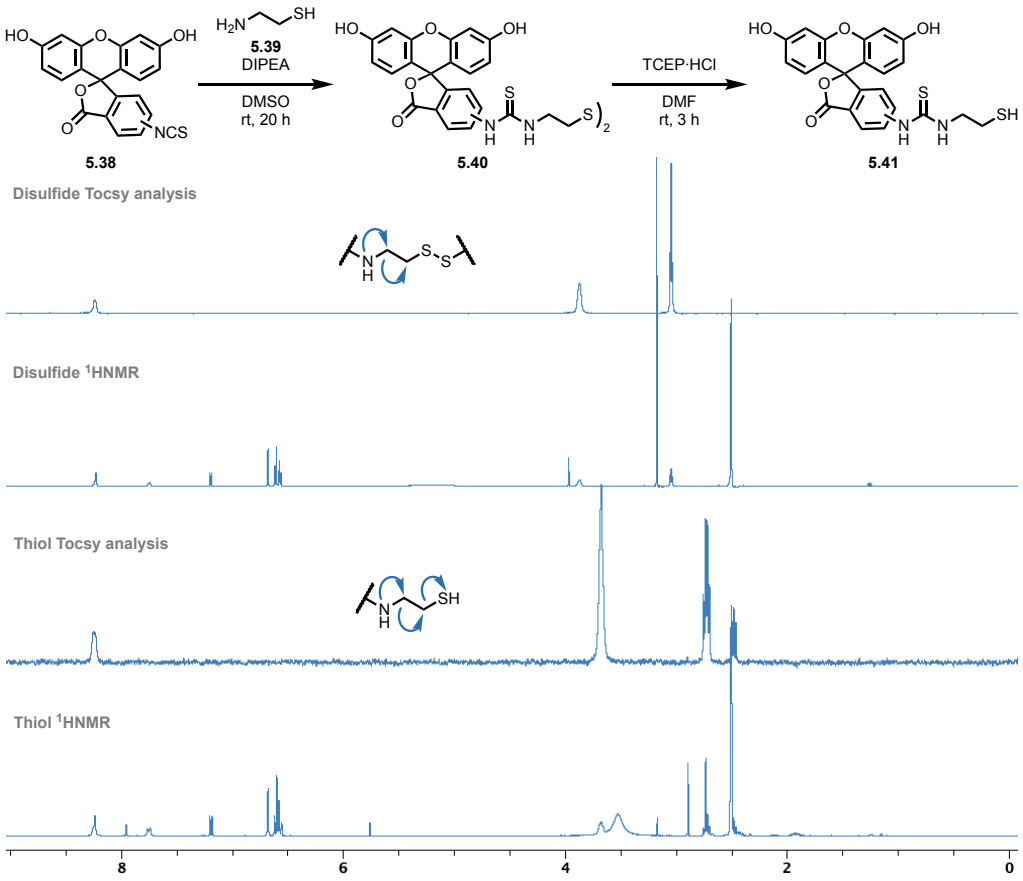

Figure 5.6: Modified synthetic route to a fluorescein thiol and NMR spectroscopic analysis showing formation of disulfide, followed by successful reduction to the thiol.

With the fluorescein thiol in hand a test TEC was conducted as for previous thiol fluorophores using allyl acetate **5.11** as the alkene substrate in the presence of DPAP in DMSO-d_6 to yield **5.42** (**Figure 5.7**). Disappointingly, no alkene consumption was observed by ^{1}H NMR spectroscopic analysis. While the previous study by the Davis and Dondoni groups report low yields for this compound,[241] in our hands it was completely unreactive in radical TEC conditions.

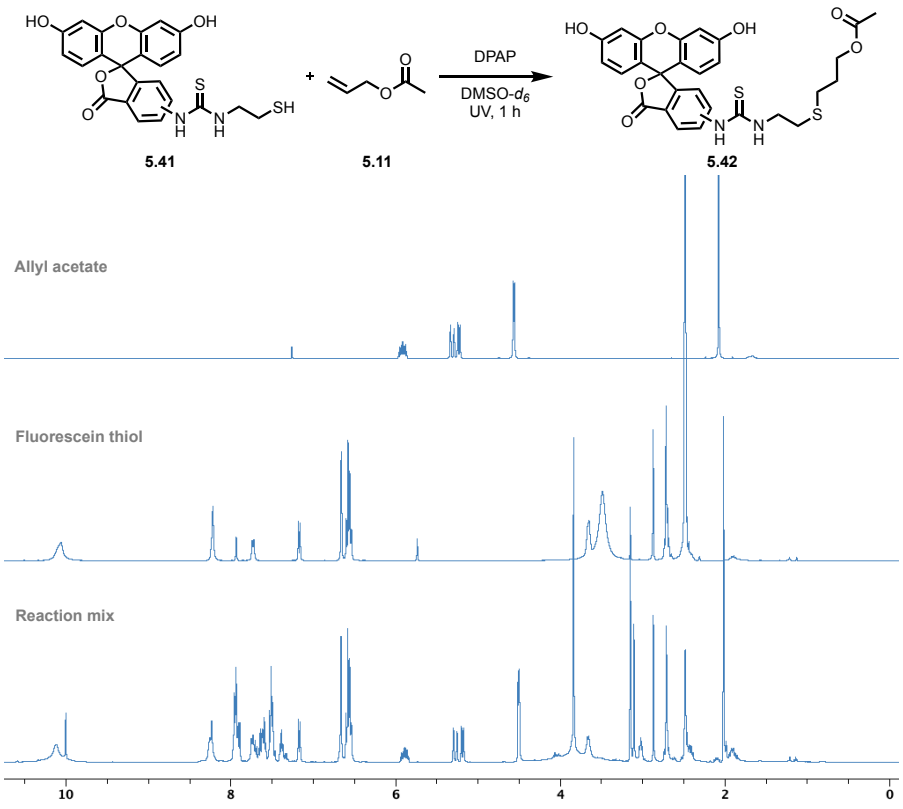

Figure 5.7: Test TEC using a fluorescein thiol.

5.3.8 Indirect Labelling Using Biotin Thiol

Following previously unsuccessful attempts to directly label alkenes using a thiol fluorophore, an alternative approach was desired that avoids the incorporation of both the thiol and fluorescent group on the same molecule. In many labelling approaches, biotin is often applied to allow study *via* strong binding of the protein streptavidin. In proteomics applications, the use of streptavidin beads is common, allowing isolation or removal of biotin-modified proteins from samples. Furthermore, fluorescent-tagged streptavidin derivatives are commercially available, in which common fluorophores are covalently attached to the protein. Therefore, an indirect approach was conceived in which a biotin thiol could be used (**Figure 5.8**).

As for the previous approach, the cells could be treated with alkene-modified sugar monomer for incorporation into glycans. However, the cells would then be treated with the biotin thiol, which would be reacted through TEC. Cells can then be treated with an AlexaFluor647-conjugated streptavidin that was commercially obtained, allowing visualisation by confocal microscopy. An added advantage of this approach is the

commercial availability of streptavidin bearing a range of tags. Additionally, PEGylated biotin thiols are commercially available, making this approach more widely accessible for a range of laboratories. Further, installation of a biotin tag, followed by pulldown using streptavidin beads or otherwise is a common approach in proteomics studies. Therefore, the use of a biotin thiol probe may also be applicable identification of glycosylated proteins *via* a proteomics approach as well as visualisation of their localisation through fluorescence microscopy.

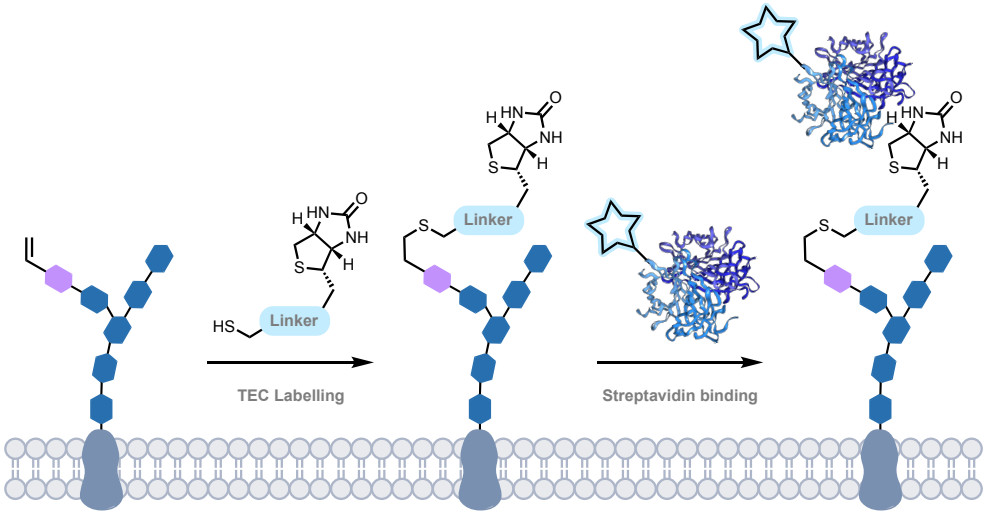

Figure 5.8: Schematic for indirect labelling using a biotin thiol and a fluorescent streptavidin[242] conjugate.

First, the synthesis of biotin thiol probe **5.44** was undertaken (**Figure 5.9**). For this purpose, biotin-OSu (**5.43**) was treated with cysteamine in the presence of TEA base in DMF overnight, followed by treatment with TCEP·HCl for 3 h to reduce any disulfide that may have been formed during the reaction, as this would prevent efficient TEC. However, isolation of the desired compound **5.44** proved challenging due to poor solubility. While it is likely that modification of the synthetic and purification procedure would overcome the purification challenge, the product would need to be soluble in aqueous conditions for application to cell glycan labelling. As a result, a different design was investigated, in which the biotin is connected to the thiol group through a PEG linker.

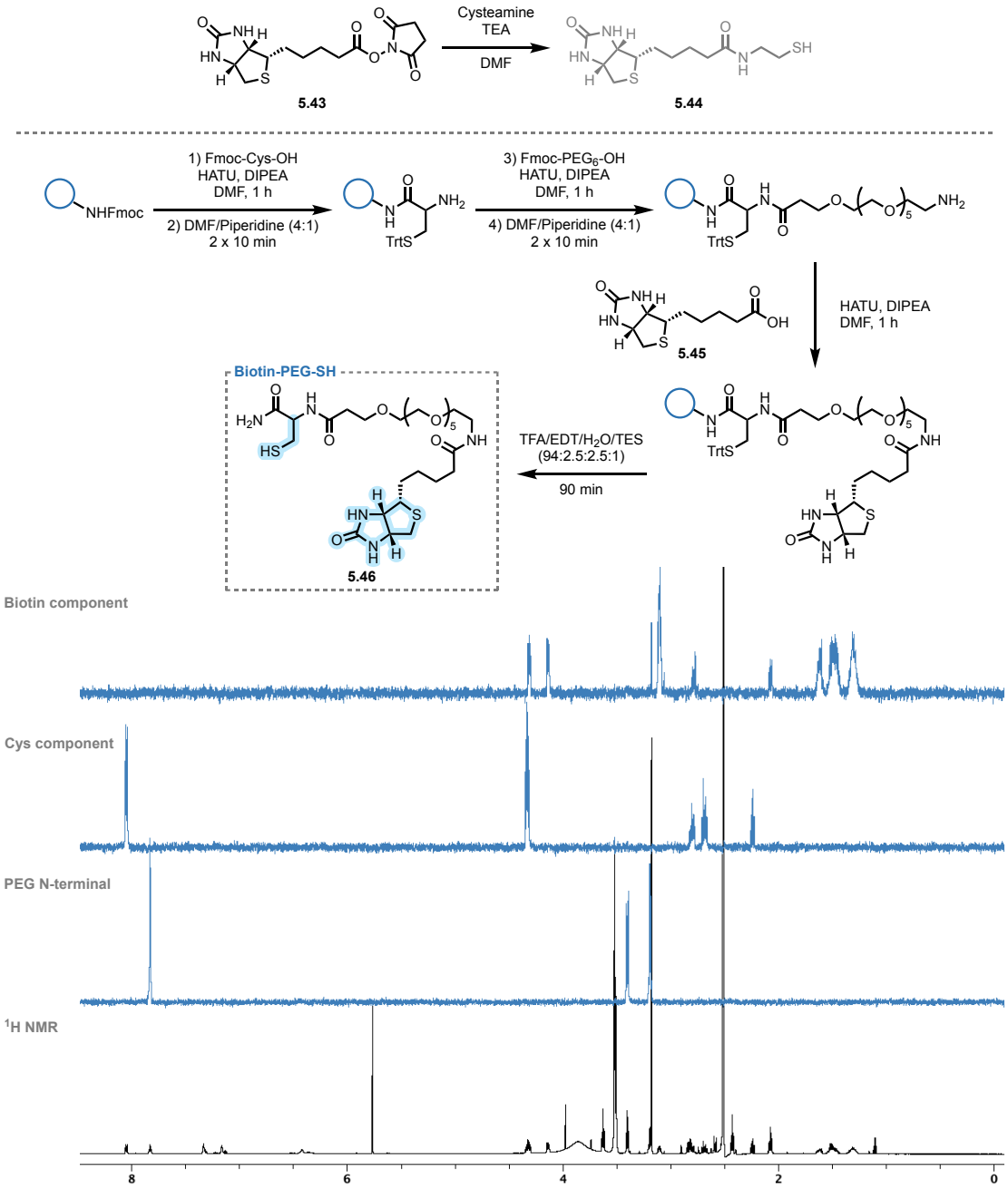

Figure 5.9: Synthesis of biotin thiol probes and NMR spectroscopic analysis (selective TOCSY & ^{1}H NMR experiments) of biotin-PEG-SH.

The primary purpose of the PEG linker is to increase solubility of the biotin thiol component, however a secondary advantage is that the linker will allow spacing of the biotin from the glycan, limiting any potential for steric hindrance to streptavidin binding. To provide an efficient synthesis route allowing for varying and sometimes difficult solubilities, a similar design to the peptide-inspired fluorophore previously synthesised (section 5.3.4) was proposed, and a similar solid-supported synthetic plan envisioned. First, coupling of Fmoc-Cys(Trt)-OH to Rink amide resin using a HATU and DIPEA coupling mix provides

the resin anchor, as well as the thiol and amine for attachment of the PEG linker. Following this, the Fmoc group is deprotected using 20% piperidine in DMF, followed by coupling of Fmoc-PEG_6-OH. After subsequent Fmoc deprotection as before, coupling of biotin (**5.45**) is again achieved by standard SPPS procedures. All acylations were confirmed by bromophenol blue test. Removal of the product from the resin and concomitant trityl deprotection were then achieved using a TFA/EDT/H_2O/TES (94:2.5:2.5:1) cocktail for 90 min. The TFA was removed under N_2 flow, and the product precipitated with cold Et_2O and isolated by centrifugation. The product was then washed with cold Et_2O (x3) and lyophilised to yield the desired biotin thiol probe **5.46**.

The reactivity of Biotin-PEG-SH probe **5.46** was then assessed in an *in vitro* test reaction using allyl acetate **5.11** at a concentration of 10 mM in the presence of DPAP in DMSO-d_6. In the initial test reaction 1.5 equivalents of both Biotin-PEG-SH and DPAP were used and the mix irradiated for 1 hour at 365 nm. ^{1}H NMR spectroscopic analysis showed approximately 50% conversion in these unoptimized conditions as judged by integration of the alkene peaks in the ^{1}H NMR spectrum. With this promising result, brief investigation into improvement of the conversion was undertaken. Blue LED initiation is desirable as the lower energy light is more favourable for cell treatment and so a blue-LED initiated experiment was conducted using thioxanthene-9-one as the initiator. Harsh reaction conditions were employed using 5 equivalents of both thiol and initiator. Again, allyl acetate **5.11** was used, this time at a concentration of 6 mM as additional solvent was required for dissolution of the photoinitiator. The mix was irradiated for 1 hour and then subjected to ^{1}H NMR spectroscopic analysis as for the previous experiment. In these conditions, approximately 60% conversion was observed. Following these results, the reaction was also attempted using the GlucNAc alkene analogue **5.6** for more direct study of the reaction of interest to form **5.47** (**Figure 5.14**). UV irradiation of a solution of carbohydrate in the presence of 3 equivalents of biotin-PEG-SH **5.46** and 2 equivalents of DPAP in DMSO-d_6 gave quantitative consumption of the alkene by ^{1}H NMR spectroscopic analysis. Formation of the new 4 carbon alkyl chain expected in the product **5.47** was confirmed by 2D NMR spectroscopic anlysis as before.

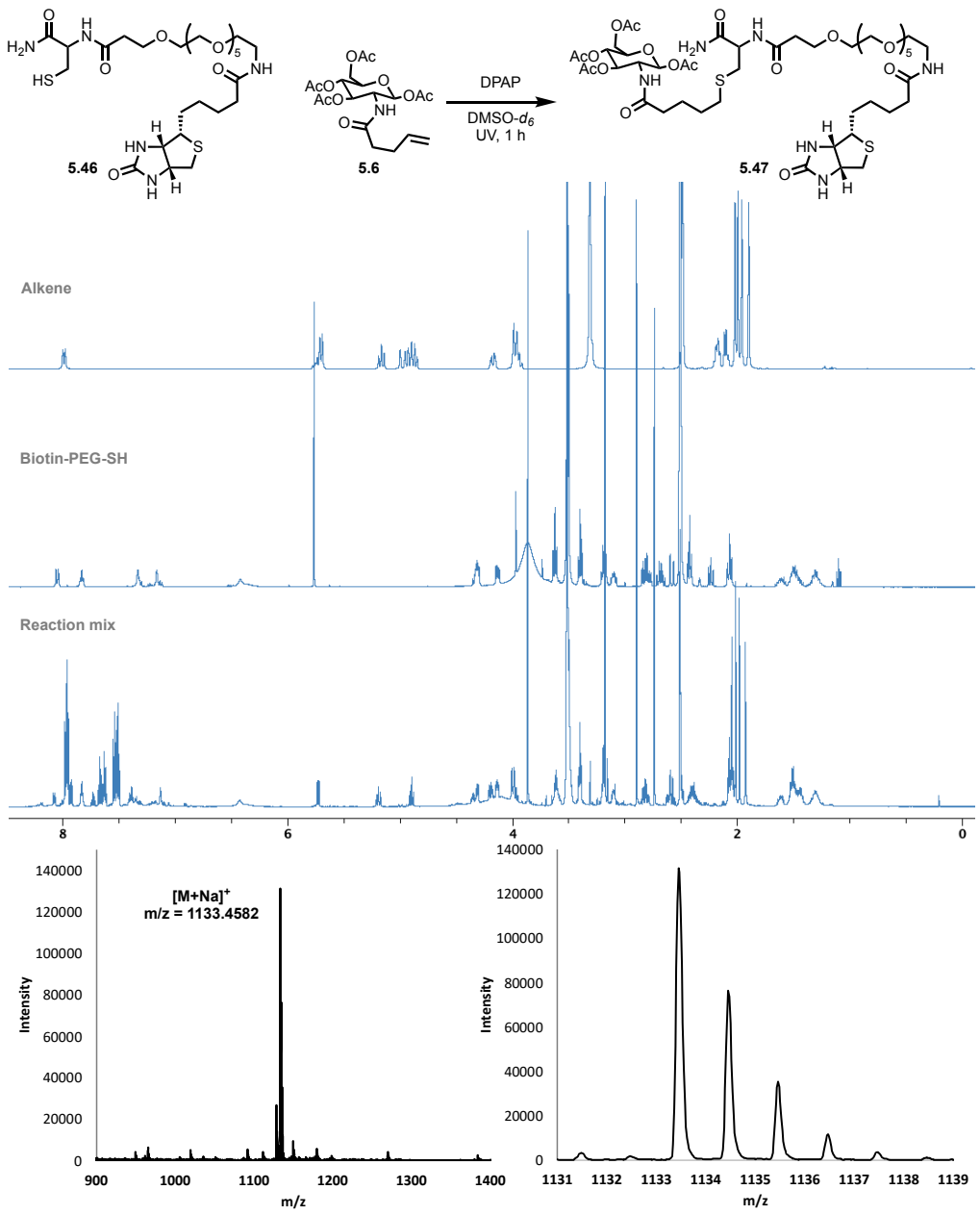

Figure 5.14: ^{1}H NMR spectroscopic and HRMS analysis of the reaction mixture for the carbohydrate test reaction.

With successful *in vitro* results for this thiol probe, we moved to perform the reaction on the cell surface for TEC labelling of modified glycans incorporated by metabolic engineering as detailed previously. First, HeLa cells were transferred to microscope cover slips and then incubated overnight in the presence of alkene-modified GlucNAc **5.6** at a concentration of either 100 or 200 μM in a 12 well plate. After this incubation, cells maintained viability at both concentrations. TEC labelling cocktails were prepared in 10% DMSO and each well was treated with 100 μL TEC cocktail. The cells were incubated with the reaction mixture for 10 min at rt in the dark, followed by UV irradiation for 5 min, and

then a further 5 min incubation. The reaction mixture was then removed by washing with 10% DMSO, then with PBS. The cells were then treated with streptavidin-AF647 solution (50 µL, 6.6 µg/mL) for 20 min at rt in the dark,[236] and again washed. The cells were then fixed by treatment with paraformaldehyde for 10 min at rt in the dark and mounted to slides using a mounting solution containing DAPI for fluorescent staining of the nuclei.

Examination of the cells by fluorescence microscopy revealed labelling of the cell surface with AF647. Importantly, this initial demonstration serves as the first use of TEC on the cell surface, expanding the potential applications of this reaction for study of biological systems. At 5 mM probe, clear labelling of the cells is observed. Even at 1 mM probe, some labelling is achieved, though not to the same extent. Some samples (**Figure 5.15**, panel d) did show some cell clumping, possibly due to cell death, and potentially as a result of slight discrepancies in the proximity to the UV source. As was expected for the healthy samples, labelling occurs on the surface of the cells where glycoproteins vital to cellular functions are present. While of course further optimisation of the labelling protocol is required, this result shows the potential for use of TEC in live biological systems.

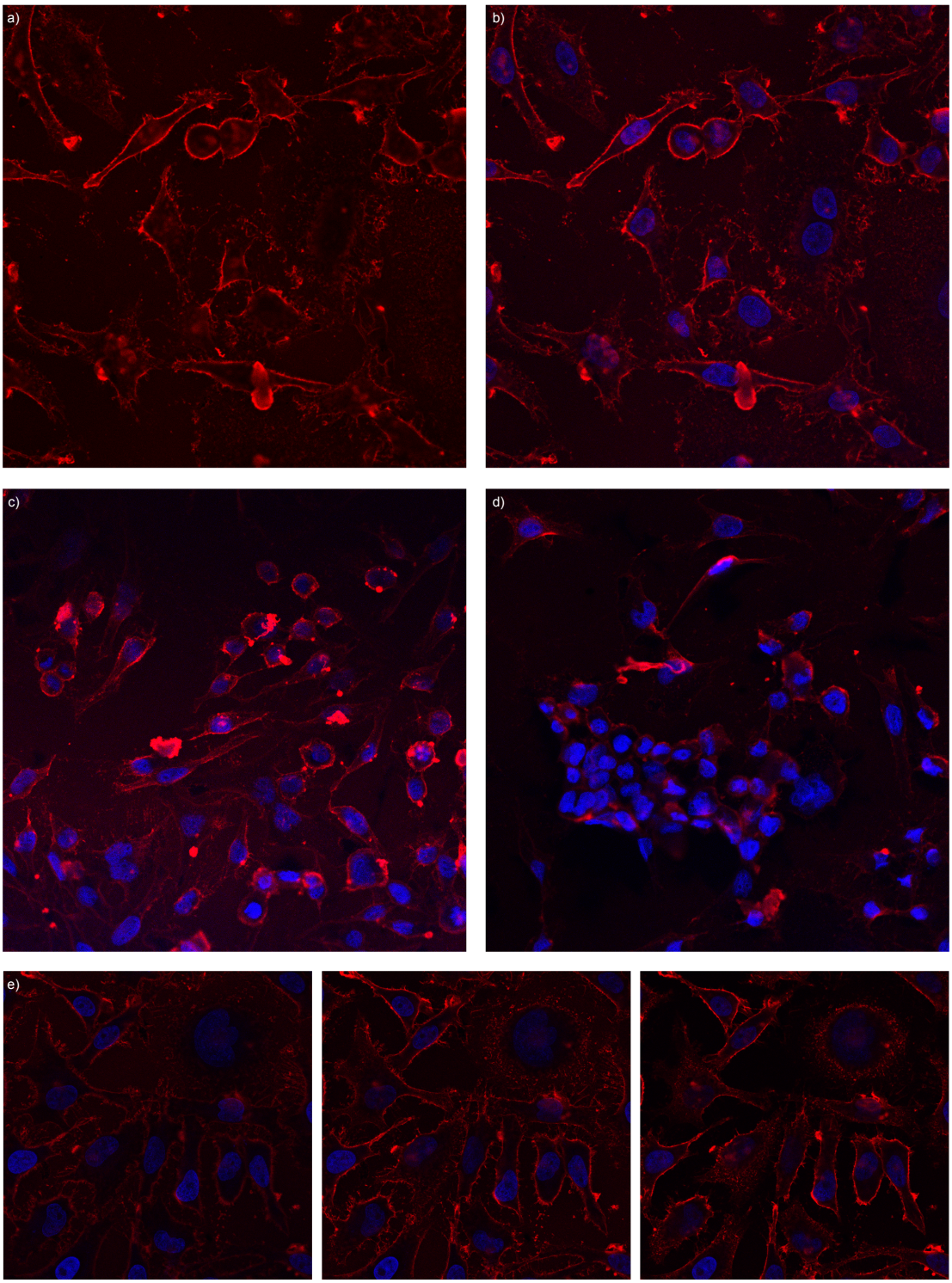

Figure 5.15: Incubation of HeLa cells with **5.6** followed by TEC labelling and treatment with streptavidin-AF647 (red) visualised by fluorescence microscopy. DAPI (blue) is used as a nuclear stain. a) Visualisation of AF647 fluorescence only and b) overlay of AF647 and DAPI fluorescence for cells treated with 5 mM probe, 1 mM DPAP and 10 mM MAP, c) 1 mM probe, 0.2 mM DPAP and 5 mM MAP, d) 2.5 mM probe, 0.2 mM DPAP and 5 mM MAP. e) Z-stack images for cells treated with 5 mM probe, 1 mM DPAP and 10 mM MAP.

5.4 Conclusions & Future Work

It is clear form this work that designing a fluorescent thiol probe suitable for TEC is not straightforward. A number of fluorescent groups including the dansyl, napthalimide and fluorescein cores were functionalised with a thiol group but showed no reactivity in TEC conditions. Attempts to impart reactivity on the designed probes by distancing of the fluorescent core and the thiol group proved fruitless.

However, use of a simple fluorescent core in an aminobenzamide thiol probe afforded a TEC reactive fluorescent thiol probe, termed AbzSH. This design showed quantitative reaction in a range of conditions that suit it for use in a biological context. The AbzSH probe was then applied in a model system to investigate its application for labelling of alkenes incorporated on a protein. For this purpose, an alkene-modified BSA was treated with AbzSH in the presence and absence of radical initiators, with both experiments giving fluorescent labelling of the protein. This could be visualised by excitation at 302 nm on an SDS-PAGE gel.

The AbzSH probe, however, cannot be easily excited using common microscopy instrumentation, owing to the low wavelength of its excitation max at 320 nm. This precludes its application to cell labelling as was the initial aim of this project. Thus, a two-step TEC glycan labelling strategy was envisaged in which a biotin thiol probe could be reacted with the alkene of interest, followed by incubation with a fluorescent-labelled streptavidin. This will facilitate use of a variety of fluorophores without concern for their compatibility with TEC conditions. A suitable biotin thiol probe, Biotin-PEG-SH, was synthesised and *in vitro* experiments showed quantitative reaction with an alkene-modified monosaccharide. Thus, this probe was brought forward for cell-based labelling. Initial experiments showed successful labelling of cell-surface glycans. Future optimisation of this glycan labelling protocol is likely to aim to use alternative irradiation and initiation sources, likely through blue-LED based methods. Additionally, the labelling will be repeated with a full range of controls. These may include use of cells not incubated with the alkene sugar, use of a radical scavenger and exclusion of either initiators or the irradiation step. Additionally, a second generation probe will be synthesised without the amide handle using trityl cysteamine resin.

The use of Biotin-PEG-SH is not limited to fluorescence labelling applications, as the biotin tag may facilitate pulldown of labelled structures for proteomics studies. Future work will make use of this advantage, allowing identification of glycoproteins on the cell surface

combined with visualisation of their localisation *via* fluorescence imaging. Similarly, applications are not limited to study of protein glycosylation, and this approach may be particularly well suited to study of protein lipidation.

Additionally, the AbzSH fluorophore proved suitable for study of alkene-modified biomolecules. This probe can be used to study protein PTMs such as lipidation, wherein a modification of a lipid substrate to introduce an alkene will allow minimal perturbation to the natural system, whilst facilitating monitoring *via* fluorescence. This may also make use of the nitrotyrosine FRET partner, allowing quenching of the fluorescence of AbzSH that reacts with an alkene partner.

Chapter 6

Summary

The work discussed in this thesis explores the applications of the TEC reaction for applications in synthesis of modified peptides as well as for investigation of biological systems. This recognises and harnesses the beneficial Click characteristics of this reaction for otherwise difficult purposes. As demonstrated in this thesis, the TEC reaction possesses great potential for further application and study in such a context.

In the first study, discussed in **Chapter 2**, the use of TEC for peptide macrocyclisation is investigated. While previous studies have used TEC chemistry for peptide stapling in stabilisation of a pre-existing structure, peptide macrocyclisation allows access to new peptide architectures with application in drug discovery. The work in this thesis shows the use of the TEC reaction for synthesis of analogues of the neuropeptide Oxytocin, as well as for cyclisation of short peptides, demonstrating utility in the efficient synthesis of known therapeutic macrocyclic peptides, as well as for access to novel candidates.

Following in the theme of peptide modification, **Chapter 3** discusses the development of a Green bioconjugation platform, utilising non-traditional DES solvents. This work first demonstrates the compatibility of the TEC reaction with these solvents, with particular focus on access to biologically relevant small molecules. Having established this system using small molecules, the expansion to peptide modification is investigated. A peptide binder for the SARS-CoV-2 spike protein is then modified using this Green system to access conjugated analogues, demonstrating the use of this Green platform to selectively modify biologically relevant peptides.

Returning to the theme of peptide macrocycles in drug discovery, **Chapter 4** discusses the development of a high-throughput combinatorial technology for diversification of peptide macrocycles through TEC chemistry. The strict confines of nanomole scale chemistry in microlitre volumes is shown to be compatible with TEC for peptide modification and is optimised to yield highly pure conjugates. These reaction mixtures may be applied directly to biological screening in a one-well-one-compound format without need for chromatographic purification. Using a fully-automated system, a 96-member library is synthesised, giving high-purity peptide conjugates.

Finally, the use of the TEC reaction for labelling of alkene-containing biomolecules is investigated in **Chapter 4**. Initially, it is made clear that the design of a TEC-reactive fluorophore bearing a thiol group is not straightforward, with a number of fluorescent cores proving incompatible. Finally, a relatively simple thiol fluorophore based on the Abz

fluorescent core is found to be suitable for this reaction. This probe is then applied to the labelling of an alkene-modified BSA conjugate, allowing fluorescent labelling of the protein target. To expand this labelling approach for microscopy applications, an indirect labelling approach is envisaged in which a biotin probe is reacted with the alkene-containing biomolecule, followed by treatment with a fluorescent streptavidin conjugate. This approach is then demonstrated for fluorescent labelling of alkene-modified sugars incorporated on the cell surface *via* metabolic engineering. This work offers a new approach to labelling within complex biological systems, complementary to existing Click chemistry methods.

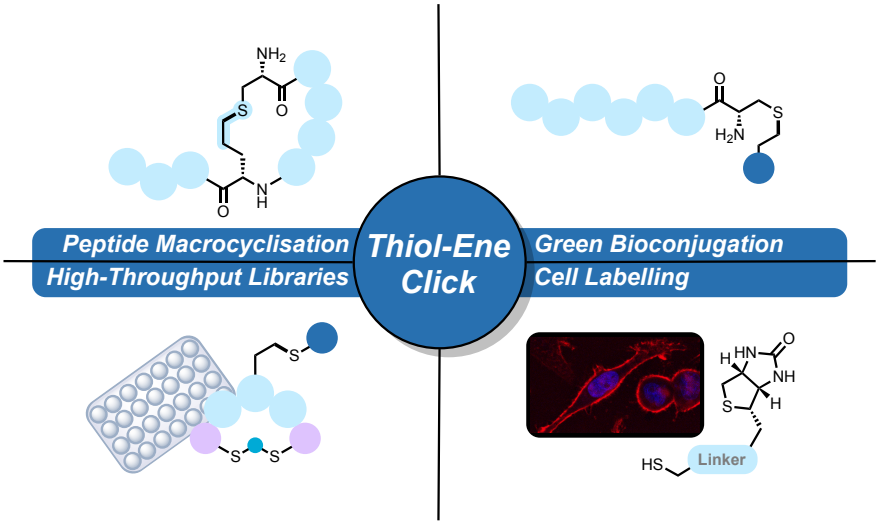

Figure 7.1: Graphical summary of work discussed in this thesis.

This work has therefore expanded the applications of TEC chemistry for biomolecular applications. This and future work, proposed in each chapter and as of yet unenvisaged should further provide useful tools for chemists and biologists alike in both drug discovery and basic science.

Chapter 7

Experimental

7.1 General Experimental

Commercial reagents and materials were purchased from Sigma Aldrich, Fluorochem, VWR, Carbosynth, Rapp Polymere and Tokyo Chemical Industry and used without further purification. Solvents for synthesis were purchased at HPLC grade. Silica gel 60 (Merck, 230-400 mesh) was used for manual flash column chromatography. Automated reverse-phase flash chromatography was performed on a Biotage system using Telos C18 flash column cartridges. TLC was performed on Merck 60 F254 silica gel plates (fluorescence indicator F_{254}, Merck) and visualised by UV light (λmax = 254 nm), ammonium molybdate, $KMnO_4$, H_2SO_4, ninhydrin or Ellman stains. SPPS was performed in polypropylene syringe vessels (Torviq) fitted with a polypropylene frit and was performed manually with continuous agitation. Deuterated solvents for NMR spectroscopic analyses were purchased from Merck, VWR and Fluorochem.

^{1}H- and ^{13}C-NMR spectroscopic analyses were performed on a 400 MHz (^{1}H, 400.13 MHz and ^{13}C, 100.61 MHz) Bruker Avance spectrometer or a 600 MHz Bruker Avance spectrometer (^{1}H, 600.13 MHz and ^{13}C, 150.90 MHz). Resonances (δ), are in ppm units downfield from an internal solvent reference. ^{1}H and ^{13}C NMR assignments were confirmed using additional experiments such as 2D COSY, HSQC, HMBC, and NOESY. NMR data was analysed using Topspin software. Analytical and semi-preparative reverse phase HPLC was performed on a Shimadzu Nexera system equipped with a photodiode array detector. For analytical HPLC, either a C18 Jupiter 5 µm, 110 Å, 250 x 4.6 mm column or a C18 Jupiter 5 µm, 110 Å, 100 x 4.6 mm column was used, with a flow rate of 1 mL/min. For semi-preparative HPLC a C18 Jupiter 5 µm, 110 Å, 250 x 10.0 mm LC column was used. UV absorption signals were detected with a PDA detector at suitable wavelengths as dictated by the resultant absorption spectrum. LC-MS analyses were performed with a UHPLC single quadrupole MS system (Shimadzu LC-MS-2020) using a C18 Phenomenex Kinetex 2.1 × 50 mm, 100 Å, 2.6 µm column. Preparative RP-HPLC was performed using a Waters system equipped with a 2489 UV detector on a C18 Xterra OBD column (19 × 250 mm, 125 Å, 10 µm). ESI mass spectra were acquired using a Bruker microTOF-Q III spectrometer interfaced to a Dionex UltiMate 3000 LC in positive and negative modes as required. The instrument was calibrated using a tune mix solution, (Agilent Technologies ESI-l Low concentration tuning mix) this was also used as an internal lock mass. Masses were recorded over the range 100-2000 m/z. Operating conditions were as follows: end-plate offset 500V capillary 4500V, nebulizer 2.0 Bar, dry gas 8.0 L/min, and dry temperature 180 ºC. MicroTof

control 3.2 and HyStar 3.2 software were used to carry out the analysis. APCI experiments were carried out on a Bruker micrOTOF-Q III spectrometer interfaced to a Dionex UltiMate 3000 LC or direct insertion probe. The instrument was operated in positive or negative mode as required. Agilent tuning mix APCI-TOF was used to calibrate the system. Masses were recorded over a range of 100-2000 m/z. Operating conditions were as follows: Capillary voltage 4000V, corona 4000nA, nebulizer gas 2.0 Bar, dry gas 3.0 L/min, dry gas temperature 100-200ºC, vap. temperature 100-400ºC. MicroTof control and HyStar software were used to carry out the analysis. IR spectra were acquired using a Perkin-Elmer Spectrum 100 FT-IR spectrometer. UV reactions were performed in a Luzchem LZC-EDU (110 V/ 60 Hz) photoreactor housing 12 UV lamps centred at 365 nm. Blue-LED reactions were performed using either a blue LED strip obtained from a domestic supplier or using 2 x Kessil PR160L lamps centred at 440 nm. Acoustic dispensing was performed using a Labcyte Echo 650 acoustic dispenser and bulk dispensing performed using a Certus FLEX. Rotational vacuum concentration (RVC) was performed on a Heraeus Multifuge 3L-R centrifuge (Thermo Scientific) with a Sorvall 75006445 rotor (radius = 19.2 cm).

7.2 Experimental for chapter 2

7.2.1 Synthesis of Vinylglycine

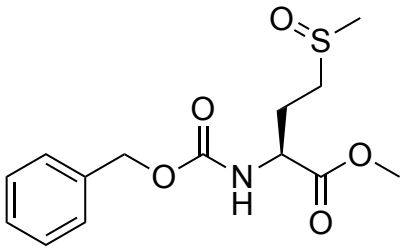

Methyl (2*S*)-2-(((benzyloxy)carbonyl)amino)-4-(methylsulfinyl)butanoate (2.9)[171]

To a solution of Cbz-Met-OMe **2.8** (16.8 mmol, 5.00 g) in MeOH (25 mL) at 0 °C, $NaIO_4$ (1.1 equiv., 18.8 mmol, 4.02 g) in H_2O (25 mL) was added dropwise. The mix was stirred under N_2 balloon for 16 hours. The mix was then filtered through celite and concentrated under reduced pressure to remove MeOH. The solution was extracted with chloroform (3 x 25 mL), dried over $MgSO_4$, and concentrated under reduced pressure to give the product as a colourless oil (5.15 g, 98%).

^{1}H NMR (400 MHz, $CDCl_3$) (mixture of rotamers at rt) δ_H 7.40-7.30 (m, 5H), 5.78 (d, J = 8.0 Hz, 1H), 5.13 (s, 2H), 4.56-4.44 (m, 1H), 3.78 (s, 3H), 2.86-2.68 (m, 2), 2.57 (s, 1.5H), 2.56 (s, 1.5H), 2.46-2.34 (m, 1H), 2.24-2.10 (m, 1H).

***m/z* HRMS (ESI$^+$)** calcd. for $C_{14}H_{19}NO_5SNa$ = 336.0876 $(M + Na)^+$, found 336.0880.

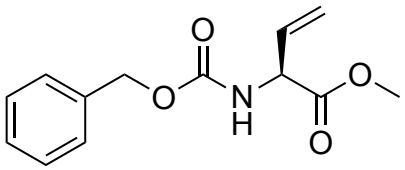

Methyl (*S*)-2-(((benzyloxy)carbonyl)amino)but-3-enoate (2.10a) [171]

A solution of **2.9** (5.10 g, 16.3 mmol) in xylene (50 mL) was heated to reflux for 72 h. The mix was concentrated *in vacuo* to give a brown oil (4.22 g) which was subjected to purification by silica gel flash chromatography (10-20% EtOAc:Hex) to afford the desired product as a colourless oil (0.81 g, 20%).

^{1}H NMR (400 MHz, $CDCl_3$) δ_H 7.42-7.32 (m, 5H), 5.93 (ddd, J = 17.1, 10.4, 8.1 Hz, 1H), 5.51 (d, J = 8.1 Hz, 1H), 5.39 (dd, J = 17.1, 1.8 Hz, 1H), 5.31 (dd, J = 10.4, 1.8 Hz, 1H), 5.15 (s, 2H), 5.00-4.93 (m, 1H), 3.79 (s, 3H).

***m/z* HRMS (ESI$^+$)** calcd. for $C_{13}H_{15}NO_4Na$ = 272.0893 $(M + Na)^+$, found 272.0891.

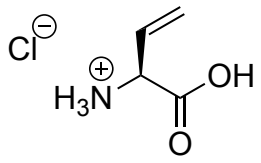

(*S*)-1-Carboxyprop-2-en-1-aminium chloride (2.11)[171]

2.10a (0.7725g, 3.10 mmol) was heated to reflux in HCl (6M, 50 mL) for 1.5 h. The mix was concentrated to dryness. The resulting off-white solid was refluxed in acetone for 10 min and filtered to afford the product as a white solid (0.276 g, 65%).

M.p.: Decomposition at 165-167 ºC. Literature value (decomposition) 175-177 ºC.

^{1}H NMR (400 MHz, D_2O) δ_H 5.86 (ddd, *J* = 17.3, 10.5, 7.5 Hz, 1H), 5.45-5.39 (m, 2H), 4.39 (d, *J* = 7.5 Hz, 1H).

***m/z* HRMS (ESI$^+$)** calcd. for $C_4H_8NO_2$ = 102.0550 $(M + H)^+$, found 102.0552.

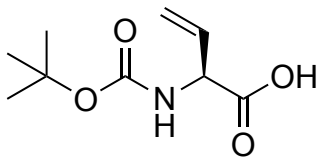

(*S*)-2-((*tert*-Butoxycarbonyl)amino)but-3-enoic acid (2.12)[171]

2.11 (0.149 g, 1.1 mmol) was dissolved in 1,4-dioxane/H_2O (1:1) (6 mL) and Boc_2O (0.355 g, 1.65 mmol) and $NaHCO_3$ (0.182 g, 2.2 mmol) were added. The mix was heated to reflux for 3 h at 100 °C and then concentrated *in vacuo*. The solid was dissolved in water (15 mL) and acidified to pH 2 using aq. HCl (1M) before extraction with chloroform (3 x 15 mL). The organics were dried using $MgSO_4$ and concentrated to give the product as a colourless oil (0.172 g, 78%).

^{1}H NMR (400 MHz, $CDCl_3$) (mixture of rotamers at rt) δ_H 8.25 (brs, 1H), 5.94 (m, 1H), 5.41 (dd, *J* = 17.1, 8.2 Hz, 1H), 5.36-5.26 (m, 1H), 4.93 (m, 0.5H) [rotamer A], 4.71 (m, 0.5H) [rotamer B], 1.48-1.45 (m, 9H).

***m/z* HRMS (ESI$^+$)** calcd. for $C_9H_{15}NO_4Na$ = 224.0893 $(M + Na)^+$, found 224.0900.

7.2.2 Synthesis of linear peptides

General Procedure: SPPS

Deprotection and first amino acid coupling:

Fmoc/tBu SPPS of peptide amides was performed manually in polypropylene syringe reaction vessels (10 mL; Torviq, MI, USA) fitted with a polypropylene frit. All reactions were performed at room temperature under continuous agitation. Rink amide aminomethyl Resin (100 - 200 mesh) was loaded in the syringe and swollen in DMF (6 mL) for 20 min and then drained. The resin bound Fmoc group was removed using 20% piperidine in DMF (2 x 5 mL, 10 min each) and the deprotected resin was washed with DMF (3 x 5 mL), DCM (3 x 5 mL) then DMF (3 x 5 mL). Coupling of the first AA to the resin was performed using PyBOP (4 equiv.), NMM (8 equiv.) and Fmoc-AA (4 equiv.) in DMF. The coupling mix was transferred to the resin in the syringe and agitated for 45 min. Excess reagents were drained from the reaction vessel and the resin was washed with DMF (3 x 5 mL), DCM (3 x 5 mL) and DMF (3 x 5 mL). Successful coupling was qualitatively monitored by treatment of a small resin sample with a solution of bromophenol blue (BPB) in DCM (0.15 mM; 0.1 mL). In the case of incomplete coupling, the above procedure was undertaken again prior to Fmoc deprotection.

Amino acid coupling:

Subsequent peptide coupling cycles consisted of (i) Fmoc deprotection using 20% piperidine in DMF (2 x 5 mL, 10 min each), (ii) resin washes with DMF (3 x 5 mL), DCM (3 x 5 mL) then DMF (3 x 5 mL), (iii) peptide coupling with addition of PyBOP (3 equiv.), NMM (6 equiv.) in DMF (3 mL) and Fmoc-AA (3 equiv.; 0.1 M) in DMF to the peptide resin for 45 min, (iv) resin washes with DMF (3 x 5 mL), DCM (3 x 5 mL) then DMF (3 x 5 mL), (v) qualitative BPB test.

Following the final coupling, the resin was treated with 20% piperidine in DMF (2 x 15 min; 5 mL) washed with 2 rounds of DMF (3 x 5 mL), DCM (3 x 5 mL), and then air dried.

Peptide cleavage from the resin:

Dried peptide resin was swollen in DCM (5 mL) under agitation for 20 min, then drained. The cleavage cocktail (TFA:TES:EDT:H_2O; 94:1:2.5:2.5; 10 mL) was added to the syringe and agitated for 90 min. The cleavage cocktail was filtered out and collected. The resin was washed with cleavage cocktail (2 x 2.5 mL) and the washings combined with the first filtrate.

TFA was removed under gentle argon flow, followed by precipitation of the peptide with Et_2O (20 mL) at 0 °C. The crude peptide suspension was centrifuged and the supernatant decanted. The peptide was washed again with Et_2O (2 x 15 mL) at 0 °C and collected by centrifugation. The crude material was then dried *in vacuo*.

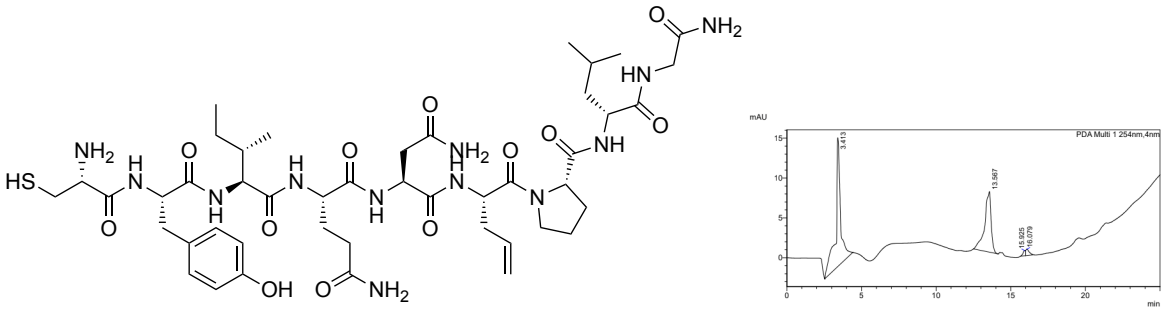

Cys-Tyr-Ile-Glu-Asn-Agl-Pro-Leu-Gly-NH_2 (2.3)

Synthesised according to the SPPS general procedure using Rink amide AM resin (0.300 g, 0.21 mmol) to afford a white solid, which was subjected to reverse-phase C_{18} flash chromatography (0-100% MeCN (0.1% TFA):H_2O (0.1% TFA)) to give the peptide as a white solid (100 mg, 48%).

R_f = 0.84 (MeCN:H_2O, 2:1, 0.1% TFA, C_{18} silica).

HPLC R_T = 13.57 min (5-95% MeCN in H_2O over 20 min, 0.1% TFA modifier, 4.6 x 250mm C18).

^{1}H NMR (600 MHz, DMSO-*d*$_6$) δ_H 9.20 (brs, 1H), 8.52 (d, *J* = 7.9 Hz, 2H), 8.25 (d, *J* = 8.6 Hz, 1H), 8.13-8.06 (m, 3H), 8.02 (d, *J* = 7.6 Hz, 1H), 7.98 (t, *J* = 6.0 Hz, 1H), 7.88 (d, *J* = 8.2 Hz, 1H), 7.32 (brs, 2H), 7.20 (brs, 2H), 7.14-7.05 (m, 4H), 6.89 (brs, 2H), 6.78 (brs, 2H), 6.66 (d, 8.3 Hz, 2H), 5.81-5.71 (m, 1H), 5.10 (d, *J* = 16.6 Hz, 1H), 5.00 (d, *J* = 10.4 Hz, 1H), 4.62-4.57 (m, 1H), 4.55-4.48 (m, 2H), 4.33-4.28 (m, 1H), 4.27-4.15 (m, 3H), 3.97-3.91 (m, 1H), 3.68-3.50 (m, 4H), 3.08-3.01 (m, 1H), 2.97-2.91 (m, 1H), 2.89-2.82 (m, 1H), 2.69-2.63 (m, 1H), 2.42-2.36 (m, 3H), 2.30-2.22 (m, 1H), 2.12-2.07 (m, 2H), 2.06-2.00 (m, 1H), 1.91-1.80 (m, 4H), 1.79-1.70 (m, 2H), 1.66-1.57 (m, 1H), 1.54-1.40 (m, 3H), 1.13-1.05 (m, 1H), 0.89 (d, *J* = 6.5 Hz, 3H), 0.85-0.79 (m, 9H).

^{13}C NMR (151 MHz, DMSO-*d*$_6$) δ_C 173.9, 172.1, 171.7, 171.2, 171.1, 170.84, 170.82, 170.75, 170.5, 169.5, 166.7, 155.8, 134.0, 130., 127.6, 117.6, 114.9, 59.6, 56.9, 54.5, 53.5,

52.1, 51.4, 50.3, 49.5, 46.8, 41.9, 36.9, 36.4, 36.2, 31.4, 30.7, 28.9, 28.1, 25.5, 24.4, 24.3, 24.1, 23., 21.5, 15.4, 10.9.

***m/z* HRMS (ESI$^+$)** calcd. for $C_{45}H_{71}N_{12}O_{12}S$ = 1003.5035 ([M+H$^+$]), found 1003.5030.

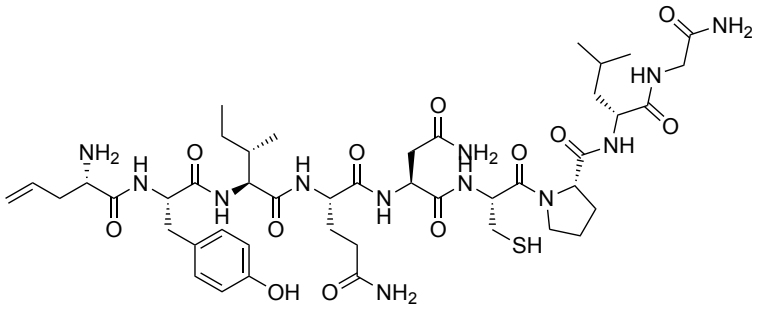

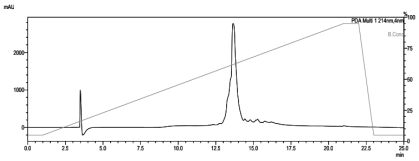

Agl-Tyr-Ile-Glu-Asn-Cys-Pro-Leu-Gly-NH$_2$ (2.4)

Synthesised according to the SPPS general procedure using Rink amide AM resin (0.150 g, 0.11 mmol) to afford a white solid, which was subjected to reverse-phase C_{18} flash chromatography (0-100% MeCN (0.1% TFA):H_2O (0.1% TFA)) to give the peptide as a white solid (57 mg, 52%).

R_f = 0.75 (MeCN:H_2O, 2:1, 0.1% TFA, C18).

HPLC R_T = 13.64 min (5-95% MeCN in H_2O over 20 min, 0.1% TFA modifier, 4.6 x 250mm C18).

^{1}H NMR (600 MHz, DMSO-*d*$_6$) δ_H 9.18 (brs, 1H), 8.55 (d, *J* = 7.9 Hz, 2H), 8.19-7.93 (m, 7H), 7.33 (brs, 2H), 7.20 (brs, 2H), 7.14-7.05 (m, 4H), 6.90 (brs, 2H), 6.79 (brs, 2H), 6.65 (d, 8.3 Hz, 2H), 5.73-5.64 (m, 1H), 5.16 (d, *J* = 17.4 Hz, 1H), 5.11 (d, *J* = 10.2 Hz, 1H), 4.66-4.57 (m, 2H), 4.54-4.50 (m, 1H), 4.33-4.28 (m, 1H), 4.27-4.17 (m, 3H), 3.82-3.77 (m, 1H), 3.68-3.50 (m, 4H), 2.93-2.89 (m, 1H), 2.80-2.73 (m, 1H), 2.70-2.58 (m, 2H), 2.46-2.36 (m, 3H), 2.12-2.02 (m, 3H), 1.93-1.80 (m, 5H), 1.79-1.70 (m, 2H), 1.67-1.59 (m, 1H), 1.54-1.39 (m, 3H), 1.13-1.05 (m, 1H), 0.89 (d, *J* = 6.5 Hz, 3H), 0.85-0.79 (m, 9H).

^{13}C NMR (151 MHz, DMSO-*d*$_6$) δ_C 173.9, 172.1, 171.7, 171.2, 170.9, 170.85, 170.82, 170.6, 170.5, 168.5, 167.9, 155.8, 131.3, 130.1, 127.6, 119.9, 114.9, 59.8, 56.9, 54.3, 53.2, 52.2, 51.42, 51.35, 49.6, 47., 41.9, 36.9, 36.5, 36.4, 31.4, 29, 28.0, 28.0, 25.4, 24.4, 24.3, 24.1, 23.0, 21.5, 15.3, 10.9.

***m/z* HRMS (ESI$^+$)** calcd. for $C_{45}H_{71}N_{12}O_{12}S$ = 1003.5035 ([M+H$^+$]), found 1003.5052.

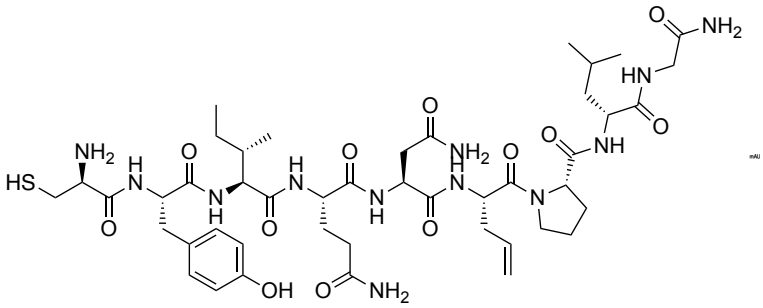

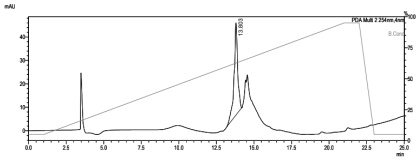

D-Cys-Tyr-Ile-Glu-Asn-Agl-Pro-Leu-Gly-NH_2 (2.27)

Synthesised according to the SPPS general procedure using Rink amide AM resin (0.150 g, 0.11 mmol) to afford a white solid, which was subjected to reverse-phase C_{18} flash chromatography (0-100% MeCN (0.1% TFA):H_2O (0.1% TFA)) to give the peptide as a white solid (35 mg, 32%).

R_f = 0.84 (MeCN:H_2O, 2:1, 0.1% TFA, C_{18} silica).

HPLC R_T = 13.80 min (5-95% MeCN in H_2O over 20 min, 0.1% TFA modifier, 4.6 x 250mm C18).

^{1}H NMR (600 MHz, DMSO-*d*$_6$) d_H 9.20 (brs, 1H), 8.52 (d, *J* = 7.9 Hz, 2H), 8.25 (d, *J* = 8.6 Hz, 1H), 8.13-8.01 (m, 4H), 7.99 (t, *J* = 6.0 Hz, 1H), 7.92-7.86 (m, 1H), 7.33 (brs, 1H), 7.21 (brs, 1H), 7.14-7.03 (m, 4H), 6.89 (brs, 1H), 6.78 (brs, 1H), 6.64 (d, 8.3 Hz, 2H), 5.81-5.72 (m, 1H), 5.10 (d, *J* = 16.6 Hz, 1H), 5.00 (d, *J* = 10.4 Hz, 1H), 4.62-4.56 (m, 1H), 4.55-4.47 (m, 2H), 4.35-4.14 (m, 4H), 3.97-3.91 (m, 1H), 3.68-3.50 (m, 4H), 3.08-3.02 (m, 1H), 2.99-2.92 (m, 1H), 2.90-2.83 (m, 1H), 2.71-2.59 (m, 1H), 2.42-2.36 (m, 3H), 2.30-2.22 (m, 1H), 2.14-2.07 (m, 2H), 2.06-2.00 (m, 1H), 1.92-1.79 (m, 4H), 1.79-1.70 (m, 2H), 1.66-1.57 (m, 1H), 1.54-1.40 (m, 3H), 1.14-1.04 (m, 1H), 0.89 (d, *J* = 6.5 Hz, 3H), 0.86-0.78 (m, 9H).

^{13}C NMR (151 MHz, DMSO-*d*$_6$) δ_C 174.4, 172.6, 172.2, 171.7, 171.3, 171.0, 170.0, 166.6, 156.4, 134.5, 130.6, 127.9, 118.1, 115.3, 60.1, 57.6, 54.2, 54.0, 52.5, 51.8, 50.7, 50.0, 47.3, 42.4, 37.4, 36.8, 35.9, 31.9, 29.4, 28.7, 26.1, 24., 24.7, 24.6, 23.5, 22.1, 15.6, 11.5.

***m/z* HRMS (ESI$^+$)** calcd. for $C_{45}H_{71}N_{12}O_{12}S$ = 1003.5035 ([M+H$^+$]), found 1003.5030.

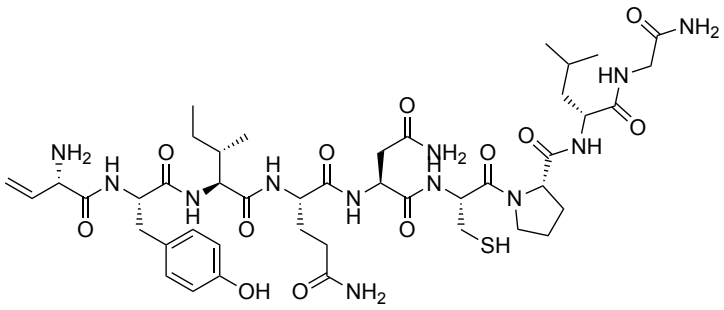

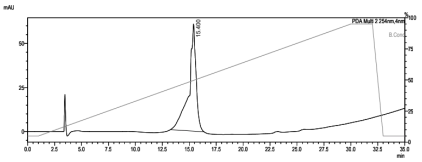

Vgl-Tyr-Ile-Glu-Asn-Cys-Pro-Leu-Gly-NH_2 (2.14)

Synthesised according to the SPPS general procedure using Rink amide AM resin (0.300 g, 0.21 mmol). For coupling of the final Vgl amino acid the resin was deprotected and dried before re-swelling in THF. The resin was then treated with solution of **2.9** (0.0845 g, 0.42 mmol, 2.0 equiv.) and IIDQ (0.1274 g, 0.042 mmol, 2.0 equiv.) in THF with agitation for 5 days. The solution was removed from the syringe and washed, followed by cleavage to afford a white solid, which was subjected to reverse-phase C_{18} flash chromatography (0-100% MeCN (0.1% TFA):H_2O (0.1% TFA)) to give the peptide as a white solid (104 mg, 50%).

R_f = 0.83 (MeCN:H_2O, 2:1, 0.1% TFA, C18).

HPLC R_T = 15.40 min (5-95% MeCN in H_2O over 30 min, 0.1% TFA modifier, 4.6 x 250mm C18).

^{1}H NMR (600 MHz, DMSO-*d*$_6$) d_H 9.19 (brs, 1H), 8.58 (dd, *J* = 8.2, 2.6 Hz) 8.33 (d, *J* = 8.0 Hz, 1H), 8.31-8.26 (m, 1H), 8.19-8.02 (m, 4H), 7.99-7.93 (m, 1H), 7.33 (s, 1H), 7.25-7.16 (m, 2H), 7.13-7.05 (m, 3H), 6.93-6.88 (m, 1H), 6.83-6.77 (m, 1H), 6.65 (d, *J* = 8.5 Hz, 2H), 5.83 (ddd, *J* = 17.3, 10.7, 6.2 Hz, 1H), 5.49 (d, *J* = 17.3 Hz, 1H), 5.41 (d, *J* = 10.7, 1H,), 4.66-4.49 (m, 3H), 4.38-4.15 (m, 4H), 3.73-3.52 (m, 4H), 2.95-2.88 (m, 1H), 2.82-2.73 (m, 1H), 2.73-2.58 (m, 1H), 2.45-2.39 (m, 2H), 2.16-2.03 (m, 3H), 1.92-1.68 (m, 5H,), 1.66-1.58 (m, 1H), 1.55-1.37 (m, 3H), 1.12-1.02 (m, 1H), 0.93-0.77 (m, 12H).

^{13}C NMR (151 MHz, DMSO-*d*$_6$) δ_C 174.4, 172.7, 172.6, 172.2, 171.8, 171.7, 171.5, 171.4, 171.3, 171.0, 166.8, 156.3, 130.9, 130.7, 128.1, 121.1, 115.4, 60.3, 57.4, 54.9, 54.4, 53.7, 52.6, 51.9, 50.1, 47.6, 42.4, 37.3, 37.0, 36.8, 31.9, 29.7, 29.5, 28.5, 24.8, 24.7, 24.6, 23.5, 21.9, 15.8, 11.4.

***m/z* HRMS (ESI$^+$)** calcd. for $C_{44}H_{69}N_{12}O_{12}S$ = 989.4873 ([M+H$^+$]), found 989.4873.

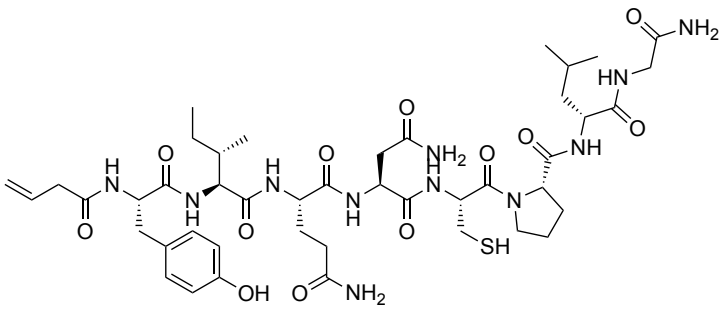

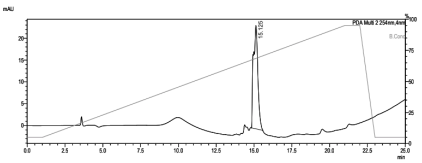

VAA-Tyr-Ile-Glu-Asn-Cys-Pro-Leu-Gly-NH_2 (2.13)

Synthesised according to the SPPS general procedure using Rink amide AM resin (0.250 g, 0.18 mmol) to afford a white solid, which was subjected to reverse-phase C_{18} flash chromatography (0-100% MeCN (0.1% TFA):H_2O (0.1% TFA)) to give the peptide as a white solid (61 mg, 36%).

R_f = 0.76 (MeCN:H_2O, 2:1, 0.1% TFA, C_{18} silica).

HPLC R_T = 15.13 min (5-95% MeCN in H_2O over 20 min, 0.1% TFA modifier, 4.6 x 250mm C18).

^{1}H NMR (600 MHz, DMSO-*d*$_6$) d_H 9.13 (brs, 1H), 8.34 (d, *J* = 9.0 Hz, 1H), 8.26 (d, *J* = 7.2 Hz, 1H), 8.20-8.01 (m, 4H), 7.99-7.92 (m, 1H), 7.33 (s, 1H), 7.26-7.16 (m, 2H), 7.13-7.01 (m, 4H), 6.93-6.87 (m, 1H), 6.82-6.75 (m, 1H), 6.65-6.59 (m, 2H), 6.57-6.49 (m, 1H,), 5.93 (d, *J* = 15.2 Hz, 1H), 5.80 (d, *J* = 11.5 Hz, 1H), 4.63-4.46 (m, 3H), 4.32-4.14 (m, 4H), 3.74-3.52 (m, 4H), 2.94-2.87 (m, 1H), 2.82-2.73 (m, 1H), 2.18-2.03 (m, 3H), 1.95 (d, *J* = 7.0, 1H), 1.92-1.80 (m, 2H), 1.78-1.70 (m, 3H), 1.65-1.58 (m, 1H), 1.55-1.40 (m, 3H), 1.11-1.04 (m, 1H), 0.92-0.77 (m, 12H).

^{13}C NMR (151 MHz, DMSO-*d*$_6$) δ_C 174.5, 172.7, 172.6, 172.0, 171.8, 171.7, 171.5, 171.4, 171.3, 166.3, 165.3, 156.1, 138.7, 130.5, 128.6, 126.0, 115.3, 61.0, 57.3, 54.5, 54.3, 52.6, 51.9, 51.2, 50.1, 47.3, 42.5, 37.2, 36.9, 36.7, 34.0, 31.9, 29.7, 29.4, 28.3, 24.9, 24.7, 24.6, 23.5, 21.9, 15.8, 11.5.

***m/z* HRMS (ESI$^+$)** calcd. for $C_{44}H_{67}N_{11}NaO_{12}S$ = 996.4584 ([M+Na^+]), found 996.4584.

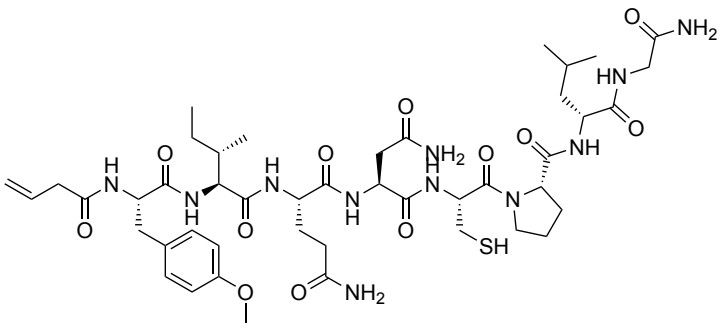

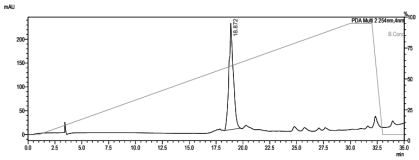

VAA-Tyr(OMe)-Ile-Glu-Asn-Cys-Pro-Leu-Gly-NH_2 (2.17a)

Synthesised according to the SPPS general procedure using Rink amide AM resin (0.250 g, 0.18 mmol) to afford a white solid, which was subjected to reverse-phase C_{18} flash chromatography (0-100% MeCN (0.1% TFA):H_2O (0.1% TFA)) to give the peptide as a white solid (96 mg, 83%).

R_f = 0.70 (MeCN:H_2O, 2:1, 0.1% TFA, C_{18} silica).

HPLC R_T = 15.86 min (20-90% MeCN in H_2O over 35 min, 0.1% TFA modifier, 4.6 x 250mm C18).

^{1}H NMR (600 MHz, DMSO-*d*$_6$) d_H 8.34 (d, *J* = 9.0 Hz, 1H), 8.26 (d, *J* = 7.2 Hz, 1H), 8.20-8.01 (m, 4H), 7.99-7.92 (m, 1H), 7.33 (s, 1H), 7.26-7.15 (m, 4H), 7.13-7.05 (m, 2H), 6.93-6.87 (m, 1H), 6.83-6.75 (m, 3H), 6.57-6.49 (m, 1H), 5.93 (d, *J* = 15.2 Hz, 1H), 5.81 (d, *J* = 11.5 Hz, 1H), 4.63-4.46 (m, 3H), 4.32-4.14 (m, 4H), 3.74-3.52 (m, 7H), 2.98-2.93 (m, 1H), 2.82-2.73 (m, 1H), 2.16-2.03 (m, 3H), 1.95 (d, *J* = 7.0, 1H), 1.92-1.80 (m, 2H), 1.78-1.70 (m, 3H), 1.65-1.58 (m, 1H), 1.55-1.40 (m, 3H), 1.11-1.04 (m, 1H), 0.92-0.77 (m, 12H,).

^{13}C NMR (151 MHz, DMSO-*d*$_6$) δ_C 174.5, 172.7, 172.6, 172.0, 171.8, 171.7, 171.5, 171.4, 171.3, 166.3, 165., 158.2 138.7, 131.0, 130.1, 126.0, 113.9, 61.0, 57.3, 55.4, 54.4, 54.3, 52.6, 51.9, 51.2, 50.1, 47.3, 42.5, 37.2, 36.9, 36.7, 34.0, 31.9, 29.7, 29.4, 28.3, 24.9, 24.7, 24.6, 23.5, 21.9, 15.8, 11.5.

***m/z* HRMS (ESI$^+$)** calcd. for $C_{45}H_{68}N_{11}NaO_{12}S$ = 986.4775 ([M-H$^-$]), found 998.4756.

7.2.3 Synthesis of cyclic peptides

General procedure for peptide cyclisation:

A sample tube was charged with a stir bar, DPAP (1 equiv.) and MAP (1 equiv.) and purged with N_2. H_2O (0.1% TFA):MeCN (1:2) solvent mix was prepared and degassed with sonication. Linear peptide (20 mg) was dissolved in the degassed solvent mix (3.0 mL) and added to the reaction vessel. The reaction was then stirred under UV for 1 h. The reaction mix was washed with EtOAc and the aqueous layer was then lyophilised to give the product peptide.

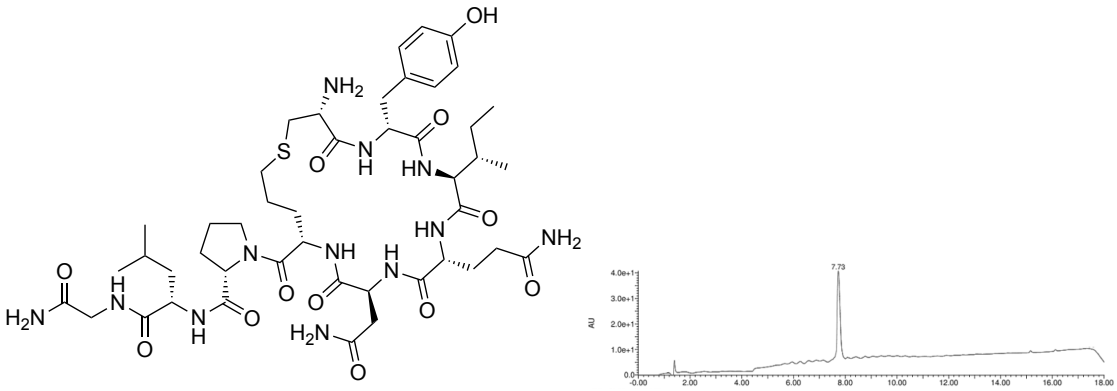

(cyclo-1,6)-Cys-Tyr-Ile-Glu-Asn-Agl-Pro-Leu-Gly-NH_2 (2.5)

HPLC R_T = 4.93 min (5-80% MeCN in H_2O over 15 min, 0.1% TFA modifier, 4.6 x 100mm C18).

^{1}H NMR (600 MHz, DMSO-*d*$_6$) δ_H 9.19 (brs, 1H), 8.72-8.61 (m, 1H), 8.31-7.86 (m, 7H), 7.37-7.31 (m, 1H), 7.29-7.16 (m, 2H), 7.15-7.01 (m, 4H), 6.94-6.86 (m, 1H), 6.85-6.76 (m, 1H), 6.65 (d, *J* = 7.86 Hz, 2H), 4.68-4.43 (m, 3H), 4.38-4.12 (m, 4H), 3.94-3.83 (m, 1H), 3.71-3.48 (m, 4H), 3.02-2.85 (m, 2H), 2.72-2.63 (m, 1H), 2.29 (t, *J* = 7.41 Hz, 1H), 2.19-1.99 (m, 3H), 1.94-1.67 (m, 6H), 1.66-1.38 (m, 4H), 1.14-1.01 (m, 1H), 0.92-0.76 (m, 12H).

^{13}C NMR (151 MHz, DMSO-*d*$_6$) δ_C 173.0, 172.1, 171.9, 171.3, 170.9, 170.84, 170.75, 170.70, 169.7, 155.9, 130.1, 127.0, 114.9, 59.4, 56.9, 54.4, 52., 51.4, 50.1, 49.5, 46.8, 41.9, 37.0, 36.6, 34.5, 31.3, 29.0, 28.7, 28.4, 24.4, 24.3, 24.1, 23.0, 21.6, 15.4, 10.9.

***m/z* HRMS (ESI$^+$)** calcd. for $C_{45}H_{71}N_{12}O_{12}S$ = 1003.5030 ([M+H$^+$]), found 1003.5030.

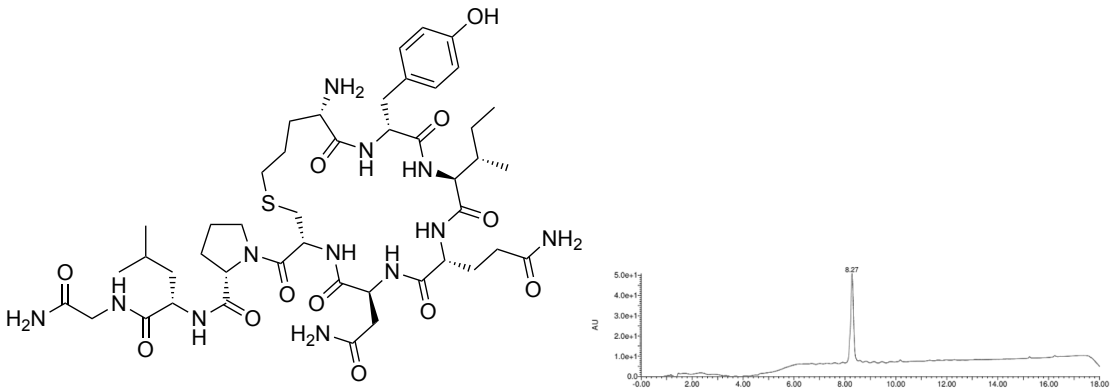

(cyclo-1,6)-Agl-Tyr-Ile-Glu-Asn-Cys-Pro-Leu-Gly-NH_2 (2.6)

HPLC R_T = 4.98 min (5-80% MeCN in H_2O over 15 min, 0.1% TFA modifier, 4.6 x 100mm C18).

^{1}H NMR (600 MHz, DMSO-*d*$_6$) δ_H 9.18 (brs, 1H), 8.72-8.57 (m, 1H), 8.35-7.86 (m, 7H), 7.38-7.30 (m, 1H), 7.30-7.20 (m, 2H), 7.20-6.99 (m, 4H), 6.95-6.84 (m, 1H), 6.70 (d, *J* = 8.2 Hz, 2H), 6.67-6.60 (m, 1H), 4.79-4.53 (m, 3H), 4.37-4.11 (m, 4H), 3.88-3.77 (m, 1H), 3.73-3.50 (m, 4H), 2.98-2.80 (m, 2H), 2.76-2.63 (m, 1H), 2.29 (t, *J* = 7.4 Hz, 1H), 2.24-2.00 (m, 3H), 1.94-1.67 (m, 6H), 1.65-1.39 (m, 4H), 1.14-1.03 (m, 1H), 0.94-0.77 (m, 12H).

^{13}C NMR (151 MHz, DMSO-*d*$_6$) δ_C 173.5, 172.6, 172.4, 171.6, 171.6, 171.4, 171.4, 171.0, 169.2, 156.4, 130.4, 128.2, 115.5, 60.3, 57.5, 54.8, 52.4, 51.9, 50.8, 49.8, 47.3, 42.5, 37.7, 36.9, 33.9, 31.8, 29.5, 29.2, 28.9, 24.9, 24.8, 24.7, 23.6, 22.0, 15.8, 11.5.

***m/z* HRMS (ESI$^+$)** calcd. for $C_{45}H_{71}N_{12}O_{12}S$ = 1003.5030 ([M+H$^+$]), found 1003.5064.

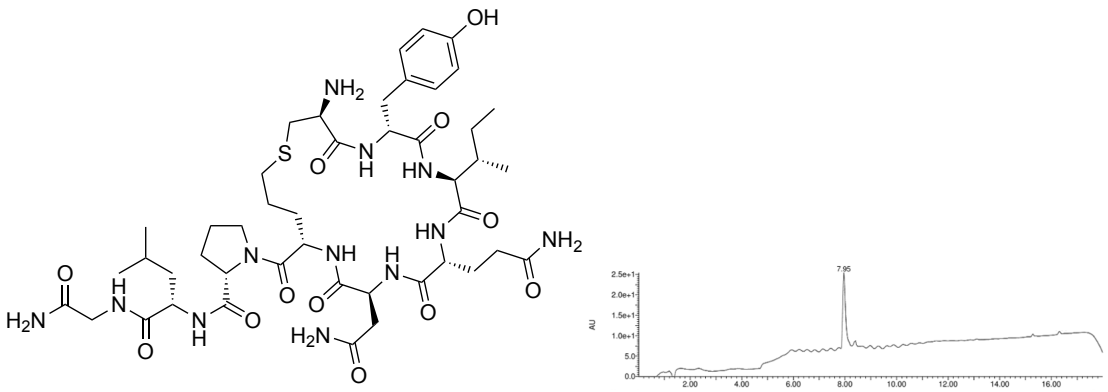

(cyclo-1,6)-D-Cys-Tyr-Ile-Glu-Asn-Agl-Pro-Leu-Gly-NH_2 (2.7)

HPLC R_T = 5.02 min (5-80% MeCN in H_2O over 15 min, 0.1% TFA modifier, 4.6 x 100mm C18).

^{1}H NMR (600 MHz, DMSO-*d*$_6$) δ_H 9.20 (brs, 1H), 8.73-8.67 (m, 2H), 8.31-7.86 (m, 7H), 7.37-7.31 (m, 1H), 7.29-7.16 (m, 2H), 7.14-6.99 (m, 4H), 6.94-6.85 (m, 1H), 6.85-6.76 (m, 1H), 6.65 (d, *J* = 7.8 Hz, 2H), 4.67-4.45 (m, 3H), 4.37-4.13 (m, 4H), 3.93-3.83 (m, 1H), 3.70-3.49 (m, 4H), 2.99-2.88 (m, 2H), 2.31-2.24 (1H), 2.18-1.99 (m, 3H), 1.95-1.68 (m, 6H), 1.66-1.39 (m, 4H), 1.14-1.03 (m, 1H), 0.92-0.76 (m, 12H).

^{13}C NMR (151 MHz, DMSO-*d*$_6$) δ_C 172.6, 172.4, 172.2, 171.7, 171.4, 171.2, 171.1, 171.0, 170.0, 156.3, 130.7, 127.5, 115.3, 59.8, 57.5, 54.2, 52.4, 51.9, 50.0, 47.3, 42.3, 36.9, 36.1, 34.0, 31.7, 29.4, 29.1, 28.7, 24.9, 24.6, 23.5, 22.6, 22.1, 15.8, 11.5.

***m/z* HRMS (ESI$^+$)** calcd. for $C_{45}H_{71}N_{12}O_{12}S$ = 1003.5030 ([M+H$^+$]), found 1003.5026.

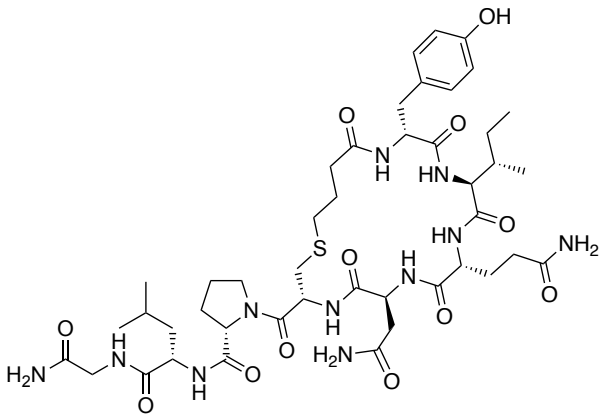

(cyclo-1,6)-VAA-Tyr-Ile-Glu-Asn-Cys-Pro-Leu-Gly-NH_2 (2.15)[243]

HPLC R_T = 18.92 min (20-90% MeCN in H_2O over 35 min, 0.1% TFA modifier, 4.6 x 250mm C18).

***m/z* HRMS (ESI$^+$)** calcd. for $C_{44}H_{67}N_{11}NaO_{12}S$ = 996.4584 ([M+Na^+]), found 996.4584

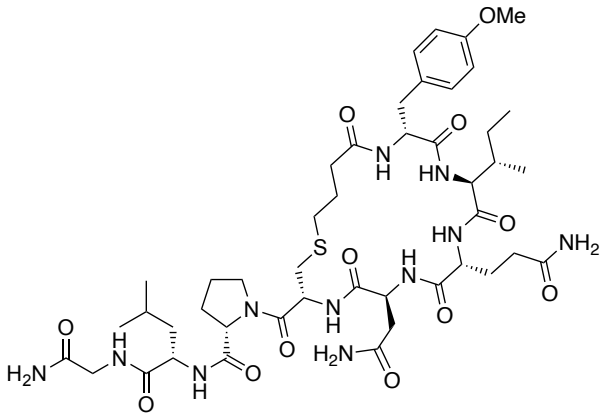

(cyclo-1,6)-VAA-Tyr(OMe)-Ile-Glu-Asn-Cys-Pro-Leu-Gly-NH_2 (2.17b)[244,245]

HPLC R_T = 18.99 min (20-90% MeCN in H_2O over 35 min, 0.1% TFA modifier, 4.6 x 250mm C18).

***m/z* HRMS (ESI$^+$)** calcd. for $C_{45}H_{69}N_{11}NaO_{12}S$ = 1010.4740 ([M+Na^+]), found 1010.4745.

7.2.4 Investigation of Cyclisation of Short Peptides

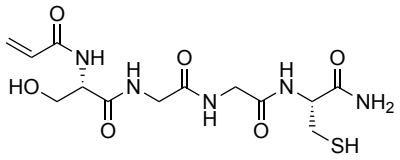

***N*-((*S*)-1-((2-((2-(((*R*)-1-amino-3-mercapto-1-oxopropan-2-yl)amino)-2-oxoethyl)amino)-2-oxoethyl)amino)-3-hydroxy-1-oxopropan-2-yl)acrylamide (2.19)**

Synthesised according to the general procedure in section 6.2.2.

HPLC R_T = 4.83 min (5% MeCN in H_2O for 7 min, 5-95% MeCN in H_2O over 5 min, 0.1% TFA modifier, 4.6 x 250mm C18).

***m/z* HRMS (ESI$^+$)** calcd. for $C_{13}H_{20}N_5O_6S$ = 374.1140 ([M-H]$^-$), found 374.1131.

General Procedure: Cyclisation of short peptides.
To a solution of **2.19** (10 mM), initiator was added and the mixture irradiated (365 nm or 440 nm) for 2 h. The reaction mixture was then subjected to ^{1}H NMR spectroscopic analysis.

7.3 Experimental for chapter 3

7.3.1 Scope examples for UV-initiated TEC

General Procedure A: UV-Initiated TEC in DESs

A solution of alkene, thiol, DPAP (0.2 equiv.) and MAP (0.2 equiv.) in DES (approx. 3.0 mL) was stirred under UV irradiation for 1 hour. The reaction was then minimally diluted with H_2O (approx. 1.0 mL) to reduce viscosity of the aqueous layer and extracted with EtOAc (10 mL). Organics were dried using $MgSO_4$, filtered and concentrated *in vacuo*. The product was then purified *via* flash chromatography on silica gel.

General Procedure B: UV-initiated ATE in DES.

A solution of alkene, thioacid, DPAP (0.2 equiv.) and MAP (0.2 equiv.) in DES (approx. 3.0 mL) was stirred under UV irradiation for 1 hour. The reaction was then minimally diluted with H_2O (approx. 1.0 mL) to reduce viscosity of the aqueous layer and extracted with EtOAc (10 mL). Organics were dried using $MgSO_4$, filtered and concentrated *in vacuo*. The product was then purified *via* flash chromatography on silica gel.

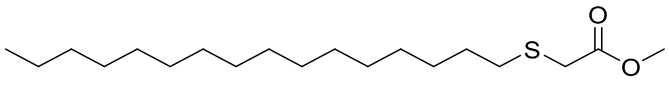

Methyl 2-(hexadecylthio)acetate (3.6a)[246]

Hexadec-1-ene (1.0 mmol, 0.082 g, 0.101 mL) was reacted with methyl 2-mercaptoacetate (1.2 mmol, 0.128 g, 0.111 mL) in ChCl:Gly in the presence of DPAP (0.2 mmol, 0.051 g) and MAP (0.2 mmol, 0.031 g) according to general procedure A. The product was purified by silica gel flash chromatography using 10% EtOAc/Hexane (v/v) to yield the desired product as a colourless oil (117 mg, 63%).

R_f = 0.71 (10% EtOAc/Hexane (v/v)).

^{1}H NMR (400 MHz, $CDCl_3$) δ_H 3.76 (s, 3H), 3.25 (s, 2H), 2.65 (t, *J* = 7.4 Hz, 2H,), 1.66-1.56 (m, 2H), 1.46-1.21 (m, 26H), 0.90 (t, *J* = 6.9 Hz, 3H).

***m/z* HRMS (ESI$^+$)** calcd. for $C_{19}H_{38}NaO_2S$ ($[M+Na]^+$): 353.2485; found: 353.2489.

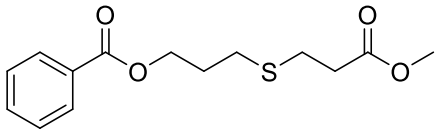

3-((3-methoxy-3-oxopropyl)thio)propyl benzoate (3.6b)

Allyl benzoate (0.4 mmol, 0.065 g, 0.064 mL) was reacted with methyl 3-mercaptopropionate (0.6 mmol, 0.072 g, 0.066 mL) in the presence of DPAP (0.04 mmol, 0.010 g) and MAP (0.04 mmol, 0.006 g) according to general procedure A. The product was purified by silica gel flash chromatography using 10-15% EtOAc/Hexane (v/v) to yield the desired product as a colourless oil (0.1023 g, 91%).

R_f = 0.48 (20% EtOAc/Hexane (v/v)).

^{1}H NMR (400 MHz, $CDCl_3$) δ_H 8.06 (d, *J* = 8.5 Hz, 2H), 7.59 (t, *J* = 7.4 Hz, 1H), 7.47 (t, *J* = 7.6 Hz, 2H), 4.44 (t, *J* = 6.2 Hz, 2H), 3.72 (s, 3H), 2.85 (t, *J* = 7.0 Hz, 2H), 2.72 (t, *J* = 7.3 Hz, 2H), 2.65 (t, *J* = 7.3 Hz, 2H), 2.11-2.08 (m, 2H).

^{13}C NMR (151 MHz, $CDCl_3$) δ_C 172.3, 166.5, 133.0, 130.2, 129.6, 128.4, 63.5, 51.8, 41.3, 34.6, 28.8, 27.0.

***m/z* HRMS (APCI$^+$)** calcd. for $C_{14}H_{18}NaO_4S$ ($[M+Na]^+$): 305.0818; found: 305.0819.

ν_{max} (film), cm^{-1}: 2952 (C-H stretch), 1734, 1714 (C=O stretch), 1457 (C-H bend), 1248, 1110 (C-O stretch).

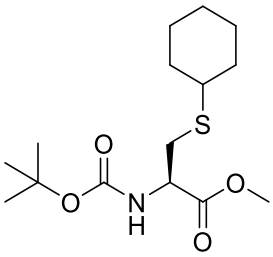

Methyl *N*-(tert-butoxycarbonyl)-*S*-cyclohexyl-L-cysteinate (3.6c)

Cyclohexene (2.0 mmol, 0.164 g, 0.202 mL) was reacted with Boc-Cys-OMe (1.0 mmol, 0.235 g, 0.206 mL) in ChCl:Gly in the presence of DPAP (0.2 mmol, 0.051 g) and MAP (0.2 mmol, 0.031 g) according to general procedure A. The product was purified by silica gel flash chromatography using 20% EtOAc/Hexane (v/v) to yield the desired product as a colourless oil (212 mg, 67%).

R_f = 0.46 (20% EtOAc/Hexane (v/v)).

^{1}H NMR (400 MHz, $CDCl_3$) δ_H (400 MHz, $CDCl_3$) 5.37 (d, *J* = 5.8 Hz, 1H), 4.57-4.54 (m, 1H), 3.78 (s, 3H), 3.00 (d, *J* = 4.7 Hz, 2H), 2.71-2.61 (m, 1H), 2.02-1.91 (m, 2H), 1.84-1.73 (m, 2H), 1.65 (s, 2H), 1.47 (s, 9H), 1.37-1.21 (m, 4H).

^{13}C NMR (151 MHz, $CDCl_3$) δ_C 171.7, 155.2, 80.1, 53.4, 52.5, 44.0, 33.6, 32.3, 28.3, 26.0, 25.7.

***m/z* HRMS (APCI$^+$)** calcd. for $C_{15}H_{27}NNaO_4S$ ($[M+Na]^+$): 340.1553; found: 340.1553.

ν_{max} (film), cm^{-1}: 2934 (N-H stretch), 1747, 1713 (C=O stretch), 1497 (C-H bend), 1208, 1161 (C-O stretch).

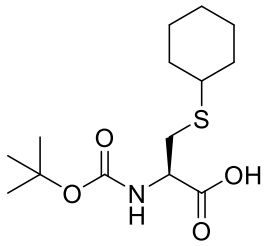

***N*-(tert-Butoxycarbonyl)-*S*-cyclohexyl-L-cysteine (3.6d)**

Cyclohexene (0.700 mmol, 0.058 g, 0.072 mL) was reacted with Boc-Cys-OH (0.350 mmol, 0.077 g) in ChCl:Gly in the presence of DPAP (0.035 mmol, 0.009 g) and MAP (0.035 mmol, 0.005 g) according to general procedure A. The product was purified by back-extraction to yield the desired product as a viscous, colourless oil (74 mg, 70%).

^{1}H NMR (400 MHz, $CDCl_3$) δ_H 5.44-5.36 (m, 1H), 4.64-4.52 (m, 1H), 3.02-2.93 (m, 2H), 2.65-2.57 (m, 1H), 1.97-1.93 (m, 2H), 1.77-1.73 (m, 2H), 1.45 (s, 11H), 1.31-1.24 (4H).

^{13}C NMR (151 MHz, $CDCl_3$) δ_C 175.3, 155.5, 78.7, 54.6, 53.2, 44.1, 33.5, 28.3, 26.0, 25.7.

***m/z* HRMS (ESI$^+$)** calcd. for $C_{14}H_{24}NO_4S$ ($[M-H]^-$): 302.1432; found 302.1436.

ν_{max} (film), cm^{-1}: 3433 (O-H stretch), 2930 (N-H stretch), 1710 (C=O stretch), 1501 (C-H bend), 1159 (C-O stretch).

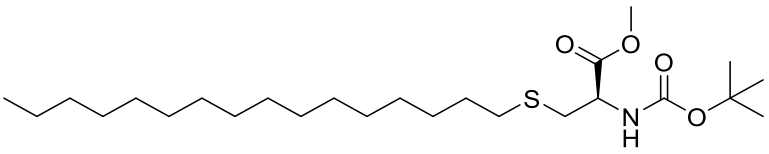

Methyl *N*-(tert-butoxycarbonyl)-*S*-hexadecyl-L-cysteinate (3.6e)

Hexadec-1-ene (0.36 mmol, 0.071 g, 0.091 mL) was reacted with Boc-Cys-OMe (0.30 mmol, 0.081 g, 0.071 mL) in ChCl:Gly in the presence of DPAP (0.06 mmol, 0.016 g) and MAP (0.06 mmol, 0.010 g) according to general procedure A. The product was purified by silica gel flash chromatography using 0-10% EtOAc/Hexane (v/v) to yield the desired product as a colourless oil, later forming a white wax when stored at -20 ºC overnight (108 mg, 78%).

R_f = 0.51 (15% EtOAc/Hexane (v/v)).

^{1}H NMR (400 MHz, $CDCl_3$) δ_H 5.37 (d, *J* = 7.1 Hz, 1H), 4.57-4.53 (m, 1H), 3.78 (s, 3H), 2.98 (d, *J* = 4.6 Hz, 2H), 2.53 (t, *J* = 7.4 Hz, 2H), 1.62-1.51 (m, 2H), 1.47 (s, 9H), 1.41-1.22 (m, 26H), 0.90 (t, *J* = 6.8 Hz, 3H).

^{13}C NMR (151 MHz, $CDCl_3$) δ_C 171.7, 155.1, 80.1, 53.3, 52.5, 34.5, 32.8, 31.9, 29.74, 29.68, 29.64, 29.59, 29.54, 29.4, 29.2, 28.8, 28.3, 22.7, 14.1.

***m/z* HRMS (APCI$^+$)** calcd. for $C_{25}H_{49}NNaO_4S$ ([M+Na]$^+$): 482.3275; found: 482.3281.

ν_{max} (film), cm^{-1}: 2916, 2847 (N-H stretch), 1751, 1683 (C=O stretch), 1497 (C-H bend), 1203, 1168 (C-O stretch).

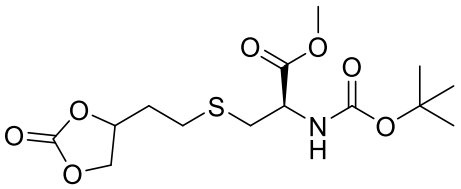

Methyl *N*-(tert-butoxycarbonyl)-*S*-(2-(2-oxo-1,3-dioxolan-4-yl)ethyl)-L-cysteinate (3.6f)

4-Vinyl-1,3-dioxolan-2-one (1.0 mmol, 0.057 g, 0.048 mL) was reacted with Boc-Cys-OMe (0.5 mmol, 0.117 g, 0.103 mL) in ChCl:Gly in the presence of DPAP (0.1 mmol, 0.026 g) and MAP (0.1 mmol, 0.016 g) according to general procedure A. The product was purified by silica gel flash chromatography using 20-60% EtOAc/Hexane (v/v) to yield the desired product as a colourless oil (103 mg, 59%).

R_f = 0.19 (40% EtOAc/Hexane (v/v)).

^{1}H NMR (400 MHz, $CDCl_3$) δ_H 5.35 (s, 1H), 4.93-4.84 (m, 1H), 4.63-4.55 (m, 2H), 4.15-4.05 (m, 1H), 3.80 (s, 3H), 3.08-2.92 (m, 2H), 2.82-2.63 (m, 2H), 2.00-1.82 (m, 2H), 1.47 (s, 9H).

^{13}C NMR (151 MHz, $CDCl_3$) δ_C 171.3, 155.2, 154.6, 80.4, 75.2, 69.1, 53.3, 52.7, 33.9, 28.3, 27.83, 27.79.

***m/z* HRMS (APCI$^+$)** calcd. for $C_{14}H_{23}NNaO_7S$ ($[M+Na]^+$): 372.1087; found: 372.1095.

ν_{max} (film), cm^{-1}: 2978, 2928 (N-H stretch), 1793, 1741, 1705 (C=O stretch), 1503 (C-H bend), 1215, 1157 (C-O stretch).

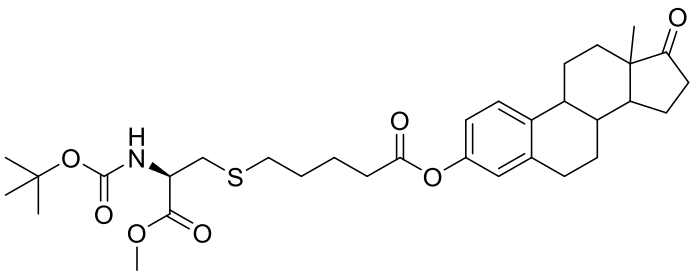

13-Methyl-17-oxo-7,8,9,11,12,13,14,15,16,17-decahydro-6H-cyclopenta[a]phenanthren-3-yl 5-(((*R*)-2-((tert-butoxycarbonyl)amino)-3-methoxy-3-oxopropyl)thio)pentanoate (3.6g)

3.10 (0.30 mmol, 0.106 g) was reacted with Boc-Cys-OMe (0.33 mmol, 0.078 g, 0.069 mL) in 20% H_2O/ChCl:Gly (v/v) in the presence of DPAP (0.6 mmol, 0.016 g) and MAP (0.06 mmol, 0.010 g) according to general procedure A. The product was purified by silica gel flash chromatography using 25-30% EtOAc/Hexane (v/v) to yield the desired product as a colourless oil (36 mg, 20%).

R_f = 0.26 (30% EtOAc/Hexane (v/v)).

^{1}H NMR (400 MHz, $CDCl_3$) δ_H 7.28 (d, *J* = 8.4 Hz, 1H), 6.88-6.79 (m, 2H), 5.46-5.34 (m, 1H), 4.65-4.50 (m, 1H), 3.77 (s, 3H), 3.03-2.87 (m, 4H), 2.63-2.46 (m, 4H), 2.44-2.36 (m, 1H), 2.33-2.24 (m, 1H), 2.21-1.92 (m, 4H), 1.89-1.79 (m, 2H), 1.75-1.39 (m, 17H), 0.91 (s, 3H).

^{13}C NMR (151 MHz, $CDCl_3$) δ_C 220.7, 172.0, 171.6, 155.1, 148.5, 138.0, 137.4, 126.4, 121.5, 118.7, 53.3, 52.6, 50.4, 47.9, 44.1, 38.0, 35.8, 34.5, 33.8, 32.3, 31.6, 29.4, 28.8, 28.3, 26.3, 25.8, 23.9, 21.6, 13.8.

***m/z* HRMS (APCI$^+$)** calcd. for $C_{32}H_{45}NNaO_7S$ ($[M+Na]^+$): 610.2809; found: 610.2813.

ν_{max} (film), cm^{-1}: 2934 (N-H stretch), 1737, 1712 (C=O stretch), 1493 (C-H bend), 1208, 1159 (C-O stretch).

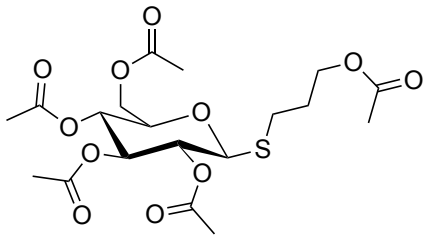

(2*R*,3*R*,4*S*,5*R*,6*S*)-2-(Acetoxymethyl)-6-((3-acetoxypropyl)thio)tetrahydro-2*H*-pyran-3,4,5-triyl triacetate (3.6h)[104]

Allyl acetate (0.5 mmol, 0.050 g, 0.054 mL) was reacted with 1-thio-β-D-glucose tetraacetate (0.6 mmol, 0.182 g) in 20% H_2O/ChCl:Gly (v/v) in the presence of DPAP (0.1 mmol, 0.026 g) and MAP (0.1 mmol, 0.016 g) according to general procedure A. The product was purified by silica gel flash chromatography using 50% EtOAc/Hexane (v/v) to yield the desired product as a colourless oil (174 mg, 75%).

R_f = 0.54 (60% EtOAc/Hexane (v/v)).

^{1}H NMR (400 MHz, $CDCl_3$) δ_H 5.20-5.16 (m, 1H), 5.07-4.95 (m, 1H), 4.45 (d, *J* = 12.2 Hz, 1H), 4.20 (dd, *J* = 12.2, 5.1 Hz, 1H), 4.16-4.09 (m, 3H), 3.71-3.64 (m, 1H), 2.79-2.61 (m, 2H), 2.06 (s, 3H), 2.03 (s, 6H), 2.01 (s, 3H), 1.99 (s, 3H), 1.93-1.85 (m, 2H).

***m/z* HRMS (APCI$^+$)** calcd. for $C_{19}H_{27}O_{11}S$ ($[M+H]^+$): 463.1279; found: 463.1275.

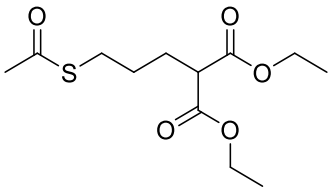

Diethyl 2-(3-(acetylthio)propyl)malonate (3.7a)[247]

Diethyl 2-allylmalonate (1.0 mmol, 0.200 g, 0.197 mL) was reacted with thioacetic acid (1.2 mmol, 0.091 g, 0.084 mL) in ChCl:Gly in the presence of DPAP (0.2 mmol, 0.051 g) and MAP (0.2 mmol, 0.031 g) according to general procedure B. The product was purified by silica gel flash chromatography using 10% EtOAc/Hexane (v/v) to yield the desired product as a colourless oil (161 mg, 71%).

R_f = 0.24 (20% EtOAc/Hexane (v/v)).

^{1}H NMR (400 MHz, $CDCl_3$) δ_H 4.22 (m, 4H), 3.35 (t, *J* = 7.2 Hz, 1H), 2.91 (t, *J* = 7.2 Hz, 2H), 2.35 (s, 3H), 1.19 (m, 2H), 1.64 (m, 2H), 1.29 (t, *J* = 7.1, 6H).

***m/z* HRMS (APCI$^+$)** calcd. for $C_{12}H_{21}O_5S$ ($[M+H]^+$): 277.1104; found: 277.1107.

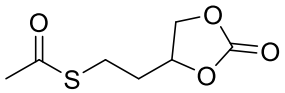

***S*-(2-(2-oxo-1,3-dioxolan-4-yl)ethyl) ethanethioate (3.7b)**[104]

4-Vinyl-1,3-dioxolan-2-one (0.5 mmol, 0.057 g, 0.048 mL) was reacted with thioacetic acid (0.6 mmol, 0.046 g, 0.043 mL) in ChCl:Gly in the presence of DPAP (0.1 mmol, 0.026 g) and MAP (0.1 mmol, 0.016 g) according to general procedure B. The product was purified by silica gel flash chromatography using 20-60% EtOAc/Hexane (v/v) to yield the desired product as a pale yellow oil (76 mg, 80%).

R_f = 0.59 (60% EtOAc/Hexane (v/v)).

^{1}H NMR (400 MHz, $CDCl_3$) δ_H 4.81-4.73 (m, 1H), 4.57 (t, *J* = 8.2 Hz, 1H), 4.14 (dd, *J* = 8.2, 6.9 Hz, 1H), 3.08-2.99 (m, 1H), 2.96-2.87 (m, 1H), 2.35 (s, 3H), 2.15-1.93 (m, 2H).

***m/z* HRMS (APCI$^+$)** calcd. for $C_7H_{10}NaO_4S$ ($[M+Na]^+$): 213.0192; found: 213.0194.

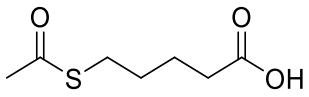

5-(Acetylthio)pentanoic acid (3.7c)[104]

4-Pentenoic acid (0.6 mmol, 0.601 g, 0.0613 mL) was reacted with thioacetic acid (0.9 mmol, 0.069 g, 0.064 mL) in the presence of DPAP (0.06 mmol, 0.015 g) and MAP (0.06 mmol, 0.009 g) according to general procedure B. The product was purified by back-extraction to yield the desired product a colourless oil, later forming white crystals when stored at -20 ºC overnight (97 mg, 91%).

^{1}H NMR (400 MHz, $CDCl_3$) δ_H 2.91 (t, *J* = 7.0 Hz, 2H), 2.40 (t, *J* = 7.0 Hz, 2H), 2.35 (s, 3H), 1.78-1.62 (m, 4H).

^{13}C NMR (151 MHz, $CDCl_3$) δ_C 195.9, 178.9, 33.3, 30.6, 28.9, 28.6, 23.7.

***m/z* HRMS (APCI$^+$)** calcd. for $C_7H_{11}O_3S$ ($[M+H]^+$): 175.0434; found: 175.0434.

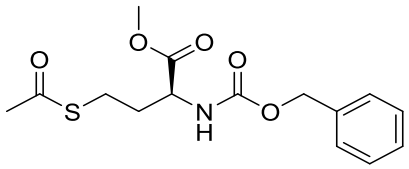

Methyl *S*-acetyl-*N*-((benzyloxy)carbonyl)-L-homocysteinate (3.7d)[248]

Cbz-Vgl-OMe (**2.8a**) (0.30 mmol, 0.075 g) was reacted with thioacetic acid (0.36 mmol, 0.027 g, 0.025 mL) in ChCl:Gly in the presence of DPAP (0.06 mmol, 0.016 g) and MAP (0.10 mmol, 0.010 g) according to general procedure B. The product was purified by silica gel flash chromatography using 20% EtOAc/Hexane (v/v) to yield the desired product as a colourless oil (57 mg, 58%).

R_f = 0.23 (20% EtOAc/Hexane (v/v)).

^{1}H NMR (400 MHz, $CDCl_3$) δ_H 7.41-7.32 (m, 5H), 5.43 (d, *J* = 5.1 Hz, 1H), 5.14 (s, 2H), 4.46 (q, *J* = 4.6, 1H), 3.78 (s, 3H), 3.01-2.94 (m, 1H), 2.91-2.85 (m, 1H), 2.34 (s, 3H), 2.19-2.14 (m, 1H), 1.99-1.93 (m, 1H).

***m/z* HRMS (APCI$^+$)** calcd. for $C_{15}H_{19}NNaO_5S$ ($[M+Na]^+$): 348.0876; found: 348.0881.

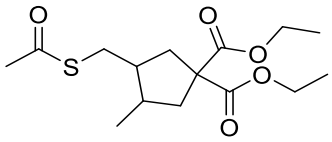

Diethyl 3-((acetylthio)methyl)-4-methylcyclopentane-1,1-dicarboxylate (3.7e)[249]

Diethyl 2,2-diallylmalonate (0.5 mmol, 0.121 g, 0.122 mL) was reacted with thioacetic acid (0.6 mmol, 0.046 g, 0.043 mL) in ChCl:Gly in the presence of DPAP (0.1 mmol, 0.026 g) and MAP (0.1 mmol, 0.016 g) at a concentration of 0.1 M, according to general procedure B. The product was purified by silica gel flash chromatography using 95% EtOAc/Hexane (v/v) to yield the desired product as a colourless oil (83 mg, 53%, 1:6 d.r.).

^{1}H NMR (400 MHz, $CDCl_3$) δ_H 4.19 (d *J* = 7.1 Hz, 4H), 2.96 (dd, *J* = 13.4, 6.5 Hz, 1H), 2.81 (dd, *J* = 13.4, 8.5 Hz, 1H), 2.50-2.39 (m, 2H), 2.34 (s, 3H), 2.30-2.17 (m, 2H), 2.09 (m, 1H), 2.01 (m, 1H), 1.25 (t, *J* = 7.1 Hz, 6H), 1.06 (d, *J* = 6.5 Hz, 0.44H), 0.94 (d, *J* = 6.5 Hz, 2.56H).

***m/z* HRMS (APCI$^+$)** calcd. for $C_{15}H_{25}O_5S$ ($[M+H]^+$): 317.1417; found: 317.1420.

7.3.2 Procedures for O_2-initiated TEC

General Procedure C: O_2-Initiated TEC in DES.

A solution of alkene and thiol in DES (approx. 3.0 mL) was heated to 64 °C with rapid stirring for 16-24 h. The reaction was cooled, minimally diluted with H_2O (approx. 1.0 mL) to reduce viscosity of the aqueous layer and extracted with EtOAc (10 mL). Organics were dried using $MgSO_4$, filtered and concentrated *in vacuo*. The product was then purified *via* flash chromatography on silica gel.

General Procedure D: O_2-Initiated ATE in DES.

A solution of alkene and thioacid in DES (approx. 3.0 mL) was heated to 64 °C with rapid stirring for 16-24 h. The reaction was cooled, minimally diluted with H_2O (approx. 1.0 mL) to reduce viscosity of the aqueous layer and extracted with EtOAc (10 mL). Organics were dried using $MgSO_4$, filtered and concentrated *in vacuo*. The product was then purified *via* flash chromatography on silica gel.

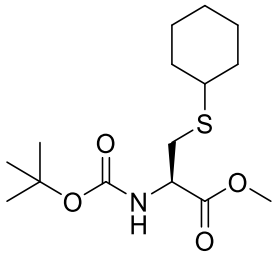

Methyl *N*-(tert-butoxycarbonyl)-*S*-cyclohexyl-L-cysteinate (3.6c)

Cyclohexene (1.0 mmol, 0.082 g, 0.101 mL) was reacted with Boc-Cys-OMe (0.5 mmol, 0.118 g, 0.103 mL) in ChCl:Gly according to general procedure C. The product was purified by silica gel flash chromatography using 20% EtOAc/Hexane (v/v) to yield the desired product as a colourless oil (67 mg, 73%).

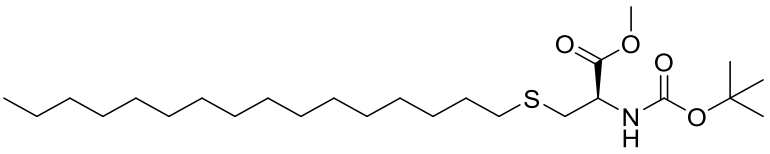

Methyl *N*-(tert-butoxycarbonyl)-*S*-hexadecyl-L-cysteinate (3.6e)

Hexadec-1-ene (0.6 mmol, 0.135 g, 0.173 mL) was reacted with Boc-Cys-OMe (0.30 mmol, 0.081 g, 0.071 mL) in ChCl:Gly according to general procedure C. The product was purified

by silica gel flash chromatography using 0-10% EtOAc/Hexane (v/v) to yield the desired product as a colourless oil, later forming a white wax when stored at -20 ºC overnight (90 mg, 65%).

ν_{max} (film), cm^{-1}: 2916, 2847 (N-H stretch), 1751, 1683 (C=O stretch), 1497 (C-H bend), 1203, 1168 (C-O stretch).

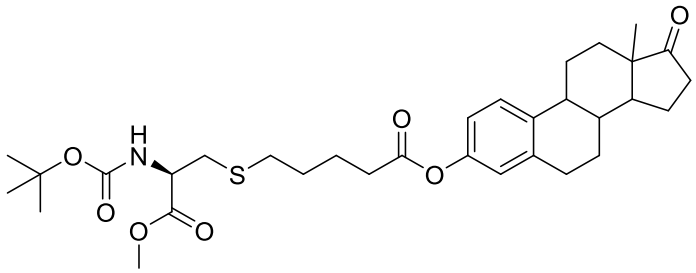

13-Methyl-17-oxo-7,8,9,11,12,13,14,15,16,17-decahydro-6H-cyclopenta[a]phenanthren-3-yl 5-(((*R*)-2-((tert-butoxycarbonyl)amino)-3-methoxy-3-oxopropyl)thio)pentanoate (3.6g)

3.10 (0.3 mmol, 0.106 g) was reacted with Boc-Cys-OMe (0.33 mmol, 0.078 g, 0.069 mL) in 20% H_2O/ChCl:Gly (v/v) according to general procedure C. The product was purified by silica gel flash chromatography using 25-30% EtOAc/Hexane (v/v) to yield the desired product as a colourless oil (95 mg, 54%).

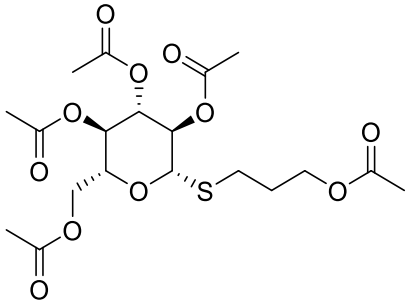

(2*R*,3*R*,4*S*,5*R*,6*S*)-2-(Acetoxymethyl)-6-((3-acetoxypropyl)thio)tetrahydro-2H-pyran-3,4,5-triyl triacetate (3.6h)[104]

Allyl acetate (0.3 mmol, 0.030 g, 0.033 mL) was reacted with 1-thio-β-D-glucose tetraacetate (0.33 mmol, 0.120 g) in 20% H_2O/ChCl:Gly (v/v) according to general procedure C. The product was purified by silica gel flash chromatography using 50% EtOAc/Hexane (v/v) to yield the desired product as a colourless oil (100 mg, 72%).

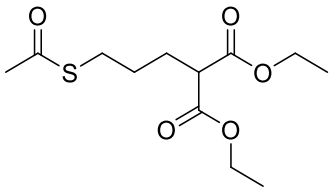

Diethyl 2-(3-(acetylthio)propyl)malonate (3.7a)

Diethyl 2-allylmalonate (1.0 mmol, 0.200 g, 0.197 mL) was reacted with thioacetic acid (2.0 mmol, 0.152 g, 0.141 mL) in ChCl:Gly according to general procedure D. The product was purified by silica gel flash chromatography using 10% EtOAc/Hexane (v/v) to yield the desired product as a colourless oil (83 mg, 37%).

7.3.3 Peptide Bioconjugation in DESs

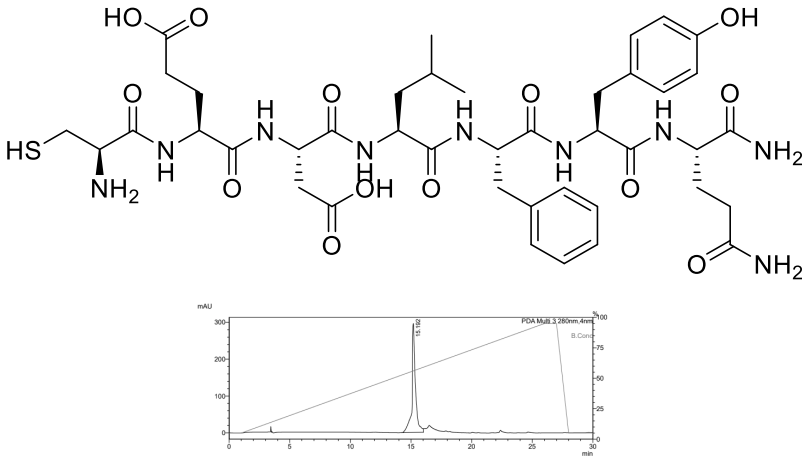

Cys-Glu-Asp-Leu-Phe-Tyr-Gln-NH_2 (3.9)

The desired sequence was prepared by standard Fmoc SPPS using 20% piperidine in DMF (2 x 10 min) for deprotection. A coupling mix consisting of Fmoc-AA (4 equiv.), PyBop (4 equiv.) and NMM (8 equiv.) in DMF was used to couple the first residue to the resin. Further couplings used Fmoc-AA (3 equiv.), PyBop (3 equiv.) and NMM (6 equiv.) in DMF. All couplings were complete after 45 min. The peptide was cleaved from the resin using TFA:H_2O:EDT:TES (94:2.5:2.5:1) cleavage cocktail. The TFA was removed under Ar flow, the peptide precipitated using cold ether and lyophilised. The product was analysed by RP-HPLC and used without further purification.

R_T (RP-HPLC) = 15.19 min (5-95% MeCN in H_2O with 0.1% TFA, 25 min).

^{1}H NMR (600 MHz, DMSO-d_6) δ_H 9.15 (brs, 1H), 8.72-8.59 (m, 1H), 8.50-8.35 (m, 1H), 8.04-7.84 (m, 3H), 7.28-7.13 (m, 8H), 7.07 (s, 1H), 7.02 (d, *J* = 8.5 Hz, 2H), 6.76 (s, 1H,), 6.64 (d, *J* = 8.46 Hz, 2H), 4.58-4.53 (m, 1H), 4.50-4.31 (m, 3H), 4.24-4.13 (m, 2H), 4.02-3.99 (m, 1H), 3.03-2.84 (m, 4H), 2.80-2.70 (m, 2H), 2.68-2.61 (m, 1H), 2.34-2.21 (m, 2H), 2.08 (t, *J* = 8.3, 2H), 1.95-1.84 (m, 2H), 1.81-1.71 (m, 2H), 1.55-1.46 (m, 1H), 1.36-1.28 (m, 1H), 0.82 (d, *J* = 6.5 Hz, 3H), 0.77 (d, *J* = 6.5 Hz, 3H).

^{13}C NMR (151 MHz, DMSO-d_6) δ_C 173.8, 173.8, 173.7, 173.07, 173.01, 171.7, 171.6, 170.8, 170.1, 155.8, 137.6, 130.0, 129.2, 127.9, 127.5, 126.1, 114.9, 54.3, 53.9, 53.6, 52.1, 51.9, 51.1, 49.3, 49.1, 39.7, 37.2, 36.5, 35.8, 31.4, 28.1, 27.7, 25.2, 24.0, 23.0, 21.4.

***m/z* HRMS (ESI$^+$)** calcd. for $C_{41}H_{58}N_9O_{13}S$ ($[M+H]^+$): 916.3888; found: 916.3870.

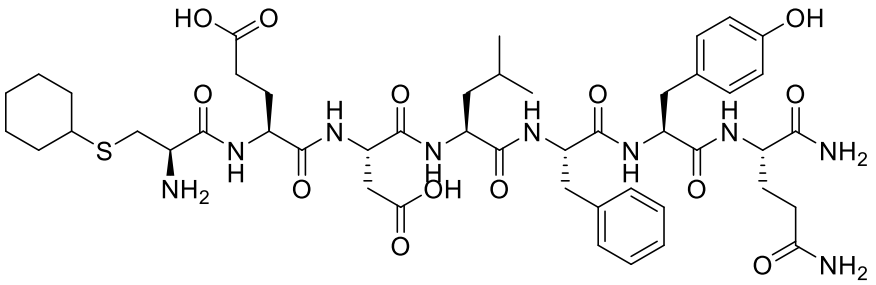

***S*-Cyclohexyl-Cys-Glu-Asp-Leu-Phe-Tyr-Gln-NH_2 (3.8a)**

To degassed ChCl:Gly/H_2O (3:2, 1 mL) was added peptide substrate (0.0090 g, 0.01 mmol, 1 equiv.), cyclohexene (0.0050 mL, 0.0040 g, 0.05 mmol, 5 equiv.), DPAP (0.0026 g, 0.01 mmol, 1 equiv.), MAP (0.0015 g, 0.01 mmol, 1 equiv.) and TES (0.0020 mL, 0.0012 g, 0.01 mmol, 1 equiv.). The mix was stirred under UV irradiation and Ar atmosphere for 3 hours. A 0.25 mL aliquot of reaction mix was added to 0.25 mL MeCN and subjected to RP-HPLC analysis which confirmed the consumption of the peptide starting material. A 0.75 mL aliquot was then subjected to semi-preparative RP-HPLC to yield the desired product as a white solid after lyophilisation (1.4 mg, 56%).

R_T (RP-HPLC) = 16.93 min (5-95% MeCN in H_2O with 0.1% TFA, 25 min).

***m/z* HRMS (ESI$^+$)** calcd. for $C_{47}H_{68}N_9O_{13}S$ ($[M+H]^+$): 998.4652; found: 998.4633.

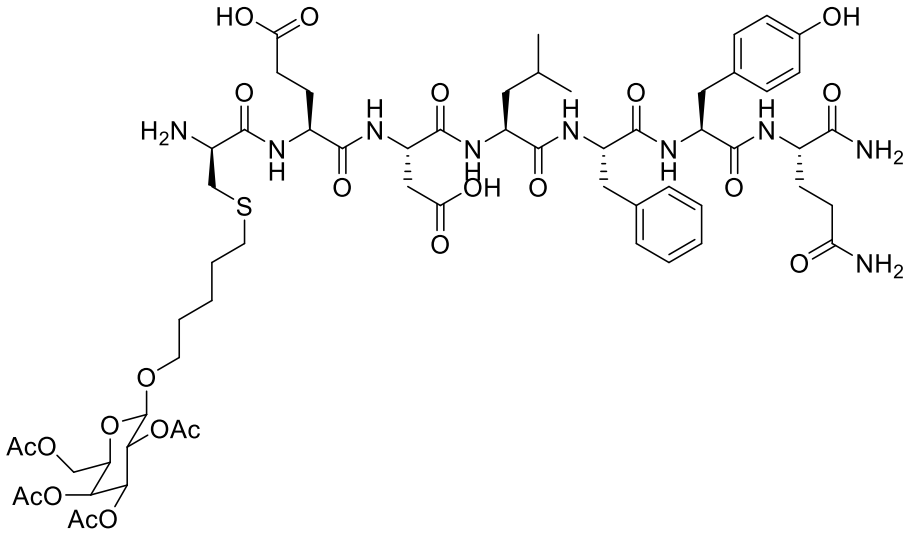

***S*-Galactosyl-Cys-Glu-Asp-Leu-Phe-Tyr-Gln-NH_2 (3.8b)**

To degassed ChCl:Gly/H_2O (3:2, 1 mL) was added peptide substrate (0.0090 g, 0.01 mmol, 1 equiv.), **3.12** (0.0208 g, 0.05 mmol, 5 equiv.), DPAP (0.0026 g, 0.01 mmol, 1 equiv.), MAP (0.0015 g, 0.01 mmol, 1 equiv.) and TES (0.0020 mL, 0.0012 g, 0.01 mmol, 1 equiv.). The

mix was stirred under UV irradiation and Ar atmosphere for 3 hours. A 0.25 mL aliquot of reaction mix was added to 0.25 mL MeCN and subjected to RP-HPLC analysis which confirmed the consumption of the peptide starting material and formation of the desired product.

R_T (RP-HPLC) = 18.15 min (5-95% MeCN in H_2O with 0.1% TFA, 25 min).

***m/z* HRMS (ESI$^+$)** calcd. for $C_{60}H_{85}N_9O_{23}S$ ([M+H]$^+$): 1332.5552; found: 1332.5418.

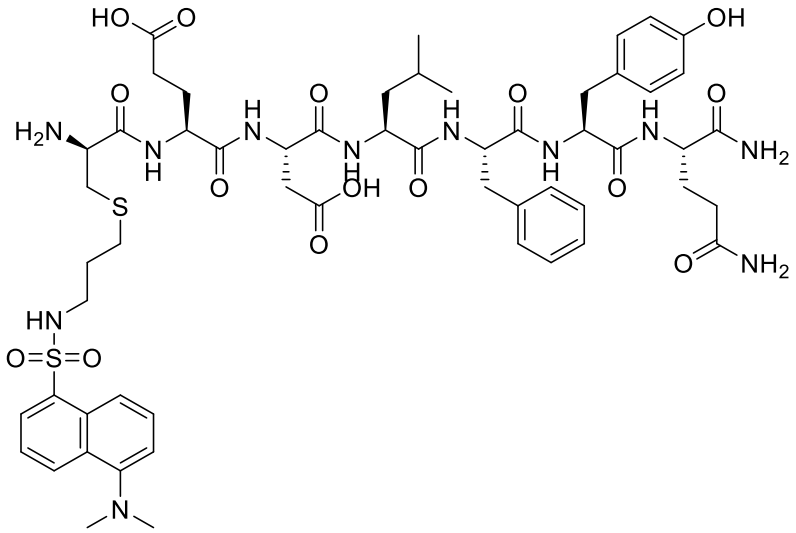

***S*-Dansyl-Cys-Glu-Asp-Leu-Phe-Tyr-Gln-NH_2 (3.8c)**

To degassed ChCl:Gly/H_2O (3:2, 1 mL) was added peptide substrate (0.0090 g, 0.01 mmol, 1 equiv.), **3.11** (0.0145 g, 0.05 mmol, 5 equiv.), DPAP (0.0026 g, 0.01 mmol, 1 equiv.), MAP (0.0015 g, 0.01 mmol, 1 equiv.) and TES (0.0020 mL, 0.0012 g, 0.01 mmol, 1 equiv.). The mixture was stirred under UV irradiation and Ar atmosphere for 3 hours. A 0.25 mL aliquot of reaction mix was added to 0.25 mL MeCN and subjected to RP-HPLC analysis which confirmed the consumption of the peptide starting material and formation of the desired product.

R_T (RP-HPLC) = 18.16 min (5-95% MeCN in H_2O with 0.1% TFA, 25 min).

***m/z* HRMS (ESI$^+$)** calcd. for $C_{56}H_{77}N_{11}O_{15}S_2$ ([M+2H]$^{2+}$): 602.7455; found: 602.7437.

7.3.4 Preparation of Synthetic Alkenes

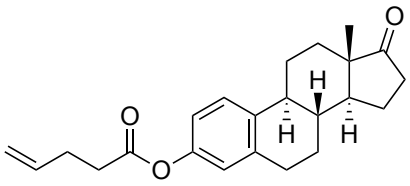

(8*R*,9*S*,13*S*,14*S*)-13-Methyl-17-oxo-7,8,9,11,12,13,14,15,16,17-decahydro-6*H*-cyclopenta[*a*]phenanthren-3-yl pent-4-enoate (3.10)[104]

To a solution of 4-pentenoic acid (1.9 mmol, 0.190 g, 0.194 mL) in dry DCM (12 mL) at 0 °C, EDC•HCl (1.9 mmol, 0.364 g) was added and stirred for 15 min. DMAP (0.4 mmol, 0.049 g) and estrone (1.5 mmol 0.406 g) was then added. The solution was warmed to rt and stirred for 24 h. The solvent was then removed *in vacuo*. The product was purified by silica gel flash chromatography using 25% EtOAc/Hexane (v/v) to yield the desired product as a colourless oil (333 mg, 66%).

^{1}H NMR (400 MHz, $CDCl_3$) δ_H 7.30 (d, J = 8.7 Hz, 1H), 6.87 (dd, J = 8.7, 2.4 Hz, 1H), 5.82 (d, J = 2.4 Hz, 1H), 5.94-5.87 (m, 1H), 5.19-5.07 (m, 2H), 2.94-2.91 (m, 2H), 2.70-2.65 (m, 2H), 2.57-2.49 (m, 3H), 2.46-2.27 (m, 2H), 2.22-1.96 (m, 4H), 1.70-1.41 (m, 6H), 0.93 (s, 3H).

^{13}C NMR (151 MHz, $CDCl_3$) δ_C 220.8, 171.8, 148.6, 138.0, 137.4, 136.4, 126.4, 121.6, 118., 115.9 50.4, 48.0, 44.2, 38.0, 35.9, 33.7, 31.6, 29.4, 28.9, 26.3, 25.8, 21.6, 13.8 (CH_3).

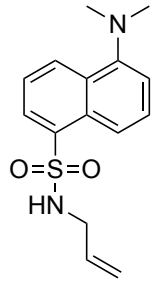

***N*-Allyl-5-(dimethylamino)naphthalene-1-sulfonamide (3.11)**[156]

To allylamine (0.37 mmol, 0.021 g, 0.028 mL) and *N,N*-diisopropylethylamine (1.85 mmol, 0.239 g, 0.322 mL) in DCM (5 mL), dansyl chloride (0.37 mmol, 0.100 g) in DCM (3 mL) was added. The mix was stirred at rt for 18h and then concentrated *in vacuo*. The product was purified by silica gel flash chromatography using 10-20% EtOAc/Hexane (v/v) to afford the desired product as a yellow waxy oil (0.08 g, 75%).

^{1}H NMR (400 MHz, $CDCl_3$) δ_H 8.66-8.62 (m, 1H), 8.39-8.35 (m, 1H), 8.30 (d, *J* = 7.3 Hz, 1H), 7.64-7.56 (m, 2H), 7.27-7.24 (m, 1H), 5.71-5.61 (m, 1H), 5.14-5.03 (m, 2H), 4.67 (m, 1H), 3.59-3.55 (m, 2H), 2.97 (s, 6H).

^{13}C NMR (151 MHz, $CDCl_3$) δ_C 147.9, 139.7, 133.0, 130.0, 129.9, 129.4, 129.3, 128.3, 123.4, 118.7, 117.5, 115.4, 46.3, 46.1.

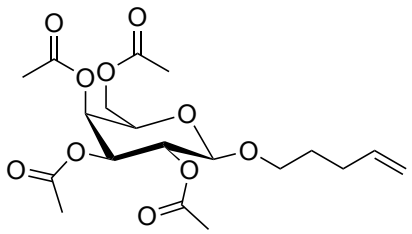

(2*R*,3*S*,4*S*,5*R*,6*R*)-2-(Acetoxymethyl)-6-(pent-4-en-1-yloxy)tetrahydro-2*H*-pyran-3,4,5-triyl triacetate (3.12)

To a stirred solution of peracetylated galactose (0.390 g, 1.0 mmol) and 4-penten-1-ol (0.399 mL, 0.3325 g, 4.0 mmol) in dry DCM (6 mL), BF_3•Et_2O (0.494 mL, 0.5677 g, 5.0 mmol) was added dropwise. The reaction was stirred overnight and then quenched by addition of H_2O. Organics were filtered through celite and then washed with 1.0 M HCl, $NaHCO_3$ and brine, followed by concentration in vacuo. The product was purified by silica gel flash chromatography using 20-40% EtOAc/Hexane (v/v) to yield the desired product as a colourless oil (175 mg, 42%).

R_f = 0.41 (40% EtOAc/Hexane (v/v)).

^{1}H NMR (400 MHz, $CDCl_3$) δ_H 5.86-5.75 (m, 1H), 5.42-5.38 (m, 1H), 5.22 (dd, *J* = 10.5, 3.4 Hz, 1H), 5.06-4.97 (m, 3H), 4.47 (m, 1H), 4.23-4.12 (m, 2H), 3.94-3.89 (m, 2H), 3.55-3.49 (m, 1H), 3.08 (s, 3H), 2.13-2.11 (m, 2H), 2.07 (s, 3H), 2.06 (s, 3H), 2.00 (s, 3H), 1.77-1.63 (m, 2H).

^{13}C NMR (151 MHz, $CDCl_3$) δ_C 170.4, 170.3, 170.2, 169.4, 137.8, 115.1, 101.4, 71.0, 70.6, 69.4, 69.0, 67.1, 61.3, 29.8, 28.6, 20.8, 20.74, 20.68, 20.6.

***m/z* HRMS (ESI$^+$)** calcd for $C_{19}H_{28}NaO_{10}$ ($[M+Na]^+$): 439.1575; found: 439.1587.

ν_{max} (film), cm^{-1}: 2970 (alkene stretch) 2905 (C-H stretch), 1741 (C=O stretch), 1214 (C-O stretch), 1173 (C-O stretch).

7.4 Experimental for chapter 4

General procedure: SPPS on disulfide resin.

Amino acid couplings were performed using HBTU and NMM for 1 h and deprotections were performed with 20% piperidine in DMF (2×5 min). Side chain deprotection was performed using TFA/TIPS/H_2O (95:2.5:2.5, v/v/v), followed by reductive release from the resin using a 100 mM solution of 1,4-butanedithiol (BDT) and TEA in DMF (2.0 mL per 25 mmol resin). Release mixtures were acidified using TFA and concentrated by RVC (30 °C, 1750 rpm, 0.1 mbar) to afford crude linear dithiol peptides.[217,218]

General procedure: Cyclisation *via bis*-electrophile.

Crude peptides were dissolved to 1 mM concentration in freshly prepared and degassed NH_4HCO_3 buffer/MeCN solution (60 mM, pH 8.0) and the desired *bis*-electrophilic linker (2.0 equiv. assuming 50% yield from SPPS) was added. The reaction was agitated for 1 h or until observed as complete by LC-MS analysis. The reaction was then quenched by addition of β-ME (8.0 equiv.) and the macrocyclic product purified by preparative RP-HPLC.

General procedure: Cyclisation *via* disulfide formation.

Crude peptides were dissolved to 1 mM concentration in freshly prepared and degassed NH_4HCO_3 buffer/MeCN solution (60 mM, pH 8.0) and approx. 20% DMSO was added. The reaction was agitated for 24 h or until observed as complete by LC-MS analysis. The macrocyclic product was then purified by preparative RP-HPLC.

General Procedure: High-throughput TEC

Peptide stock solutions (40 nmol, 1 mL from 40 mM solution in DMSO) were dispensed using a LabCyte Echo 650 acoustic dispenser into a 1536-well plate, centrifuged and concentrated *via* RVC to give dried peptide pellets. DPAP (40 nmol, 1 equiv.), TES (200 nmol, 5 equiv.) and thiol (400 nmol,) were dispensed as a 4 mL of a single solution of 10 mM DPAP, 50 mM TES and 100 mM thiol in degassed DMSO using a CERTUS Flex automated bulk dispenser. Final concentrations were 10 mM peptide, 10 mmol DPAP, 50 mmol TES and 100 mmol thiol. The plates were centrifuged and sealed under argon atmosphere and then irradiated using a custom LED array and nail curing lamp setup for 1 h,

following RVC to yield dried peptide thioether pellets. For analysis, peptides were dissolved in DMSO (4 mL), of which 2 mL was diluted 10-fold in water:MeCN (1:1) for LC-MS injection.

Table 7.1: Characterisation data for alkene peptide substrates synthesised and isolated *via* the general procedure for disulfide resins.

X = Agl, **O** = Alloc Lys, **β** = β-Agl, **B** = *N*-allylglycine

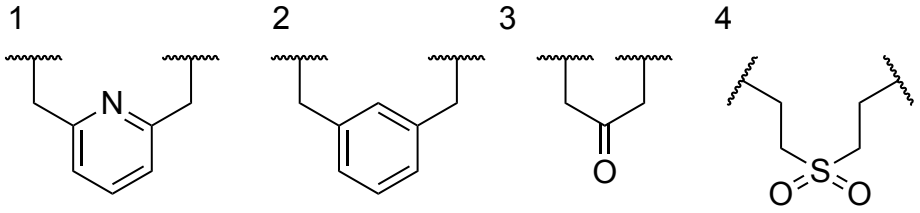

Compound	Sequence	Linker	t_R (min)	Formula	Ion	Calculated	Found
4.11a	Y**X**G	3	2.66	$C_{24}H_{32}N_4O_6S_2$	$[M+H]^+$	537.18	537.15
4.11b	Y**X**G	S-S	2.65	$C_{21}H_{28}N_4O_5S_2$	$[M+H]^+$	481.15	481.05
4.13a	K**X**Y	1	2.61	$C_{32}H_{44}N_6O_5S_2$	$[M+H]^+$	657.29	657.20
4.13b	L**X**Y	1	3.21	$C_{32}H_{43}N_5O_5S_2$	$[M+H]^+$	642.28	642.30
4.13c	W**X**Y	1	3.29	$C_{37}H_{42}N_6O_5S_2$	$[M+H]^+$	715.27	715.20
4.13d	E**X**Y	1	2.70	$C_{30}H_{37}N_5O_7S_2$	$[M+H]^+$	658.24	658.20
4.13e	Y**X**G	1	2.82	$C_{28}H_{35}N_5O_5S_2$	$[M+H]^+$	586.22	586.20
4.13f	Y**X**G	2	3.31	$C_{29}H_{36}N_4O_5S_2$	$[M+H]^+$	585.22	585.20
4.13g	Y**X**G	3	2.66	$C_{24}H_{32}N_4O_6S_2$	$[M+H]^+$	537.18	537.15
4.13h	Y**X**G	4	2.81	$C_{25}H_{36}N_4O_7S_3$	$[M+H]^+$	569.21	569.20
4.13i	WA**X**	3	3.20	$C_{27}H_{35}N_5O_5S_2$	$[M+H]^+$	574.22	574.20
4.13j	WA**O**	3	3.40	$C_{32}H_{44}N_6O_7S_2$	$[M+H]^+$	689.28	689.25
4.13k	WA**β**	3	3.19	$C_{27}H_{35}N_5O_5S_2$	$[M+H]^+$	574.22	574.20
4.13l	WA**B**	3	3.21	$C_{28}H_{37}N_5O_5S_2$	$[M+H]^+$	588.23	588.25

7.5 Experimental for chapter 5

7.5.1 Carbohydrate synthesis

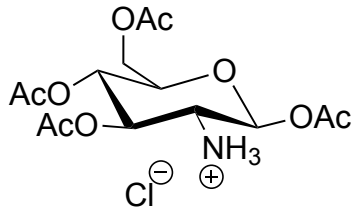

(2*S*,3*R*,4*R*,5*S*,6*R*)-2,4,5-triacetoxy-6-(acetoxymethyl)tetrahydro-2*H*-pyran-3-aminium chloride (5.47)[250]

D-Glucosamine hydrochloride (6.038 g, 28.0 mmol) was dissolved in NaOH (1.0 M, 30 mL) and *p*-anisaldehyde (3.748 mL, 4.194 g, 30.8 mmol) was added. The mix was cooled in an ice bath and stirred at 0 ºC for 2 h. The precipitate was then collected by vacuum filtration and washed with ice-cold H_2O (100 mL) and Et_2O/EtOAc (1:1, 100 mL). This material (4.000 g) was then redissolved in pyridine (22 mL) at 0 ºC and Ac_2O (12.00 mL) was added dropwise. The mix was stirred at 0 ºC until a homogeneous mixture was obtained, followed by stirring overnight at rt, then poured into ice-cold H_2O (250 mL). The precipitate was extracted with DCM (3 x 100 mL) and the organics washed with $CuSO_4$ (75 mL) and H_2O (100 mL) and then concentrated *in vacuo*. This material (4.189 g) was then redissolved in acetone (60 mL) at 30 ºC and HCl (5.0 M, 2.25 mL) was added dropwise. The mix was then cooled to 0 ºC and Et_2O (60 mL) was added, followed by stirring for 3 h. The precipitate was then isolated by vacuum filtration and washed with ice-cold Et_2O (120 mL) to yield the product as a white solid (3.4540 g, 37% yield).

M.p.: 215-217 ºC. Literature value 221-222 ºC.

^{1}H NMR (600 MHz, CD_3OD) δ_H 5.86 (d, *J* = 9.0 Hz, 1H), 5.36 (dd, *J* = 10.5, 9.0 Hz, 1H), 5.14-5.08 (m, 1H), 4.33 (dd, *J*.= 12.6, 4.6 Hz, 1H), 4.14 (dd, *J* = 12.6, 2.2 Hz, 1H), 4.06-4.01 (m, 1H), 3.34-3.59 (m, 1H), 2.21 (s, 3H), 2.12 (s, 3H), 2.06 (s, 3H), 2.05 (s, 3H).

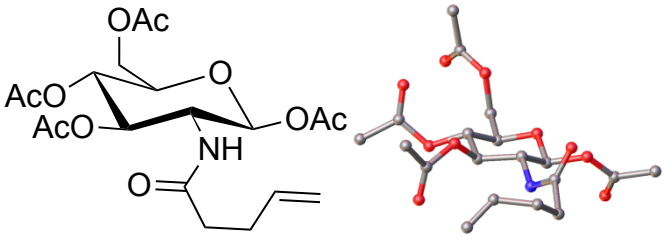

(2*S*,3*R*,4*R*,5*S*,6*R*)-6-(Acetoxymethyl)-3-(pent-4-enamido)tetrahydro-2*H*-pyran-2,4,5-triyl triacetate (5.6)

To a suspension of (2*S*,3*R*,4*R*,5*S*,6*R*)-2,4,5-triacetoxy-6-(acetoxymethyl)tetrahydro-2*H*-pyran-3-aminium chloride (peracetylated glucosamine hydrochloride) (2.993 g, 7.8 mmol) and pentenoyl chloride (1.291 mL, 1.387 g, 11.7 mmol) at 0 ºC, triethylamine (3.262 mL, 2.368 g, 23.4 mmol) was added dropwise. The mixture was then allowed to warm to rt and stirred for a further 3 h. The mix was then diluted with DCM and washed with H_2O, 1.0 M NaOH and brine. The organics were dried over $MgSO_4$, filtered, and concentrated *in vacuo*. The product was purified by silica gel flash chromatography using 40-60% EtOAc/Hexane (v/v) to yield the desired product as white crystals (2.675 g, 80%).

M.p.: 173 ºC.

R_f = 0.40 (60% EtOAc/Hexane (v/v)).

^{1}H NMR (600 MHz, $CDCl_3$) δ_H 5.81-5.74 (m, 1H), 5.71 (d, *J* = 8.8 Hz, 1H), 5.59 (d, *J* = 9.4 Hz, 1H), 5.18-5.13 (m, 2H), 5.08-5.04 (m, 1H), 5.01 (d, *J* = 10.2 Hz, 1H), 4.36-4.31 (m, 1H), 4.29 (dd, *J* = 12.5, 4.62 Hz, 1H), 4.15 (dd, *J* = 12.5, 2.10 Hz, 1H), 3.84-3.80 (m, 1H), 2.36-2.32 (m, 2H), 2.25-2.22 (m, 2H), 2.12 (s, 3H), 2.06 (s, 3H), 2.05 (s, 3H).

^{13}C NMR (151 MHz, $CDCl_3$) δ_C 172.3, 171.2, 170.7, 169.5, 169.3, 136.5, 115.8, 92.7, 73.0, 72.5, 67.7, 61.7, 52.9, 35.7, 29.2, 20.9, 20.7, 20.7, 20.6.

***m/z* HRMS (ESI$^+$)** calcd. for $C_{19}H_{27}NO_{10}Na$ ($[M+Na]^+$): 452.1527; found: 452.1532.

Crystal Data for $C_{19}H_{27}NO_{10}$ (*M* =429.41 g/mol): monoclinic, space group $P2_1$ (no. 4), *a* = 5.2450(2) Å, *b* = 18.4373(6) Å, *c* = 11.2088(4) Å, *β* = 98.9340(12)°, *V* = 1070.78(7) Å^3, *Z* = 2, *T* = 100(2) K, μ(Cu Kα) = 0.922 mm^{-1}, *Dcalc* = 1.332 g/cm^3, 15707 reflections measured (7.984° ≤ 2Θ ≤ 139.976°), 4009 unique (R_{int} = 0.0498, R_{sigma} = 0.0389) which were used in all calculations. The final R_1 was 0.0554 (I > 2σ(I)) and wR_2 was 0.1423 (all data).

7.5.2 Synthesis of thiol fluorophores

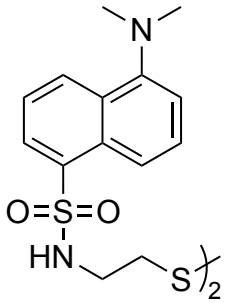

***N*,*N*'-(disulfanediylbis(ethane-2,1-diyl))bis(5-(dimethylamino)naphthalene-1-sulfonamide)[237] (5.8)**

Dansyl chloride (0.200 g, 0.741 mmol) was dissolved in a mixture of acetone (4.5 mL) and water (1.5 mL). Cystamine dihydrochloride (0.0835 g, 0.37 mmol) was dissolved in aqueous $NaHCO_3$ (0.1 M, 5 mL) and added to the reaction mixture dropwise. The reaction was stirred for 2 h, following which it was diluted with $CHCl_3$ (50 mL) and washed with $NaHCO_3$ (3 x 30 mL) and H_2O (30 mL), then dried over $MgSO_4$, filtered, and concentrated *in vacuo* to yield the product as a flocculent yellow solid (0.1616 g, 37%).

M.p.: 70 ºC. Literature value 71-72 ºC.

R_f = 0.40 (30% Acetone/Hexane (v/v)).

^{1}H NMR (400 MHz, $CDCl_3$) δ_H 8.57 (d, *J* = 8.2 Hz, 1H), 8.28-8.23 (m, 2H), 7.59-7.50 (m, 2H), 7.20 (d, *J* = 7.4 Hz, 1H), 5.16 (brs, 1H), 3.10 (q, *J* = 6.3 Hz, 2H), 2.90 (s, 6H) 2.50 (t, *J* = 6.3 Hz, 2H).

***m/z* HRMS (ESI$^+$)** calcd. for $C_{28}H_{35}N_4O_4S_4$ ($[M+H]^+$): 619.1536; found: 619.1529.

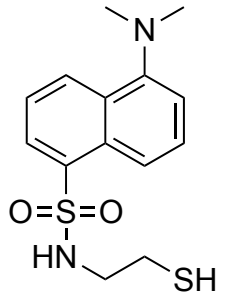

5-(dimethylamino)-*N*-(2-mercaptoethyl)naphthalene-1-sulfonamide (5.9)[237]

Bi-dansyl cystamine **5.8** (0.150 g, 0.243 mmol) was dissolved in EtOH (30 mL). Finely powdered zinc dust (0.850 g) and acetic acid (1.900 mL, 1.995 g, 33.2 mmol) were then

added alternately in portions and the reaction was then stirred for a further 4 h. The mixture was concentrated *in vacuo*, then redissolved in $CHCl_3$ (50 mL) and washed with H_2O (2 x 50 mL), dilute $NaHCO_3$ (30 mL) and brine (30 mL), then dried over $MgSO_4$, filtered, and concentrated *in vacuo* to yield the product as a yellow/green film (0.1505 g, 78%).

^{1}H NMR (400 MHz, $CDCl_3$) δ_H 8.59 (d, *J* = 8.2 Hz, 1H), 8.31-8.25 (m, 2H), 7.61-7.52 (m, 2H), 7.22 (d, *J* = 7.6 Hz, 1H), 5.17 (t, *J* = 6.0 Hz, 1H), 3.09 (q, *J* = 6.3 Hz, 2H), 2.92 (s, 6H), 2.54-2.48 (m, 2H).

R_f = 0.50 (30% Acetone/Hexane (v/v)).

***m/z* HRMS (ESI$^+$)** calcd. for $C_{14}H_{19}N_2O_2S_2$ ($[M+H]^+$): 311.0882; found: 311.0886.

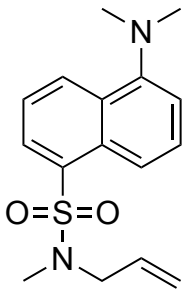

***N*-Allyl-5-(dimethylamino)-*N*-methylnaphthalene-1-sulfonamide (5.16)**

Dansyl chloride (0.500 g, 1.85 mmol) was dissolved in dry DCM and *N*-allylmethylamine (0.373 mL, 0.2767 g, 3.89 mmol) was added. The mix was then stirred for 3 h, following which the reaction was concentrated *in vacuo*. The crude was run through a silica plug with EtOAc/Hexane (1:1) eluent, and then concentrated *in vacuo* to yield the product as a fluorescent yellow/green oil (0.5640 g, > 99%).

R_f = 0.41 (20% EtOAc/Hexane (v/v)).

^{1}H NMR (400 MHz, $CDCl_3$) δ_H 8.58 (d, *J* = 8.2, 1H), 8.39 (d, *J* = 8.2 Hz, 1H), 8.23 (dd, *J* = 7.3, 1.2 Hz, 1H), 7.59-7.53 (m, 2H), 7.21 (d, *J* = 7.3 Hz), 5.79-5.69 (m, 1H), 5.34-5.17 (m, 2H), 3.85 (d, *J* = 6.3 Hz, 2H), 2.91 (s, 6H), 2.79 (s, 3H).

^{13}C NMR (151 MHz, $CDCl_3$) δ_C 151.7, 134.1, 132.9, 130.4, 130.3, 130.1, 130.1, 128.0, 123.2, 119.7, 119.1, 115.2, 52.3, 45.4, 33.7.

***m/z* HRMS (ESI$^+$)** calcd. for $C_{16}H_{21}N_2O_2S$ ($[M+H]^+$): 305.1318; found: 305.1316.

ν_{max} (film), cm^{-1}: 3081 (alkene C-H stretch), 2942, 2832 (C-H stretch), 1643, 1571 (aromatic C-H bend), 1320 (S=O stretch).

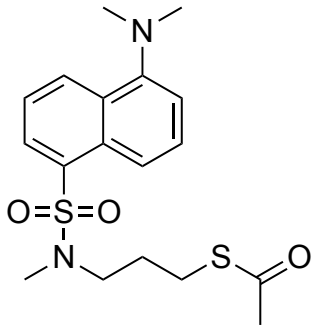

***S*-(3-((5-(dimethylamino)-*N*-methylnaphthalene)-1-sulfonamido)propyl) ethanethioate (5.17)**

Dansyl alkene **5.16** (0.079 g, 0.26 mmol), DPAP (0.067 g, 0.26 mmol) and MAP (0.039 g, 0.26 mmol) were dissolved in DCM which was acidified with 2-3 drops of TFA. Thioacetic acid (0.093 mL, 0.099 g, 1.30 mmol) was then added and the mix was stirred under UV irradiation for 3 h. The organics were then washed with $NaHCO_3$ (3 x 50 mL), dried over $MgSO_4$ and concentrated *in vacuo*. The product was purified by silica gel flash chromatography using 10-25% EtOAc/Hexane (v/v) to yield the desired product as a highly viscous yellow oil (0.0549 g, 56%).

$\mathbf{R_f}$ = 0.49 (25% EtOAc/Hexane (v/v)).

^{1}H NMR (400 MHz, $CDCl_3$) δ_H 8.55 (d, *J* = 8.4 Hz, 1H), 8.34 (d, *J* = 8.4 Hz, 1H) 8.16 (dd, *J* = 7.3, 1.24 Hz, 1H), 7.56-7.50 (m, 2H), 7.18 (d, *J* = 7.3 Hz, 1H), 3.24 (t, *J* = 6.9 Hz, 2H), 2.89 (s, 6H), 2.84 (s, 3H), 2.80 (t, *J* = 6.9 Hz, 1H), 2.29 (s, 3H), 1.85-1.77 (m, 2H).

^{13}C NMR (151 MHz, $CDCl_3$) δ_C 195.6, 151.7, 134.0, 130.4, 130.3, 130.1, 130.0, 128.0, 123.2, 119.7, 115.3, 48.4, 45.5, 34.2, 30.6, 27.7, 26.1.

***m/z* HRMS (ESI$^+$)** calcd. for $C_{18}H_{25}N_2O_3S_2$ ($[M+H]^+$): 381.1301; found: 381.1306.

ν_{max} (film), cm^{-1}: 2940, 2867 (C-H stretch), 1686 (C=O stretch), 1572 (aromatic C-H bend), 1320 (S=O stretch).

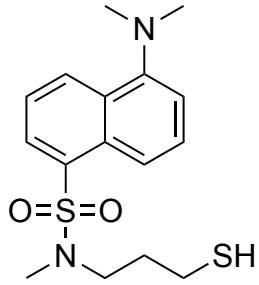

5-(dimethylamino)-*N*-(3-mercaptopropyl)-*N*-methylnaphthalene-1-sulfonamide (5.18)[251]

Dansyl thioester **5.17** (0.024 g, 0.064 mmol) was dissolved in MeOH/H_2O (2:1, 2.0 mL) and K_2CO_3 (0.027 g, 0.192 mmol) was added. The mix was stirred for 3 h, following which the mix was diluted with H_2O, acidified with 1.0 M HCl, and extracted with DCM. The organics were dried over $MgSO_4$, filtered, and concentrated *in vacuo* to yield the product as a viscous yellow oil (0.013 g, 60%).

R_f = 0.22 (30% EtOAc/Hexane (v/v)).

^{1}H NMR (400 MHz, $CDCl_3$) δ_H 8.78-8.62 (m, 1H), 8.50-8.38 (m, 1H), 8.18 (d, *J* = 5.7 Hz, 1H), 7.65-7.53 (m, 2H), 7.35-7.22 (m, 1H), 3.29 (t, *J* = 5.7 Hz, 2H), 2.98 (s, 6H), 2.84 (s, 3H), 2.57 (t, *J* = 5.6 Hz, 2H), 1.97-1.86 (m, 2H), 1.25 (t, *J* = 7.0 Hz, 1H).

***m/z* HRMS (ESI$^+$)** calcd. for $C_{16}H_{23}N_2O_2S_2$ ($[M+H]^+$): 339.1195; found: 339.1178.

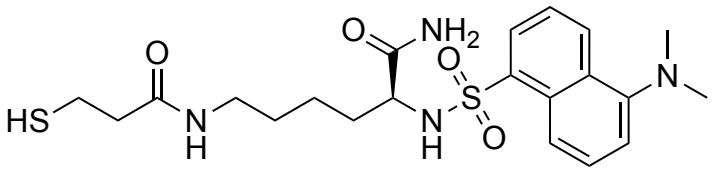

(*S*)-2-((5-(Dimethylamino)naphthalene)-1-sulfonamido)-6-(3-mercaptopropanamido)hexanamide (5.21)

Rink amide resin (0.350 g, 0.273 mmol) was swelled in DMF and the Fmoc group removed by treatment with 20% 4-methylpiperidine in DMF for 2 x 10 min. A solution of Fmoc-Lys(Mtt)-OH (0.512 g, 0.819 mmol), DIPEA (0.286 mL, 0.2115 g, 1.636 mmol) and HATU (0.311 g, 0.819 mmol) in DMF (5.0 mL) was then added to the resin and agitated for 1 h. The resin was drained and washed with DMF (3 x 7 mL), DCM (3 x 7 mL) and again DMF (3 x 7 mL). The resin was then treated with DCM/TFA/TES (90:5:5) mix for 5 x 1 min and washed as before. A solution of 3-(tritylthio)propanoic acid (0.285 g, 0.819 mmol), DIPEA

(0.286 mL, 0.212 g, 1.636 mmol) and HATU (0.311 g, 0.819 mmol) in DMF (5.0 mL) was then added to the resin and agitated for 1 h and washed as before. The resin was again treated with 20% 4-methylpiperidine in DMF for 2 x 10 min and again washed. Dansyl chloride (0.221 g, 0.819 g) and DIPEA (0.143 mL, 0.106 g, 0.819 mmol) were dissolved in DMF (5 mL), added to the resin and agitated for 2 h. The resin was then again drained, washed, and dried. The resin was re-swelled in DCM and then treated with TFA/H_2O/EDT/TES (94:2.5:2.5:0.1) for 90 min. The solution was transferred to a falcon tube and the TFA removed under N_2 flow. Et_2O was added to precipitate the product, which was then washed with Et_2O (3 x 12 mL) and then lyophilised to yield a highly viscous yellow oil (0.1064 g, 84%).

^{1}H NMR (600 MHz, DMSO) δ_H 8.45 (d, *J* = 8.5, 1H), 8.34 (d, *J* = 8.5, 1H), 8.13 (d, *J* = 2.8, 1H), 8.08 (d, *J* = 8.5 Hz, 1H), 7.67 (t, *J* = 5.5 Hz, 1H), 7.61-7.57 (m, 2H), 7.27 (d, *J* = 7.5 Hz, 1H), 7.16 (s, 1H), 6.90 (s, 1H), 3.58-3.54 (m, 1H), 2.84 (s, 6H), 2.74-2.59 (m, 4H), 2.31 (t, *J* = 7.0 Hz, 2H), 2.23 (t, *J* = 8.0 Hz, 1H), 1.42-1.34 (m, 2H), 1.11-0.97 (m, 3H), 0.89-0.83 (m, 1H).

^{13}C NMR (151 MHz, DMSO) δ_C 172.8, 169.8, 136.4, 129.3, 129.1, 128.9, 128.3, 127.6, 123.4, 119.7, 115.1, 55.8, 45.1, 38.0, 32.2, 28.3, 22.2, 19.9.

***m/z* HRMS (ESI$^+$)** calcd. for $C_{21}H_{31}N_4O_4S_2$ ($[M+H]^+$): 467.1781; found: 467.1785.

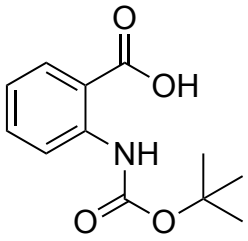

2-((*tert*-Butoxycarbonyl)amino)benzoic acid (5.25)[252]

To a suspension of anthranilic acid (5.00 g, 36.46 mmol) in THF/H_2O (1:1, 80 mL), 2 M NaOH was added until pH 8 was achieved. Boc_2O (8.76 g, 40.10 mmol) was then added and the reaction stirred overnight. The THF was then removed *in vacuo* and the mixture acidified to pH 4 with citric acid (10% w/v) to give a white precipitate. The mixture was then extracted with DCM (3 x 150 mL) and the combined organics washed with citric acid (10% w/v, 3 x 150 mL), dried over $MgSO_4$, filtered, and concentrated *in vacuo* to yield the product as an off-white solid (8.48 g, 98%), which was used without further purification.

M.p.: 143-146 ºC. Literature value 148-151 ºC

^{1}H NMR (400 MHz, $CDCl_3$) δ_H 10.01 (brs, 1H), 8.47 (d, *J* = 7.6 Hz, 1H), 8.10 (d, *J* = 7.9 Hz, 1H), 7.57 (t, *J* = 7.9 Hz, 1H), 7.04 (t, *J* = 7.6 Hz, 1H), 1.55 (s, 9H).

***m/z* HRMS (ESI$^+$)** calcd. for $C_{12}H_{15}NO_4Na$ ([M+Na]$^+$): 260.0893; found: 260.0900.

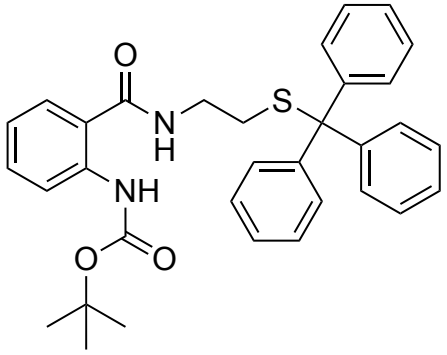

***tert*-Butyl (2-((2-(tritylthio)ethyl)carbamoyl)phenyl)carbamate (5.29)**

2-((*tert*-Butoxycarbonyl)amino)benzoic acid (0.890 g, 3.75 mmol), EDC·HCl (0.959 g, 5.00 mmol) and DIPEA (0.873 mL, 0.646 g, 5.00 mmol) were dissolved in dry DCM (20 mL) at 0 ºC and stirred for 45 min at 0 ºC. 2-Tritylthio-1-ethylamine hydrochloride (0.890 g, 2.50 mmol) was then added and the reaction allowed warm to rt and stirred for 24 h. The reaction was then diluted with DCM (100 mL) and washed with H_2O (50 mL), saturated $NaHCO_3$ (50 mL)and brine (50 mL), then dried over $MgSO_4$, filtered, and concentrated *in vacuo*. The product was then purified by silica gel flash chromatography using 10-20% EtOAc/Hexane (v/v) to yield the desired product as a fine pale yellow powder (0.4679 g, 35%).

M.p.: 192-193 ºC.

R_f = 0.48 (20% EtOAc/Hexane (v/v)).

^{1}H NMR (400 MHz, DMSO) δ_H 10.09 (brs, 1H), 8.39 (d, *J* = 8.5 Hz, 1H), 7.48-7.21 (m, 17H), 7.01 (t, *J* = 7.0 Hz, 1H), 6.24 (brs, 1H), 3.29 (t, *J* = 6.1 Hz, 2H), 2.56 (t, *J* = 6.2 Hz), 1.54 (s, 9H).

^{13}C NMR (151 MHz, $CDCl_3$) δ_C 168.7, 153.1, 144.5, 140.4, 132.6, 129.5, 128.0, 126.9, 126.9, 126.6, 121.3, 119.8, 119.5, 80.2, 67.0, 38.3, 32.0, 28.4.

***m/z* HRMS (ESI$^+$)** calcd. for $C_{33}H_{34}N_2O_3SNa$ ([M+Na]$^+$): 561.2182; found: 561.2195.

ν_{max} (film), cm^{-1}: 3309 (N-H stretch), 1696, 1641 (C=O stretch).

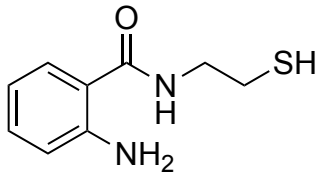

2-amino-*N*-(2-mercaptoethyl)benzamide (5.24)[253]

tert-Butyl (2-((2-(tritylthio)ethyl)carbamoyl)phenyl)carbamate **5.29** (0.4310 g, 0.80 mmol) was dissolved in a DCM/TFA/H_2O/TES/EDT (44:50:2.5:1.0:2.5, 20 mL) cocktail. The mixture was stirred for 1 h, following which the TFA was removed under a N_2 flow. The product was then purified by silica gel flash chromatography using 25-40% EtOAc/Hexane (v/v) to yield the desired product as a highly viscous yellow oil (0.1518 g, 97%).

R_f = 0.40 (50% EtOAc/Hexane (v/v)).

^{1}H NMR (400 MHz, $CDCl_3$) δ_H 7.38 (d, *J* = 7.8 Hz, 1H), 7.25 (d, 7.4 Hz, 1H), 6.75-6.69 (m, 2H), 6.53 (brs, 1H), 3.63 (q, *J* = 7.1 Hz, 2H), 2.81 (q, *J* = 7.1 Hz 2H), 1.44 (t, *J* = 8.5 Hz, 1H).

***m/z* HRMS (ESI$^+$)** calcd. for $C_9H_{13}N_2OS$ ($[M+H]^+$): 197.0743; found: 197.0753.

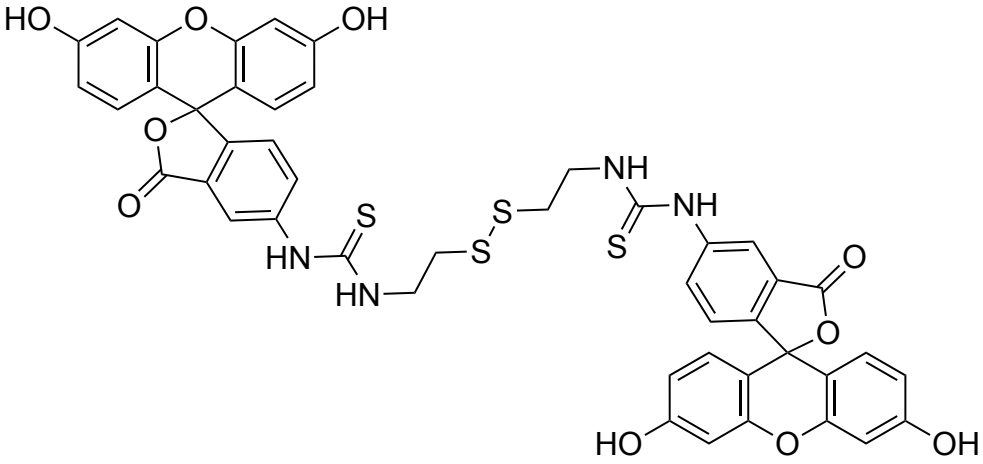

1,1'-(disulfanediylbis(ethane-2,1-diyl))bis(3-(3',6'-dihydroxy-3-oxo-3H-spiro[isobenzofuran-1,9'-xanthen]-5-yl)thiourea) (5.40)

Fluorescein 5(6)-isothiocyanate (0.0584 g, 0.15 mmol) was dissolved in dry DMSO (0.75 mL) and DIPEA (0.0523 mL, 0.0388 g, 0.30 mmol) was added, followed by cysteamine (0.0116 g, 0.15 mmol). The mix was stirred for 20 h, and then diluted with ice-cold H_2O. The precipitate was then isolated by centrifugation to yield the product as a red solid (0.0700 g, > 99%).

M.p.: 226-230 ºC (decomposition).

^{1}H NMR (600 MHz, DMSO) δ_H 10.07 (s, 2H), 8.23 (s, 2H), 7.75 (d, *J* = 7.5 Hz, 2H), 7.19 (d, *J* = 8.3 Hz, 2H), 6.71-6.67 (m, 4H), 6.62-6.55 (m, 8H), 3.90-3.84 (m, 4H), 3.04 (t, *J* = 6.7 Hz, 4H).

^{13}C NMR (151 MHz, $CDCl_3$) δ_C 180.5, 168.4, 159.5, 158.4, 158.1, 151.9, 141.1, 129.0, 126.6, 124.1, 116.7, 112.6, 109.7, 102.2, 55.0, 42.9, 36.2.

***m/z* HRMS (ESI$^+$)** calcd. for $C_{46}H_{35}N_4O_{10}S_4$ ($[M+H]^+$): 931.1231; found: 931.1229.

ν_{max} (film), cm^{-1}: 2988 (N-H stretch), 1580 (C=S stretch).

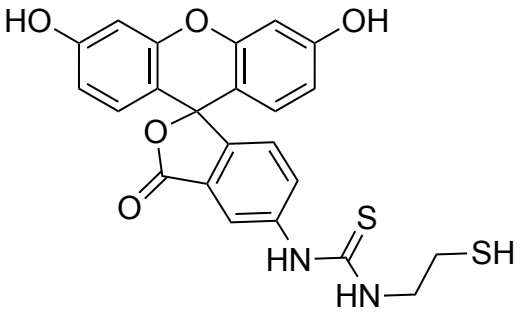

1-(3',6'-Dihydroxy-3-oxo-3H-spiro[isobenzofuran-1,9'-xanthen]-5-yl)-3-(2-mercaptoethyl)thiourea (5.41) [241]

1,1'-(Disulfanediylbis(ethane-2,1-diyl))bis(3-(3',6'-dihydroxy-3-oxo-3H-spiro[isobenzofuran-1,9'-xanthen]-5-yl)thiourea) (0.047 g, 0.075 mmol) was dissolved in dry DMF (0.5 mL). Separately, TCEP·HCl (0.129 g, 0.450 mmol) was dissolved in DMF/H_2O (1:1, 0.5 mL) and then added to the fluorescein solution. The reaction mixture was then agitated for 3 h and then diluted with ice-cold H_2O. The precipitate was then isolated by centrifugation to yield the product as an orange solid (0.0350 g, 87%).

M.p. 217-219 ºC (decomposition).

^{1}H NMR (400 MHz, DMSO) δ_H 10.09 (s, 1H), 8.23 (s, 1H), 7.75 (d, *J* = 8.0 Hz, 1H), 7.19 (d, *J* = 8.0 Hz, 1H), 6.71-6.67 (m, 2H), 6.62-6.55 (m, 4H), 3.68 (d, *J* = 5.8 Hz, 2H), 2.76-2.73-2.68 (m, 2H), 2.49 (t, *J* = 8.53 Hz, 2H).

^{13}C NMR (151 MHz, $CDCl_3$) δ_C 180.5, 168.4, 162.27, 159.5, 151.8, 147.3, 141.1, 129.0, 126.5, 124.1, 116.1, 112.5, 109.7, 102.2, 46.8, 26.0, 22.7.

***m/z* HRMS (ESI$^+$)** calcd. for $C_{23}H_{19}N_2O_5S_2$ ($[M+H]^+$): 467.0730; found: 467.0734.

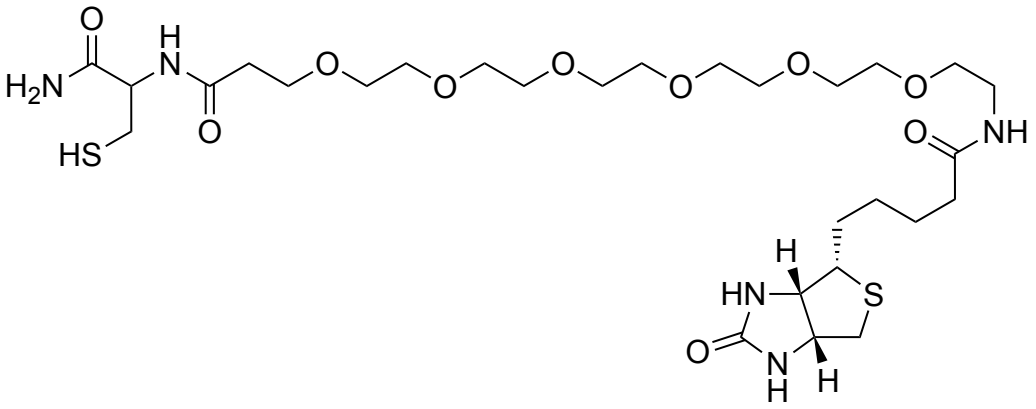

2-(Mercaptomethyl)-23-(5-((3a*S*,4*S*,6a*R*)-2-oxohexahydro-1*H*-thieno[3,4-*d*]imidazol-4-yl)pentanamido)-6,9,12,15,18,21-hexaoxa-3-azatricosanamide (5.46)

Rink amide resin (0.250 g, 0.195 mmol) was swelled in DMF and the Fmoc group removed by treatment with 20% piperidine in DMF for 2 x 10 min. A solution of Fmoc-Cys(Trt)-OH (0.3426 g, 0.585 mmol), DIPEA (0.204 mL, 0.0.1429 g, 1.170 mmol) and HBTU (0.2220 g, 0.585 mmol) in DMF (3.5 mL) was then added to the resin and agitated for 1 h. The resin was drained and washed with DMF (x3), DCM (x3) and again DMF (x3). Fmoc deprotection was achieved using 20% piperidine in DMF for 2 x 10 min. Fmoc-PEG_6-OH (0.3367 g, 0.585 mmol) and biotin (0.1249 g, 0.585 mmol) were coupled using the same conditions. The compound was then cleaved from the resin by treatment with TFA/H_2O/EDT/TES (94:2.5:2.5:0.1) for 90 min. The TFA was removed under N_2 flow. Et_2O was added to precipitate the product, which was then washed with Et_2O (x3) and lyophilised to yield the product as a highly viscous colourless syrup (0.1030 g, 77%).

^{1}H NMR (600 MHz, DMSO) δ_H 8.04 (d, *J* = 8.1 Hz, 1H), 7.83 (t, *J* = 5.6 Hz, 1H), 7.33 (brs, 1H), 7.16 (brs, 1H), 6.41 (brs, 2H), 4.35-4.29 (m, 2H), 4.12 (dd, *J* = 7.7, 4.4 Hz, 1H), 3.62 (t, *J* = 6.4 Hz, 2H), 3.52-3.49 (m, 20H), 3.39 (t, *J* = 6.4 Hz, 2H), 3.21-3.16 (m, 2H), 3.12-3.07 (m, 2H), 2.85-2.76 (m, 1H), 2.74-2.63 (m, 2H) 2.25-2.21 (m, 1H), 2.06 (t, *J* = 7.4 Hz, 2H) 1.66-1.24 (m, 8H).

^{13}C NMR (151 MHz, DMSO) δ_C 172.1, 171.6, 170.4, 162.7, 69.7, 69.7, 69.7, 69.5, 69.1, 66.9, 61.0, 59.1, 55.4, 55.0, 54.9, 54.7, 54.6, 54.6, 48.5, 38.4, 36.0, 35.1, 28.2, 28.0, 26.0, 25.2.

t_R (RP-HPLC) = 8.39 min (5-95% MeCN in H_2O with 0.1% TFA, 10 min).

***m/z* HRMS (ESI$^+$)** calcd. for $C_{28}H_{52}N_5O_{10}S_2$ ($[M+H]^+$): 682.3150; found: 682.3152.

7.5.3 Synthesis of NHS Esters

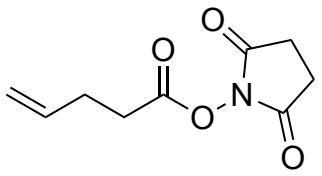

2,5-Dioxopyrrolidin-1-yl pent-4-enoate (5.31)[254]

N-hydroxysuccinimide (0.096 g, 0.83 mmol) and DMAP (0.010, 0.08 mmol) were dissolved in dry DCM. DCC (0.137 mL, 0.171 g, 0.83 mmol) was added, followed by pent-4-enoic acid (0.077 mL, 0.075 g, 0.75 mmol). The mix was stirred under Ar for 24 h, filtered, and concentrated *in vacuo*. The product was purified by silica gel flash chromatography using 0.2-0.4% MeOH/DCM (v/v) to yield the desired product as a white solid (0.1107 g, 75%).

M.p.: 40 ºC. Literature value 44-45 ºC.[255]

R_f = 0.41 (0.2% MeOH/DCM (v/v)).

^{1}H NMR (400 MHz, $CDCl_3$) δ_H 5.90-5.80 (m, 1H), 5.16-5.07 (m, 2H), 2.84 (s, 4H), 2.72 (t, *J* = 7.36 Hz, 2H), 2.52-2.46 (m, 2H).

***m/z* HRMS (ESI$^+$)** calcd. for $C_9H_{11}NO_4Na$ ($[M+Na]^+$): 220.0580; found: 220.0580.

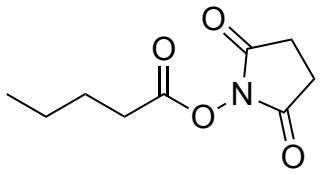

2,5-dioxopyrrolidin-1-yl pentanoate (5.48)[256]

N-hydroxysuccinimide (0.096 g, 0.83 mmol) and DMAP (0.010, 0.08 mmol) were dissolved in dry DCM DCC (0.137 mL, 0.171 g, 0.83 mmol) was added, followed by pentanoic acid (0.081 mL, 0.077 g, 0.75 mmol). The mix was stirred under Ar for 24 h, filtered, and concentrated *in vacuo*. The product was then purified by silica gel flash chromatography using 0.4% MeOH/DCM (v/v) to yield the desired product as a colourless oil (0.0.1307 g, 87%).

R_f = 0.45 (0.2% MeOH/DCM (v/v)).

^{1}H NMR (400 MHz, $CDCl_3$) δ_H 2.83 (s, 4H), 2.61 (t, *J* = 7.5 Hz, 2H), 1.78-1.69 (m, 2H), 1.49-1.39 (m, 2H), 0.95 (t, *J* = 7.34 Hz, 3H).

***m/z* HRMS (ESI$^+$)** calcd. for $C_9H_{13}NO_4Na$ ($[M+Na]^+$): 222.0737; found: 222.0736.

References

(1) Best, C. H.; Scott, D. A. The Preparation of Insulin. *J. Biol. Chem.* **1923**, *57* (3), 709–723. https://doi.org/10.1016/s0021-9258(18)85482-5.

(2) Gause, G. F.; Brazhnikova, M. G. Gramicidin S and Its Use in the Treatment of Infected Wounds. *Nature* **1944**, *154* (3918), 703-703. https://doi.org/10.1038/154703a0.

(3) Erlanger, B. F.; Goode, L. Gramicidin S: Relationship of Cyclic Structure to Antibiotic Activity. *Nature* **1954**, *174* (4435), 840–841. https://doi.org/10.1038/174840a0.

(4) Spiliotis, B. E. Recombinant Human Growth Hormone in the Treatment of Turner Syndrome. *Ther. Clin. Risk Manag.* **2008**, *4* (6), 1177–1183. https://doi.org/10.2147/TCRM.S1440.

(5) Brennan, B. P.; Kanayama, G.; Hudson, J. I.; Pope, H. G. Human Growth Hormone Abuse in Male Weightlifters. *Am. J. Addict.* **2011**, *20* (1), 9–13. https://doi.org/10.1111/j.1521-0391.2010.00093.x.

(6) Pechkova, E.; Bragazzi, N.; Bozdaganyan, M.; Belmonte, L.; Nicolini, C. A Review of the Strategies for Obtaining High-Quality Crystals Utilizing Nanotechnologies and Microgravity. *Crit. Rev. Eukaryot. Gene Expr.* **2014**, *24* (4), 325–339. https://doi.org/10.1615/CritRevEukaryotGeneExpr.2014008275.

(7) De Vos, A. M.; Ultsch, M.; Kossiakoff, A. A. Human Growth Hormone and Extracellular Domain of Its Receptor: Crystal Structure of the Complex. *Science.* **1992**, *255* (5042), 306–312. https://doi.org/10.1126/science.1549776.

(8) Bergen, P. J.; Landersdorfer, C. B.; Lee, H. J.; Li, J.; Nation, R. L. "Old" Antibiotics for Emerging Multidrug-Resistant Bacteria. *Curr. Opin. Infect. Dis.* **2012**, *25* (6), 626–633. https://doi.org/10.1097/QCO.0B013E328358AFE5.

(9) Driggers, E. M.; Hale, S. P.; Lee, J.; Terrett, N. K. The Exploration of Macrocycles for Drug Discovery — an Underexploited Structural Class. *Nat. Rev. Drug Discov.* **2008**, *7* (7), 608–624. https://doi.org/10.1038/nrd2590.

(10) Schneider, J. J.; Unholzer, A.; Schaller, M.; Schäfer-Korting, M.; Korting, H. C. Human Defensins. *J. Mol. Med.* **2005**, *83* (8), 587–595. https://doi.org/10.1007/s00109-005-0657-1.

(11) Rastogi, S.; Shukla, S.; Kalaivani, M.; Singh, G. N. Peptide-Based Therapeutics: Quality Specifications, Regulatory Considerations, and Prospects. *Drug Discov. Today* **2019**, *24* (1), 148–162. https://doi.org/10.1016/j.drudis.2018.10.002.

(12) Hopkins, A. L.; Groom, C. R. The Druggable Genome. *Nat. Rev. Drug Discov.* **2002**, *1* (9), 727–730. https://doi.org/10.1038/nrd892.

(13) Russ, A. P.; Lampel, S. The Druggable Genome: An Update. *Drug Discov. Today*. **2005**, *23* (10) 1607–1610. https://doi.org/10.1016/S1359-6446(05)03666-4.

(14) Tsomaia, N. Peptide Therapeutics: Targeting the Undruggable Space. *Eur. J. Med. Chem.* **2015**, *94* (1), 459–470. https://doi.org/10.1016/j.ejmech.2015.01.014.

(15) Doak, B. C.; Zheng, J.; Dobritzsch, D.; Kihlberg, J. How Beyond Rule of 5 Drugs and Clinical Candidates Bind to Their Targets. *J. Med. Chem.* **2016**, *59* (6), 2312–2327. https://doi.org/10.1021/acs.jmedchem.5b01286.

(16) Villar, E. A.; Beglov, D.; Chennamadhavuni, S.; Porco, J. A.; Kozakov, D.; Vajda, S.; Whitty, A. How Proteins Bind Macrocycles. *Nat. Chem. Biol.* **2014**, *10* (9), 723–731. https://doi.org/10.1038/nchembio.1584.

(17) Duffy, F. J.; O'Donovan, D.; Devocelle, M.; Moran, N.; O'Connell, D. J.; Shields, D. C. Virtual Screening Using Combinatorial Cyclic Peptide Libraries Reveals Protein Interfaces Readily Targetable by Cyclic Peptides. *J. Chem. Inf. Model.* **2015**, *55* (3), 600–613. https://doi.org/10.1021/CI500431Q.

(18) Wang, L.; Wang, N.; Zhang, W.; Cheng, X.; Yan, Z.; Shao, G.; Wang, X.; Wang, R.; Fu, C. Therapeutic Peptides: Current Applications and Future Directions. *Signal Transduct. Target. Ther.* **2022**, *7* (1), 1–27. https://doi.org/10.1038/s41392-022-00904-4.

(19) Di, L. Strategic Approaches to Optimizing Peptide ADME Properties. *AAPS J.* **2015**, *17* (1), 134–143. https://doi.org/10.1208/s12248-014-9687-3.

(20) Jón Tryggvi Njardarson. *Top Pharmaceuticals Poster | Njarðarson*. https://njardarson.lab.arizona.edu/content/top-pharmaceuticals-poster (accessed 2020-05-13).

(21) Vinogradov, A. A.; Yin, Y.; Suga, H. Macrocyclic Peptides as Drug Candidates: Recent Progress and Remaining Challenges. *J. Am. Chem. Soc.* **2019**, *141* (10), 4167–4181. https://doi.org/10.1021/jacs.8b13178.

(22) Zorzi, A.; Deyle, K.; Heinis, C. Cyclic Peptide Therapeutics: Past, Present and Future. *Curr. Opin. Chem. Biol.* **2017**, *38* (1), 24–29. https://doi.org/10.1016/j.cbpa.2017.02.006.

(23) Dougherty, P. G.; Sahni, A.; Pei, D. Understanding Cell Penetration of Cyclic Peptides. *Chem. Rev*. **2019**, *119* (17) 10241–10287. https://doi.org/10.1021/acs.chemrev.9b00008.

(24) Li, X.; Craven, T. W.; Levine, P. M. Cyclic Peptide Screening Methods for Preclinical Drug Discovery. *J. Med. Chem.* **2022**, *65* (18), 11913-11926. https://doi.org/10.1021/acs.jmedchem.2C01077.

(25) Wang, C. K.; Swedberg, J. E.; Harvey, P. J.; Kaas, Q.; Craik, D. J. Conformational Flexibility Is a Determinant of Permeability for Cyclosporin. *J. Phys. Chem. B* **2018**, *122* (8), 2261–2276. https://doi.org/ 10.1021/acs.jpcb.7b12419.

(26) Bhardwaj, G.; O'Connor, J.; Rettie, S.; Huang, Y. H.; Ramelot, T. A.; Mulligan, V. K.; Alpkilic, G. G.; Palmer, J.; Bera, A. K.; Bick, M. J.; Di Piazza, M.; Li, X.; Hosseinzadeh, P.; Craven, T. W.; Tejero, R.; Lauko, A.; Choi, R.; Glynn, C.; Dong, L.; Griffin, R.; van Voorhis, W. C.; Rodriguez, J.; Stewart, L.; Montelione, G. T.; Craik, D.; Baker, D. Accurate de Novo Design of Membrane-Traversing Macrocycles. *Cell* **2022**, *185* (19), 3520-3532. https://doi.org/10.1016/j.cell.2022.07.019.

(27) Kosfeld, M.; Heinrichs, M.; Zak, P. J.; Fischbacher, U.; Fehr, E. Oxytocin Increases Trust in Humans. *Nature* **2005**, *435* (7042), 673–676. https://doi.org/10.1038/nature03701.

(28) Attilakos, G.; Psaroudakis, D.; Ash, J.; Buchanan, R.; Winter, C.; Donald, F.; Hunt, L.; Draycott, T. Carbetocin versus Oxytocin for the Prevention of Postpartum Haemorrhage Following Caesarean Section: The Results of a Double-Blind Randomised Trial. *BJOG An Int. J. Obstet. Gynaecol.* **2010**, *117* (8), 929–936. https://doi.org/10.1111/j.1471-0528.2010.02585.x.

(29) Hostetler, M. A.; Smith, C.; Nelson, S.; Budimir, Z.; Modi, R.; Woolsey, I.; Frerk, A.; Baker, B.; Gantt, J.; Parkinson, E. I. Synthetic Natural Product Inspired Cyclic Peptides. *ACS Chem. Biol.* **2021**, *16* (11), 2604–2611. https://doi.org/10.1021/acschembio.1c00641.

(30) Martens, E.; Demain, A. L. The Antibiotic Resistance Crisis, with a Focus on the United States. *J. Antibiot.* **2017**, *70* (5), 520–526. https://doi.org/10.1038/JA.2017.30.

(31) Newman, D. J.; Cragg, G. M. Natural Products as Sources of New Drugs over the Nearly Four Decades from 01/1981 to 09/2019. *J. Nat. Prod.* **2020**, *83* (3), 770–803. https://doi.org/ 10.1021/acs.jnatprod.9b01285.

(32) Götze, S.; Vij, R.; Burow, K.; Thome, N.; Urbat, L.; Schlosser, N.; Pflanze, S.; Müller, R.; Hänsch, V. G.; Schlabach, K.; Fazlikhani, L.; Walther, G.; Dahse, H.-M.; Regestein, L.; Brunke, S.; Hube, B.; Hertweck, C.; Franken, P.; Stallforth, P. Ecological Niche-Inspired Genome Mining Leads to the Discovery of Crop-Protecting Nonribosomal Lipopeptides Featuring a Transient Amino Acid Building Block. *J. Am. Chem. Soc.* **2023**, *145* (4), 2342–2353. https://doi.org/ 10.1021/jacs.2c11107.

(33) Ziemert, N.; Alanjary, M.; Weber, T. The Evolution of Genome Mining in Microbes – a Review. *Nat. Prod. Rep.* **2016**, *33* (8), 988–1005. https://doi.org/10.1039/C6NP00025H.

(34) Bauman, K. D.; Butler, K. S.; Moore, B. S.; Chekan, J. R. Genome Mining Methods to Discover Bioactive Natural Products. *Nat. Prod. Rep.* **2021**, *38* (11), 2100–2129. https://doi.org/10.1039/D1NP00032B.

(35) Newton, M. S.; Cabezas-Perusse, Y.; Tong, C. L.; Seelig, B. In Vitro Selection of Peptides and Proteins-Advantages of MRNA Display. *ACS Synth. Biol.* **2020**, *9* (2), 181–190. https://doi.org/ 10.1021/acssynbio.9b00419.

(36) Derda, R.; Tang, S. K. Y.; Li, S. C.; Ng, S.; Matochko, W.; Jafari, M. R. Diversity of Phage-Displayed Libraries of Peptides during Panning and Amplification. *Molecules* **2011**, *16* (2), 1776–1803. https://doi.org/10.3390/molecules16021776.

(37) Ebrahimizadeh, W.; Rajabibazl, M. Bacteriophage Vehicles for Phage Display: Biology, Mechanism, and Application. *Curr. Microbiol.* **2014**, *69* (2), 109–120. https://doi.org/10.1007/S00284-014-0557-0.

(38) Cotten, S. W.; Zou, J.; Wang, R.; Huang, B. C.; Liu, R. MRNA Display-Based Selections Using Synthetic Peptide and Natural Protein Libraries. *Methods Mol. Biol.* **2012**, *805* (1), 287–297. https://doi.org/10.1007/978-1-61779-379-0_16.

(39) Smith, G. P. Filamentous Fusion Phage: Novel Expression Vectors That Display Cloned Antigens on the Virion Surface. *Science* **1985**, *228* (4705), 1315–1317. https://doi.org/10.1126/SCIENCE.4001944.

(40) Roberts, R. W.; Szostak, J. W. RNA-Peptide Fusions for the in Vitro Selection of Peptides and Proteins. *Proc. Natl. Acad. Sci. U. S. A.* **1997**, *94* (23), 12297–12302. https://doi.org/10.1073/PNAS.94.23.12297.

(41) Heinis, C. Combining Biological and Chemical Diversity. *Nat. Chem.* **2021**, *13* (6), 512–513. https://doi.org/10.1038/s41557-021-00722-1.

(42) Habeshian, S.; Merz, M. L.; Sangouard, G.; Mothukuri, G. K.; Schüttel, M.; Bognár, Z.; Díaz-Perlas, C.; Vesin, J.; Bortoli Chapalay, J.; Turcatti, G.; Cendron, L.; Angelini, A.; Heinis, C. Synthesis and Direct Assay of Large Macrocycle Diversities by Combinatorial Late-Stage Modification at Picomole Scale. *Nat. Commun.* **2022**, *13* (1), 1–14. https://doi.org/10.1038/s41467-022-31428-8.

(43) Merrifield, R. B. Solid Phase Peptide Synthesis. I. The Synthesis of a Tetrapeptide. *J. Am. Chem. Soc.* **1963**, *85* (14), 2149–2154. https://doi.org/10.1021/ja00897a025.

(44) Mäde, V.; Els-Heindl, S.; Beck-Sickinger, A. G. Automated Solid-Phase Peptide Synthesis to Obtain Therapeutic Peptides. *Beilstein J. Org. Chem.* **2014**, *10* (1), 1197–1212. https://doi.org/10.3762/BJOC.10.118.

(45) Muttenthaler, M.; Albericio, F.; Dawson, P. E. Methods, Setup and Safe Handling for Anhydrous Hydrogen Fluoride Cleavage in Boc Solid-Phase Peptide Synthesis. *Nat. Protoc.* **2015**, *10* (7), 1067–1083. https://doi.org/10.1038/NPROT.2015.061.

(46) Chang, C. -D; Meienhofer, J. Solid-Phase Peptide Synthesis Using Mild Base Cleavage of NαFluorenylmethyloxycarbonylamino Acids, Exmplified by a Synthesis of Dihydrosomatostatin. *Int. J. Pept. Protein Res.* **1978**, *11* (3), 246–249. https://doi.org/10.1111/j.1399-3011.1978.tb02845.x.

(47) Fields, G. B.; Noble, R. L. Solid Phase Peptide Synthesis Utilizing 9-Fluorenylmethoxycarbonyl Amino Acids. *Int. J. Pept. Protein Res.* **1990**, *35* (3), 161–214. https://doi.org/10.1111/J.1399-3011.1990.TB00939.X.

(48) Hartrampf, N.; Saebi, A.; Poskus, M.; Gates, Z. P.; Callahan, A. J.; Cowfer, A. E.; Hanna, S.; Antilla, S.; Schissel, C. K.; Quartararo, A. J.; Ye, X.; Mijalis, A. J.; Simon, M. D.; Loas, A.; Liu, S.; Jessen, C.; Nielsen, T. E.; Pentelute, B. L. Synthesis

of Proteins by Automated Flow Chemistry. *Science* **2020**, *368* (6494), 980–987. https://doi.org/10.1126/science.abb2491.

(49) Dawson, P. E.; Muir, T. W.; Clark-Lewis, I.; Kent, S. B. H. Synthesis of Proteins by Native Chemical Ligation. *Science* **1994**, *266* (5186), 776–779. https://doi.org/10.1126/science.7973629.

(50) Muir, T. W.; Sondhi, D.; Cole, P. A. Expressed Protein Ligation: A General Method for Protein Engineering. *Proc. Natl. Acad. Sci. U. S. A.* **1998**, *95* (12), 6705–6710. https://doi.org/10.1073/PNAS.95.12.6705.

(51) Shelton, P. T.; Jensen, K. J. Synthesis of C-Terminal Peptide Thioesters Using Fmoc-Based Solid-Phase Peptide Chemistry. Methods Mol. Biol*. Vol. 1047*, Humana Press (2015). https://doi.org/10.1007/978-1-62703-544-6_8.

(52) Wang, Y. C.; Peterson, S. E.; Loring, J. F. Protein Post-Translational Modifications and Regulation of Pluripotency in Human Stem Cells. *Cell Res.* **2013**, *24* (2), 143–160. https://doi.org/10.1038/cr.2013.151.

(53) Blom, N.; Sicheritz-Pontén, T.; Gupta, R.; Gammeltoft, S.; Brunak, S. Prediction of Post-Translational Glycosylation and Phosphorylation of Proteins from the Amino Acid Sequence. *Proteomics*. **2004**, *4* (6), 1633-1649. https://doi.org/10.1002/pmic.200300771.

(54) Ramazi, S.; Zahiri, J. Post-Translational Modifications in Proteins: Resources, Tools and Prediction Methods. *Database* **2021**, *2021* (1), 1-20. https://doi.org/10.1093/database/baab012/6214407.

(55) Yang, A.; Cho, K.; Park, H. S. Chemical Biology Approaches for Studying Posttranslational Modifications. *RNA Biol.* **2017**, *15* (4), 427–440. https://doi.org/10.1080/15476286.2017.1360468.

(56) Emenike, B.; Nwajiobi, O.; Raj, M. Covalent Chemical Tools for Profiling Post-Translational Modifications. *Front. Chem.* **2022**, *10*, 868773. https://doi.org/10.3389/fchem.2022.868773.

(57) Byk, G.; Halle, D.; Zeltser, I.; Bitan, G.; Selinger, Z.; Gilon, C. Synthesis and Biological Activity of NK-1 Selective, N-Backbone Cyclic Analogs of the C-Terminal Hexapeptide of Substance P. *J. Med. Chem.* **1996**, *39* (16), 3174–3178. https://doi.org/10.1021/jm960154i.

(58) Hess, S.; Linde, Y.; Ovadia, O.; Safrai, E.; Shalev, D. E.; Swed, A.; Halbfinger, E.; Lapidot, T.; Winkler, I.; Gabinet, Y.; Faier, A.; Yarden, D.; Xiang, Z.; Portillo, F. P.; Haskell-Luevano, C.; Gilon, C.; Hoffman, A. Backbone Cyclic Peptidomimetic Melanocortin-4 Receptor Agonist as a Novel Orally Administrated Drug Lead for Treating Obesity. *J. Med. Chem.* **2008**, *51* (4), 1026–1034. https://doi.org/10.1021/jm701093y.

(59) Lau, Y. H.; De Andrade, P.; Wu, Y.; Spring, D. R. Peptide Stapling Techniques Based on Different Macrocyclisation Chemistries. *Chem. Soc. Rev.* **2015**, *44* (1), 91–102. https://doi.org/10.1039/c4cs00246f.

(60) Do, T.; Link, A. J. Protein Engineering in Ribosomally Synthesized and Post-Translationally Modified Peptides (RiPPs). *Biochemistry* **2023**, *62* (2), 201–209. https://doi.org/ 10.1021/acs.biochem.1c00714.

(61) Arnison, P. G.; Bibb, M. J.; Bierbaum, G.; Bowers, A. A.; Bugni, T. S.; Bulaj, G.; Camarero, J. A.; Campopiano, D. J.; Challis, G. L.; Clardy, J.; Cotter, P. D.; Craik, D. J.; Dawson, M.; Dittmann, E.; Donadio, S.; Dorrestein, P. C.; Entian, K. D.; Fischbach, M. A.; Garavelli, J. S.; Göransson, U.; Gruber, C. W.; Haft, D. H.; Hemscheidt, T. K.; Hertweck, C.; Hill, C.; Horswill, A. R.; Jaspars, M.; Kelly, W. L.; Klinman, J. P.; Kuipers, O. P.; Link, A. J.; Liu, W.; Marahiel, M. A.; Mitchell, D. A.; Moll, G. N.; Moore, B. S.; Müller, R.; Nair, S. K.; Nes, I. F.; Norris, G. E.; Olivera, B. M.; Onaka, H.; Patchett, M. L.; Piel, J.; Reaney, M. J. T.; Rebuffat, S.; Ross, R. P.; Sahl, H. G.; Schmidt, E. W.; Selsted, M. E.; Severinov, K.; Shen, B.; Sivonen, K.; Smith, L.; Stein, T.; Süssmuth, R. D.; Tagg, J. R.; Tang, G. L.; Truman, A. W.; Vederas, J. C.; Walsh, C. T.; Walton, J. D.; Wenzel, S. C.; Willey, J. M.; Van Der Donk, W. A. Ribosomally Synthesized and Post-Translationally Modified Peptide Natural Products: Overview and Recommendations for a Universal Nomenclature. *Nat. Prod. Rep.* **2012**, *30* (1), 108–160. https://doi.org/10.1039/C2NP20085F.

(62) DeGruyter, J. N.; Malins, L. R.; Baran, P. S. Residue-Specific Peptide Modification: A Chemist's Guide. *Biochemistry* **2017**, *56* (30), 3863–3873. https://doi.org/10.1021/acs.biochem.7b00536.

(63) Agouridas, V.; El Mahdi, O.; Cargoët, M.; Melnyk, O. A Statistical View of Protein Chemical Synthesis Using NCL and Extended Methodologies. *Bioorg. Med. Chem.*

2017, *25* (18), 4938–4945. https://doi.org/10.1016/j.bmc.2017.05.050.

(64) Haynes, W.M. *CRC Handbook of Chemistry and Physics,* Vol 97, CRC Press (2016). https://doi.org/10.1201/9781315380476.

(65) Pahari, S.; Sun, L.; Alexov, E. PKAD: A Database of Experimentally Measured PKa Values of Ionizable Groups in Proteins. *Database* **2019**, *2019* (1). https://doi.org//10.1093/database/baz024/5359213.

(66) Modell, A. E.; Marrone, F.; Panigrahi, N. R.; Zhang, Y.; Arora, P. S. Peptide Tethering: Pocket-Directed Fragment Screening for Peptidomimetic Inhibitor Discovery. *J. Am. Chem. Soc.* **2022**, *144* (3), 1198–1204. https://doi.org/ 10.1021/jacs.1c09666.

(67) Smith, M. E. B.; Schumacher, F. F.; Ryan, C. P.; Tedaldi, L. M.; Papaioannou, D.; Waksman, G.; Caddick, S.; Baker, J. R. Protein Modification, Bioconjugation, and Disulfide Bridging Using Bromomaleimides. *J. Am. Chem. Soc.* **2010**, *132* (6), 1960–1965. https://doi.org/10.1021/ja908610s.

(68) Ceballos, J.; Grinhagena, E.; Sangouard, G.; Heinis, C.; Waser, J. Cys–Cys and Cys–Lys Stapling of Unprotected Peptides Enabled by Hypervalent Iodine Reagents. *Angew. Chem. Int. Ed.* **2021**, *60* (16), 9022–9031. https://doi.org/10.1002/ANIE.202014511.

(69) Frei, R.; Waser, J. A Highly Chemoselective and Practical Alkynylation of Thiols. *J. Am. Chem. Soc.* **2013**, *135* (26), 9620–9623. https://doi.org/10.1021/ja4044196.

(70) Allouche, E. M. D.; Grinhagena, E.; Waser, J. Hypervalent Iodine-Mediated Late-Stage Peptide and Protein Functionalization. *Angew. Chem. Int. Ed.* **2022**, *61* (1), e202112287. https://doi.org/10.1002/ANIE.202112287.

(71) Baumann, A. L.; Schwagerus, S.; Broi, K.; Kemnitz-Hassanin, K.; Stieger, C. E.; Trieloff, N.; Schmieder, P.; Hackenberger, C. P. R. Chemically Induced Vinylphosphonothiolate Electrophiles for Thiol-Thiol Bioconjugations. *J. Am. Chem. Soc.* **2020**, *142* (20), 9544–9552. https://doi.org/ 10.1021/jacs.0c03426.

(72) Stieger, C. E.; Franz, L.; Körlin, F.; Hackenberger, C. P. R. Diethynyl Phosphinates for Cysteine-Selective Protein Labeling and Disulfide Rebridging. *Angew. Chem. Int. Ed.* **2021**, *60* (28), 15359–15364. https://doi.org/10.1002/ANIE.202100683.

(73) Dickens, F. Interaction of Halogenacetates and SH CompoundsThe Reaction of

Halogenacetic Acids with Glutathione and Cysteine. The Mechanism of Iodoacetate Poisoning of Glyoxalase. *Biochem. J.* **1933**, *27* (4), 1141–1151. https://doi.org/10.1042/BJ0271141.

(74) Goto, Y.; Suga, H. The RaPID Platform for the Discovery of Pseudo-Natural Macrocyclic Peptides. *Acc. Chem. Res.* **2021**, *54* (18), 3604–3617. https://doi.org/ 10.1021/acs.accounts.1c00391.

(75) Freidmann, E.; Marrian, D. H.; Simonreuss, I. Antimitotic Action of Maleimide and Related Substances. *Br. J. Pharmacol. Chemother.* **1949**, *4* (1), 105-105. https://doi.org/10.1111/J.1476-5381.1949.TB00521.X.

(76) Ford-Moore, A. H. Divinyl Sulphone and Allied Compounds. *J. Chem. Soc.* **1949**, *1* (1) 2433–2440. https://doi.org/10.1039/jr9490002433.

(77) Heinis, C.; Rutherford, T.; Freund, S.; Winter, G. Phage-Encoded Combinatorial Chemical Libraries Based on Bicyclic Peptides. *Nat. Chem. Biol.* **2009**, *5* (7), 502–507. https://doi.org/10.1038/nchembio.184.

(78) Kale, S. S.; Bergeron-Brlek, M.; Wu, Y.; Kumar, M. G.; Pham, M. V.; Bortoli, J.; Vesin, J.; Kong, X. D.; Franco Machado, J.; Deyle, K.; Gonschorek, P.; Turcatti, G.; Cendron, L.; Angelini, A.; Heinis, C. Thiol-to-Amine Cyclization Reaction Enables Screening of Large Libraries of Macrocyclic Compounds and the Generation of Sub-Kilodalton Ligands. *Sci. Adv.* **2019**, *5* (8), eaaw2851. https://doi.org/10.1126/sciadv.aaw2851.

(79) Gehringer, M.; Laufer, S. A. Emerging and Re-Emerging Warheads for Targeted Covalent Inhibitors: Applications in Medicinal Chemistry and Chemical Biology. *J. Med. Chem.* **2019**, *62* (12), 5673–5724. https://doi.org/ acs.jmedchem.8b01153.

(80) Lechner, V. M.; Nappi, M.; Deneny, P. J.; Folliet, S.; Chu, J. C. K.; Gaunt, M. J. Visible-Light-Mediated Modification and Manipulation of Biomacromolecules. *Chem. Rev.* **2021**, *122* (2), 1752-1829. https://doi.org/10.1021/acs.chemrev.1c00357.

(81) Linsley, C. S.; Quach, V. Y.; Agrawal, G.; Hartnett, E.; Wu, B. M. Visible Light and Near-Infrared-Responsive Chromophores for Drug Delivery-on-Demand Applications. *Drug Deliv. Transl. Res.* **2015**, *5* (6), 611–624. https://doi.org/10.1007/S13346-015-0260-0.

(82) Choi, H.; Kim, M.; Jang, J.; Hong, S. Visible-Light-Induced Cysteine-Specific

Bioconjugation: Biocompatible Thiol–Ene Click Chemistry. *Angew. Chem. Int. Ed.* **2020**, *59* (50), 22514–22522. https://doi.org/10.1002/anie.202010217.

(83) Fancy, D. A.; Kodadek, T. Chemistry for the Analysis of Protein–Protein Interactions: Rapid and Efficient Cross-Linking Triggered by Long Wavelength Light. *Proc. Natl. Acad. Sci.* **1999**, *96* (11), 6020–6024. https://doi.org/10.1073/PNAS.96.11.6020.

(84) Sato, S.; Nakamura, H. Ligand-Directed Selective Protein Modification Based on Local Single-Electron-Transfer Catalysis. *Angew. Chem. Int. Ed.* **2013**, *52* (33), 8681–8684. https://doi.org/10.1002/ANIE.201303831.

(85) Wan, C.; Wang, Y.; Lian, C.; Chang, Q.; An, Y.; Chen, J.; Sun, J.; Hou, Z.; Yang, D.; Guo, X.; Yin, F.; Wang, R.; Li, Z.; Wan, C.; Wang, Y.; Lian, C.; Chang, Q.; An, Y.; Chen, J.; Sun, J.; Hou, Z.; Yang, D.; Guo, X.; Yin, F.; Wang, R.; Li, Z. Histidine-Specific Bioconjugation via Visible-Light-Promoted Thioacetal Activation. *Chem. Sci.* **2022**, *13* (1), 8289-8296. https://doi.org/10.1039/D2SC02353A.

(86) King, J. L.; Jukes, T. H. Non-Darwinian Evolution. *Science.* **1969**, *164* (3881), 788–798. https://doi.org/ 10.1126/science.164.3881.788.

(87) Yu, Y.; Zhang, L. K.; Buevich, A. V.; Li, G.; Tang, H.; Vachal, P.; Colletti, S. L.; Shi, Z. C. Chemoselective Peptide Modification via Photocatalytic Tryptophan β-Position Conjugation. *J. Am. Chem. Soc.* **2018**, *140* (22), 6797–6800. https://doi.org/10.1021/JACS.8B03973.

(88) Kim, J.; Li, B. X.; Huang, R. Y.-C.; Qiao, J. X.; Ewing, W. R.; Macmillan, D. W. C. Site-Selective Functionalization of Methionine Residues via Photoredox Catalysis. *J. Am. Chem. Soc.* **2020**, *142* (51), 21260–21266. https://doi.org/10.1021/jacs.0c09926.

(89) Kolb, H. C.; Finn, M. G.; Sharpless, K. B. Click Chemistry: Diverse Chemical Function from a Few Good Reactions. *Angew. Chem. Int. Ed.* **2001**, *40* (11), 2004–2021. https://doi.org/10.1002/1521-3773(20010601)40:11<2004::AID-ANIE2004>3.0.CO;2-5.

(90) *The Nobel Prize in Chemistry*, https://www.nobelprize.org/prizes/chemistry/2022/summary/ (accessed 2023-10-22).

(91) Huisgen, R. 1,3-Dipolar Cycloadditions. Past and Future. *Angew. Chem. Int. Ed.*

1963, *2* (10), 565–598. https://doi.org/10.1002/ANIE.196305651.

(92) Rostovtsev, V. V.; Green, L. G.; Fokin, V. V.; Sharpless, K. B. A Stepwise Huisgen Cycloaddition Process: Copper(I)-Catalyzed Regioselective "Ligation" of Azides and Terminal Alkynes. *Angew. Chem. Int. Ed.* **2002**, *41* (14), 2596-2599. https://doi.org/10.1002/1521-3773(20020715)41:14<2596::AID-ANIE2596>3.0.CO;2-4.

(93) Tornøe, C. W.; Christensen, C.; Meldal, M. Peptidotriazoles on Solid Phase: [1,2,3]-Triazoles by Regiospecific Copper(I)-Catalyzed 1,3-Dipolar Cycloadditions of Terminal Alkynes to Azides. *J. Org. Chem.* **2002**, *67* (9), 3057–3064. https://doi.org/10.1021/JO011148J.

(94) Meldal, M.; Tomøe, C. W. Cu-Catalyzed Azide - Alkyne Cycloaddition. *Chem. Rev*. **2008**, *108* (8), 2952-3015. https://doi.org/10.1021/cr0783479.

(95) Liang, L.; Astruc, D. The Copper(I)-Catalyzed Alkyne-Azide Cycloaddition (CuAAC) "Click" Reaction and Its Applications. An Overview. *Coord. Chem. Rev*. **2011**, 255 (23), 2933-2945. https://doi.org/10.1016/j.ccr.2011.06.028.

(96) Agard, N. J.; Prescher, J. A.; Bertozzi, C. R. A Strain-Promoted [3 + 2] Azide-Alkyne Cycloaddition for Covalent Modification of Biomolecules in Living Systems. *J. Am. Chem. Soc.* **2004**, *126* (46), 15046–15047. https://doi.org/10.1021/ja044996f.

(97) Laughlin, S. T.; Baskin, J. M.; Amacher, S. L.; Bertozzi, C. R. In Vivo Imaging of Membrane-Associated Glycans in Developing Zebrafish. *Science* **2008**, *320* (5876), 664–667. https://doi.org/10.1126/science.1155106.

(98) Finn, M. G.; Kolb, H. C.; Sharpless, K. B. Click Chemistry Connections for Functional Discovery. *Nat. Synth.* **2022**, *1* (1), 8–10. https://doi.org/10.1038/s44160-021-00017-w.

(99) Posner, T. Beiträge Zur Kenntniss Der Ungesättigten Verbindungen. II. Ueber Die Addition von Mercaptanen an Ungesättigte Kohlenwasserstoffe. *Ber. Dtsch. Chem. Ges.* **1905**, *38* (1), 646–657. https://doi.org/10.1002/cber.190503801106.

(100) Hoyle, C. E.; Bowman, C. N. Thiol-Ene Click Chemistry. *Angew. Chem. Int. Ed.*. February 22, 2010, pp 1540–1573. https://doi.org/10.1002/anie.200903924.

(101) Cesana, P. T.; Li, B. X.; Shepard, S. G.; Ting, S. I.; Hart, S. M.; Olson, C. M.;

Martinez Alvarado, J. I.; Son, M.; Steiman, T. J.; Castellano, F. N.; Doyle, A. G.; MacMillan, D. W. C.; Schlau-Cohen, G. S. A Biohybrid Strategy for Enabling Photoredox Catalysis with Low-Energy Light. *Chem.* **2021**, *8* (1), 1–12. https://doi.org/10.1016/j.chempr.2021.10.010.

(102) Taylor, N. C.; McGouran, J. F. Investigating Eosin Y as a Photocatalyst for the Radical-Dependent Activity-Based Probing of Deubiquitinating Enzymes. *Org. Biomol. Chem.* **2021**, *19* (10), 2177–2181. https://doi.org/10.1039/D1OB00253H.

(103) Triola, G.; Brunsveld, L.; Waldmann, H. Racemization-Free Synthesis of S-Alkylated Cysteines via Thiol-Ene Reaction. *J. Org. Chem.* **2008**, *73* (9), 3646–3649. https://doi.org/10.1021/jo800198s.

(104) McCourt, R. O.; Scanlan, E. M. Atmospheric Oxygen Mediated Radical Hydrothiolation of Alkenes. *Chem. – A Eur. J.* **2020**, *26* (68), 15804–15810. https://doi.org/10.1002/CHEM.202002542.

(105) Nolan, M. D.; Mezzetta, A.; Guazzelli, L.; Scanlan, E. M. Radical-Mediated Thiol-Ene 'Click' Reactions in Deep Eutectic Solvents for Bioconjugation. *Green Chem.* **2022**, *24* (4), 1456–1462. https://doi.org/10.1039/d1gc03714e.

(106) McSweeney, L.; Dénès, F.; Scanlan, E. M. Thiyl-Radical Reactions in Carbohydrate Chemistry: From Thiosugars to Glycoconjugate Synthesis. *Eur. J. Org. Chem.* **2016**, *2016* (12), 2080–2095. https://doi.org/10.1002/ejoc.201501543.

(107) Hoyle, C. E.; Lee, T. Y.; Roper, T. Thiol-Enes: Chemistry of the Past with Promise for the Future. *J. Polym. Sci. Part A Polym. Chem.* **2004**, *42* (21), 5301–5338. https://doi.org/10.1002/pola.20366.

(108) Nolan, M. D.; Scanlan, E. M. Applications of Thiol-Ene Chemistry for Peptide Science. *Front. Chem*. **2020**, *8* (1), 583272. https://doi.org/10.3389/fchem.2020.583272.

(109) McLean, J. T.; Benny, A.; Nolan, M. D.; Swinand, G.; Scanlan, E. M. Cysteinyl Radicals in Chemical Synthesis and in Nature. *Chem. Soc. Rev*. **2021**, *50* (1) 10857–10894. https://doi.org/10.1039/d1cs00254f.

(110) Ahangarpour, M.; Kavianinia, I.; Harris, P. W. R.; Brimble, M. A. Photo-Induced Radical Thiol–Ene Chemistry: A Versatile Toolbox for Peptide-Based Drug Design. *Chem. Soc. Rev.* **2021**, *50* (1), 898-944. https://doi.org/10.1039/D0CS00354A.

(111) Northrop, B. H.; Coffey, R. N. Thiol-Ene Click Chemistry: Computational and Kinetic Analysis of the Influence of Alkene Functionality. *J. Am. Chem. Soc.* **2012**, *134* (33), 13804–13817. https://doi.org/10.1021/JA305441D/.

(112) Fındık, V.; Degirmenci, I.; Çatak, Ş.; Aviyente, V. Theoretical Investigation of Thiol-Ene Click Reactions: A DFT Perspective. *Eur. Polym. J.* **2019**, *110*, 211–220. https://doi.org/10.1016/J.EURPOLYMJ.2018.11.030.

(113) Cramer, N. B.; Reddy, S. K.; O'Brien, A. K.; Bowman, C. N. Thiol - Ene Photopolymerization Mechanism and Rate Limiting Step Changes for Various Vinyl Functional Group Chemistries. *Macromolecules* **2003**, *36* (21), 7964–7969. https://doi.org/10.1021/MA034667S.

(114) McCourt, R. O.; Dénès, F.; Sanchez-Sanz, G.; Scanlan, E. M. Rapid Access to Thiolactone Derivatives through Radical-Mediated Acyl Thiol-Ene and Acyl Thiol-Yne Cyclization. *Org. Lett.* **2018**, *20* (10), 2948–2951. https://doi.org/ 10.1021/acs.orglett.8b00996.

(115) Narendra, N.; Thimmalapura, V. M.; Hosamani, B.; Prabhu, G.; Kumar, L. R.; Sureshbabu, V. V. Thioacids – Synthons for Amide Bond Formation and Ligation Reactions: Assembly of Peptides and Peptidomimetics. *Org. Biomol. Chem.* **2018**, *16* (19), 3524–3552. https://doi.org/10.1039/C8OB00512E.

(116) McCourt, R. O.; Scanlan, E. M. A Sequential Acyl Thiol-Ene and Thiolactonization Approach for the Synthesis of δ-Thiolactones. *Org. Lett.* **2019**, *21* (9), 3460–3464. https://doi.org/ 10.1021/acs.orglett.9b01271.

(117) Tian, Y.; Li, J.; Zhao, H.; Zeng, X.; Wang, D.; Liu, Q.; Niu, X.; Huang, X.; Xu, N.; Li, Z. Stapling of Unprotected Helical Peptides via Photo-Induced Intramolecular Thiol–Yne Hydrothiolation. *Chem. Sci.* **2016**, *7* (5), 3325–3330. https://doi.org/10.1039/c6sc00106h.

(118) Nador, F.; Mancebo-Aracil, J.; Zanotto, D.; Ruiz-Molina, D.; Radivoy, G. Thiol-Yne Click Reaction: An Interesting Way to Derive Thiol-Provided Catechols. *RSC Adv.* **2021**, *11* (4), 2074–2082. https://doi.org/10.1039/D0RA09687C.

(119) Ryss, J. M.; Turek, A. K.; Miller, S. J. Disulfide-Bridged Peptides That Mediate Enantioselective Cycloadditions through Thiyl Radical Catalysis. *Org. Lett.* **2018**, *20* (6), 1621–1625. https://doi.org/10.1021/acs.orglett.8b00364.

(120) Shin, N. Y.; Ryss, J. M.; Zhang, X.; Miller, S. J.; Knowles, R. R. Light-Driven Deracemization Enabled by Excited-State Electron Transfer. *Science* **2019**, *366* (6463), 364–369. https://doi.org/10.1126/science.aay2204.

(121) Hashimoto, T.; Kawamata, Y.; Maruoka, K. An Organic Thiyl Radical Catalyst for Enantioselective Cyclization. *Nat. Chem.* **2014**, *6* (8), 702–705. https://doi.org/10.1038/nchem.1998.

(122) Hoppmann, C.; Kühne, R.; Beyermann, M. Intramolecular Bridges Formed by Photoswitchable Click Amino Acids. *Beilstein J. Org. Chem*. **2012**, *8* (1), 884–889. https://doi.org/10.3762/bjoc.8.100.

(123) Tian, Y.; Li, J.; Zhao, H.; Zeng, X.; Wang, D.; Liu, Q.; Niu, X.; Huang, X.; Xu, N.; Li, Z. Stapling of Unprotected Helical Peptides via Photo-Induced Intramolecular Thiol–Yne Hydrothiolation. *Chem. Sci.* **2016**, *7* (5), 3325–3330. https://doi.org/10.1039/c6sc00106h.

(124) Cochrane, S. A.; Huang, Z.; Vederas, J. C. Investigation of the Ring-Closing Metathesis of Peptides in Water. *Org. Biomol. Chem.* **2012**, *11* (4), 630–639. https://doi.org/10.1039/C2OB26938D.

(125) Aimetti, A. A.; Shoemaker, R. K.; Lin, C.-C.; Anseth, K. S. On-Resin Peptide Macrocyclization Using Thiol–Ene Click Chemistry. *Chem. Commun.* **2010**, *46* (23), 4061. https://doi.org/10.1039/c001375g.

(126) Zhao, B.; Zhang, Q.; Li, Z. Constructing Thioether-Tethered Cyclic Peptides via on-Resin Intra-Molecular Thiol–Ene Reaction. *J. Pept. Sci.* **2016**, 540–544. https://doi.org/10.1002/psc.2902.

(127) Hoppmann, C.; Schmieder, P.; Heinrich, N.; Beyermann, M. Photoswitchable Click Amino Acids: Light Control of Conformation and Bioactivity. *ChemBioChem* **2011**, *12* (17), 2555–2559. https://doi.org/10.1002/cbic.201100578.

(128) Levalley, P. J.; Ovadia, E. M.; Bresette, C. A.; Sawicki, L. A.; Maverakis, E.; Bai, S.; Kloxin, A. M. Design of Functionalized Cyclic Peptides through Orthogonal Click Reactions for Cell Culture and Targeting Applications. *Chem. Commun.* **2018**, *54* (50), 6923–6926. https://doi.org/10.1039/c8cc03218a.

(129) Wang, Y.; Chou, D. H. C. A Thiol-Ene Coupling Approach to Native Peptide Stapling and Macrocyclization. *Angew. Chem. Int. Ed.* **2015**, *54* (37), 10931–10934.

https://doi.org/10.1002/anie.201503975.

(130) Lynch, D. M.; Scanlan, E. M. Thiyl Radicals: Versatile Reactive Intermediates for Cyclization of Unsaturated Substrates. *Molecules* **2020**, *25* (13), 3094-3134. https://doi.org/10.3390/molecules25133094.

(131) Wang, Y.; Bruno, B. J.; Cornillie, S.; Nogieira, J. M.; Chen, D.; Cheatham, T. E.; Lim, C. S.; Chou, D. H. C. Application of Thiol–Yne/Thiol–Ene Reactions for Peptide and Protein Macrocyclizations. *Chem. - A Eur. J.* **2017**, *23* (29), 7087–7092. https://doi.org/10.1002/chem.201700572.

(132) Paterson, D. L.; Flanagan, J. U.; Shepherd, P. R.; Harris, P. W. R.; Brimble, M. A. Variable-Length Ester-Based Staples for α-Helical Peptides by Using A Double Thiol-Ene Reaction. *Chem. - A Eur. J.* **2020**, *26* (47), 10826–10833. https://doi.org/10.1002/chem.202001478.

(133) Apweiler, R.; Hermjakob, H.; Sharon, N. On the Frequency of Protein Glycosylation, as Deduced from Analysis of the SWISS-PROT Database. *Biochim. Biophys. Acta - Gen. Subj.* **1999**, *1473* (1), 4–8. https://doi.org/10.1016/S0304-4165(99)00165-8.

(134) Spiro, R. G. Protein Glycosylation: Nature, Distribution, Enzymatic Formation, and Disease Implications of Glycopeptide Bonds. *Glycobiology* **2002**, *12* (4), 43R-56R. https://doi.org/10.1093/glycob/12.4.43R.

(135) Scanlan, E. M.; Corcé, V.; Malone, A. Synthetic Applications of Intramolecular Thiol-Ene "Click" Reactions. *Molecules* **2014**, *19* (11) 19137–19151. https://doi.org/10.3390/molecules191119137.

(136) Dondoni, A.; Massi, A.; Nanni, P.; Roda, A. A New Ligation Strategy for Peptide and Protein Glycosylation: Photoinduced Thiol-Ene Coupling. *Chem. - A Eur. J.* **2009**, *15* (43), 11444–11449. https://doi.org/10.1002/chem.200901746.

(137) Floyd, N.; Vijayakrishnan, B.; Koeppe, J. R.; Davis, B. G. Thiyl Glycosylate of Olefinic Proteins: S-Linked Glycoconjugate Synthesis. *Angew. Chem. Int. Ed.* **2009**, *48* (42), 7798–7802. https://doi.org/10.1002/anie.200903135.

(138) Lo Conte, M.; Pacifico, S.; Chambery, A.; Marra, A.; Dondoni, A. Photoinduced Addition of Glycosyl Thiols to Alkynyl Peptides: Use of Free-Radical Thiol-Yne Coupling for Post-Translational Double-Glycosylation of Peptides. *J. Org. Chem.*

2010, *75* (13), 4644–4647. https://doi.org/10.1021/jo1008178.

(139) Markey, L.; Giordani, S.; Scanlan, E. M. Native Chemical Ligation, Thiol-Ene Click: A Methodology for the Synthesis of Functionalized Peptides. *J. Org. Chem.* **2013**, *78* (9), 4270–4277. https://doi.org/10.1021/jo4001542.

(140) Rojas-Ocáriz, V.; Compañón, I.; Aydillo, C.; Castro-Lopez, J.; Jiménez-Barbero, J.; Hurtado-Guerrero, R.; Avenoza, A.; Zurbano, M. M.; Peregrina, J. M.; Busto, J. H.; Corzana, F. Design of α-S-Neoglycopeptides Derived from MUC1 with a Flexible and Solvent-Exposed Sugar Moiety. *J. Org. Chem.* **2016**, *81* (14), 5929–5941. https://doi.org/10.1021/acs.joc.6b00833.

(141) Fiore, M.; Chand Daskhan, G.; Thomas, B.; Renaudet, O. Orthogonal Dual Thiol-Chloroacetyl and Thiol-Ene Couplings for the Sequential One-Pot Assembly of Heteroglycoclusters. *Beilstein J. Org. Chem* **2014**, *10*, 1557–1563. https://doi.org/10.3762/bjoc.10.160.

(142) Su, Y.; Tian, L.; Yu, M.; Gao, Q.; Wang, D.; Xi, Y.; Yang, P.; Lei, B.; Ma, P. X.; Li, P. Cationic Peptidopolysaccharides Synthesized by "click" Chemistry with Enhanced Broad-Spectrum Antimicrobial Activities. *Polym. Chem.* **2017**, *8* (25), 3788–3800. https://doi.org/10.1039/c7py00528h.

(143) Chen, Y.; Yu, L.; Zhang, B.; Feng, W.; Xu, M.; Gao, L.; Liu, N.; Wang, Q.; Huang, X.; Li, P.; Huang, W. Design and Synthesis of Biocompatible, Hemocompatible, and Highly Selective Antimicrobial Cationic Peptidopolysaccharides via Click Chemistry. *Biomacromolecules* **2019**, *20* (6), 2230–2240. https://doi.org/10.1021/acs.biomac.9b00179.

(144) Majorek, K. A.; Porebski, P. J.; Dayal, A.; Zimmerman, M. D.; Jablonska, K.; Stewart, A. J.; Chruszcz, M.; Minor, W. Structural and Immunologic Characterization of Bovine, Horse, and Rabbit Serum Albumins. *Mol. Immunol.* **2012**, *52* (3), 174–182. https://doi.org/10.1016/J.MOLIMM.2012.05.011.

(145) Hamman, J. H.; Enslin, G. M.; Kotzé, A. F. Oral Delivery of Peptide Drugs: Barriers and Developments. *BioDrugs*. Springer (2005). https://doi.org/10.2165/00063030-200519030-00003.

(146) Simerska, P.; Moyle, P. M.; Toth, I. Modern Lipid-, Carbohydrate-, and Peptide-Based Delivery Systems for Peptide, Vaccine, and Gene Products. *Med. Res. Rev.*

2011, *31* (4), 520–547. https://doi.org/10.1002/med.20191.

(147) Zhang, L.; Bulaj, G. Converting Peptides into Drug Leads by Lipidation. *Curr. Med. Chem.* **2012**, *19* (11), 1602–1618. https://doi.org/10.2174/092986712799945003.

(148) Cochrane, S. A.; Vederas, J. C. Lipopeptides from Bacillus and Paenibacillus Spp.: A Gold Mine of Antibiotic Candidates. *Med. Res. Rev.* **2016**, *36* (1), 4–31. https://doi.org/10.1002/med.21321.

(149) Al Ayed, K.; Ballantine, R. D.; Hoekstra, M.; Bann, S. J.; Wesseling, C. M. J.; Bakker, A. T.; Zhong, Z.; Li, Y. X.; Brüchle, N. C.; van der Stelt, M.; Cochrane, S. A.; Martin, N. I. Synthetic Studies with the Brevicidine and Laterocidine Lipopeptide Antibiotics Including Analogues with Enhanced Properties and in Vivo Efficacy. *Chem. Sci.* **2022**, *13* (12), 3563–3570. https://doi.org/10.1039/D2SC00143H.

(150) Wright, T. H.; Brooks, A. E. S.; Didsbury, A. J.; Williams, G. M.; Harris, P. W. R.; Dunbar, P. R.; Brimble, M. A. Direct Peptide Lipidation through Thiol-Ene Coupling Enables Rapid Synthesis and Evaluation of Self-Adjuvanting Vaccine Candidates. *Angew. Chem. Int. Ed.* **2013**, *52* (40), 10616–10619. https://doi.org/10.1002/anie.201305620.

(151) Yang, S. H.; Harris, P. W. R.; Williams, G. M.; Brimble, M. A. Lipidation of Cysteine or Cysteine-Containing Peptides Using the Thiol-Ene Reaction (CLipPA). *Eur. J. Org. Chem.* **2016**, *2016* (15), 2608–2616. https://doi.org/10.1002/ejoc.201501375.

(152) Yim, V. V.; Kavianinia, I.; Cameron, A. J.; Harris, P. W. R.; Brimble, M. A. Direct Synthesis of Cyclic Lipopeptides Using Intramolecular Native Chemical Ligation and Thiol–Ene CLipPA Chemistry. *Org. Biomol. Chem.* **2020**, *18* (15), 2838–2844. https://doi.org/10.1039/d0ob00203h.

(153) Yim, V. V; Cameron, A. J.; Kavianinia, I.; Harris, P. W. R.; Brimble, M. A. Thiol-Ene Enabled Chemical Synthesis of Truncated S-Lipidated Teixobactin Analogs. *Front. Chem.* **2020**, *8* (1), 4–10. https://doi.org/10.3389/fchem.2020.00568.

(154) Yim, V.; Kavianinia, I.; Knottenbelt, M. K.; Ferguson, S. A.; Cook, G. M.; Swift, S.; Chakraborty, A.; Allison, J. R.; Cameron, A. J.; Harris, P. W. R.; Brimble, M. A. "CLipP"ing on Lipids to Generate Antibacterial Lipopeptides. *Chem. Sci.* **2020**, *11*

(1), 5759-5765. https://doi.org/10.1039/d0sc01814g.

(155) Karmann, L.; Kazmaier, U. Thiol-Ene Click Reactions - Versatile Tools for the Modification of Unsaturated Amino Acids and Peptides. *Eur. J. Org. Chem.* **2013**, *31* (1), 7101–7109. https://doi.org/10.1002/ejoc.201300672.

(156) Healy, J.; Rasmussen, T.; Miller, S.; Booth, I. R.; Conway, S. J. The Photochemical Thiol-Ene Reaction as a Versatile Method for the Synthesis of Glutathione S-Conjugates Targeting the Bacterial Potassium Efflux System Kef. *Org. Chem. Front.* **2016**, *3* (4), 439–446. https://doi.org/10.1039/c5qo00436e.

(157) Petracca, R.; Bowen, K. A.; McSweeney, L.; O'Flaherty, S.; Genna, V.; Twamley, B.; Devocelle, M.; Scanlan, E. M. Chemoselective Synthesis of N-Terminal Cysteinyl Thioesters via β,γ-C,S Thiol-Michael Addition. *Org. Lett.* **2019**, *21* (9), 3281–3285. https://doi.org/10.1021/acs.orglett.9b01013.

(158) Rafie, K.; Gorelik, A.; Trapannone, R.; Borodkin, V. S.; Van Aalten, D. M. F. Thio-Linked UDP-Peptide Conjugates as O-GlcNAc Transferase Inhibitors. *Bioconjug. Chem.* **2018**, *29* (6), 1834–1840. https://doi.org/10.1021/acs.bioconjchem.8b00194.

(159) Li, F.; Allahverdi, A.; Yang, R.; Lua, G. B. J.; Zhang, X.; Cao, Y.; Korolev, N.; Nordenskiöld, L.; Liu, C. F. A Direct Method for Site-Specific Protein Acetylation. *Angew. Chem. Int. Ed.* **2011**, *50* (41), 9611–9614. https://doi.org/10.1002/anie.201103754.

(160) Valkevich, E. M.; Guenette, R. G.; Sanchez, N. A.; Chen, Y. C.; Ge, Y.; Strieter, E. R. Forging Isopeptide Bonds Using Thiol-Ene Chemistry: Site-Specific Coupling of Ubiquitin Molecules for Studying the Activity of Isopeptidases. *J. Am. Chem. Soc.* **2012**, *134* (16), 6916–6919. https://doi.org/10.1021/ja300500a.

(161) Serniwka, S. A.; Shaw, G. S. The Structure of the UbcH8-Ubiquitin Complex Shows a Unique Ubiquitin Interaction Site. *Biochemistry* **2009**, *48* (51), 12169–12179. https://doi.org/10.1021/BI901686J.

(162) Garber, K. C. A.; Carlson, E. E. Thiol-Ene Enabled Detection of Thiophosphorylated Kinase Substrates. *ACS Chem. Biol.* **2013**, *8* (8), 1671–1676. https://doi.org/10.1021/cb400184v.

(163) Taylor, N. C.; Hessman, G.; Kramer, H. B.; McGouran, J. F. Probing Enzymatic Activity-a Radical Approach. *Chem. Sci.* **2020**, *11* (11), 2967–2972.

https://doi.org/10.1039/c9sc05258e.

(164) Gori, A.; Gagni, P.; Rinaldi, S. Disulfide Bond Mimetics: Strategies and Challenges. *Chem. - A Eur. J.* **2017**, *23* (60), 14987–14995. https://doi.org/10.1002/chem.201703199.

(165) Lee, H. J.; Macbeth, A. H.; Pagani, J. H.; Scott Young, W. Oxytocin: The Great Facilitator of Life. *Prog. Neurobiol.* **2009**, *88* (2), 127–151. https://doi.org/10.1016/j.pneurobio.2009.04.001.

(166) Du Vigneaud, V.; Ressler, C.; Trippett, S. The Sequence of Amino Acids in Oxytocin, with a Proposal for the Structure of Oxytocin. *J. Biol. Chem.* **1953**, *205* (2), 949–957.

(167) Du Vigneaud, V.; Ressler, C.; Swan, J. M.; Roberts, C. W.; Katsoyannis, P. G.; Gordon, S. The Synthesis of an Octapeptide Amide With The Hormonal Activity of Oxytocin. *J. Am. Chem. Soc.* **1953**, *75* (19), 4879–4880. https://doi.org/10.1021/ja01115a553.

(168) du Vigneaud, V.; Resslbr, C.; Swan, J. M.; Roberts, C. W.; Katsoyannis, P. G. The Synthesis of Oxytocin. *J. Am. Chem. Soc.* **1954**, *76* (12), 3115–3121. https://doi.org/10.1021/ja01641a004.

(169) *The Nobel Prize in Chemistry 1955 - NobelPrize.org*. https://www.nobelprize.org/prizes/chemistry/1955/summary/ (accessed 2020-04-20).

(170) Gude, M.; Ryf, J.; White, P. D. An Accurate Method for the Quantitation of Fmoc-Derivatized Solid Phase Supports. *Lett. Pept. Sci. 2002 94* **2002**, *9* (4), 203–206. https://doi.org/10.1023/A:1024148619149.

(171) Afzali-Ardakani, A.; Rapoport, H. L-Vinylglycine. *J. Org. Chem.* **1980**, *45* (24), 4817–4820. https://doi.org/10.1021/jo01312a002.

(172) McLean, J. T.; Milbeo, P.; Lynch, D. M.; McSweeney, L.; Scanlan, E. Radical-Mediated Acyl-Thiol-Ene Reaction for Rapid Synthesis of Biomolecular Thioester Derivatives. *Eur. J. Org. Chem.* **2021**, *2021* (1), 4148-4164. https://doi.org/10.1002/EJOC.202100615.

(173) Valeur, E.; Bradley, M. Amide Bond Formation: Beyond the Myth of Coupling Reagents. *Chem. Soc. Rev.* **2009**, *38* (2), 606–631. https://doi.org/10.1039/B701677H.

(174) Love, D. M.; Kim, K.; Goodrich, J. T.; Fairbanks, B. D.; Worrell, B. T.; Stoykovich, M. P.; Musgrave, C. B.; Bowman, C. N. Amine Induced Retardation of the Radical-Mediated Thiol-Ene Reaction via the Formation of Metastable Disulfide Radical Anions. *J. Org. Chem.* **2018**, *83* (5), 2912–2919. https://doi.org/10.1021/acs.joc.8b00143.

(175) Colak, B.; Da Silva, J. C. S.; Soares, T. A.; Gautrot, J. E. Impact of the Molecular Environment on Thiol-Ene Coupling for Biofunctionalization and Conjugation. *Bioconjug. Chem.* **2016**, *27* (9), 2111–2123. https://doi.org/10.1021/acs.bioconjchem.6b00349.

(176) Wang, B.; Muir, T. W. Regulation of Virulence in Staphylococcus Aureus: Molecular Mechanisms and Remaining Puzzles. *Cell Chem. Biol.* **2016**, *23* (2), 214–224. https://doi.org/10.1016/j.chembiol.2016.01.004.

(177) Tal-Gan, Y.; Stacy, D. M.; Foegen, M. K.; Koenig, D. W.; Blackwell, H. E. Highly Potent Inhibitors of Quorum Sensing in Staphylococcus Aureus Revealed through a Systematic Synthetic Study of the Group-III Autoinducing Peptide. *J. Am. Chem. Soc.* **2013**, *135* (21), 7869–7882. https://doi.org/10.1021/ja3112115.

(178) *Goal 12 | Department of Economic and Social Affairs*. https://sdgs.un.org/goals/goal12 (accessed 2023-05-18).

(179) Bryan, M. C.; Dalton, C.; Doerfler, J.; Engl, O. D.; Ferguson, P.; Molina, A. G.; Harawa, V.; Hosford, J.; Howell, G. P.; Kelly, C. B.; Li, W.; Munday, R. H.; Navarro, A.; Parmentier, M.; Pawlas, J.; Richardson, P. F.; Steven, A.; Takale, B. S.; Terrett, J. A.; Treitler, D. S.; Zeng, M. Green Chemistry Articles of Interest to the Pharmaceutical Industry. *Org. Process Res. Dev.* **2022**, *26* (9), 2550–2559. https://doi.org/10.1021/ACS.OPRD.2C00274.

(180) Welton, T. Editorial Overview: UN Sustainable Development Goals: How Can Sustainable/Green Chemistry Contribute? There Can Be More than One Approach. *Curr. Opin. Green Sustain. Chem.* **2018**, *13* (1), A7–A9. https://doi.org/10.1016/j.cogsc.2018.09.005.

(181) Kar, S.; Sanderson, H.; Roy, K.; Benfenati, E.; Leszczynski, J. Green Chemistry in the Synthesis of Pharmaceuticals. *Chem. Rev.* **2021**, *122* (3), 3637-3710. acs.chemrev.1c00631. https://doi.org/ 10.1021/acs.chemrev.1c00631.

(182) Colombo Dugoni, G.; Mezzetta, A.; Guazzelli, L.; Chiappe, C.; Ferro, M.; Mele, A. Purification of Kraft Cellulose under Mild Conditions Using Choline Acetate Based Deep Eutectic Solvents. *Green Chem.* **2020**, *22* (24), 8680–8691. https://doi.org/10.1039/d0gc03375h.

(183) Mamilla, J. L. K.; Novak, U.; Grilc, M.; Likozar, B. Natural Deep Eutectic Solvents (DES) for Fractionation of Waste Lignocellulosic Biomass and Its Cascade Conversion to Value-Added Bio-Based Chemicals. *Biomass Bioenergy* **2019**, *120*, 417–425. https://doi.org/10.1016/j.biombioe.2018.12.002.

(184) Husanu, E.; Mero, A.; Rivera, J. G.; Mezzetta, A.; Ruiz, J. C.; D'andrea, F.; Pomelli, C. S.; Guazzelli, L. Exploiting Deep Eutectic Solvents and Ionic Liquids for the Valorization of Chestnut Shell Waste. *ACS Sustain. Chem. Eng.* **2020**, *8* (50), 18386–18399. https://doi.org/10.1021/acssuschemeng.0c04945.

(185) de Almeida Pontes, P. V.; Ayumi Shiwaku, I.; Maximo, G. J.; Caldas Batista, E. A. Choline Chloride-Based Deep Eutectic Solvents as Potential Solvent for Extraction of Phenolic Compounds from Olive Leaves: Extraction Optimization and Solvent Characterization. *Food Chem.* **2021**, *352* (1), 129346. https://doi.org/10.1016/j.foodchem.2021.129346.

(186) Wu, J.; Liang, Q.; Yu, X.; Qiu-Feng, L.; Ma, L.; Qin, X.; Chen, G.; Li, B. Deep Eutectic Solvents for Boosting Electrochemical Energy Storage and Conversion: A Review and Perspective. *Adv. Funct. Mater.* **2021**, 31(1), 2011102. https://doi.org/10.1002/adfm.202011102.

(187) Arnaboldi, S.; Mezzetta, A.; Grecchi, S.; Longhi, M.; Emanuele, E.; Rizzo, S.; Arduini, F.; Micheli, L.; Guazzelli, L.; Mussini, P. R. Natural-Based Chiral Task-Specific Deep Eutectic Solvents: A Novel, Effective Tool for Enantiodiscrimination in Electroanalysis. *Electrochim. Acta* **2021**, *380* (1), 138189. https://doi.org/10.1016/j.electacta.2021.138189.

(188) Pätzold, M.; Siebenhaller, S.; Kara, S.; Liese, A.; Syldatk, C.; Holtmann, D. Deep Eutectic Solvents as Efficient Solvents in Biocatalysis. *Trends Biotechnol.* **2019**, *37* (9), 943–959. https://doi.org/10.1016/j.tibtech.2019.03.007.

(189) Hooshmand, S. E.; Afshari, R.; Ramón, D. J.; Varma, R. S. Deep Eutectic Solvents: Cutting-Edge Applications in Cross-Coupling Reactions. *Green Chem.* **2020**, *22* (12), 3668–3692. https://doi.org/10.1039/d0gc01494j.

(190) Chien, C. Y.; Yu, S. S. Ester-Mediated Peptide Formation Promoted by Deep Eutectic Solvents: A Facile Pathway to Proto-Peptides. *Chem. Commun.* **2020**, *56* (80), 11949–11952. https://doi.org/10.1039/d0cc03319g.

(191) Vidal, C.; García-Álvarez, J.; Hernán-Gõmez, A.; Kennedy, A. R.; Hevia, E. Introducing Deep Eutectic Solvents to Polar Organometallic Chemistry: Chemoselective Addition of Organolithium and Grignard Reagents to Ketones in Air. *Angew. Chem. Int. Ed.* **2014**, *53* (23), 5969–5973. https://doi.org/10.1002/anie.201400889.

(192) Alonso, D. A.; Baeza, A.; Chinchilla, R.; Guillena, G.; Pastor, I. M.; Ramón, D. J. Deep Eutectic Solvents: The Organic Reaction Medium of the Century. *Eur. J. Org. Chem.* **2016**, *2016* (4), 612–632. https://doi.org/10.1002/ejoc.201501197.

(193) Smith, E. L.; Abbott, A. P.; Ryder, K. S. Deep Eutectic Solvents (DESs) and Their Applications. *Chem. Rev*. **2014**, *114* (21), 11060–11082. https://doi.org/10.1021/cr300162p.

(194) Abbott, A. P.; Boothby, D.; Capper, G.; Davies, D. L.; Rasheed, R. K. Deep Eutectic Solvents Formed between Choline Chloride and Carboxylic Acids: Versatile Alternatives to Ionic Liquids. *J. Am. Chem. Soc.* **2004**, *126* (29), 9142–9147. https://doi.org/10.1021/ja048266j/.

(195) Abbott, A. P.; Capper, G.; Davies, D. L.; Rasheed, R. K.; Tambyrajah, V. Novel Solvent Properties of Choline Chloride/Urea Mixtures. *Chem. Commun.* **2003**, *1* (1), 70–71. https://doi.org/10.1039/B210714G.

(196) Abbott, A. P.; Capper, G.; Davies, D. L.; Munro, H. L.; Rasheed, R. K.; Tambyrajah, V. Preparation of Novel, Moisture-Stable, Lewis-Acidic Ionic Liquids Containing Quaternary Ammonium Salts with Functional Side Chains. *Chem. Commun.* **2001**, *1* (19), 2010–2011. https://doi.org/10.1039/B106357J.

(197) Migliorati, V.; Sessa, F.; D'Angelo, P. Deep Eutectic Solvents: A Structural Point of View on the Role of the Cation. *Chem. Phys. Lett.* **2019**, *737* (1), 100001. https://doi.org/10.1016/j.cpletx.2018.100001.

(198) Chen, W.; Xue, Z.; Wang, J.; Jiang, J.; Zhao, X.; Mu, T. Investigation on the Thermal Stability of Deep Eutectic Solvents. *Acta Phys. - Chim. Sin.* **2018**, *34* (8), 904–911. https://doi.org/10.3866/PKU.WHXB201712281.

(199) Agieienko, V.; Buchner, R. Densities, Viscosities, and Electrical Conductivities of Pure Anhydrous Reline and Its Mixtures with Water in the Temperature Range (293.15 to 338.15) K. *J. Chem. Eng. Data* **2019**, *64* (11), 4763–4774. https://doi.org/10.1021/acs.jced.9b00145.

(200) González-Rivera, J.; Husanu, E.; Mero, A.; Ferrari, C.; Duce, C.; Tinè, M. R.; D'Andrea, F.; Pomelli, C. S.; Guazzelli, L. Insights into Microwave Heating Response and Thermal Decomposition Behavior of Deep Eutectic Solvents. *J. Mol. Liq.* **2020**, *300* (1), 112357. https://doi.org/10.1016/j.molliq.2019.112357.

(201) Mjalli, F. S.; Naser, J.; Jibril, B.; Alizadeh, V.; Gano, Z. Tetrabutylammonium Chloride Based Ionic Liquid Analogues and Their Physical Properties. *J. Chem. Eng. Data* **2014**, *59* (7), 2242–2251. https://doi.org/10.1021/je5002126.

(202) Majid, M. F.; Mohd Zaid, H. F.; Kait, C. F.; Ghani, N. A.; Jumbri, K. Mixtures of Tetrabutylammonium Chloride Salt with Different Glycol Structures: Thermal Stability and Functional Groups Characterizations. *J. Mol. Liq.* **2019**, *294* (1), 111588. https://doi.org/10.1016/j.molliq.2019.111588.

(203) Panda, D. K.; Bhargava, B. L. Intermolecular Interactions in Tetrabutylammonium Chloride Based Deep Eutectic Solvents: Classical Molecular Dynamics Studies. *J. Mol. Liq.* **2021**, *335* (1), 116139. https://doi.org/10.1016/j.molliq.2021.116139.

(204) Kruse, J. A. Methanol and Ethylene Glycol Intoxication. *Crit. Care Clin.* **2012**, *28* (4), 661–711. https://doi.org/10.1016/J.CCC.2012.07.002.

(205) Zhang, N.; Steininger, F.; Meyer, L. E.; Koren, K.; Kara, S. Can Deep Eutectic Solvents Sustain Oxygen-Dependent Bioprocesses? - Measurements of Oxygen Transfer Rates. *ACS Sustain. Chem. Eng.* **2021**, *9* (25), 8347–8353. https://doi.org/10.1021/acssuschemeng.1c03547.

(206) Huang, L.; Bittner, J. P.; Domínguez de María, P.; Jakobtorweihen, S.; Kara, S. Modeling Alcohol Dehydrogenase Catalysis in Deep Eutectic Solvent/Water Mixtures. *ChemBioChem* **2020**, *21* (6), 811–817. https://doi.org/10.1002/cbic.201900624.

(207) Huo, C.; Wang, Y.; Yuan, Y.; Chen, F.; Tang, J. Auto-Oxidative Hydroxysulfenylation of Alkenes. *Chem. Commun.* **2016**, *52* (45), 7233–7236. https://doi.org/10.1039/C6CC01937D.

(208) Larue, R. C.; Xing, E.; Kenney, A. D.; Zhang, Y.; Tuazon, J. A.; Li, J.; Yount, J. S.; Li, P. K.; Sharma, A. Rationally Designed ACE2-Derived Peptides Inhibit SARS-CoV-2. *Bioconjug. Chem.* **2021**, *32* (1), 215–223. https://doi.org/10.1021/acs.bioconjchem.0c00664.

(209) Sadremomtaz, A.; Al-Dahmani, Z. M.; Ruiz-Moreno, A. J.; Monti, A.; Wang, C.; Azad, T.; Bell, J. C.; Doti, N.; Velasco-Velázquez, M. A.; De Jong, D.; De Jonge, J.; Smit, J.; Dömling, A.; Van Goor, H.; Groves, M. R. Synthetic Peptides That Antagonize the Angiotensin-Converting Enzyme-2 (ACE-2) Interaction with SARS-CoV-2 Receptor Binding Spike Protein. *J. Med. Chem.* **2022**, *65* (4), 2836–2847. https://doi.org/10.1021/acs.jmedchem.1c00477.

(210) Hammond, O. S.; Bowron, D. T.; Edler, K. J. The Effect of Water upon Deep Eutectic Solvent Nanostructure: An Unusual Transition from Ionic Mixture to Aqueous Solution. *Angew. Chem. Int. Ed.* **2017**, *56* (33), 9782–9785. https://doi.org/10.1002/ANIE.201702486.

(211) Thomas, R. P.; Heap, R. E.; Zappacosta, F.; Grant, E. K.; Pogány, P.; Besley, S.; Fallon, D. J.; Hann, M. M.; House, D.; Tomkinson, N. C. O.; Bush, J. T. A Direct-to-Biology High-Throughput Chemistry Approach to Reactive Fragment Screening. *Chem. Sci.* **2021**, *12* (36), 12098–12106. https://doi.org/10.1039/d1sc03551g.

(212) Aatkar, A.; Vuorinen, A.; Longfield, O. E.; Gilbert, K.; Peltier-Heap, R.; Wagner, C. D.; Zappacosta, F.; Rittinger, K.; Chung, C.; House, D.; Tomkinson, N. C. O.; Bush, J. T. Efficient Ligand Discovery Using Sulfur(VI) Fluoride Reactive Fragments. *ACS Chem. Biol.* **2023**. https://doi.org/10.1021/ACSCHEMBIO.3C00034.

(213) Kaguchi, R.; Katsuyama, A.; Sato, T.; Takahashi, S.; Horiuchi, M.; Yokota, S.; Ichikawa, S. Discovery of Biologically Optimized Polymyxin Derivatives Facilitated by Peptide Scanning and In Situ Screening Chemistry. *J. Am. Chem. Soc.* **2023**, *145* (6), 3665-3681. https://doi.org/10.1021/jacs.2c12971.

(214) Gehrtz, P.; Marom, S.; Bührmann, M.; Hardick, J.; Kleinbölting, S.; Shraga, A.; Dubiella, C.; Gabizon, R.; Wiese, J. N.; Müller, M. P.; Cohen, G.; Babaev, I.; Shurrush, K.; Avram, L.; Resnick, E.; Barr, H.; Rauh, D.; London, N. Optimization of Covalent MKK7 Inhibitors via Crude Nanomole-Scale Libraries. *J. Med. Chem.* **2022**, *65* (15), 10341–10356. https://doi.org/10.1021/ACS.JMEDCHEM.1C02206.

(215) Kitamura, S.; Zheng, Q.; Woehl, J. L.; Solania, A.; Chen, E.; Dillon, N.; Hull, M. V.;

Kotaniguchi, M.; Cappiello, J. R.; Kitamura, S.; Nizet, V.; Sharpless, K. B.; Wolan, D. W. Sulfur(VI) Fluoride Exchange (SuFEx)-Enabled High-Throughput Medicinal Chemistry. *J. Am. Chem. Soc.* **2020**, *142* (25), 10899–10904. https://doi.org/10.1021/jacs.9b13652.

(216) Liu, Z.; Li, J.; Li, S.; Li, G.; Sharpless, K. B.; Wu, P. SuFEx Click Chemistry Enabled Late-Stage Drug Functionalization. *J. Am. Chem. Soc.* **2018**, *140* (8), 2919–2925. https://doi.org/10.1021/jacs.7b12788.

(217) Habeshian, S.; Sable, G. A.; Schüttel, M.; Merz, M. L.; Heinis, C. Cyclative Release Strategy to Obtain Pure Cyclic Peptides Directly from the Solid Phase. *ACS Chem. Biol.* **2022**, *17* (1), 181–186. https://doi.org/10.1021/acschembio.1c00843.

(218) Bognar, Z.; Mothukuri, G. K.; Nielsen, A. L.; Merz, M. L.; Pânzar, P. M. F.; Heinis, C. Solid-Phase Peptide Synthesis on Disulfide-Linker Resin Followed by Reductive Release Affords Pure Thiol-Functionalized Peptides. *Org. Biomol. Chem.* **2022**, *20* (29), 5699–5703. https://doi.org/10.1039/d2ob00910b.

(219) Mothukuri, G. K.; Kale, S. S.; Stenbratt, C. L.; Zorzi, A.; Vesin, J.; Bortoli Chapalay, J.; Deyle, K.; Turcatti, G.; Cendron, L.; Angelini, A.; Heinis, C. Macrocycle Synthesis Strategy Based on Step-Wise "Adding and Reacting" Three Components Enables Screening of Large Combinatorial Libraries. *Chem. Sci.* **2020**, *11* (30), 7858–7863. https://doi.org/10.1039/d0sc01944e.

(220) Assem, N.; Ferreira, D. J.; Wolan, D. W.; Dawson, P. E. Acetone-Linked Peptides: A Convergent Approach for Peptide Macrocyclization and Labeling. *Angew. Chem. Int. Ed.* **2015**, *54* (30), 8665–8668. https://doi.org/10.1002/ANIE.201502607.

(221) Lin, S.; Dikler, S.; Blincoe, W. D.; Ferguson, R. D.; Sheridan, R. P.; Peng, Z.; Conway, D. V.; Zawatzky, K.; Wang, H.; Cernak, T.; Davies, I. W.; DiRocco, D. A.; Sheng, H.; Welch, C. J.; Dreher, S. D. Mapping the Dark Space of Chemical Reactions with Extended Nanomole Synthesis and MALDI-TOF MS. *Science.* **2018**, *361* (6402). https://doi.org/10.1126/science.AAR6236.

(222) Ellson, R.; Mutz, M.; Browning, B.; Lee, L.; Miller, M. F.; Papen, R. Transfer of Low Nanoliter Volumes between Microplates Using Focused Acoustics—Automation Considerations. *JALA J. Assoc. Lab. Autom.* **2003**, *8* (5), 29–34. https://doi.org/10.1016/s1535-5535-03-00011-x.

(223) Ellson, R. Picoliter: Enabling Precise Transfer of Nanoliter and Picoliter Volumes. *Drug Discov. Today* **2002**, *7* (5), S32–S34. https://doi.org/10.1016/s1359-6446(02)02176-1.

(224) *NIST Chemistry WebBook*. https://webbook.nist.gov/chemistry/# (accessed 2023-04-07).

(225) Rahaman, R.; Hoque, M. T.; Maiti, D. K. Organophotoredox-Catalyzed Sulfurization of Alkenes and Alkynes: Selective and Controlled Synthesis of Sulfoxides, β-Hydroxysulfoxides, and β-Keto Sulfides. *Org. Lett.* **2022**, *24* (38), 6885–6890. https://doi.org/10.1021/acs.orglett.2c02307.

(226) Griffiths, R. C.; Smith, F. R.; Long, J. E.; Williams, H. E. L.; Layfield, R.; Mitchell, N. J. Site-Selective Modification of Peptides and Proteins via Interception of Free-Radical-Mediated Dechalcogenation. *Angew. Chem. Int. Ed.* **2020**, *59* (52), 23659–23667. https://doi.org/10.1002/ANIE.202006260.

(227) Griffiths, R. C.; Smith, F. R.; Long, J. E.; Scott, D.; Williams, H. E. L.; Oldham, N. J.; Layfield, R.; Mitchell, N. J. Site-Selective Installation of Nϵ-Modified Sidechains into Peptide and Protein Scaffolds via Visible-Light-Mediated Desulfurative C–C Bond Formation. *Angew. Chem. Int. Ed.* **2022**, *61* (2), e202110223. https://doi.org/10.1002/anie.202110223.

(228) Shaabani, S.; Xu, R.; Ahmadianmoghaddam, M.; Gao, L.; Stahorsky, M.; Olechno, J.; Ellson, R.; Kossenjans, M.; Helan, V.; Dömling, A. Automated and Accelerated Synthesis of Indole Derivatives on a Nano-Scale. *Green Chem.* **2019**, *21* (2), 225–232. https://doi.org/10.1039/C8GC03039A.

(229) Gao, K.; Shaabani, S.; Xu, R.; Zarganes-Tzitzikas, T.; Gao, L.; Ahmadianmoghaddam, M.; Groves, M. R.; Dömling, A. Nanoscale, Automated, High Throughput Synthesis and Screening for the Accelerated Discovery of Protein Modifiers. *RSC Med. Chem.* **2021**, *12* (5), 809–818. https://doi.org/10.1039/D1MD00087J.

(230) Sangouard, G.; Zorzi, A.; Wu, Y.; Ehret, E.; Schüttel, M.; Kale, S.; Díaz-Perlas, C.; Vesin, J.; Bortoli Chapalay, J.; Turcatti, G.; Heinis, C. Picomole-Scale Synthesis and Screening of Macrocyclic Compound Libraries by Acoustic Liquid Transfer. *Angew. Chem. Int. Ed.* **2021**, *60* (40), 21702–21707. https://doi.org/10.1002/ANIE.202107815.

(231) Gao, L.; Shaabani, S.; Reyes Romero, A.; Xu, R.; Ahmadianmoghaddam, M.; Dömling, A. 'Chemistry at the Speed of Sound': Automated 1536-Well Nanoscale Synthesis of 16 Scaffolds in Parallel. *Green Chem.* **2023**, *25* (4), 1380–1394. https://doi.org/10.1039/d2gc04312b.

(232) *CERTUS FLEX Micro Dispenser - Trajan Scientific and Medical - LEAP*. https://www.leaptec.com/products/certus-flex-high-end-digital-dispenser (accessed 2023-04-10).

(233) Luchansky, S.H.; Argade, S; Hayes B.K; Bertozzi C.R. Metabolic Functionalization of Recombinant Glycoproteins. *Biochemistry* **2004**, *43* (38), 12358–12366. https://doi.org/10.1021/BI049274F.

(234) Dube, D. H.; Prescher, J. A.; Quang, C. N.; Bertozzi, C. R. Probing Mucin-Type O-Linked Glycosylation in Living Animals. *Proc. Natl. Acad. Sci.* **2006**, *103* (13), 4819–4824. https://doi.org/10.1073/PNAS.0506855103.

(235) Sletten, E. M.; Bertozzi, C. R. Bioorthogonal Chemistry: Fishing for Selectivity in a Sea of Functionality. *Angew. Chem. Int. Ed.* **2009**, *48* (38), 6974–6998. https://doi.org/10.1002/ANIE.200900942.

(236) Niederwieser, A.; Späte, A. K.; Nguyen, L. D.; Jüngst, C.; Reutter, W.; Wittmann, V. Two-Color Glycan Labeling of Live Cells by a Combination of Diels–Alder and Click Chemistry. *Angew. Chem. Int. Ed.* **2013**, *52* (15), 4265–4268. https://doi.org/10.1002/ANIE.201208991.

(237) Robinson, C.; Hartman, R. F.; Rose, S. D. Emollient, Humectant, and Fluorescent α,β-Unsaturated Thiol Esters for Long-Acting Skin Applications. *Bioorg. Chem.* **2008**, *36* (6), 265–270. https://doi.org/10.1016/J.BIOORG.2008.06.004.

(238) Teders, M.; Henkel, C.; Anhäuser, L.; Strieth-Kalthoff, F.; Gómez-Suárez, A.; Kleinmans, R.; Kahnt, A.; Rentmeister, A.; Guldi, D.; Glorius, F. The Energy-Transfer-Enabled Biocompatible Disulfide–Ene Reaction. *Nat. Chem.* **2018**, *10* (9), 981–988. https://doi.org/10.1038/s41557-018-0102-z.

(239) Li, Y.; Yang, M.; Huang, Y.; Song, X.; Liu, L.; Chen, P. R. Genetically Encoded Alkenyl-Pyrrolysine Analogues for Thiol-Ene Reaction Mediated Site-Specific Protein Labeling. *Chem. Sci.* **2012**, *3* (9), 2766–2770. https://doi.org/10.1039/c2sc20433a.

(240) Olatunji, S.; Yu, X.; Bailey, J.; Huang, C. Y.; Zapotoczna, M.; Bowen, K.; Remškar, M.; Müller, R.; Scanlan, E. M.; Geoghegan, J. A.; Olieric, V.; Caffrey, M. Structures of Lipoprotein Signal Peptidase II from Staphylococcus Aureus Complexed with Antibiotics Globomycin and Myxovirescin. *Nat. Commun.* **2020**, *11* (1), 1–11. https://doi.org/10.1038/s41467-019-13724-y.

(241) Lo Conte, M.; Staderini, S.; Marra, A.; Sanchez-Navarro, M.; Davis, B. G.; Dondoni, A. Multi-Molecule Reaction of Serum Albumin Can Occur through Thiol-Yne Coupling. *Chem. Commun.* **2011**, *47* (39), 11086–11088. https://doi.org/10.1039/c1cc14402b.

(242) Fairhead, M.; Krndija, D.; Lowe, E. D.; Howarth, M. Plug-and-Play Pairing via Defined Divalent Streptavidins. *J. Mol. Biol.* **2014**, *426* (1), 199–214. https://doi.org/10.1016/J.JMB.2013.09.016.

(243) Adachi, Y.; Sakimura, K.; Shimizu, Y.; Nakayama, M.; Terao, Y.; Yano, T.; Asami, T. Potent and Selective Oxytocin Receptor Agonists without Disulfide Bridges. *Bioorganic Med. Chem. Lett.* **2017**, *27* (11), 2331–2335. https://doi.org/10.1016/j.bmcl.2017.04.030.

(244) Wiśniewski, K.; Alagarsamy, S.; Galyean, R.; Tariga, H.; Thompson, D.; Ly, B.; Wiśniewska, H.; Qi, S.; Croston, G.; Laporte, R.; Rivière, P. J. M.; Schteingart, C. D. New, Potent, and Selective Peptidic Oxytocin Receptor Agonists. *J. Med. Chem.* **2014**, *57* (12), 5306–5317. https://doi.org/10.1021/JM500365S.

(245) Wesche, F.; De Maria, L.; Leek, T.; Narjes, F.; Bird, J.; Su, W.; Czechtizky, W. Automated High-Throughput in Vitro Assays to Identify Metabolic Hotspots and Protease Stability of Structurally Diverse, Pharmacologically Active Peptides for Inhalation. *J. Pharm. Biomed. Anal.* **2022**, *211*, 114518. https://doi.org/10.1016/J.JPBA.2021.114518.

(246) Mansueto, M.; Kreß, K. C.; Laschat, S. Sulfur Makes the Difference: Synthesis and Mesomorphic Properties of Novel Thioether-Functionalized Imidazolium Ionic Liquid Crystals. *Tetrahedron* **2014**, *70* (36), 6258–6264. https://doi.org/10.1016/j.tet.2014.03.050.

(247) Hakimelahi, G. H.; Just, G. The Synthesis of 4-Decarboxy-4-phosphono-O-2-isooxacephems, -isopenams and -isooxacephems Containing Phosphorus at the 3-Position. *Helv. Chim. Acta* **1982**, *65* (5). https://doi.org/10.1002/hlca.19820650505.

(248) Jeffrey A. Robl, *; Chong-Qing Sun; Jay Stevenson; Denis E. Ryono; Ligaya M. Simpkins; Maria P. Cimarusti; Tamara Dejneka; William A. Slusarchyk; Sam Chao; Leslie Stratton; Raj N. Misra; Mark S. Bednarz; Magdi M. Asaad; Hong Son Cheung; Benoni E. Abboa-Offei; Patricia L. Smith; Parker D. Mathers; Maxine Fox; Thomas R. Schaeffer; Andrea A. Seymour, and; Trippodo, N. C. Dual Metalloprotease Inhibitors: Mercaptoacetyl-Based Fused Heterocyclic Dipeptide Mimetics as Inhibitors of Angiotensin-Converting Enzyme and Neutral Endopeptidase. *J. Med. Chem.* **1997**, *40* (11), 1570–1577. https://doi.org/10.1021/JM970041E.

(249) Kuehne, M. E.; Damon, R. E. Thiyl Radical Induced Cyclizations of Dienes. Cyclization of α-Acoradiene, α-Bulnesene, and Geranyl Acetate to Cedrane, Patchulane, and Cyclogeranyl Acetate Products. *J. Org. Chem.* **1977**, *42* (11), 1825–1832. https://doi.org/10.1021/JO00431A001.

(250) Biswas, N. N.; Yu, T. T.; Kimyon, Ö.; Nizalapur, S.; Gardner, C. R.; Manefield, M.; Griffith, R.; Black, D. S. C.; Kumar, N. Synthesis of Antimicrobial Glucosamides as Bacterial Quorum Sensing Mechanism Inhibitors. *Bioorg. Med. Chem.* **2017**, *25* (3), 1183–1194. https://doi.org/10.1016/J.BMC.2016.12.024.

(251) Magnus, N. A.; Ducry, L.; Rolland, V.; Wonnacott, S.; Gallagher, T. Direct C-11 Functionalisation of Anatoxin-a. Application to Thesynthesis of New Ligand-Based Structural Probes. *J. Chem. Soc. Perkin Trans.* **1997**, *16* (1), 2313–2318. https://doi.org/10.1039/A702087B.

(252) Vilaivan, T. A Rate Enhancement of Tert-Butoxycarbonylation of Aromatic Amines with Boc2O in Alcoholic Solvents. *Tetrahedron Lett.* **2006**, *47* (38), 6739–6742. https://doi.org/10.1016/J.TETLET.2006.07.097.

(253) Hurst, R. D.; Nieves, A.; Brichacek, M. Expanding Glycomic Investigations through Thiol-Derivatized Glycans. *Molecules* **2023**, *28* (4), 1956-1975. https://doi.org/10.3390/molecules28041956.

(254) Lee, Y. J.; Yadagiri, K.; Yang, Y.; Torres-Kolbus, J.; Deiters, A.; Liu, W. R. Genetically Encoded Unstrained Olefins for Live Cell Labeling with Tetrazine Dyes. *Chem. Commun.* **2014**, *50* (86), 13085–13088. https://doi.org/10.1039/C4CC06435F.

(255) Smulik, J. A.; Diver, S. T.; Pan, F.; Liu, J. O. Synthesis of Cyclosporin A-Derived Affinity Reagents by Olefin Metathesis. *Org. Lett.* **2002**, *4* (12), 2051–2054.

https://doi.org/10.1021/OL0258987.

(256) Oh, C.; Li, M.; Kim, E. H.; Park, J. S.; Lee, J. C.; Ham, S. W. Antioxidant and Radical Scavenging Activities of Ascorbic Acid Derivatives Conjugated with Organogermanium. *Bull. Korean Chem. Soc.* **2010**, *31* (12), 3513–3514. https://doi.org/10.5012/BKCS.2010.31.12.3513.